INSTRUMENTATION FOR OBSERVATION OF HIGH FREQUENCY SIGNALS

IN THE SCANNING ELECTRON MICROSCOPE

by

SAAD A.W.A.R. ALSHABAN

B.Sc, M.Sc (Dundee Univ)

A thesis submitted to the Faculty of Science

University of Edinburgh for the degree

of Doctor of Philosophy

Department of Electrical Engineering

1983

ABSTRACT

Stroboscopy and sampling in the scanning electron microscope (SEM) were developed to observe high frequency signals on integrated circuit specimens under test as a valuable tool in the field of microcircuit design and testing. Voltage contrast in the SEM can be directly observed only for d.c. or slowly varying signals, due to the SEM bandwidth limitation. For frequencies above a few KHz, stroboscopic techniques must be used to study devices under dynamic conditions, where the sampling function is performed by chopping the electron beam. A survey of approaches to produce sampling systems shows their various limitations, and experimental results identify the nature of the difficulties (such as timing jitter in the reconstructed waveform).

A digital sampling system has been designed and developed to produce a digitally switched time delay to enable computer control of sampling. This overcomes the above problems and shows an improvement over the past work, with automated control for observing and measuring high frequency signals on the specimen. A colour stroboscopy technique was used to display timing and delay information throughout the specimen with signals up to 10 MHz frequency. A significant improvement with respect to the frequency limitation of the previous work in colour stroboscopy is achieved.

DECLARATION

I declare that this thesis was written by myself and that the work described in it was performed by me, unless otherwise indicated.

ACKNOWLEDGEMENTS

TO MY WIFE SHATHA,AND

MY DAUGHTERS

REEM AND RAYI

CONTENTS

CHAPTER 4: <u>OBSERVATION OF HIGH FREQUENCY SIGNALS</u>
            <u>USING ANALOGUE CIRCUITRY</u>

CHAPTER ONE

INTRODUCTION

Stroboscopic and sampling modes in the scanning electron micro-scope (SEM) are convenient and versatile tools which have found a wide field of applications for testing and diagnosis of integrated circuit devices under dynamic operation with repetitive phenomena to observe and measure high frequency signals where the electron beam is used as a circuit probe. Stroboscopic techniques in the SEM must be used for displaying voltage contrast of frequencies above a few kHz, due to the SEM collector bandwidth limitation.

The SEM utilised in the voltage - contrast stroboscopic mode can be used to give very precise timing information about voltage waveforms in integrated circuits. This information is normally displayed as either 2-D picture of voltage contrast at a particular phase point or as a waveform at a particular point on the surface.

A survey of past work shows that analogue sampling systems have timing jitter problems which seriously disturb the time resolution measurement of the system and shows the phase instability of this kind of sampling system.

New types of chopping plates and delay lines are produced by the present work. An improvement over past systems of analogue circuitry is achieved by a digital sampling system using digitally switched time delays to produce better performance and reproducibility. The present design of the delay units is found to be the only suitable source for generating time delays to test devices and analyse signal waveforms by colour stroboscopy, which is advantageous over the traditional way of

the sampling mode.

Chapter Two presents stroboscopy and sampling principles and a short review on the past work of stroboscopy and sampling in the SEM, with comparison and comment .

Chapter Three deals with definitions on chopping systems,the principle of electron beam chopping systems in the SEM,asurvey of the past work, the design and construction of different shapes of ⟨   ⟩ plates with comparisonsand suggestion . given.

Chapter Four surveys the analogue sampling systems reported by other workers. Most of the work which has been mentioned with the SEM in the past used analogue circuitry depending on the conventional sampling oscilloscope principle. Analogue circuitry is utilised at present for measurement and observation of high frequency signals on MOS specimens, by developing sampling techniques to produce waveforms which are composites of the waveforms value at a number of sampling phases plotted against time delay (phase change), using the chopped electron beam as the circuit probe.

Chapter Five involves the core of the present work, aimed towards producing a digital sampling system in the SEM. However it was identified that programmability is a necessary requirement for the future sampling system. New models of delay lines have been designed and constructed for producing time delays of low and high frequency signals.

Improvements over the previous sampling techniques are discussed. Comparisons between the analogue and digital system approaches are also given. Computer programmes for controlling the sampling system and delay units functions are discussed.

Chapter Six includes colour stroboscopy which is used to analyse signals at high frequency. The present work aims to give timing information in the form of colour on a 2-D image of the specimen. The colour is at present generated in a real-time analogue video system, although it is envisaged that a similar principle could be used with a computer-generated synthetic colour overlay of the previous system.

Colour stroboscopy is useful to study the slowing down of signal rise time under test when propagating through long strips of the specimen, where the signal rise time changes. Also to display time delays in colour, which is important as a diagnostic tool for microcircuit engineering. Hardware and software are implemented to perform colour stroboscopy in the SEM working up to 10 MHz repetitive signal frequency.

It is considered that the original work of this thesis comprises chapters five, and six, which detail the contribution of the practical studies on the design and construction of the sampling system in the SEM; and also describes the basics of the signal analysis by colour stroboscopy.

Chapter seven deals with a conclusion on present work performance and future work.

CHAPTER TWO

REVIEW OF STROBOSCOPY AND SAMPLING IN THE SEM

2.1 INTRODUCTION

In the ordinary SEM as in Figure 2.1 the electron probe is scanned over the specimen by the scanning coils, electrons penetrate the specimen producing electron emission; these electrons are deflected by the electric field above the specimen under test towards the collector which contains a scintillator/photomultiplier. This emitted electron current is a function of specimen surface properties at the point of incidence. A certain proportion of this current is collected, amplified and converted to modulating the brightness of the C.R.T spot which is scanned in synchronism with the electron probe.

A microcircuit chip with static voltage distribution on the surface can be examined qualitatively by conventional SEM. Voltage contrast in the SEM can be readily observed for dc or slowly varying signals. For frequencies above a few KHz, however, stroboscopic techniques must be used. This chapter includes stroboscopy and sampling principles and a short review of the basic ideas using SEM in the stroboscopic and sampling modes in the literature, mainly to study semiconductor devices under high frequency (H.F) dynamic conditions, where the sampling function is performed by chopping the electron beam used as probe.

2.2 STROBOSCOPY PRINCIPLE

The most straight forward technique for observing an a.c signal is

SEM

electron gun

Chopping assembly

condenser lens 1

condenser lens 2

final condenser
lens

scanning coils

magnification
unit

specimen

vacuum
systems

scanning
circuit

display
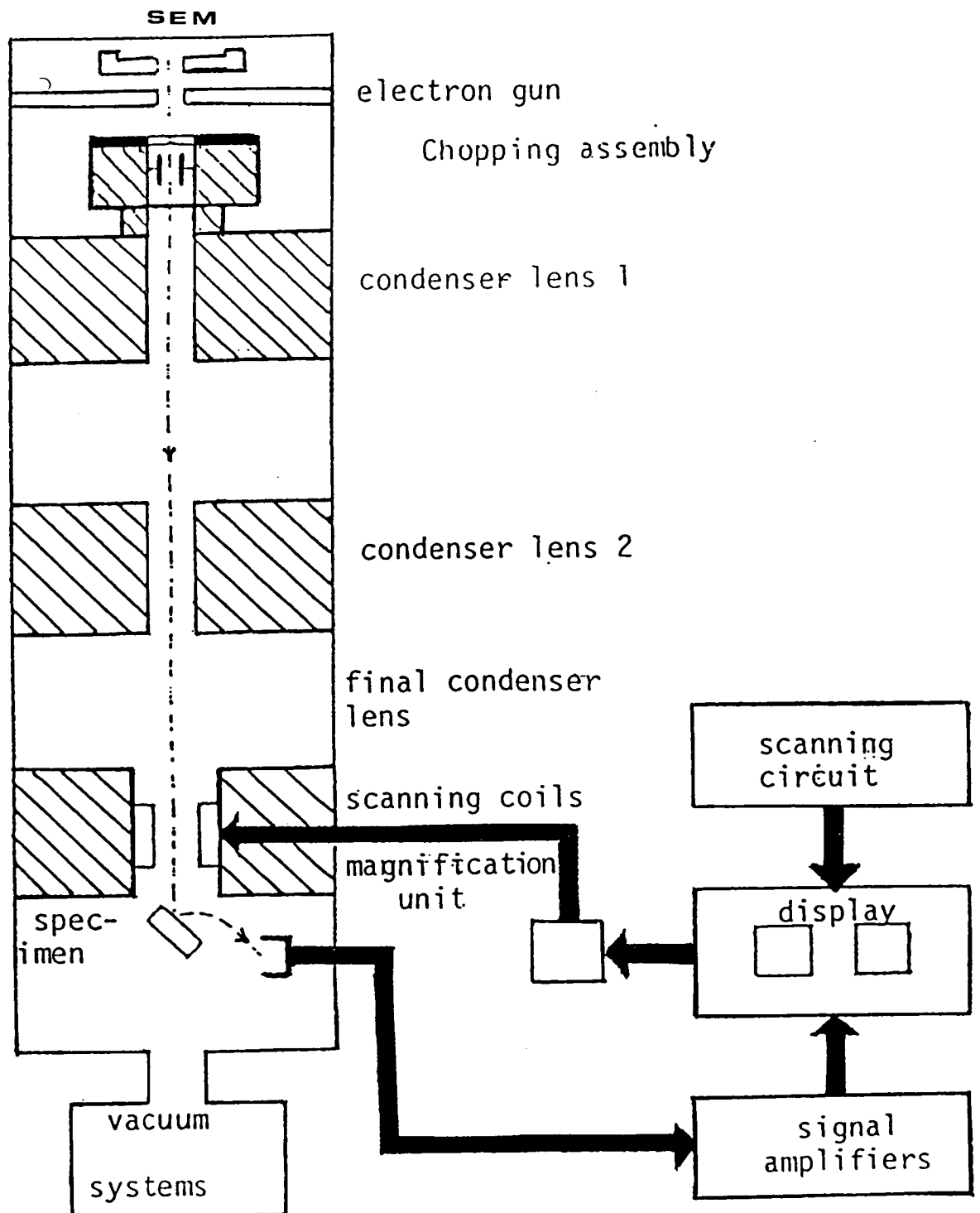
signal
amplifiers

Figure 2.1:   Shows block schematic diagram of
basic operating principles (SEM).

to stop the electron beam on the point of interest and examine the signal coming out of the detector system. However, if the frequency of the signal is outside the pass band of the detector system, an alternative must be found. The technique adopted, originally described by Plows and Nixon (1968) is to chop the electron beam at a high frequency related to the frequency of the signal on the circuit. The electron stream being emitted from the specimen will therefore be modulated both by this frequency and the frequency of the voltage on the specimen. The modulated signal can be arranged to have a frequency within the bandwidth of any detector system, and if the two frequencies are locked together, the output has a d.c component, and this is known as the "stroboscopic mode".

The use of this technique is that the specimen to be tested should be put into its dynamic operation in full operating mode and that the electron beam of the SEM should be switched "on" and "off" in synchronism with the waveform to be investigated. This is arranged by having a set of chopping plates placed at the top of the electron optical column, and the beam is pulsed by these plates(see Figure 2. 2). "If a changing phenomenon is periodic in time, and illuminated for a short time compared with the period, this shows the state of the system frozen at the chosen phase"(from Hill(1974)).

Two logic states to show stroboscopy:

(a)   When binary "1" is for both trigger pulse —
and electron beam pulse, then the area is dark.

(b)   When the area is at binary "0" (low)the area shown is bright, see Figure 2 .2 .

The signal fed to the chopping plates deflects the electron beam
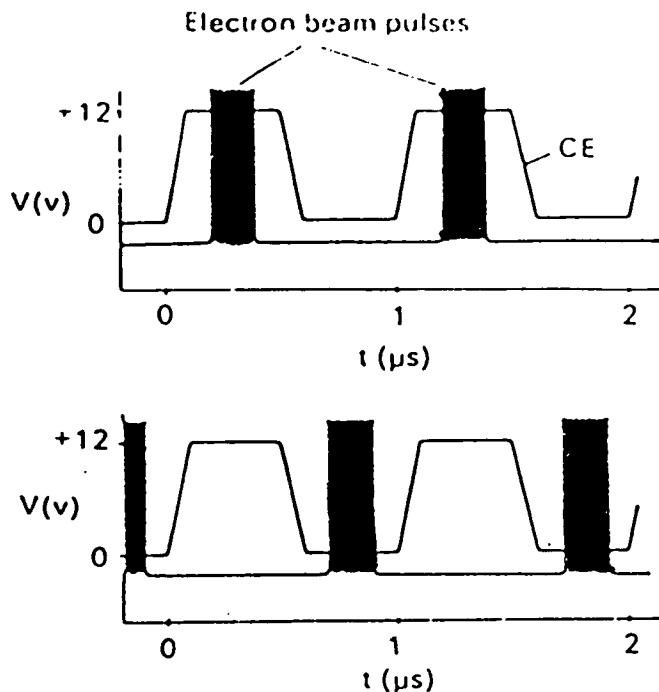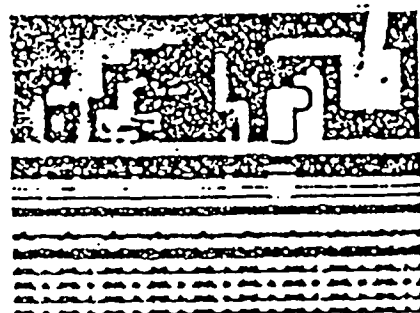
Figure 2.2 : Stroboscopic principle. The electron beam is
only unblanked when the specimen assumes a
certain logical state. In the upper representation
this is the case when the external clock CE is
at 12V ('1'). In the lower representations, CE
is at 0V ('0'). (From Wolfgang 1981)
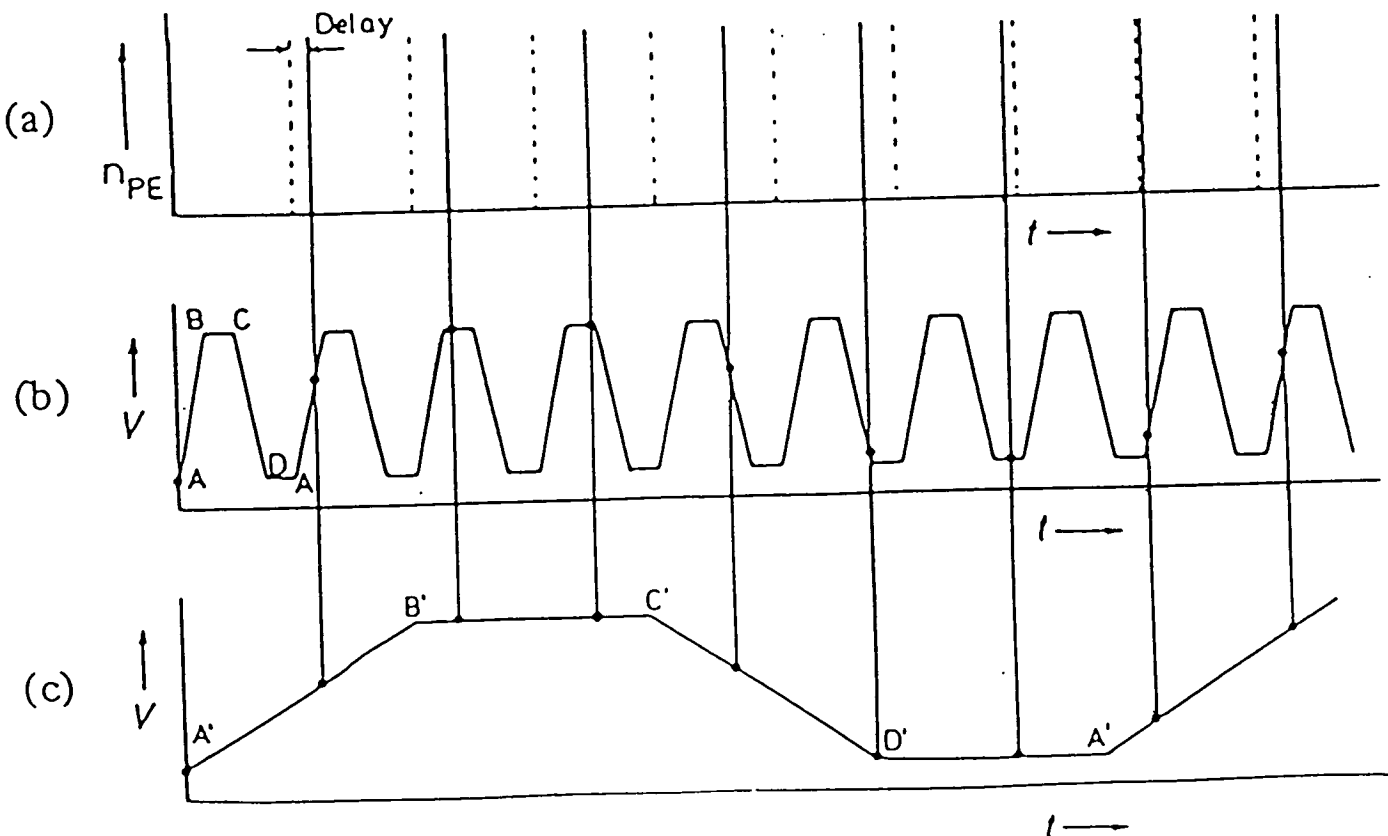
Figure 2.3 : The sampling technique.

so that it does not reach the specimen for the bulk of the time. At a well defined moment of time and for a certain length of time a pulse is fed to the plates, which allows the electron beam to penetrate down into the column and investigate the waveform of interest at the same point on each successive cycle.

A counter circuit may be used, to ensure the waveform of interest is investigated once in every two cycles or once in every eight cycles or whatever according to the frequency of the waveform and the maximum frequency allowed by the chopping plates, more details will be given in following Chapters.

2.3   SAMPLING   PRINCIPLE

"If a short time interval window is chosen from a repetitive waveform during every cycle of the waveform, this time is normally smaller than the period of the waveform, and the phase between time window and the waveform is constant. The resulting waveform is then a series of pulses which gives a d.c level proportional to the average waveform level during the window, if it is integrated" (from Hill(1974)).

The phase of the sampling pulse is changed in steps and the output d.c. level changes with respect to the waveform at each phase (see Figure 2.3). Therefore a trace of averaged signal value against phase is observed to be the same shape as the repetitive waveform. "The sampling repetition frequency must be equal to the specimen frequency, the phase between them is controlled to vary slowly with the time base of the display device; the actual waveform of the signal can be observed" (from Dinnis(1979)).

Most sampling circuitry depends on the basis of the conventional sampling oscilloscope as shown in Figure 2.4. More circuitry details will be given later. "In the sampling mode, the chopping pulse is moved continuously in time with respect to the waveform to be investigated, hence rather than sampling at the same point on successive cycles of the waveform, the movement of the sampling pulse causes the waveform to be sampled at a given number of intervals during its period, so that an overall picture of the complete period of the waveform is reconstructed.

One of the applications of this mode is that of monitoring the rise time of digital waveforms, here the sampling pulse is moved in time over only a fraction of the period of the waveform on successive periods" (from Gopinath and Hill (1974)).

" Both stroboscopic and sampling modes in the SEM allow analogue signals to be monitored as they progress through the functional blocks of an IC and allow observation of the propagation delays of logic signals as they progress through the circuit to be obtained " (from Gopinathan and Gopinath (1978)).

These modes are undoubtedly a great diagnostic and failure analysis tool in microcircuit engineering. The main difference between these modes is that the phase is changed manually in steps throughout the waveform in the stroboscopic mode while it is changed automatically in the sampling mode.

2.4 GENERAL REVIEW

Plows and Nixon (1968) were the first to report on stroboscopy in the SEM while varying the surface voltage distribution periodically. The voltage contrast image is "frozen" over the whole image surface at
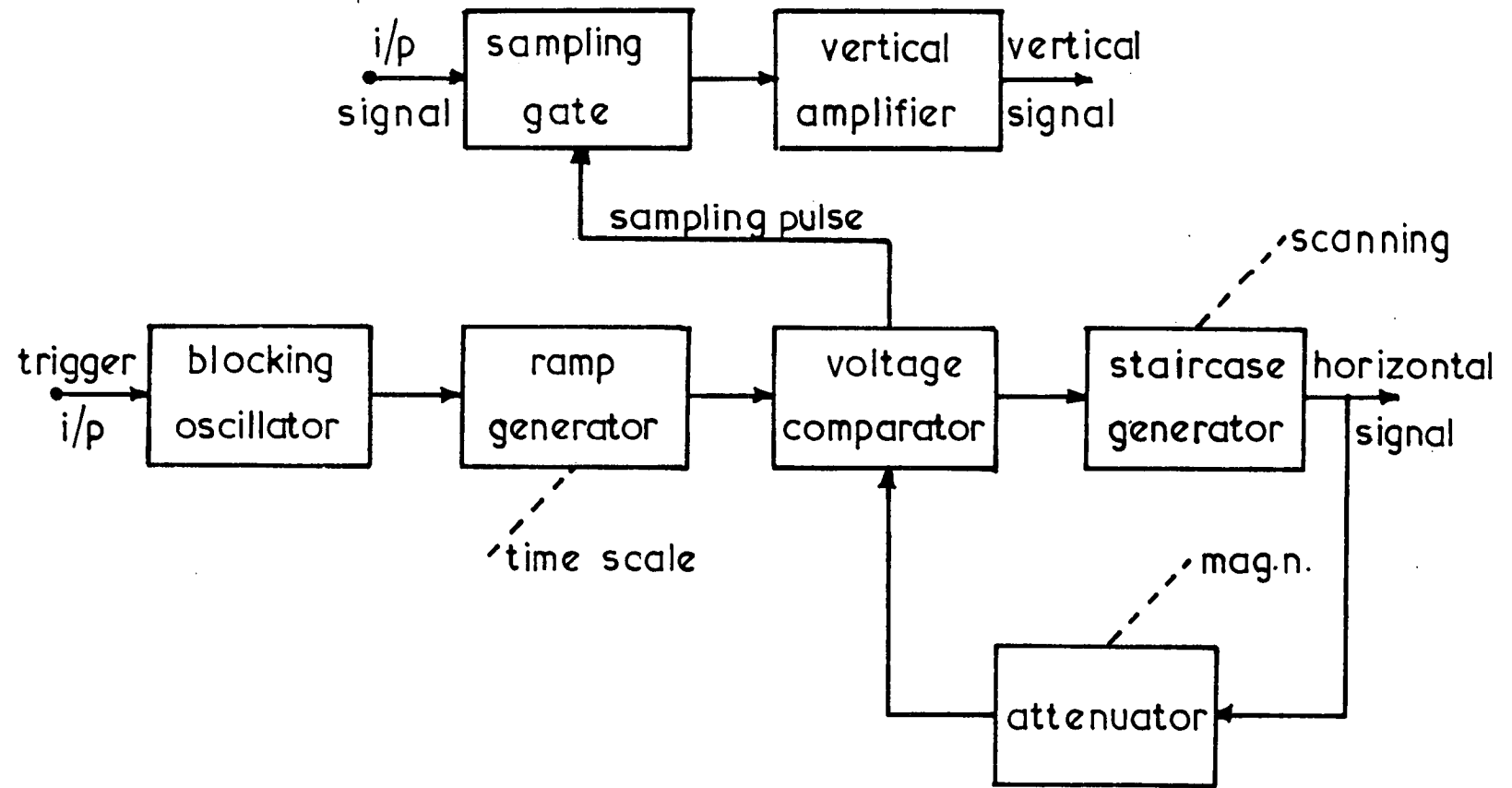
Figure 2.4: Shows block diagram of sampling oscilloscope (from Cooper 1978)

any chosen phase to give an easily interpreted picture of the distribution at that phase.

Robinson et al (1968) have reported a stroboscopic SEM mode using the Plows and Nixon principle to study and test the high field domains in a Gunn effect diode operating in the transit-time mode with time resolution of 20ns to record the sampled data; they used electrostatic plates to achieve subnanosecond transit time.

MacDonald et al (1969) have used a sampling oscilloscope to record the sampled data; they used electrostatic plate travelling wave deflection to provide short duration electron beam pulses. They used a computer to position the electron beam and to store topographical features. They also reported on degradation in spatial resolution with rapid chopping of the primary beam by a 57 MHz sine wave. The time resolution was determined only by the pulse shape and the width of the primary beam pulse at the surface of the specimen.

They described that the velocities of the deflection signal and electron beams should be the same when propagating through the deflection structure. They have mentioned that sampled data could be recorded on a sampling oscilloscope. They reported that with rapid deflection of the electron beam across an aperture, astigmatism in the primary beam at the target is possible, as well as degradation in spatial resolution as the blanking frequency increases.

Plows and Nixon (1971) have used the stroboscopic SEM to observe and test large scale integration (LSI) with repetitive pulses up to GHz for testing a 24-bit dynamic shift register, using both image and waveform modes. They mentioned that charging by the electron probe can affect the performance of some circuits, and they described the princi-

ple of the stroboscopic SEM image mode by pulsing the electron probe of the microscope in synchronisation with the fundamental of the periodic excitation appearing on the specimen surface. " As the electron probe scans the specimen surface, the electron pulses arrive at the same phase the "sampling phase", in succeeding cycles of the fundamental and in succeeding spatial positions along the scan raster (from Plows and Nixon(1971)).

They described the sampling technique in the waveform mode, the scan was stopped and the pulsed electron probe stationed at a point of interest on the specimen surface. " The sampling phase was then swept through the period of the specimen signal fundamental; this could be done manually or by phase modulation or by slight difference in frequency between specimen fundamental and sampling frequency. The collected electron current was then used not to form an image but to vertically deflect the cathode ray tube (C.R.T) spot in the oscilloscope, the horizontal C.R.T deflection was made proportional to the phase sweep and the stroboscopic SEM acted as a sampling oscilloscope "(from Plows and Nixon(1971)). The waveform could be shown by C.R.T or X-Y plotter.

They also mentioned that noise was visible on the stroboscopic waveform and the manual rather than automatic sweep led to a little shakiness in the stroboscopic waveform. The time resolution achieved was better than 0.01 ns. No computer monitoring in testing had been used so far and no details of electronic circuitry for performing stroboscopy in the SEM had been mentioned.

Robinson (1971) has reported stroboscopic SEM at GHz frequency, by pulsing the primary electron beam with travelling wave electro-static deflection plates with electron beam pulses of less than 200 ps duration, to study solid state devices. Astigmatism of the primary beam across an aperture, resulting in degradation of the spatial resolution

had been found. No electronic circuitry for stroboscopy was mentioned.

Szentesi (1972) has used stroboscopy in the electron mirror microscope at frequencies up to 100 MHz to study microcircuits under dynamic conditions and was the first to give some details of the electronic circuitry used to provide variable phase shift up to 66 MHz, with frequency range 30-70 MHz. This stroboscopy arrangement can be applied to other microscopes (see Figure 2.5).

Hill and Gopinath(1973), Gopinath and Hill(1974) have given a review of electron beam chopping systemson the SEM

as well as types of beam switches for developing micro wave devices; more details will be given in Chapter 3. No electronic circuit details were reported, but mainly they concentrated on the stroboscopic SEM setup, also mentioning the sampling mode by taking samples every nth cycle. They also reported about the problem of jitter in the timing of the pulses, considering phase instability as an important factor, but they have not discussedthe problem.

They developed techniques to sample the video signal by using an electronic gate, and using an R-C filter to remove high frequency noise and they suggested use of a slower line scan to improve S/N ratio by taking many scans along the same line, and averaging the values for each particular point on the line scan using a computer.

Fujioka et al (1980) have suggested the instrumentation for stroboscopic SEM as shown in Figure 2.6.

Gonzales andPowell (1975) have reported stroboscopic SEM employed to analyse high speed dynamic RAM (randomaccess memory) operations with 20 ns time resolution by making the SEM work as a sampling oscilloscope to display timing waveforms of MOS LSI devices (MCM6605); no electronic circuitry detail was mentioned.
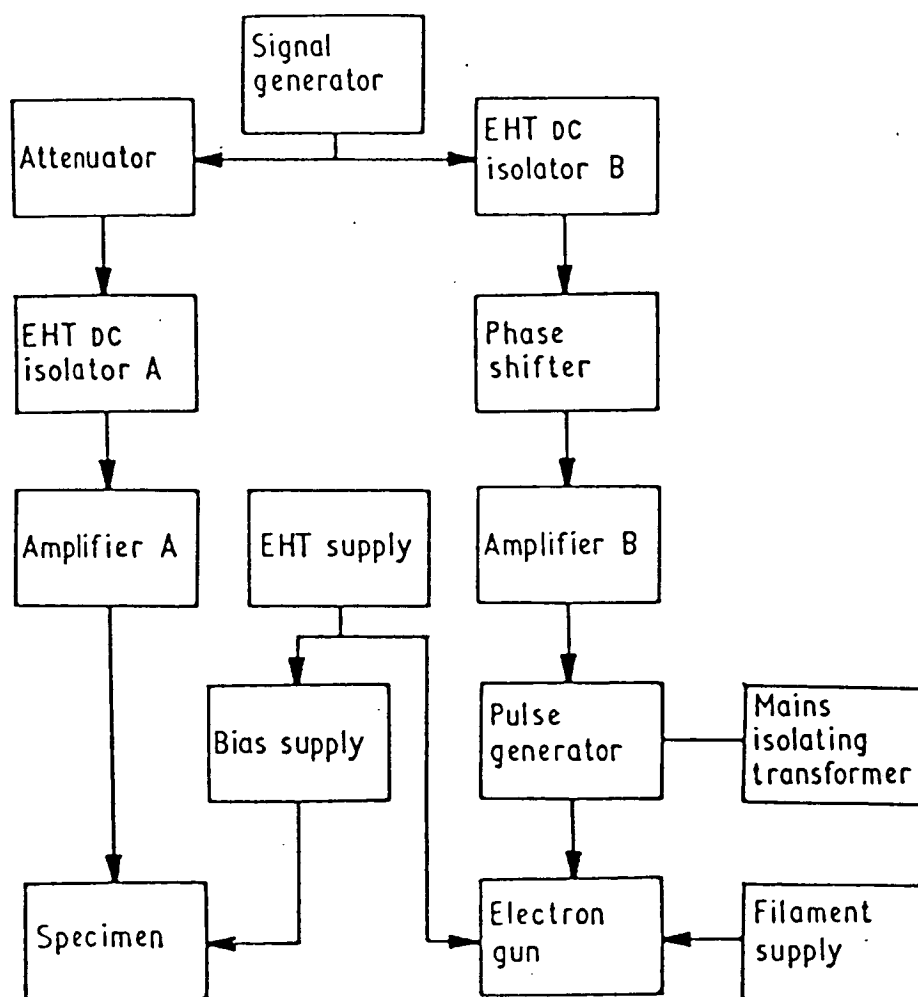
Figure 2.5: Simplified block diagram of the
electronics of the stroboscopic
electron mirror microscope.(from Szentesi 1972)
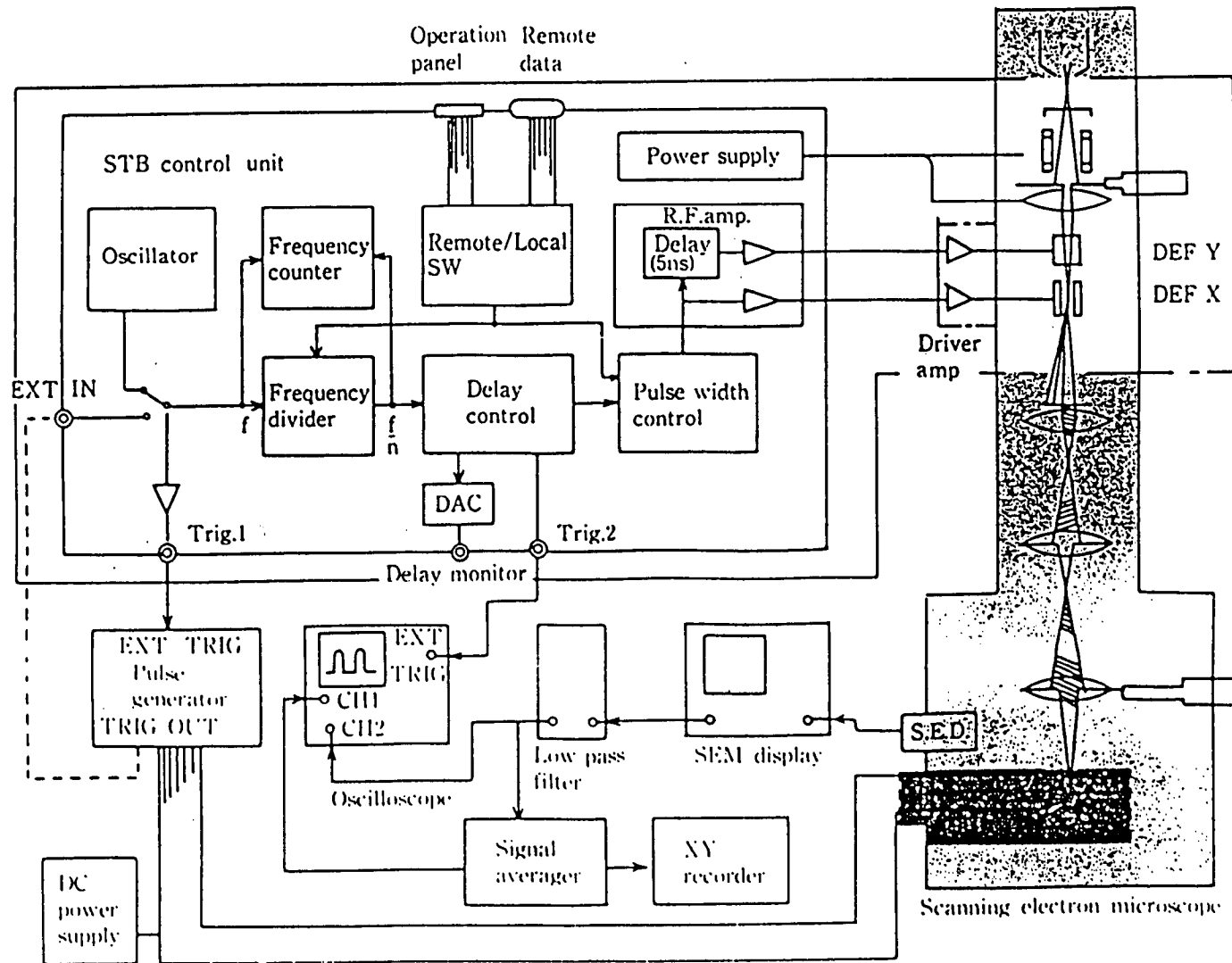
Figure 2.6 : Shows a block diagram of stroboscopic SEM produced by JEOL Ltd USA depending on Fujioka et al 1980)

Wolfgang et al (1976) have reported stroboscopic voltage contrast of MOS (RAM) by using a simple stroboscopic set up; no electronic circuitry was mentioned here either.

Thomas et al (1976) were the first who reported sampling techniques with analogue circuitry details, to display the oscillographs of high speed signals on devices in the SEM, mainly by interfacing the SEM with sampling circuitry on the lines of a sampling oscilloscope(see Figures 2.4, 2.7, and 2.8). The sampling circuitry operated up to a maximum frequency of 1 MHz, and the periodic signals at high frequency up to 18 GHz are sampled and measured at some sub-harmonic or below this 1 MHz frequency with beam sampling pulse width of 100 ps. A delay trigger pulse was produced by using fast and slow ramp generators(see Figure 2.8b).

Balk et al (1976) reported a set-up for stroboscopic and voltage measurement, to study a NAND gate with electron energy of 2keV with repetition rate of 350 KHz.

Gonzales and Powell (1975) have used the stroboscopic SEM to test RAM devices (MOS memories) with time resolution of 0.3 ns as a tool of failure analysis.

Ura et al (1977) have reported stroboscopic SEM to observe two-dimensional and dynamic potential distribution of semiconductor devices. They demonstrated blanking plates and alignment coils with a buncher for microwave frequency blanking with a complicated set up with no electronic circuitry details.

Hosokawa et al (1978) have developed GHz stroboscopy with the SEM
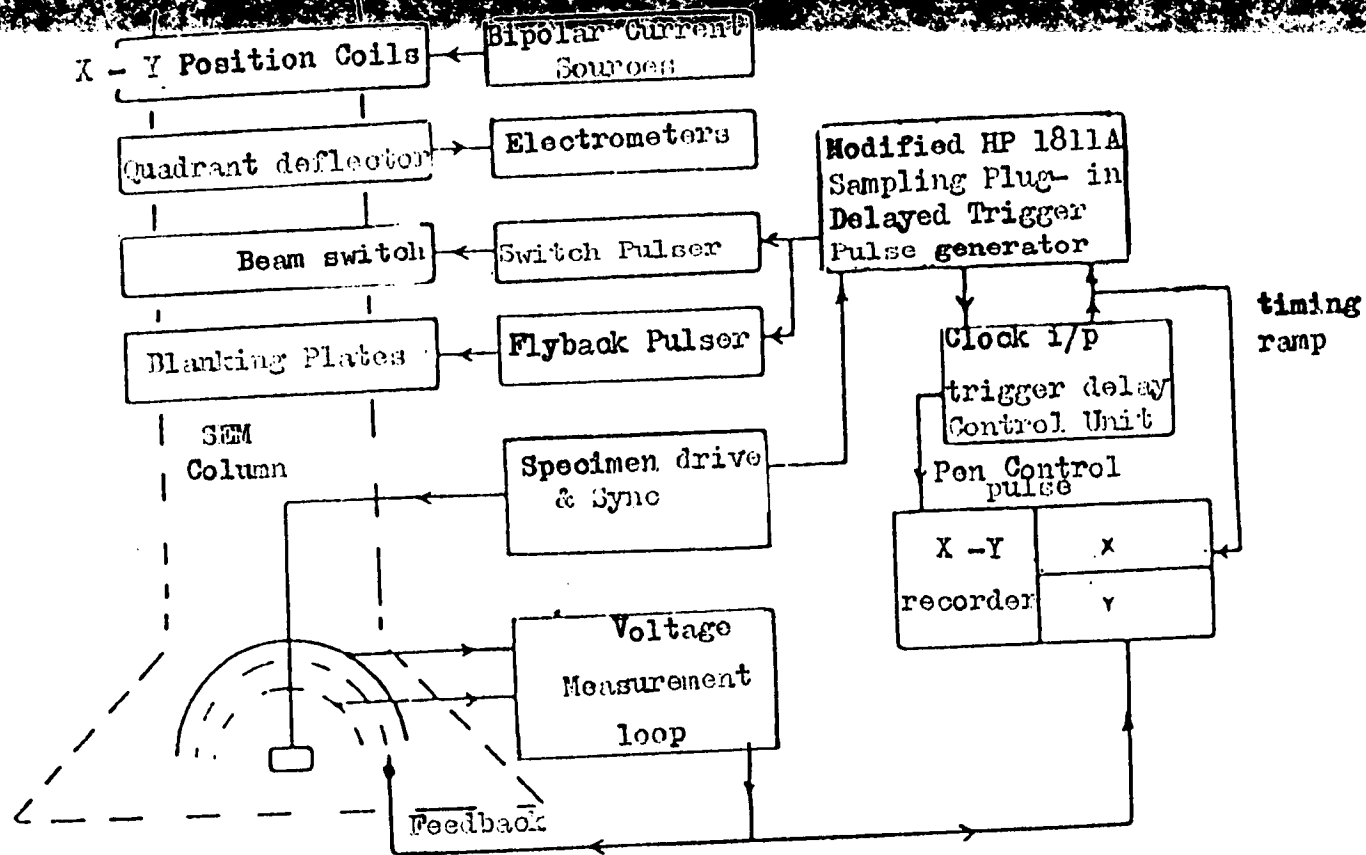
Figure 2.7: Complete system schematic. (from Thomas et al 1976).

(a)

sampled points

input signal

controlled trigger delays

trigger.
pulses
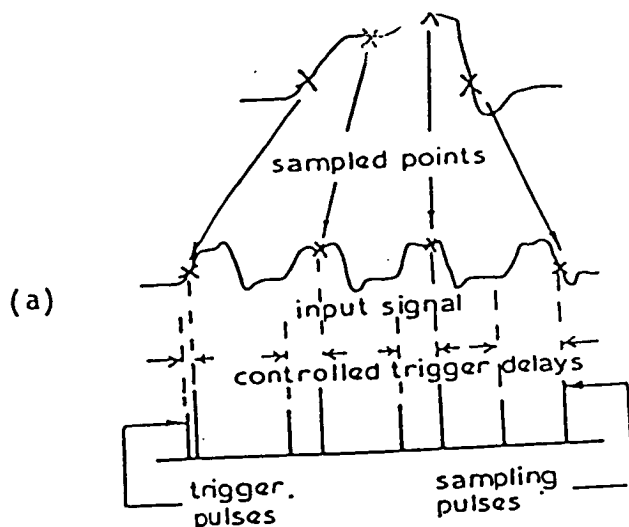
sampling
pulses

Figure 2.8: Illustration of conventional   (from   Thomas et al 1976).
sampling oscilloscope technique.

(b)

Bipolar
current
generators

Signal input
(periodic)

Schmitt
trigger

1 GHz
(max)

Trigger
circuit

Gate
latch

Hold-off
period

20 MHz (max)
synchronised

Timing-
ramp
generator

1 MHz
repetition

C_r

Time/division
attenuator

Precision
comparator

Digital
staircase
input

Strobe
driver

1 MHz (max)
delayed-
trigger output
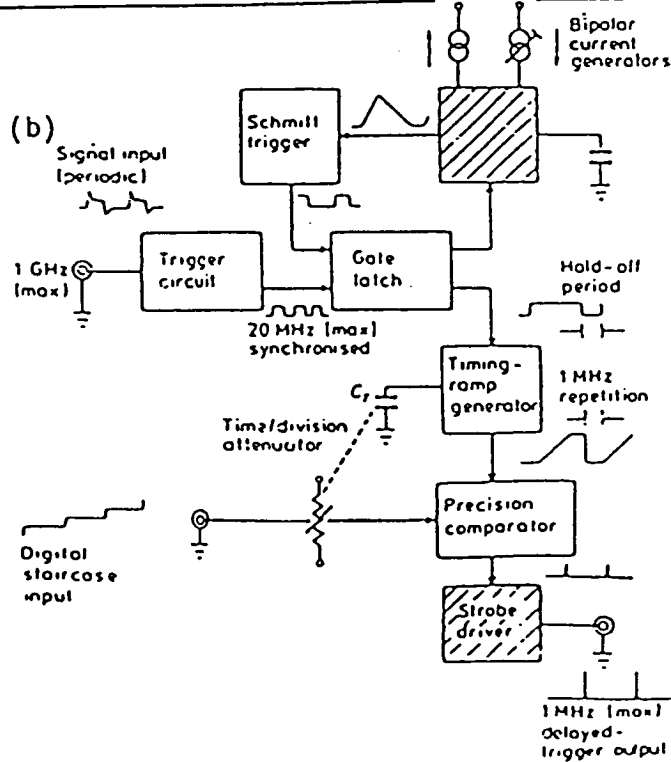
to test Gunn effect devices by using deflection and bunching modes; no excessive degradation of S/N ratio was achieved with a pulse operation device. Simple circuitry to show stroboscopy is mentioned. A microcomputer was developed to control the position of the electron beam, store output signals from the SEM, process the signals, and to generate data display, with time resolution of 7.6 ps.

Gopinathan and Gopinath (1978) have reported on a sampling SEM, to study high speed bipolar logic circuits (ECL devices) and to resolve the periodic voltage waveform at any point on the specimen. The electron beam is used as the sampling probe (see Figures 2.8 and 2.11), the waveform is sampled in successive periods with increasing phase or time-delay and the displayed values plotted against time delay; more details are given in following Chapters . The technique of modifying the time base circuitry of a sampling oscilloscope type of (HP1181) will be discussed.

Fujioka et al (1978) have used a microcomputer controlled stroboscopic SEM and developed a technique to observe signal waveforms at a frequency of 14.3 MHz with a time resolution of 0.2ns and voltage resolution of 50 mV.

Masuda et al (1979) reported using a stroboscopic SEM to study planar Gunn diodes with 1 GHz pulsed electron beam.

Wolfgang et al (1979) have used the stroboscopic voltage contrast mode, to study failure analysis of word-line defect of 4-K bit MOS RAM, dynamic memory devices, 16K bit memory HYB4116, and microprocessor (4 bit microprocessor) with both demonstration of hardware and software techniques·

Feuerbaum (1979) has developed the sampling mode to observe
waveforms in the MHz frequency range to study 64K MOS RAM with 2.5 keV ac-
celerating energy(see Figures 2.10 & 2.12).
Hill(1974) has reported on SEM stroboscopy types as shown in Figure 2.9.

Menzel and Kubalek (1979) have used stroboscopic voltage contrast
to study VLSI (very large scale integration) circuits, they used a modi-
fied SEM (S180 Cambridge Instruments) with short deflection plates, us-
ing an additional magnetic lens to control electron beam focusing
through the SEM column when blanking at high speed.

Dinnis (1979) has reported on demonstration of stroboscopic and
sampling SEM, see Figure 2.13, to measure high frequency signal voltage
contrast in the SEM, depending on Plows and Nixons' principle by chop-
ping the electron beam at high frequency related to the frequency of
the signal on the circuit. The actual waveform of the signal can be ob-
served as shown in Figure 2.14. He has mentioned that this process is
identical to that employed in sampling oscilloscope. No electronic cir-
cuitry is suggested.

Fujioka et al (1980) have developed a stroboscopic SEM for func-
tional testing of bipolar ICs and LSIs with time resolution of sub-
nanoseconds. A microcomputer was used to control the SEM for internal
circuit operation testing with 1024 bit programmable read only memory
(PROM) in the MHz region. They improved the S/N ratio by higher primary
beam current and longer recording time. They mentioned the beam current
fluctuations due to contamination of the internal surfaces of the elec-
tron column.

Obyden, et al (1980) have reported a new principle of forming
stroboscopy images in real time in a colour SEM, for viewing phases of
luminescence and its correlation with the topographic features of the

Figure 2.9: A periodic event sampled synchronously
and types of stroboscopic SEM.
(from Hill PhD Thesis 1974)
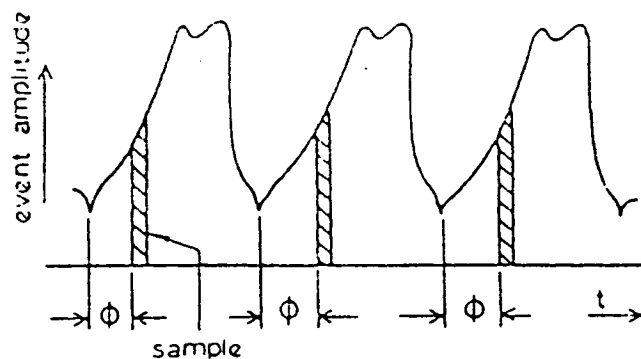
- a -
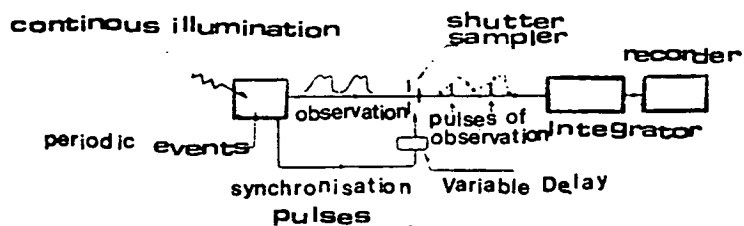
- b -
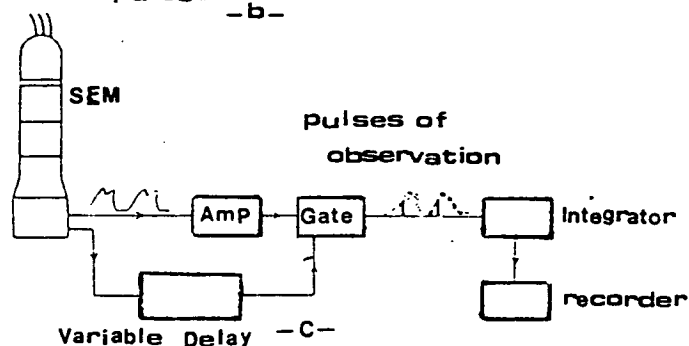
- c -
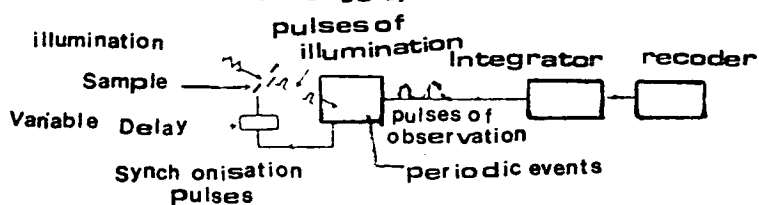
- d -
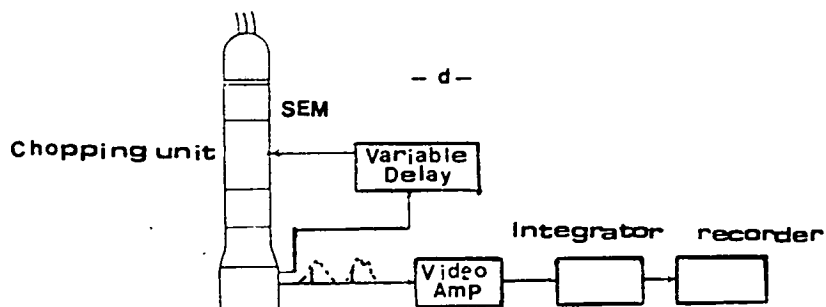
a sampled observation visual stroboscope.
b gated video signal SEM stroboscope.
c pulsed illumination visual stroboscope.
d pulsed beam SEM stroboscope.
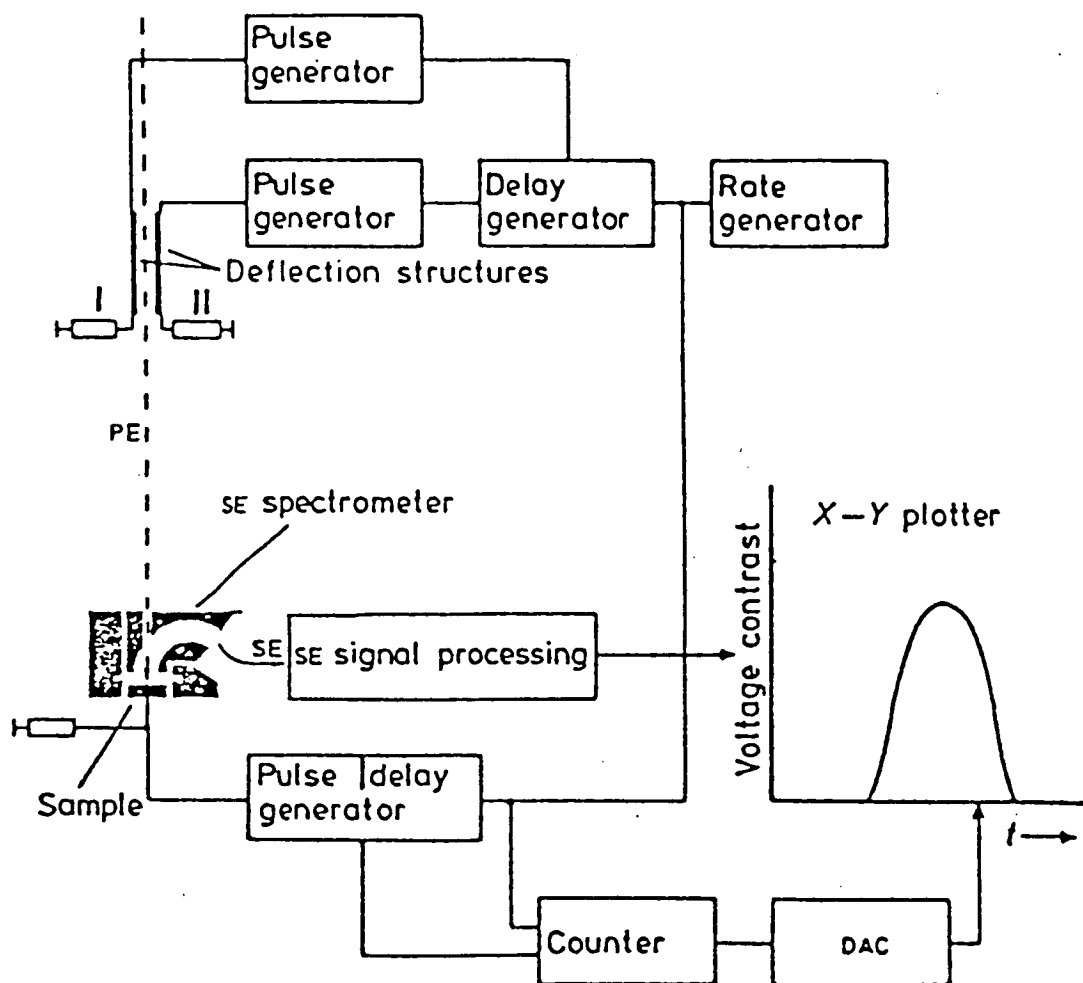
Figure 2.10: Experimental set-up. (from Feuerbaum 1979)
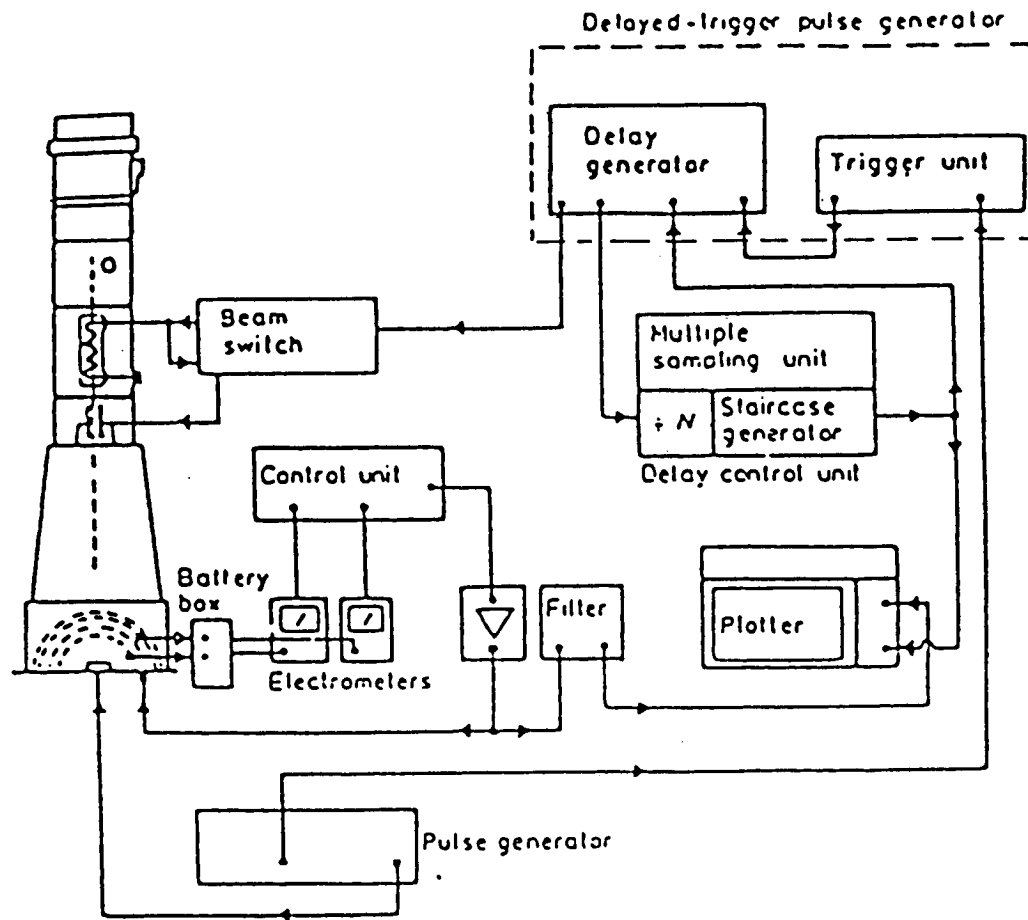
Figure 2.11: Sampling SEM set-up. (from Gopinathan and Gopinath 1978)

Figure 2.12: Schematic experimental set-up for measuring waveforms using the sampling mode. (From Feuerbaum 1979).
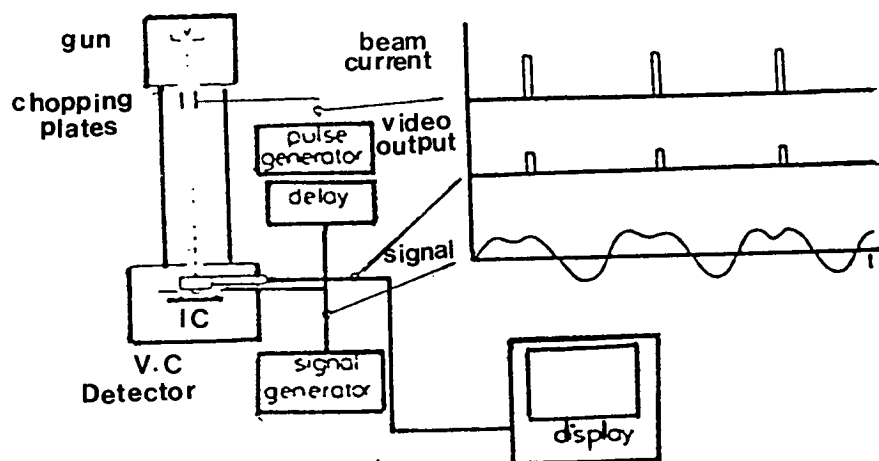
Figure 2.13 Stroboscopic mode voltage contra
(from Dinnis 1979)
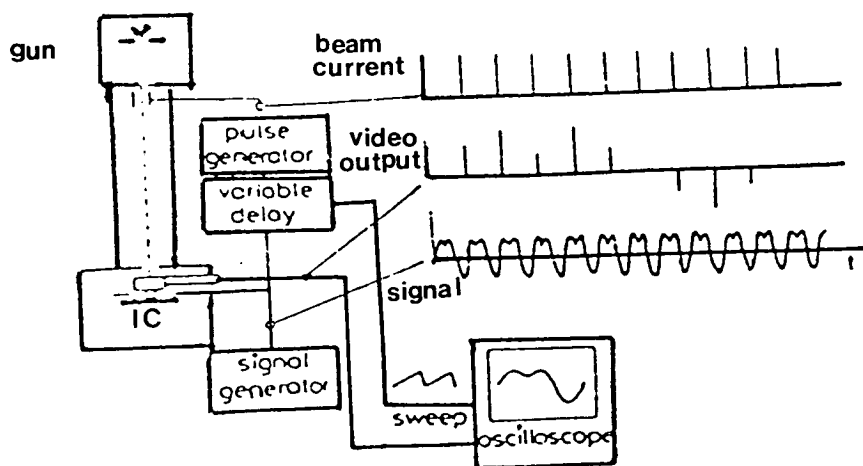
Figure 2.14 : Sampling mode voltage contras
(from Dinnis 1979)

SEM COLUMN **SYNCHRONIZING CIRCUITRY** **MICROCOMPUTL**
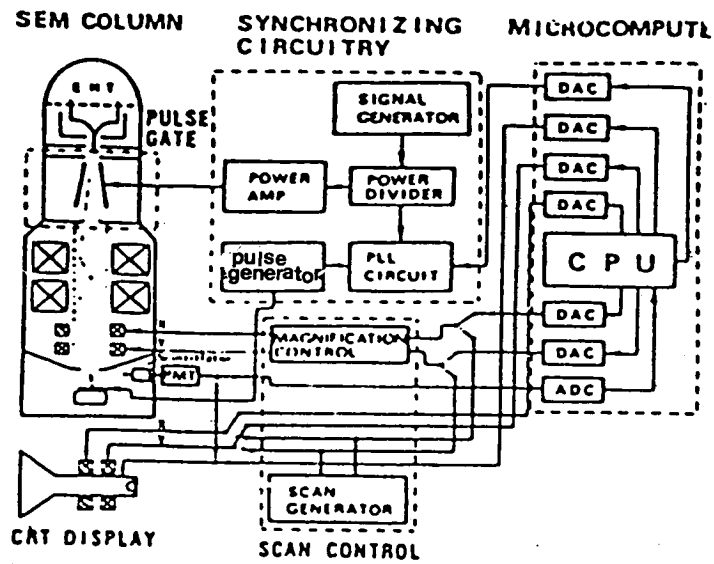
Block diagram of the stroboscopic SEM.
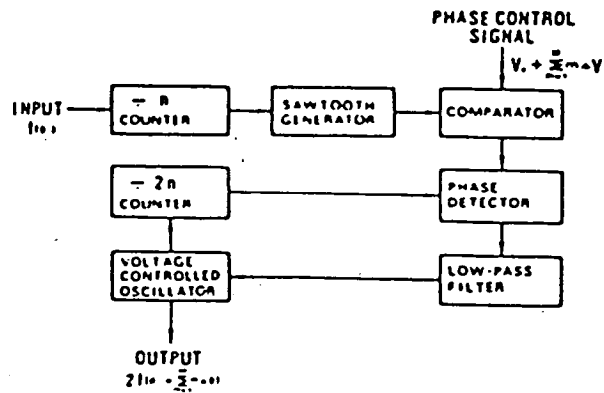
Figure 2.15: Block diagram of the PLL circuit.
(from Fujioka et al 1980)

object, with a new SEM mode colour Y-modulation which makes it possible to estimate the intensity of cathodo-luminescence and chromaticity at a point. This technique was used to study a ZnS crystal. They have reported the principle of stroboscopic transformation of the signal, as well as colour Y-modulation; with condition that the repetition frequencies of the electron beam and strobing pulses are equal to the horizontal sweep frequency, for formation of vertical row of stroboscopic pixel. This technique was used to obtain a real time colour display up to 10 ms. The SEM collector developed for this work used three photomultipliers for three primary colour of RGB.

They reported using strobing pulse of 200 ns in length, at reptition frequency of 15 kHz, with exciting pulse length of 5 µs, the electron beam energy of 20 kev. This principle is some what complicated in comparison to Dinnis principle as is mentioned below.

Rau, et al (1980) have reported colour encoding of video signals in the SEM.

Crewe (1980) reported colour conversion in electron microscopy, to show colour TV image formation, using a modified colour TV receiver to display RGB signals.

Dinnis (1980) has reported colour display of voltage contrast in the SEM, described a colour stroboscopy set up and was the first to show the basic principle as :" particular digital pulse is chosen to correspond with a given colour, then the appropriate gun in the display tube is switched in synchronism with the pulse so all conductors carrying that particular repetitive pulse will be readily identified " from Dinnis(1980)). More details will be discussed in Chapter Six.

Fujioka et al (1981) have reported using combined stroboscopic SEM - Microprocessor Systems for functional testing of bipolar and MOS LSI circuits. The microcomputer is interfaced to the SEM for sampling and storing the signal waveforms, performing an operation of signal processing and generating a data display or data output in numerics. They show some software used for sampling waveforms, they tested a 8085A microprocessor chip with passivation layer with accelerating voltage of 1 keV by image mode, waveform and logic state mapping modes. They have mentioned that passivated MOS devices can be inspected as well as non-passivated ones by using an electron probe with low accelerating voltage (see Figure 2.16).

Ranasinghe and Proctor (to be published) have demonstrated electronic circuitry to produce delay by using a fast speed(ECL) monostable multivibrator as a delay unit on the lines of a sampling oscilloscope; to show waveforms on test at 2 MHz frequency and to study the ring oscillator (see Figure 2.17).

Fazekas et al (1982) have reported a sampling SEM (see Figures 2.18, 2.19 and 2.20) to show logic-state mapping as one of the methods of waveform measurement in the SEM. In electron probe sampling short primary electron pulses take over the function of the electronic time window; the beam pulses are generated by a blanking capacitor which is driven by the timing unit and pulses the beam in such a way that it strikes the measurement point only in a defined phase of the applied signal. This set up was used to study a 4K by 1 bit ECL memory, also a 64K MOS RAM with voltage resolution of 10 to 20 mV. They submitted a logic state mapping for an 8085 microprocessor, 2.5 keV was used as accelerating voltage.
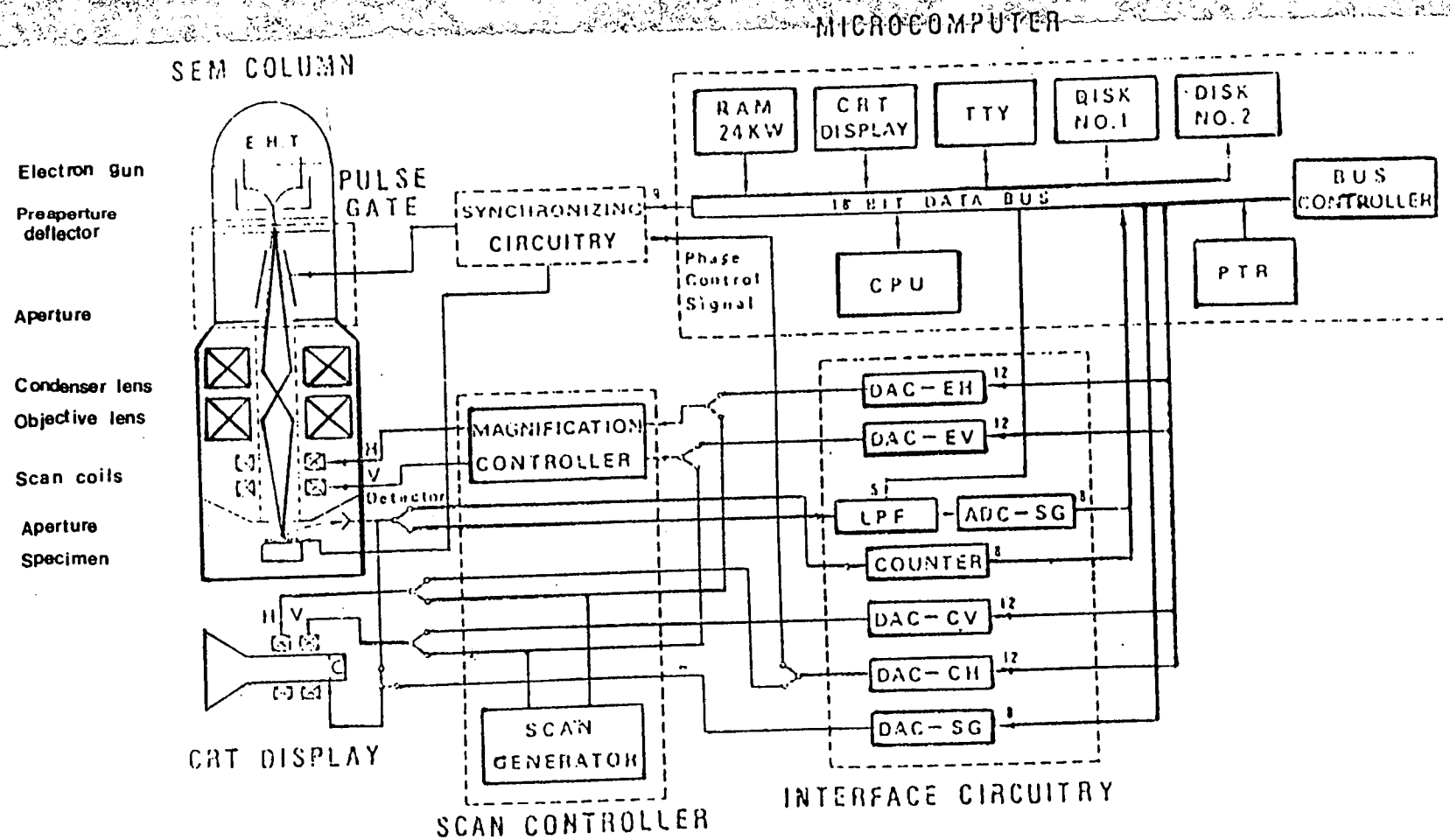
Figure 2.16.: Block diagram of SEM microcomputer test system.
(from Fujioka et al 1981)
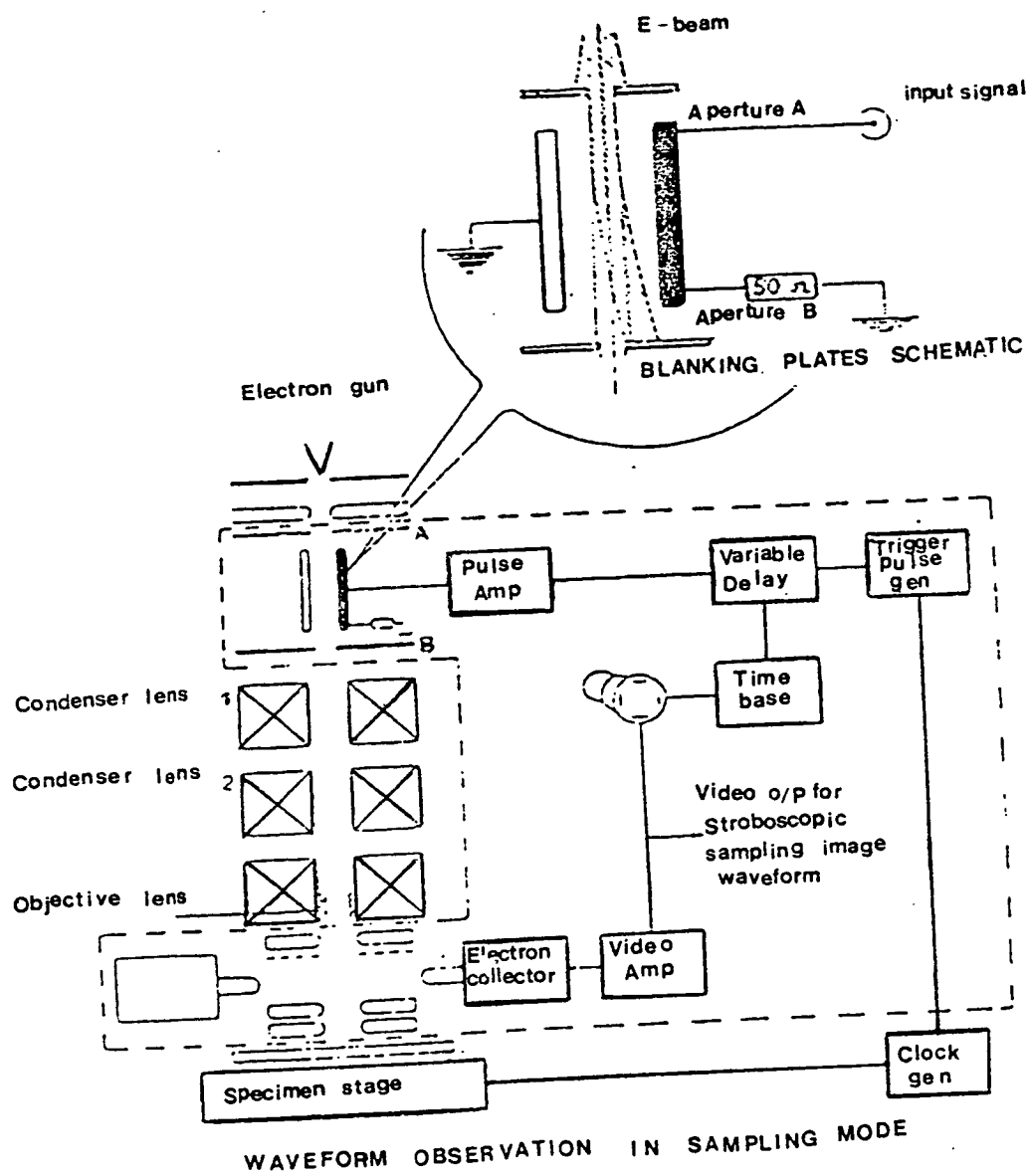
Figure 2.17 : The overall system for examining the dynamic operation of integrated circuits. (from Ranasingh and Proctor to be published)

ELECTRON GUN

BLANKING CAPACITOR

PRIMARY ELECTRON BEAM

TIMING UNIT

LENSES

SCAN COILS

SECONDARY ELECTRONS

COLLECTOR

INTEGRATED-CIRCUIT DRIVE UNIT

MICROSCOPE'S SIGNAL PROCESSING AND DISPLAY ELECTRONICS

INTEGRATED CIRCUIT UNDER TEST

SPECIMEN CHAMBER

X,Y STAGE
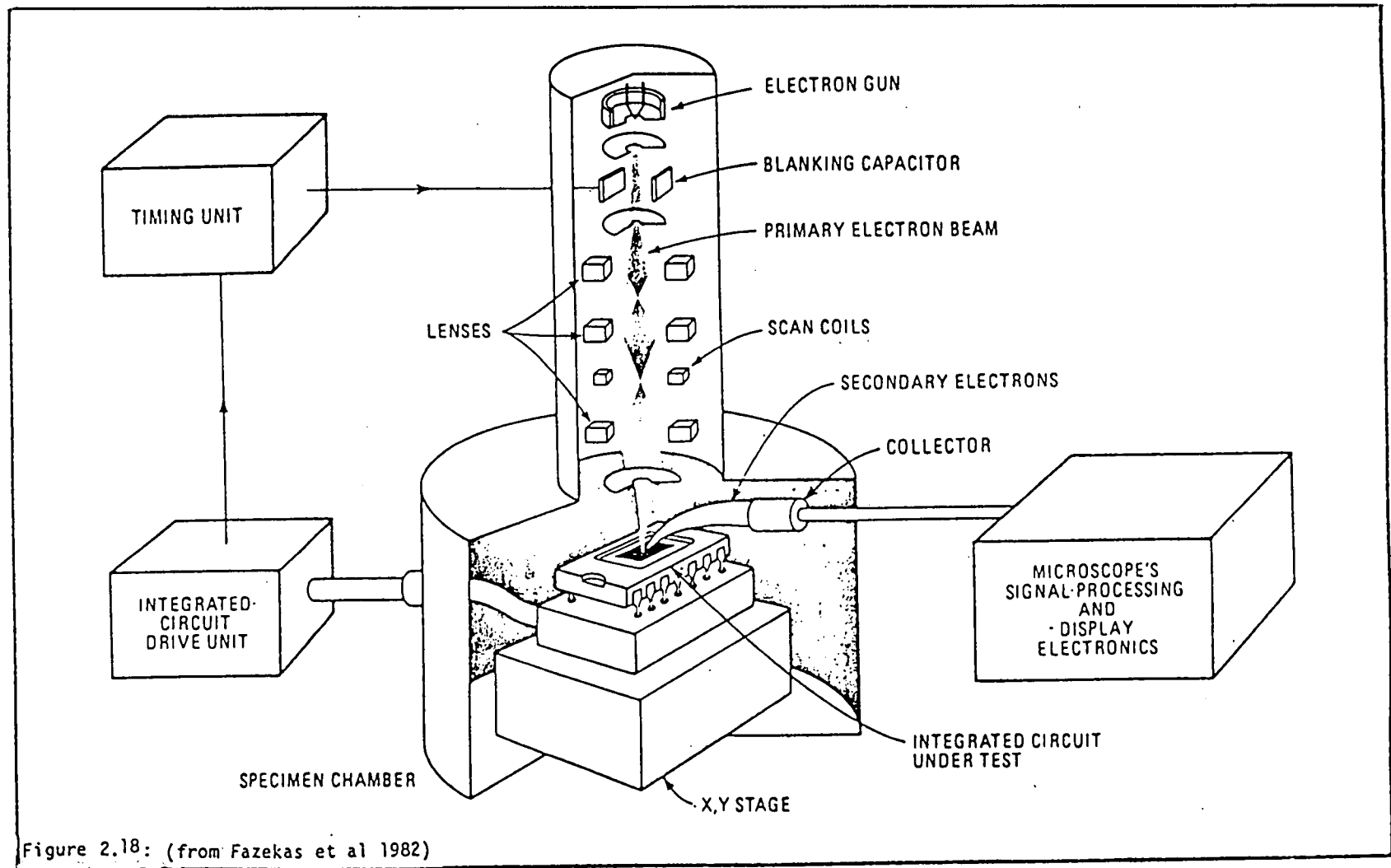
Figure 2.18: (from Fazekas et al 1982)

Electron-beam probing. A packaged IC without a lid is put in a sampling electron microscope's specimen chamber. A pulsed beam of electrons is focused on a point on the IC, and the resulting secondary electrons are collected and displayed on a CRT or logic analyzer.
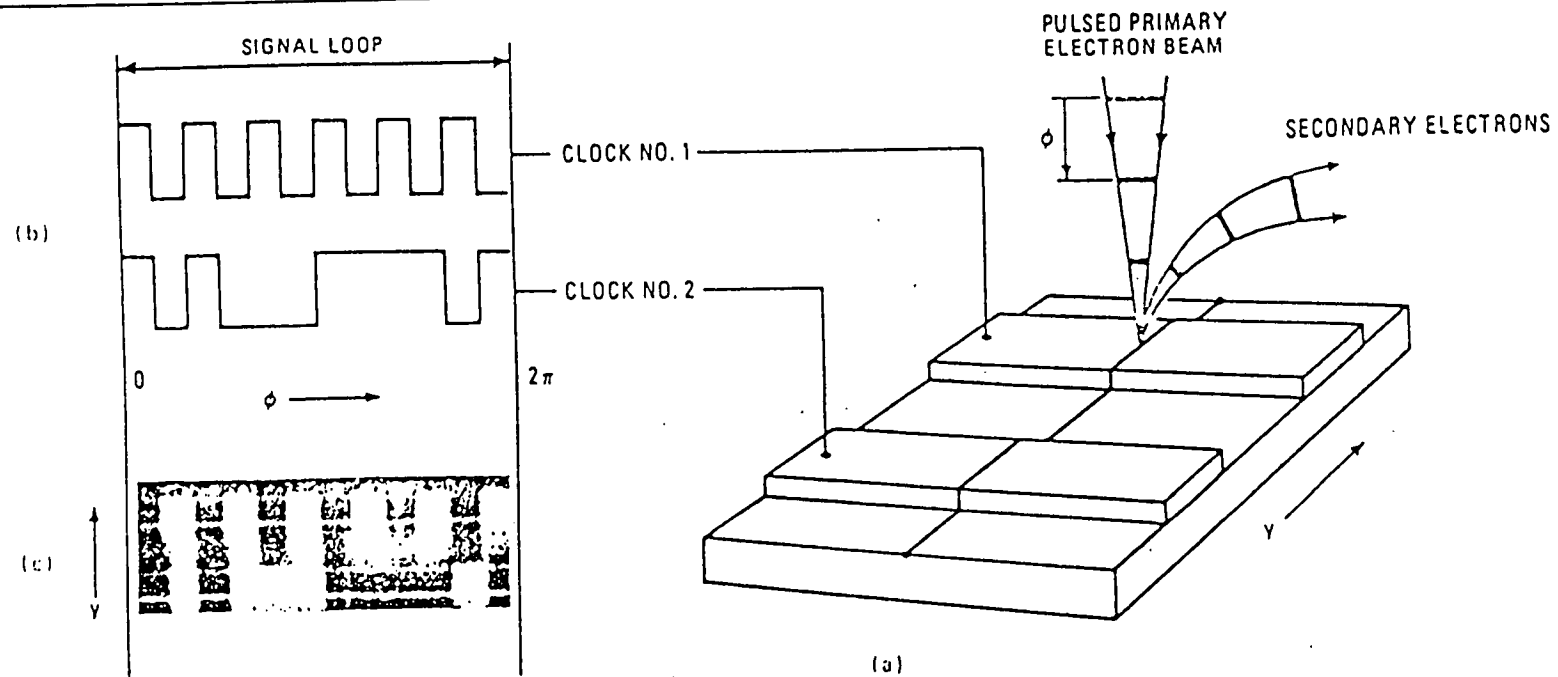
Figure 2.19: (from Fazekas et al 1982)

Logically mapped. In logic-state mapping, the primary electron beam scans a line (a). After each scan, the phase is shifted. The clock signals are shown in (b). A logic state mapping of the loop is shown in (c), where dark bars are logic 1s and light bars are logic 0s.

SIGNAL LOOP

(b)

CLOCK NO. 1

CLOCK NO. 2

0          $\phi \longrightarrow$ 2π

E

PULSED PRIMARY
ELECTRON BEAM

SECONDARY ELECTRONS
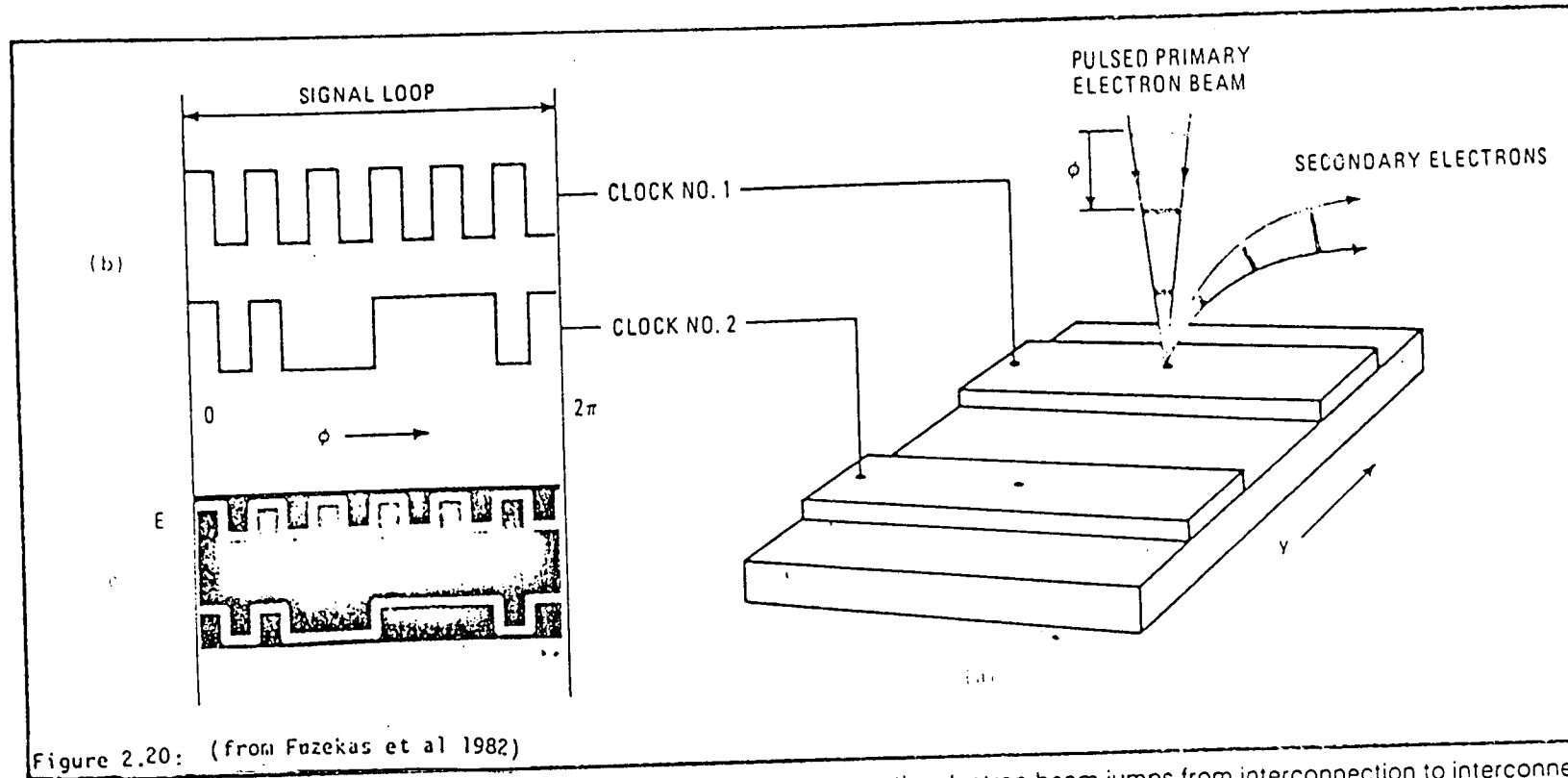
Figure 2.20: (from Fazekas et al 1982)

Timing diagram. In the course of generating a logic-state timing diagram, the electron beam jumps from interconnection to interconne
(a). Applied clock signals are displayed at left in (b), and (c) represents scanned data as it is displayed on a logic analyzer.

Ura et al[*] have reported stroboscopic observations of passivated microprocessor chips in the SEM, by using another stroboscopic mode of operation, the phase-stepping image mode. This gives both spatial and temporal information at once on a single voltage contrast image. They have also mentioned that the time properties on the passivated microprocessor are found to agree well with that on the non-passivated chip. They developed a new synchronising circuitry for the stroboscopic SEM system, which was described in previous papers, but had been modified as shown in Figures 2.21 and 2.22, so as to observe a 8085 microprocessor in the phase-stepping image mode. " Generation of electron beam pulses is realised by the double deflection method, the repetition rate of the generated beam pulse applied to the Y deflector, while the pulse width is determined by X deflection as shown in Figure 2.23. Applying a voltage sine wave with a frequency of f/4 (f; the external clock of 8085A) to the X deflector results in the beam pulse with repetition rate of f/2. Then, the application of a voltage pulse with a frequency of f/2N to the Y deflector which is set perpendicularly to the X deflector enables it to generate the beam pulse whose repetition rate is f/2N. The synchronising circuitry controlled by a microcomputer has a phase shifter which allows two stepping modes of time stepping (mode A) (see Figure 2.21) and coarse stepping (mode B). Mode A allows setting up the sampling phase, in 100 steps with a stepping width of 5 nS, from 0 to 495 nS, while mode B, in N steps with stepping width of 2/f from 0 to 2(N - 1)/f. The number N is programmable in 48 steps from 2 to 49 " (from Ura et al[*]).

* N.B : To be published.
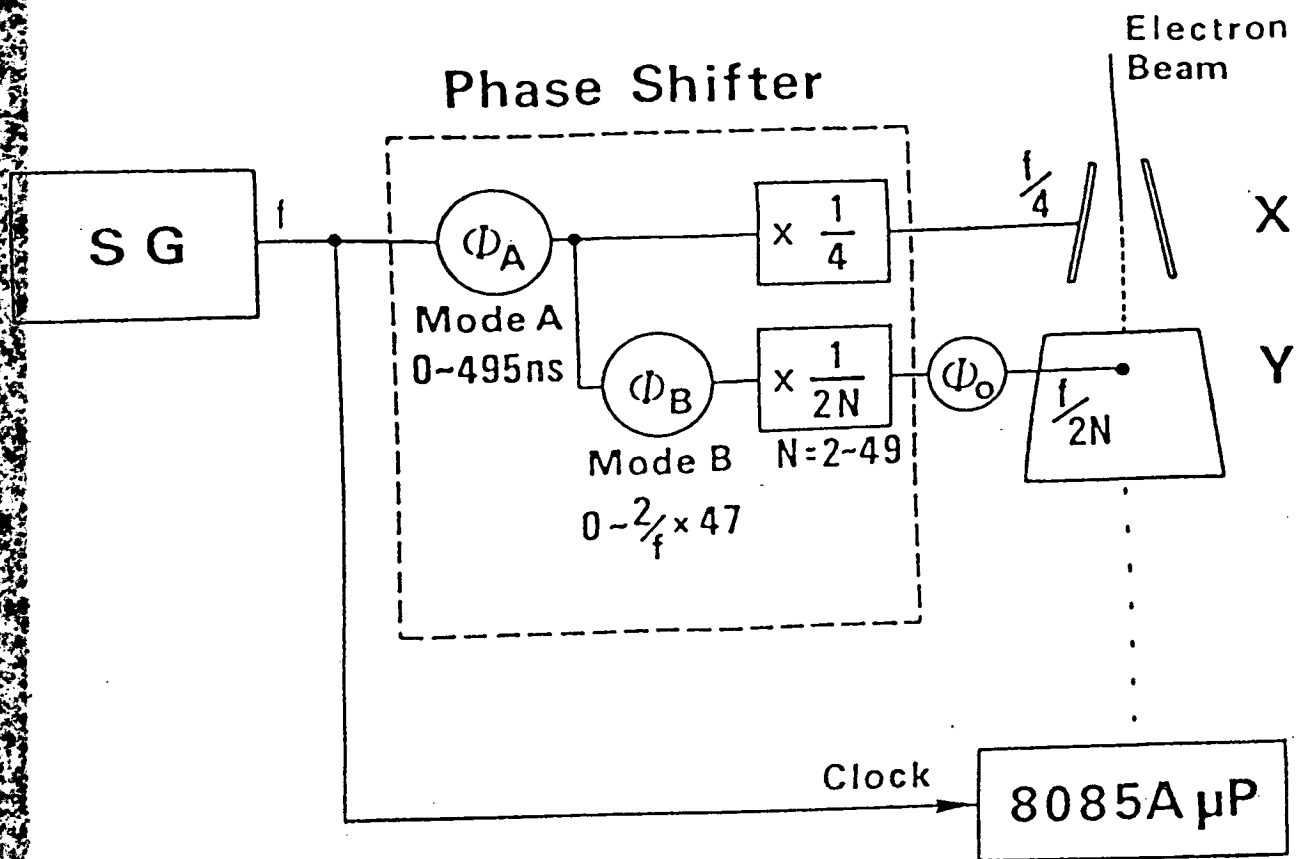
Figure 2.21: Shows synchronizing circuitry of the stroboscopic SEM
(from Ura et al to be published).

Figure 2.22: Shows technique of determining the beam pulse
width (from Ura et al).
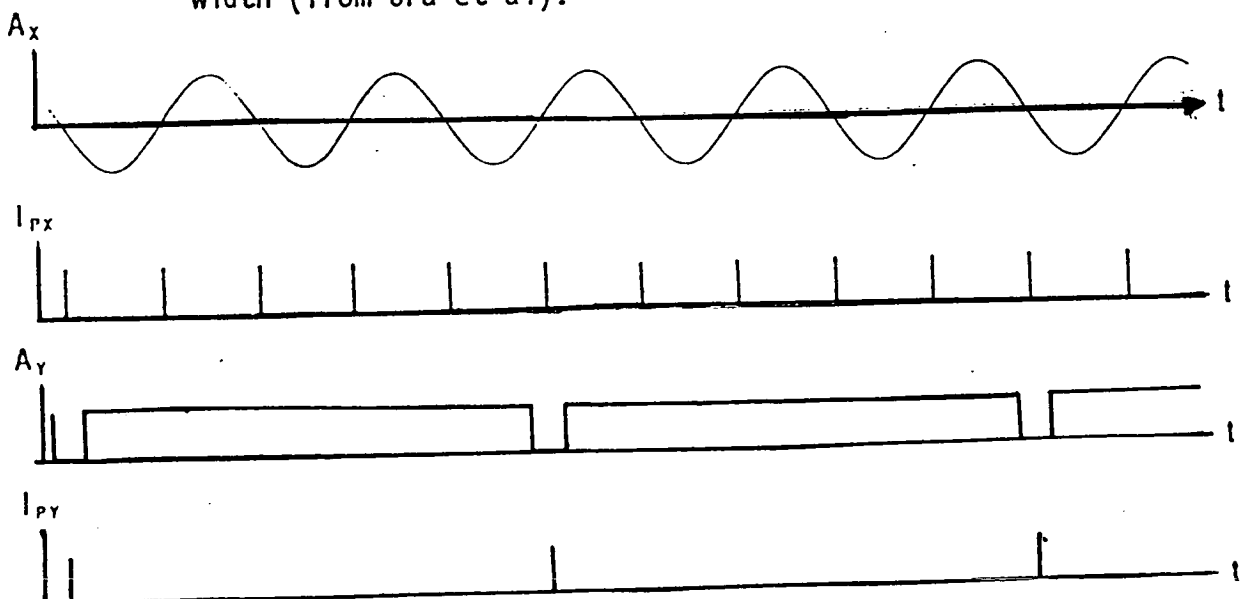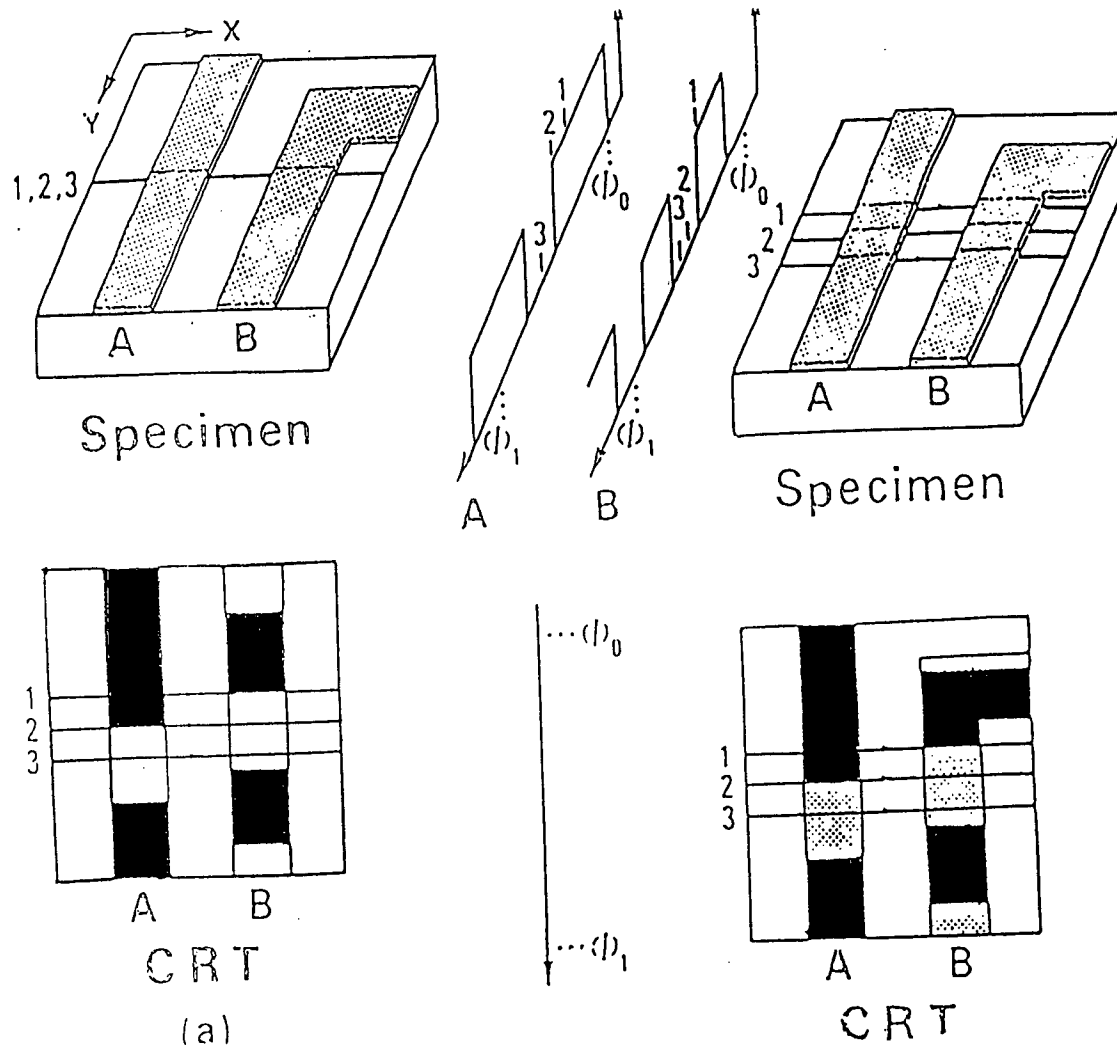
Figure 2.23: Shows phase-stepping image mode (from Ura et al to be published).

CHAPTER THREE

ELECTRON BEAM SWITCH

3.1 INTRODUCTION

This chapter mainly deals with the development of a beam chopping system in the SEM; also included are: definitions, basic principles of chopping techniques, beam switch review, present work problems, chopping system performance, and a discussion section. Since the deflection chopping scheme is the most widely used among chopping systems and is very simple to implement, it is covered in this chapter.

Switching of the electron beam is entirely based on deflection of the primary electron beam by an electrostatic chopping assembly. This is made of simple capacitor plates which have a beam transit time limitation. Two types of deflecting plates were fitted and developed in the SEM column of an S2 Cambridge machine.

MOS devices are more sensitive to electron beam damage than bipolar devices. To minimise the damage, low primary electron beam energies are used (less than 2.5 kev) and the beam is only turned on when essential.

3.2 DEFINITIONS

3.2.1 Deflection Angle

The electron beam is assumed to be filamentary and non-

relativistic. The deflection angle is defined as the angle between the final deflected beam and the original beam direction. The transverse velocity of the electron beam is not more than 1% of the longitudinal velocity, therefore deflection defocusing is neglected.

Gopinath and Hill (1974) have discussed the deflection ray and assumed the moving of the source in the deflection to a new position, which is the intersection of this ray with the column axis; since the deflection angle is small, this movement may be assumed to be along the source plane. Beam cut-off occurs when it is deflected beyond the edge of a centrally placed chopping aperture. The beam pulse width is determined by the time taken for the beam to reach the aperture edge.

3.2.2 Deflection Sensitivity

The electron beam passes through a gap between two parallel plates across which a suitable voltage is applied hence a transverse velocity is added to the electrons causing a parabolic trajectory between the plates. The deflection action of the plates can be understood by assuming the deflection to be at the mid plane of the plates. When the beam is deflected beyond the edge of the aperture, it is switched off at the specimen, this mainly depends on many factors, the plate length, the gap between plates, the electron beam accelerating energy, and the potential difference across plates.

3.2.3 Degrad ation

The degrad ation of the electron beam spot size, caused by the chopping action results in a reduction of spatial resolution and should

therefore be minimised so as to allow its compensation by the astigmatism control in the SEM. " The degrad ation occurs because the electron beam is deflected away from the electron optical axis of the SEM and the electrons appear to originate from a crossover which is not positioned on the electron optical axis. This movement with rising deflection voltage causes an enlargement of the effective electron beam probe at high frequency(from Gopinath and Hill (1974)).

Menzel and Kubalek (1979) have reported the degrad ation for a deflection system between the gun and first lens. The degrad ation ratio D is given by :

$$D = \frac{2.f + d_g}{d_g} \qquad (3.1)$$

where d_g is the cross over diameter, f is the apparent movement of the cross over in its plane. This only influences the final beam spot size if it occurs within the field ofviewwhich is determined by the diameter of the first aperture and final aperture image above the first lens . All electrons within the field of view that pass through the FAI (Final Aperture Image) reach the specimen.

The movement of the crossover is coupled with the movement of the first aperture so that the field of view (determined by this aperture), also moves with the deflection. For a beam cut-off it is necessary to move the crossover out of this moving field of view, which equals a deflection of the external electron rays of the beam. Degrad ation of the probe-forming spot is kept to a minimum by selection of an appropriate lens current (Gopinath and Hill (1977)).

3.2.4 Transit Time

This is the time required for electrons to pass through the chopping plates. The deflection plates length is limited by consideration of this transit time; higher transit angles are inefficient and also produce lateral displacement of the beam. If the transit time is smaller than the pulse rise time, the beam deflection time is determined by the transit time of the electrons through the deflection structure.

3.2.5 Final Aperture Image (FAI)

The central aperture in the final lens may be assumed to be at one of its principle planes. An electron passing through the FAI aperture reaches the specimen, but if it is obstructed by this image aperture then, although it may travel down the column to the actual final aperture, it will not reach the specimen. " If all lens parameters are known, the size and position of these FAIs can be determined, their position may be approximately estimated by neglecting the effect of the final lens field and thin lens optics. The second and first lenses progressively demagnify the size of the final aperture image which may be used as the accurately aligned chopping aperture for the deflection-chopping system"(from Gopinath and Hill(1977)).

The reason for using FAI apertures instead of mechanical ones is that most deflection-chopping systems use an image aperture more by default than by design because these images are in general very small in diameter. A mechanical aperture needs to be very small, of the order of 10 μm diameter or less; it also requires to be accurately aligned with consequent complexity in the mechanical design for precision adjustments. Thus it is simpler in most situations to use the image aperture.

Gopinath and Hill (1976) have reported that burn marks on the chopping plates structure charge up intermittently, causing difficulty in alignment and repeatability. The maximum deflection depends on the dimensions of the deflection structure.

Lin and Bauchamp (1973) have suggested placing the crossover at the centre of the chopping line, so no movement of the crossover occurred during chopping. The beam diverged through half the structure, and the deflection angle of the extremal ray defined by the top aperture is easily estimated.

Gopinath and Hill(1976), Menzel and Kubalek(1979) have developed an extra lens in SEM column for their chopping systems. If this system is fitted between first and second lenses this may result in poor demagnification of the focussed electron beam. This extra lens has its focus at the gun crossover; since the crossover is finite the beam is slightly diverging.

3.2.6 Pulse Width And Beam Current

The average beam current Ip is given by the product of the d.c beam current Id, the beam pulse width (T) , and the pulse repetition rate when(n)pulses are produced per deflection cycle f. Ip is given by:

$$Ip= n.f.T .Id \qquad (3.2)$$

(from Fujioka and Ura(1983))

This relation shows that the pulse width in the nanosecond region can be simply estimated by measuring the ratio of chopped to unchopped beam current. This method is not a precise way to measure the electron beam pulse width ,due to the fact that a primary electron beam current flows in

the pauses between pulses(Feuerbaum and Otto (1982)),which means that the electron beam is not chopped completely.

3.3 BASIC PRINCIPLE OF BLANKING SYSTEM

3.3.1 Deflection by Electrostatic Field

(1) Primary beam pulsing

Plows and Nixon (1968) have discussed the theoretical concept of flat-plate electrostatic beam chopping systems to pulsing the electron beam. The pulse repetition frequency was equal to the specimen voltage frequency.   The time duration of the pulse would be variable and it was possible to make this short compared with the period.

A voltage sine wave was applied to the deflection plates, and the effective blanking aperture was considered as the entrance window of the system. The deflection voltage amplitude, T, the period and τ the current pulse duration is:

$$\text{deflection voltage} = V_D \sin (2\pi t/ T) \qquad (3.3)$$

$$\text{and } V_D = V_{min} \text{ cosec } (\pi\tau/T) \qquad (3.4)$$

Each deflection voltage produces two current pulses. As $V_{\square}$ is de-creased, the current pulses are seen to increase in duration. The beam pulse width is determined by the deflection time from beam cut-off on one side of the aperture to beam cut-off on the other side of the aper-ture.

Gopinath and Hill[1977] expressed the deflection angle as:

$$\alpha = \alpha_0 \frac{\sin wh/2V_y}{wh/2V_y} \qquad (3.5)$$

where w   is angular frequency
α is the a.c. excitation deflection angle
α_0 is the d.c. excitation deflection angle
V_y is the longitudinal electron velocity
h   h is the deflection structure length
$wh/2V_y$ is the transit time angle θ'.

so

$$\alpha = \alpha_0 \frac{\sin\theta'}{\theta'} \qquad (3.6)$$

Lee (1946) was the first who analysed the effect of a.c field exci-tation on the electron beam chopping system. His work has provided the basic principles for electrostatic deflection of electron beams and it is compared with the work of other workers who used his equations in this field to analyse their experiments results.

Hill (1977) has reported the deflection angle of the flat chop-ping plate system as follows:

$$\tan \alpha_0 \simeq \alpha_0 = \frac{V_d \, fl.h}{2V_{b.d}} \qquad (3.7)$$

Menzel and Kubalek (1979) reported the dependence of deflection angle on frequency. If the deflection field alters during the time of flight the effective deflection angle decreases to:

$$\alpha(f) = \frac{V_{dfl}.h}{2V_{b.d}} \cdot \frac{\sin(\pi fh/Vel)}{(\pi fh/Vel)} \qquad (3.8)$$

where V_{dfl} = deflection structure voltage

d = distance between plates

V_b = V_{acc} = beam accelerating voltage

h = deflection structure length

f = frequency of the deflection voltage

V_{el} = longitudinal electron velocity

The dependence of the normalised deflection angle $\alpha(f)/\alpha_o$ on $\pi fh/v_{el}$. Equation 3.8, is the same as equation 3.6 has been mentioned by Lee (1946). Menzel and Kubalek have proved this equation experimentally.

Beam cut-off occurs when it is deflected beyond the edge of a centrally placed chopping aperture, which shows the chopping aperture deflection sensitivity of the plates as:

$$S = 1/V_{dfl \ min} \qquad (3.9)$$

Equations 3.7 & 3.9 correspond with experimental results from the present chopping plates, as a combination of 3.7 & 3.9 gives:

$$s = \frac{L.h}{x.2V_{b}.d} \qquad (3.10)$$

where L = deflection distance, x = deflection at aperture plane, this shows the dependence of (s) on the geometrical arrangement and accelerating voltage. All mentioned equations are valid for parallel plates chopper.

If a sine wave is applied to the plates, this results in a sinusoidal movement of the beam across the aperture. When no electrical field exists between the plates, electrons reach the specimen and beam pulses are generated. The problem of obtaining two pulses per period can be solved either by applying an additional offset voltage to the plates resulting in longer beam pulses or by adding a second pair of the plates perpendicular to the first.

Gopinath and Hill (1976), Menzel and Kubalek (1979) have fed these plates with a 90° phase shifted deflection voltage pulse with a suitable offset voltage. Excitation of the plates by deflection voltage pulses results in electron beam pulse widths determined by the chopper sensitivity, the rise and fall times and the amplitude of the deflection voltage. This technique is widely used in high frequency stroboscopic SEM by different workers, up to 1 GHz.

(2)   Gun Pulsing

The electron gun in the SEM is a triode with a heated tungsten hairpin filament cathode, solid Wehnelt cylinder and solid earthed anode; these each have a central hole for the electron beam to pass through. The cylinder is biased negatively with respect to the filament and focuses the electrons to a crossover very close to the filament (Hain and Einstein(1952)). Thus pulses applied to the cylinder give a pulsed beam.

Wienfield and Bouchoule (1976) reported the gun crossover as a

function of the Wehnelt grid potential, and thus it moves during the switching process. The crossover is seen at the specimen under test as the beam spot and any vertical motion of the crossover gives rise to defocusing of the beam spot. The frequency of the beam pulsing is limited.

Davidson (1981) has reported gun modulation to 50 MHz frequency.

(3)   Beam bunching

This technique is used at microwave frequencies and mainly depends on velocity modulation of the electron beam, which produces chromatic aberrations when electrons pass through the lenses in the SEM. The long drift length allows a small amplitude modulation for low resolution. The buncher is a resonant cavity and it is mechanically tunable. More detail is given elsewhere (Hill(1974)).

3.3.2   Deflection by Magnetic Field

In principle, when sufficient current passes through the coil the electron beam is deflected on to an aperture, and is there by prevented from proceeding further down the column. Electrostatic deflection systems are very sensitive to contamination problems, as already mentioned, so sometimes magnetic deflection is preferred, especially for low frequency applications.

The deflection angle is:

$$\alpha_o = V_{el} \; \frac{L.B}{2V_b} \qquad\qquad (3.11)$$

where L = length of magnetic field

   V_{el} = velocity

   B = induction (**magnetic flux density**)

   V_b = accelerating voltage

This sort of deflection has the problem of self inductance and self capacitance at MHz frequency.

Gonzales and Powel (1975) have reported the development of a chopping technique, based on Equation 3.11. A repetitive frequency of 10 MHz and electron beam pulses of 10 ns duration were achieved but shorter pulses with high repetitive frequencies could not be obtained.

Ohiwa (1977) has reported details of coil design. The proposed tilt angle of 6° at a magnification of (X500) is suggested in such a way that the beam passes through the chopping assembly. Design of deflection coils basically depends on the Lorentz force equation for a particle moving in magnetic fields as:

$$\overrightarrow{F} = - e . \overrightarrow{V_{el}} \times \overrightarrow{B} \tag{3.12}$$

where $\overrightarrow{F}$ = force on electron beam

   $\overrightarrow{V_{el}}$ = electron velocity

   $\overrightarrow{B}$ = magnetic flux density (induction)

   e = electronic charge = 1.6×10^{-19} Coulomb, and by using

Amperes' law :

  $\oint H . dl = I$

hence $H_{air} . l_{air} = N . I \tag{3.13}$

where N = number of turns, H = magnetic field intensity, I = current. Equation 3.13 was used to design the present deflection coils.

3.4 BEAM SWITCH REVIEW

Plows and Nixon (1968) have reported capacitor plates used in a blanking unit fitted above the first column lens and an electron deflection pulsing structure as shown in Figure 3.1.

Hill and Gopinath (1973) were the first to suggest the theoretical and practical analysis of blanking the electron beam in the SEM column in the stroboscopic mode at 9 GHz. They mentioned four methods of pulsing the electron beam:

(1) Beam bunching.

(2) Deflecting the electron beam back and forth across an aperture.

(3) Using an electrostatic deflection system, by applying a d.c voltage across the beam to produce one pulse per cycle.

(4) Pulsing the electron gun.

Methods of (2) and (3) were adopted.

The comparison shows that each of these systems has only been designed for a restricted range of applications. The repetition rate of the pulses must be synchronous with the signal on the specimen.

Hill and Gopinath (1973) have developed the meander line and helix as an ideal deflection system that can pass any frequency up to 10 GHz (see Figure 3.2). They show that the transit time is an important factor in selecting the type of blanking system, also they suggested that

Specimen position

final image in L_3

Final aperture (F A)

Lens 3

FA image

Lens 2

Entrance window

Lens 1

Deflection plates

First aperture

Crossover.

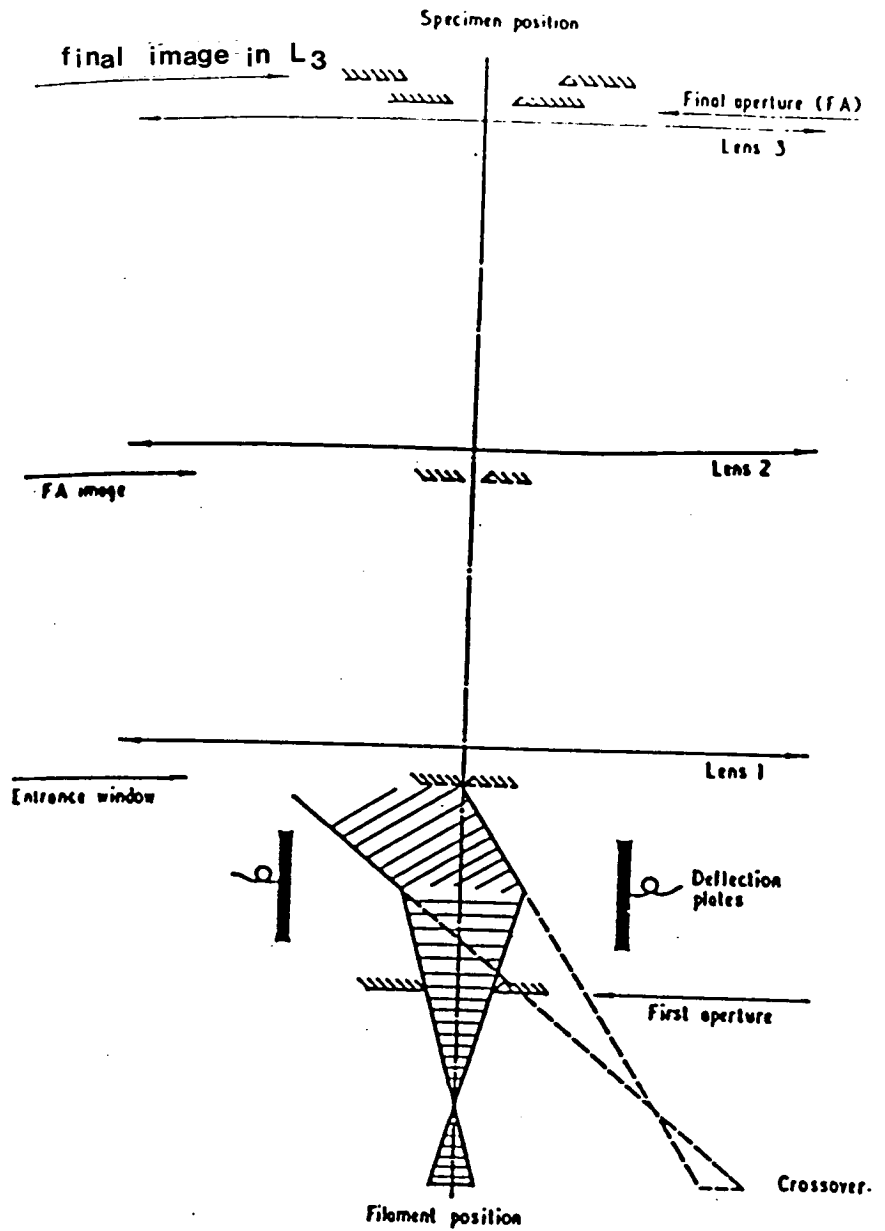Filament position

Figure 3.1: Schematic diagram of the stroboscopic scanning electron microscope showing deflection pulsing (from Plows and Nixon. 1968)
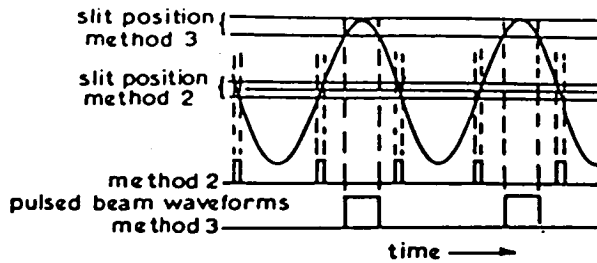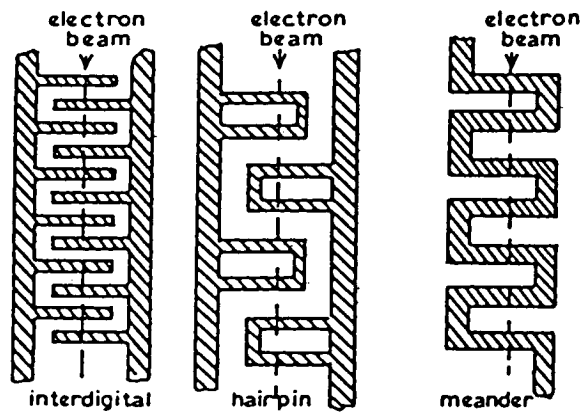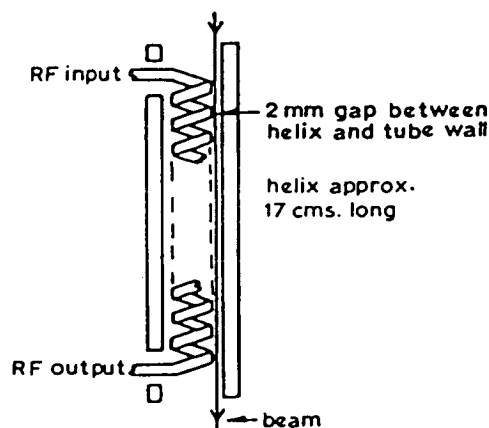
Figure 3.2 (a): Theoretical comparison of beam pulses using
method 2 and method 3 (assuming infinitely
small beam diameter). (from Hill and Gopinath 1973).

(b) Slow wave structure showing path of e-beam.

(c): Helical slow wave structure.

the chopping system must permit the use of variable beam energies; for MOS devices smaller than 2.5 kev energy is required.

Ura and Morimura (1973) have described a technique for producing beam pulses as short as 6 ps, using a combination of the resonant cavity and beam deflection methods. Degradation problems due to fringe fields were experienced·

Lin andBeauchamp (1973) have used a magnetic deflection system and beam blanking unit in a commercial SEM for application to electron lithography; they reported a comparison between electrostatic and magnetic deflection systems. " With electrostatic deflection, astigmatic aberration in the deflected beam was found to be worse than with magnetic deflection, but this effect was greatly reduced for small deflection angles. The basic problem arose from the effect of differential electro-static charging of the deflection plates by electrons; these plates were easily contaminated, allowing electrons or other charged particles to accumulate on the contaminated surface. When a voltage was applied across the plates to deflect the beam, charge no longer accumulated equally on the two plates, and unequal charges on the plates produced an unwanted deflection of the beam and hence a deflection error " (from Lin andBeauchamp(1973)). They suggested a technique to reduce this effect by using the beam blanking method in Figure 3.3, by turning the electron beam "on" and "off" by electrically switching either the accelerating potential or the bias potential of the electron gun. They preferred to blank or unblank the beam at high speed to electrostatically deflecting the beam against an aperture-stop, this involved the use of a pair of deflection plates.

Hill (1974) in his PhD thesis has reported pulsing the electron gun with 50V(see figure 3.4) but this required high current at high fre-

IST CONDENSER LENS
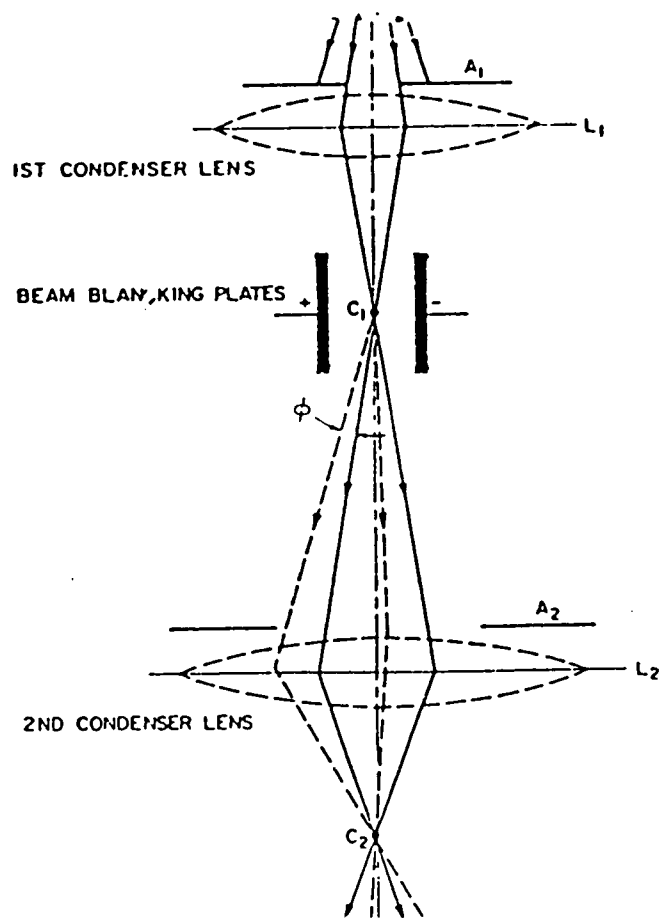
BEAM BLANKING PLATES

2ND CONDENSER LENS

Figure 3.3: Pertinent components of the deflection system and their locations in the objective lens structure. (from Lin and Beauchamp 1973)

quency. "Several difficulties were encountered, especially the defocus-
ing of the beam spot due to the gun crossover moving vertically during
the switching process. This technique was limited to 100 MHz; to obtain
a faster speed, it is necessary to redesign the Wehnelt cylinder to be a
microwave cavity"(from Hill(1974)).

He has also reported on beam bunching, depending on velocity modu-
lation of the electron beam where the density of bunches depends on the
magnitude and frequency of the velocity modulation. This technique
depends on microwave klystrons, with disadvantages of lack of monitoring
as well as chromatic aberrations.

Gopinath and Hill (1974) have reported an electron beam pulsing
system for performing stroboscopic SEM. They developed gun pulsing and
the screened meander line as electron beam chopper techniques (see Fig-
ure 3.5). Gun crossover movement which causes spot degradation has
been reported (see Figure 3.6).

They suggested placing apertures in the deflection pulsing system,
to reduce the field of view of the source; so that no source movement is
seen at the specimen; also they placed a deflection structure between
the gun and the first lens in the SEM column, which does not require a
lot of column modification, but gives less deflection sensitivity and
large deflection angle. This will be discussed later in more detail.

Gopinath and Hill (1977) have made a theoretical analysis for de-
flection beam chopping in the SEM which is the basis of the author's
work, where the deflection system is placed between the gun and the top
of the first lens in the SEM column (see Figures 3.7,3.8). They have
also suggested different deflection structures in the three lens SEM
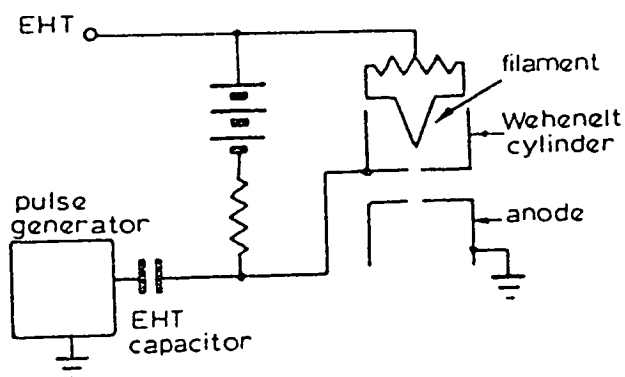
Figure 3.4: A gun pulsing circuit.
(from Hill thesis 1974).
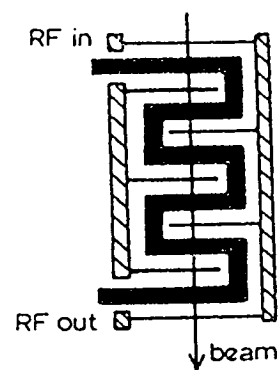
Figure 3.5: Screened meander line.
(from Hill thesis 1974)
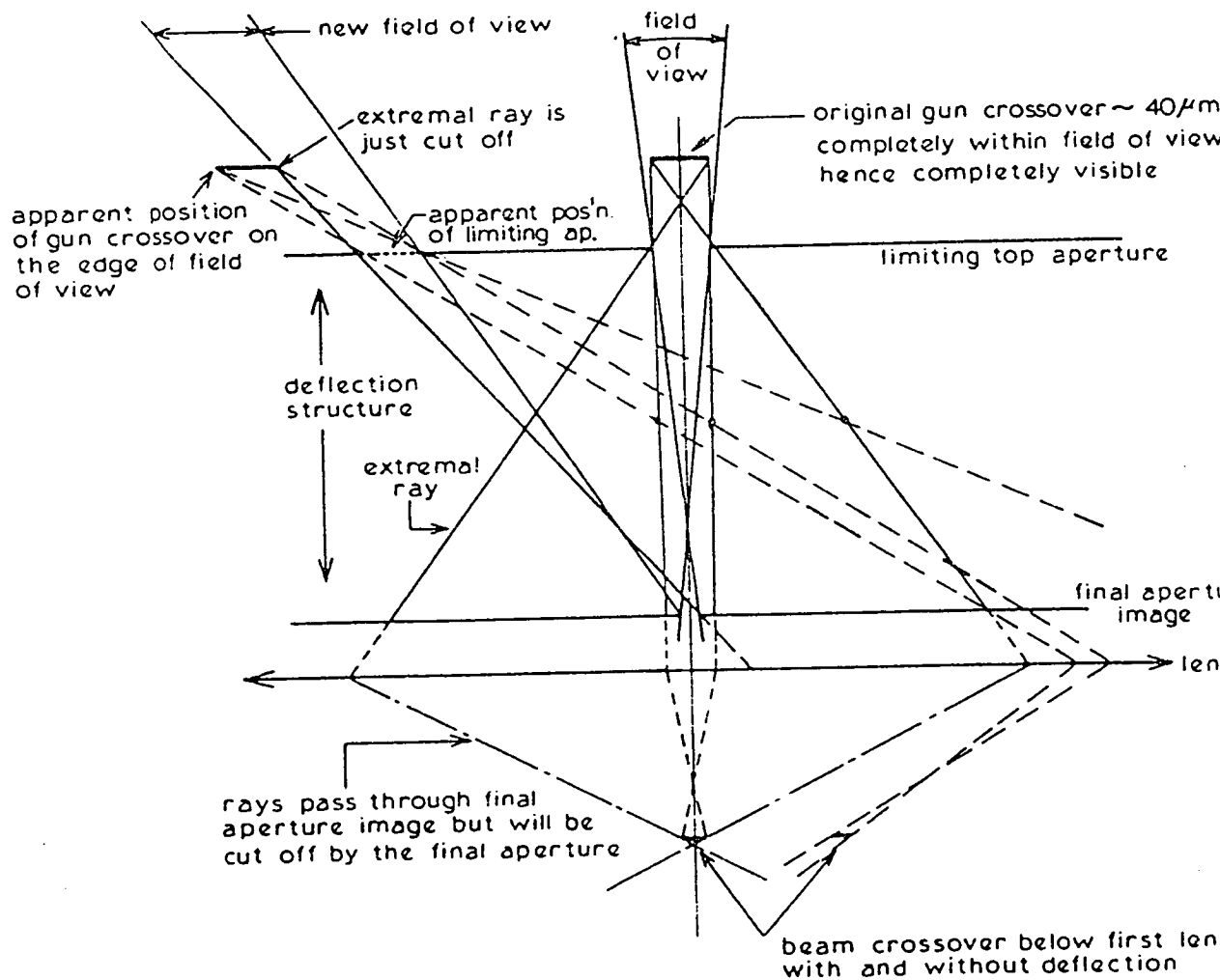
Figure 3.6: Ray diagram of deflection structure between gun and first lens
(unfocussed system). (from Gopinath and Hill 1974)
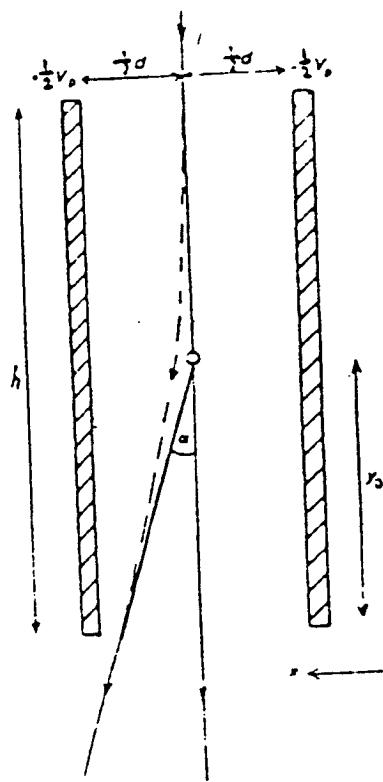
Figure 3.7: A schematic diagram of deflection of a filamentry beam by a pair of electrostatic plates. (from Gopinath and Hill 1977)
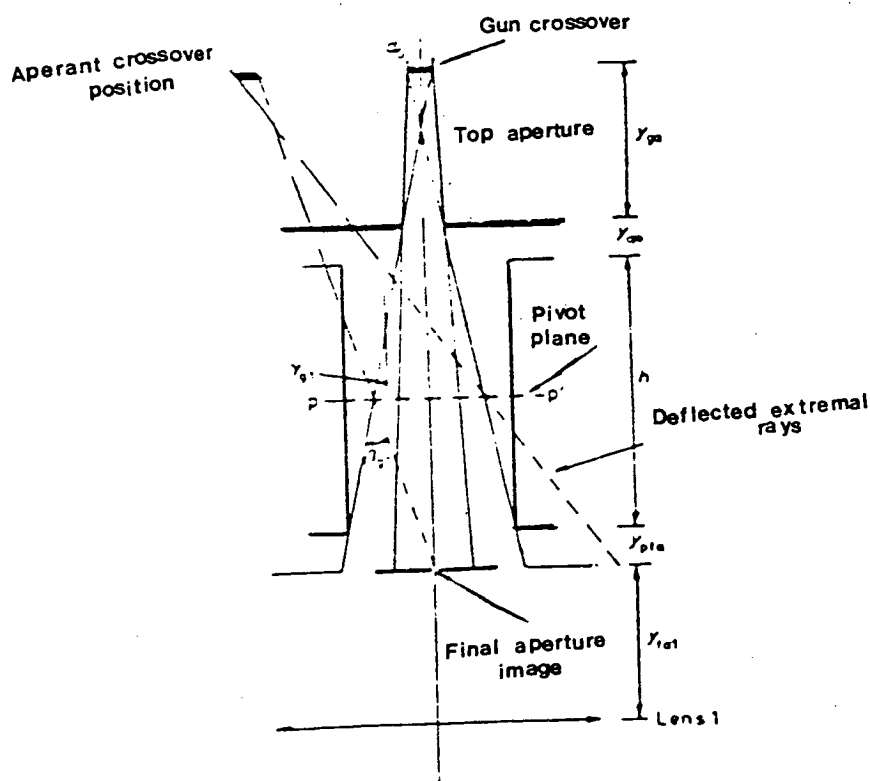
Figure 3.8: Ray diagram of the deflection chopping of a finite diameter beam, with the deflection structure between the gun and lens 1. (from Gopinath and Hill 1977)

column.

Ura et al (1977) have used a complicated set up for the blanking system, to provide ps pulses for the stroboscopic SEM as shown in Figure 3.9, by using a deflector, chopping aperture and a buncher. The deflector was a re-entrant cavity with 1 GHz operating frequency, while the buncher works at a frequency of 4 GHz. They have developed this technique to observe two dimensional voltage contrast images, with nano and pico-sec time resolutions

Heike et al (1977) have developed a technique using an electrostatic beam blanking system for the SEM. Deflection repetition rates up to 1 GHz were achieved with a 300 mV deflection voltage; a 2.5 keV accelerating energy was used to study a ring oscillator. The time resolution of the blanking system was 500 ps. The electron beam pulse width of less than 1ns was reported. A very small gap of 1 μm between the chopping plates has reported.

Gopinath and Hill (1977) have employed a screened meander line in a travelling wave deflection source with high deflection sensitivity (see Figure 3.5). They used a pulse of the order of 100 ps, and pulsed the electron beam, and electrostatically deflected it across an aperture for blanking during fly back (double plates of chopping and blanking types were used).

They placed the structure between the top and intermediate condenser lenses, so that the convergent beam passed through the meander line. 350 mV was required to turn the beam current off at V_{acc} = 12.5 keV. They reported using the final aperture image (FAI) as the beam chopping aperture. They developed circuitry for pulse shaping, which is used for fast electron beam switching as in Figures 3.10 &

W-FILAMENT

ANODE

PRE-APERTURE
HOLE DIA. 10,20,40μm

49

1ST DEFLECTOR

ALIGNMENT COILS

271

BUNCHER

82

CHOPPING APERTURE
HOLE DIA. 50μm
        100μm
        200μm

113

CONDENSER LENS
APERTURE DIA. 250μm

247

SCANNING COILS
STIGMATOR
OBJECTIVE LENS
SPECIMEN PLANE
2ND DEFLECTOR

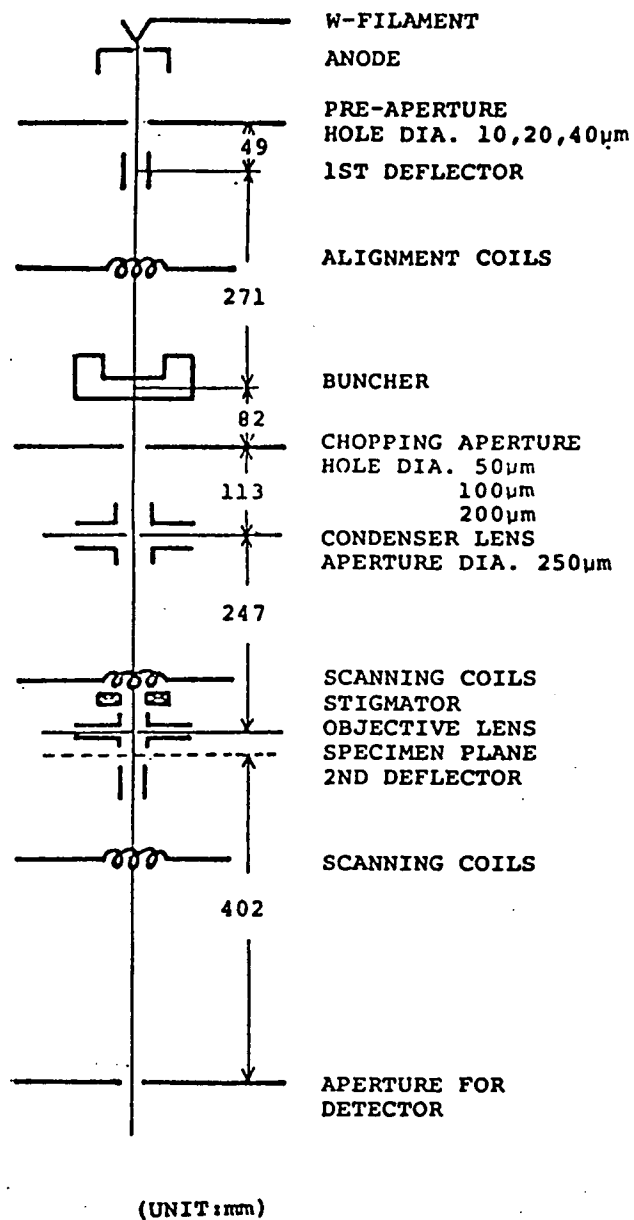SCANNING COILS

402

APERTURE FOR
DETECTOR

(UNIT:mm)

Figure 3.9: Schematic figure of electron optical disposition.
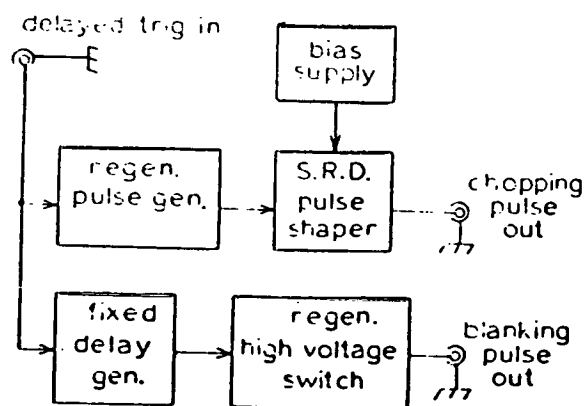(from Ura et al 1977)

Figure 3.10: Schematic of beam switch and
blanking plate pulse generators. (from Gopinath and Hill
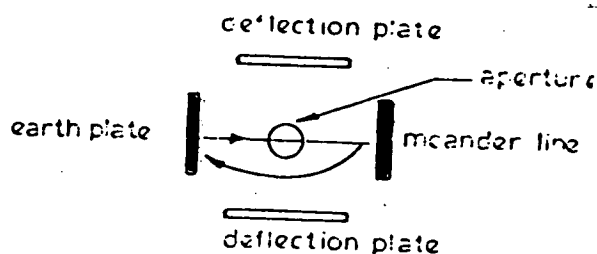1977)

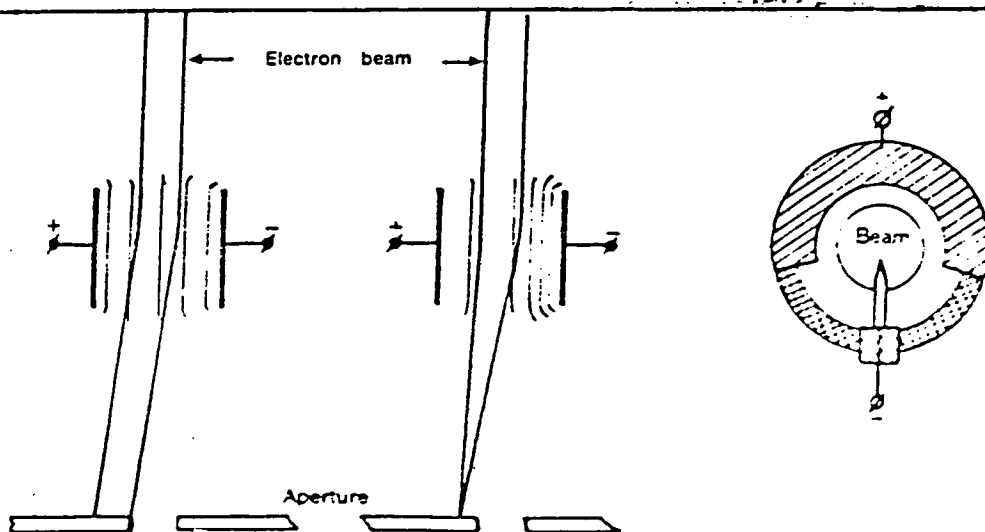Figure 3.11: Beam chopping trajectory.　　(from Gopinath and Hill
1977)

Figure 3.12: Design principle of the beam blanking system.
(from Rau et al 1980)

3.11.

By employing non-linear devices, they found that the delayed trigger pulse did not have a fast enough edge to obtain a 100 ps beam pulse width. In order to achieve this, the sensitivity of the meander line demanded a drive signal with a rate of increase in voltage by at least 35 MV/s. A step recovery diode (SRD) has been used for such requirements with a 2V output pulse into the 50 ohms load; a rise time of 500 ps was achieved. This technique is useful and considered at present as essential for comparison.

Menzel and Kubalek (1979) have reported using EBCS (Electron Beam Chopping System) for the generation of electron beam pulses for variable pulse widths in the SEM. They suggested that EBCS must permit the use of variable beam energies as non-destructive stroboscopic voltage contrast measurement on MOS circuits can only be carried out at energies smaller than 2.5 keV, whereas bipolar circuits can be examined at higher beam energies resulting in better spatial resolution. They have also mentioned that since stroboscopic voltage contrast depends on the primary electron beam current to show voltage and time resolution, then the maximum primary beam current must not be affected by the electron beam chopper.

They have employed different blanking systems of the plate capacitor type and a travelling wave deflection structure of the screened meander line type of Gopinath and Hill(1974), which has been mentioned before (see Figure 3.5). They reported different methods of driving electron chopping systems as shown in Figure 3.13, the dependence of minimum deflection voltage on the primary electron energy, the deflection angle on the frequency of the chopping system, electron velocity and plate length (see Figures 3.15, 3.16, 3.17, and 3.21).
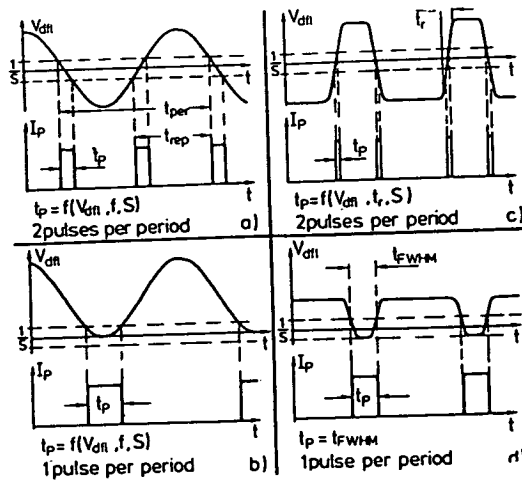
Figure 3.13: Different methods of driving electron
beam chopping systems. (from Menzel and Kubalek 1979)
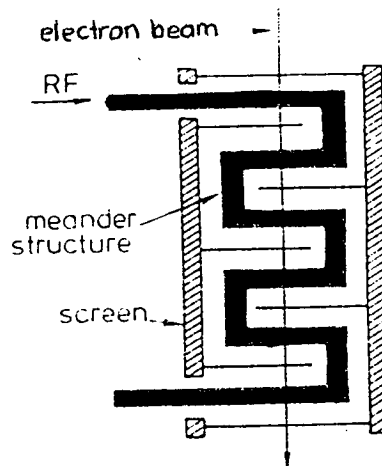
Figure 3.14: Chopping system with travelling wave deflection
structure (screened meander).
(from Menzel and Kubalek 1979)
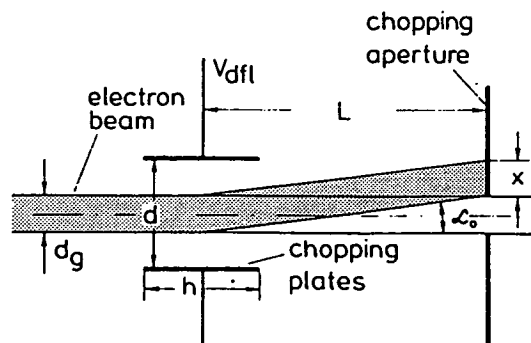
Figure 3.15: Chopping of the electron beam by a plate capacitor
and a chopping aperture. (from Menzel and Kubalek 1979)
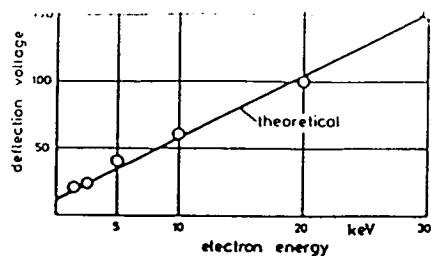
Figure 3.16:⸱ ⸱ependence of the minimum deflection voltage on
the primary electron energy (experimental:
circles, theoretical: solid line).   (from Menzel and Kubalek 1979)
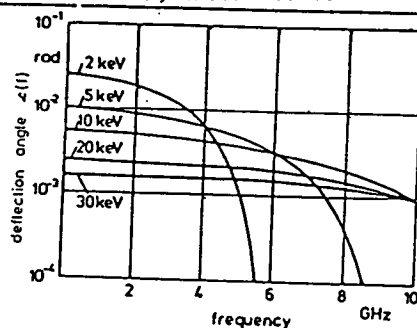
Figure 3.17: Dependence of the deflection angle on the frequency
of the new chopping system. (ᶠrom Menzel and Kubalek 1979)
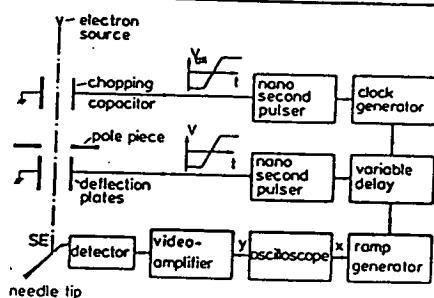
Figure 3.18: Experimental set up for direct measurements of
short electron beam pulses with high time   (from Menzel and
                                              resolution   Kubalek 1979)
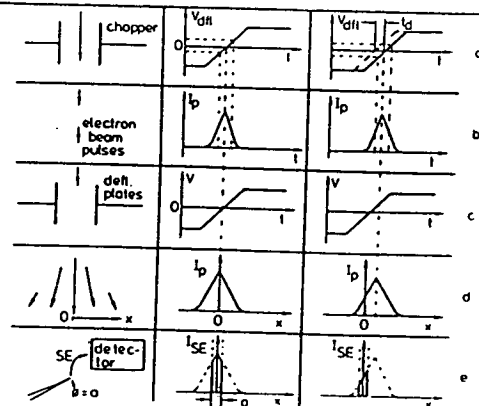
Figure 3.19: Principle of function of short electron
beam pulse measurements. (from Menzel and Kubalek 1979)
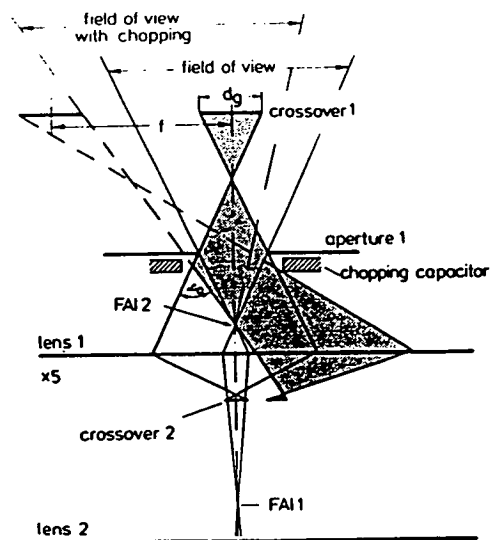
Figure 3.20: EBCS with chopping plate capacitor and aperture
between electron gun and first lens in the SEM.

(from Menzel and Kubalek 1979)
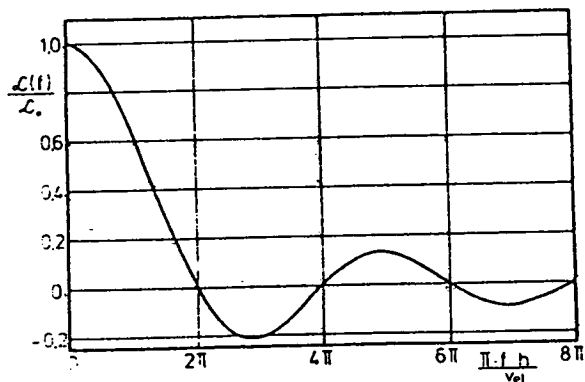
Figure 3.21: Dependence of the normalized deflection angle on
frequency, electron velocity, and plate length.
(from Menzel and Kubalek 1979)
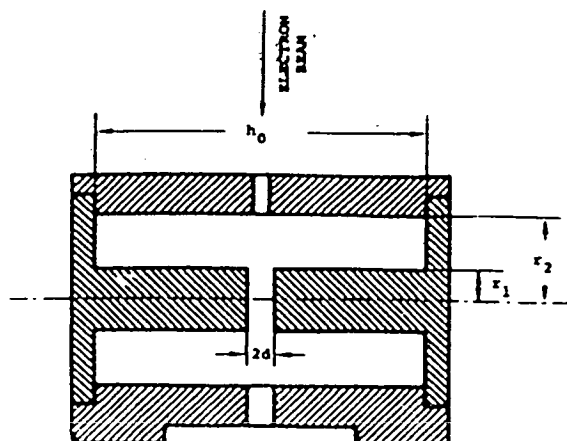
Figure 3.22: Schematic diagram of the pulse gate and assumed
electric field in the deflector. (from Menzel and
Kubalek 1979)

They developed similar techniques to those of Gopinath and Hill by using chopping and blanking plates which were positioned perpendicular to each other, to produce short electron beam pulses with high time resolution as shown in Figures 3.11 and 3.18. They described the principle for measuring the electron beam pulse length actually achieved as in Figure 3.19.

A blanking system (EBCS) was placed above the first electron lens in the SEM column, provided with a chopping structure between gun and first lens, which is the scheme adopted for the present work and will be discussed later (see Figure 3.20). Also a chopping structure below the first lens was reported which corresponds with the Gopinath and Hill analysis (1977).

Chopping by parallel plates can not be carried out at such high frequency where the time period of the chopping pulse is comparable to the transit time of electrons in the field between the plates, so they suggested using travelling wave structures and a buncher as shown in Figures 3.14, 3.22, instead for these higher frequencies. They have reviewed most of previous work with a new development of beam switch and some mathematical expressions for deflection sensitivity of electron beam .

Hosokawa et al(1978) have reported the generation and measurement of subpicosecond electron beam pulses by using transverse longitudinal combination gate systems as shown in Figure 3.23. They have discussed in detail these types of deflection system, which used transverse deflection and longitudinal modulation of the beam, as in Figure 3.24. Their work is very similar to Ura et al (1977) approach.

Feuerbaum and Otto (1978) have developed an externally adjustable

Figure 3.23: Schematic diagram of the pulse gate and
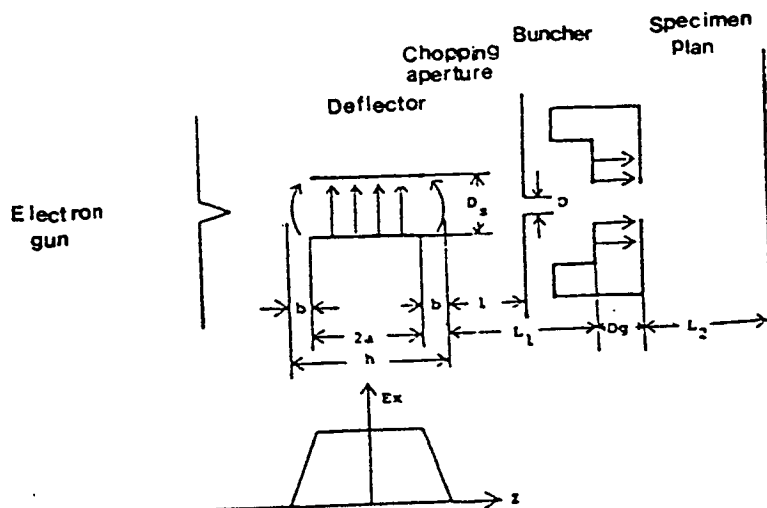assumed electric field in the deflector.
(from Hosokawa et al 1978)
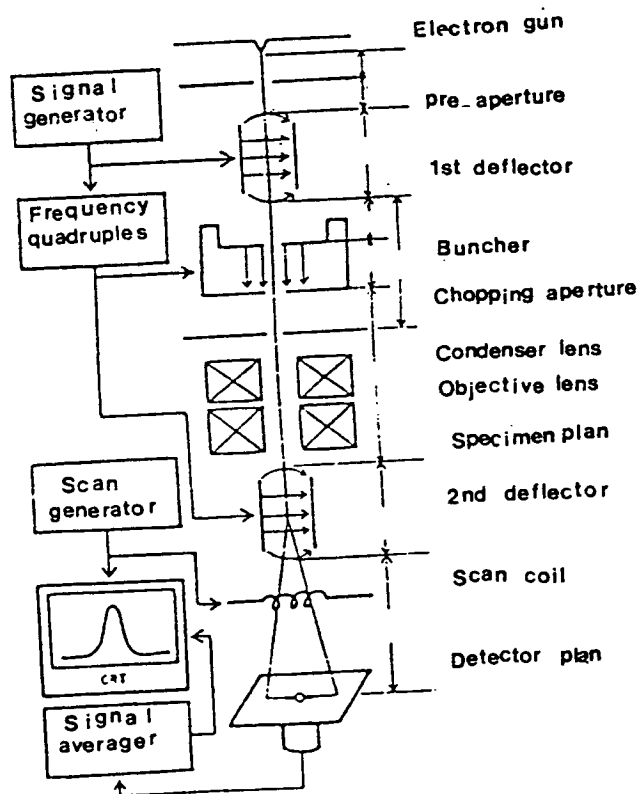
Figure 3.24: Experimental arrangement for the generation
and measurement of the subpicosecond electron
beam pulses. (from Hosokawa et al 1978)

beam deflection system, which is useful in alignment of electron beam and the chopping system with respect to SEM column externally as shown in Figure 3.25 by using a trough type travelling-wave structure (see Figure 3.26). They used the electrostatic field of a symmetrical deflection system with bandwidth of 8 GHz and a pulse width of 250 ps for the stroboscopic mode in the SEM. They have used previous suggestions of Gopinath and Hill (1977) of fitting the beam blanking system in the SEM column; they reported a relationship between deflection voltage and specimen current as shown in Figure 3.27.

Gopinath and Hill (1977), Menzel and Kubalek (1979) have used an additional fourth lens in the electron optical column. They placed the chopping system of parallel plates between the gun and the additional lens to optimise the deflection sensitivity.

Menzel and Kubalek(1979) have developed new techniques by making chopping plates as short as possible to produce a high repetition rate. They reported a 2 mm plate length for higher electron energies, This results in lower deflection angles. In order to compensate for this reduction and to obtain high deflection sensitivity the distance between plates and aperture has to be high, and the deflection on the aperture plane has to be as small as possible.

" The beam is cut-off when the apparent crossover completely moves out of the fieldofview resulting in a small deflection angle which is dependent on the geometrical arrangement and the size of the first crossover (from Menzel and Kubalek(1979)). A pulse width of about 10 ps at any primary electron energy between 2 and 30 kev was reported. 300 ps rise time of a step function was measured at a bond pad of an IC by stroboscopic voltage contrast.
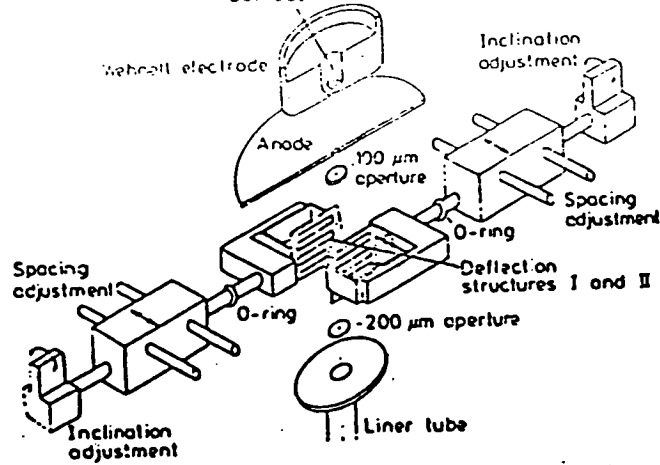
Figure 3.25: Beam deflection system. The spacing and inclination
of the deflection structures can be adjusted to an
accuracy of about 10μm and 2' respectively.

(from Feuerbaum and Otto 1978)
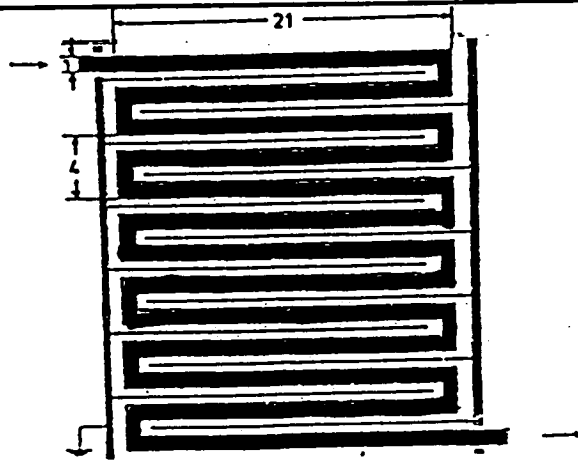
Figure 3.26: One of the two trough-type travelling-wave structures
(dimensions in millimetres).
(from Feuerbaum and Otto 1978)
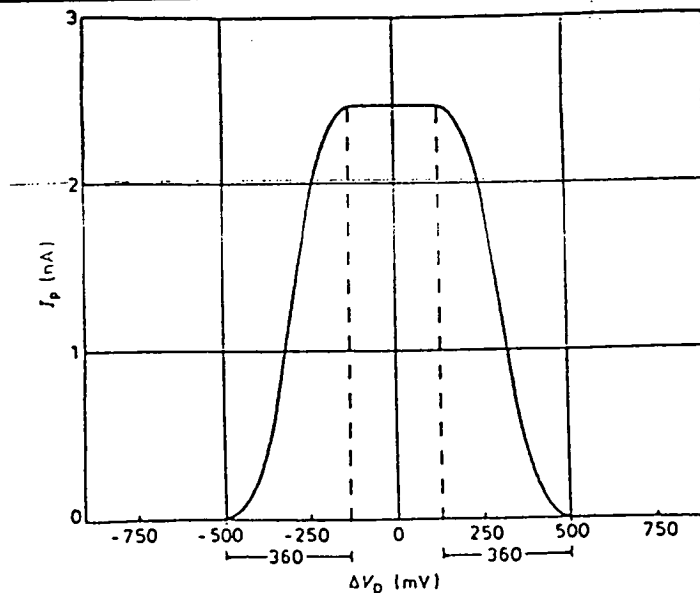
Figure 3.27: Specimen current lp as a function of a direct
voltage ΔV_D between the deflection structures.

(from Feuerbaum and Otto 1978)

Rau et al (1980) have used a beam blanking system with an inhomogeneous radial field developed to study dynamic processes and to improve the spatial resolution, they reported that the beam is completely cut-off at a significantly lower value of the field as compared with the conventional system of plane parallel plates. An inhomogeneous electric deflecting field is induced between the cylindrical channel and the blade edge. They have suggested using inhomogeneous field systems which are roughly one order of magnitude more sensitive as they claimed and exhibit better temporal characteristics compared with homogeneous field system.

3.5 PRESENT WORK

All reported work was on electron beam chopping systems built to suit special purposes and fitted for different SEM machines. So developing a suitable chopping system at present was essential. For the present electron beam switch, it was decided to adopt the principles of Gopinath and Hill(1977), and Kubalek and Menzel(1979).

Problems to be overcome for present work are mainly:

1.   Electron beam alignment

2.   Contamination

3.   Beam switch efficiency

4.   Electronic circuits design for beam switch

3.5.1 Introduction

There are some electron optical problems associated with chopping the electron beam by electrostatic deflection across an aperture. These include spot size degrad ation due to apparent movement of the gun crossover and instabilities due to oil contamination which becomes electrostatically charged.

For the development of a reliable chopping system these problems must be solved. Another important requirement of an efficient beam chopping system is that the beam can be switched off as it traverses the most radiation-sensitive areas of MOS devices, minimising beam induced damage.

3.5.2 Electron Beam Alignment

The gap between the chopping plates must be kept small in order that the voltage required to drive them should be kept down to a few volts. This means that the gap should be around 1-3 mm. This in turn means that the aperture to be placed above them must be approximately 100 um in diameter, and is used on the present system. The whole assembly should also be aligned precisely with the electron-optical axis. One possibility would be to use mechanical adjustments controlled from outside the column, as was developed by Feuerbaum and Otto (1978), see Figure 3.25, but this would mean quite major changes to the microscope and so an alternative method has been devised. The chopping assembly is machined and adjusted as accurately as possible on the mechanical axis of the column.

An electro-magnetic beam deflector (as shown in Figure 3.28) is positioned between the electron gun and the chopping assembly; this is
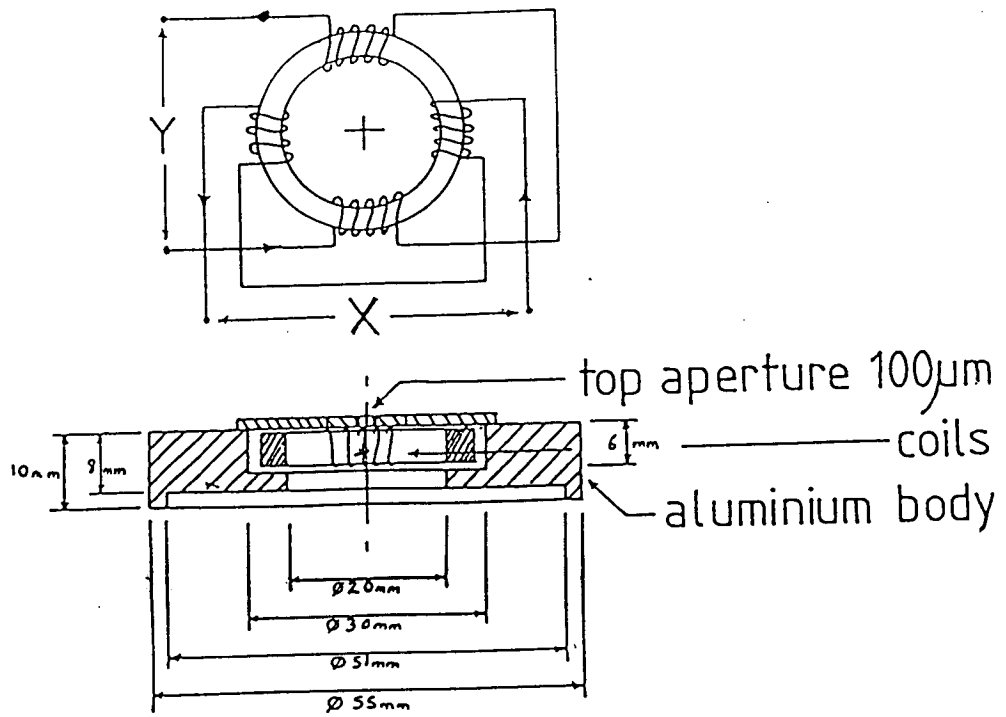
Figure 3.28: Shows present design of deflection coil used for electron beam alignment.

used for electron beam alignment and for low frequency chopping applications. This has proved successful, but does make the accurate alignment of the electron beam more critical. Therefore, it is suggested to ignore using the deflection coils for beam non- alignment problem, but using manual methods to fit the plates with the electron column in the present chopping assembly.

The design of these coils depends on equations 3.12 and 3.13. An aluminium body is used to fix the coils above the chopping assembly. The deflection angle $\alpha_o = 7°$ for v_b = 10 keV, $V_{el} = 5.93 \times 10^7$ m/s, H = 190 AT/m, and $\alpha_o = 6°$ for v_b = 15 keV have been estimated. A wire of (0.125 inch) in diameter is used to produce the deflection coils (See Figure 3.28). Polythene bars were used as coil cores. Using curved plates was found helpful in solving electron beam non-alignment.

3.5.3 Contamination

The Cambridge Stereoscan S2 machine used for this work has oil diffusion vacuum pumps and has many greased "O"-rings in the column. Therefore a film of oil is deposited on all surfaces inside the column and specimen chamber. Under electron bombardment this oil polymerises to form an insulating film which can retain charge from the electron beam.

Contamination layers on the specimen are generated by the polymerisation of hydrocarbons by the electron beam (Miller (1978)). This is not a serious problem for the present work mainly because the film is deposited symmetrically around apertures placed in the column. However, one of the beam chopping plates will be covered in a thicker film than the other, as the beam is held off for a large fraction of the time. This leads to very inconsistent performance of the plates, this practi-

cal conclusion agrees with Lin andBeauchamp (1973). As it is imprac-
tical to improve the vacuum condition in this machine to the extent re-
quired, the solution adopted is to place a small aperture of 100 μm im-
mediately before the electron chopping plates so that ⟩ the electron
beam can not directly strike either of the plates.

To reduce contamination, the vacuum chamber should be thoroughly
cleaned with ethanol in order to replace non-volatile adsorbed hydrocar-
bons on the surfaces by the easily volatile ethanol (Harada et al 1978).
It is suggested to use an oil free getter -ion pump, or cryo-pump which
were not available.

A dark mark is produced on the chopping plates. One method to
measure contamination in the SEM is to use a crystal oscillator. This
depends upon the idea that if the crystal surface thickness increases, a
change in oscillation frequency takes place. It was found experimental-
ly that very little change in surface thickness of the crystal for long
running times was achieved. Therefore contamination is not a severe
problem in the present work, probably due to the use of a thermoelectri-
cally cooled baffle above the diffusion pump.

3.6 ELECTRON BEAM SWITCH

3.6.1 Transit Time Aspect

An important factor in designing the chopping plates is the
transit time, especially in the high frequency range. In the present
design of the chopping plates (see Figures 3.29 and 3.30), the following
are considered; the geometrical dimensions, Vacc , and gaps between
plates:

$$t_t = \frac{\ell}{V}$$

(3.14)
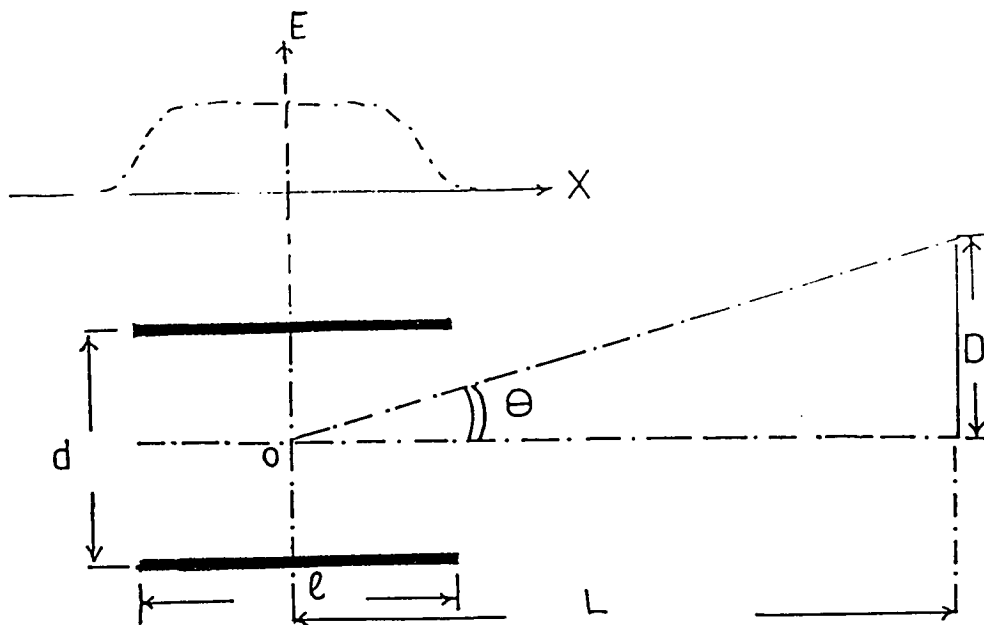
Figure 3.29   The electrostatic deflection (flat plates).
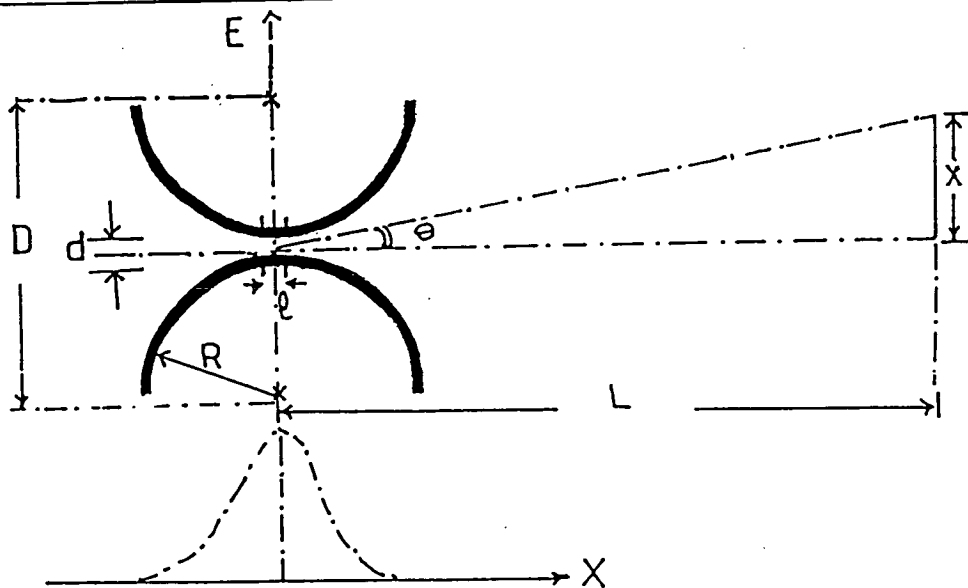
Figure 3.30   Shows fields of two parallel conducting cylinder (curved plates).

where t_t = transit time

ℓ = effective plate length

V_{el} = electron velocity = $5.93 \times 10^5 \sqrt{V_{acc}}$ m/s

V_{acc} = accelerating voltage

If 1 is fixed

t_t α effective plate length (ℓ)

$$t_t \; \alpha \; \frac{\ell}{\sqrt{V}_{acc}} \qquad (3.15)$$

This equation coresponds to Lee [1946]

Since the chopping assembly is positioned at the top of the first lens, large deflection angles with less deflection sensitivities are expected (Gopinath and Hill 1977).

Lee (1946) has reported that in parallel electrostatic deflection plates, the decrease in sensitivity at high frequency due to transit time effect and is given by:

$$\text{relative dynamic sensitivity} = \frac{\sin w\theta/2}{w\theta/2} \qquad (3.16)$$

where w is the angular frequency of deflection voltage, θ is the time taken for the electron to pass between the plates. Equation 3.15 neglects the action of the stray fields at the end of the deflection plates.

Fringe field effects around the flat plates edges have been neglected for the present since the central field is the primary source of electron beam deflection.

3.6.2 The Field Distribution Effect on the Electron Beam Deflection

Figures 3.29 & 3.30 show the approximate axial electric field strength for two parallel plates in flat and curved shapes. The electric field is distributed linearly inside the flat plates. This causes the electron beam to deflect effectively along the plates while at the plates edges fringing fieldsdisturb the electron beam and cause deflection defocusing problem, especially when a small gap between plates is used.

In the curved plates the electric field is distributed non-linearly along the curvature of the plates . It is expected that the field is more effective in the centre of the plates, than at the plates edges. To prove this further work is required using computer simulation, to show the deflection sensitivity of the curved plates is effective at the center. At the plates edges a weak field effective on the deflection of the electron beam with respect to the flat type. These might be the reasons for the curved plates to solve the problem of electron beam non-alignment and to chop the electron beam smoothly. **For more detail of mathematical expressions, see Appendix(II).**

For further work , it is recommended to use Khursheed(1983) computer programme for modelling of the electron beam through flat and curved plates; to study field analysis in three dimensional pattern of the electron beam deflection across the plates with respect to electric field strength,plates length, deflection angles, potential difference across the plates, accelerating energy, etc. This study will be helpful for plates design, and to suggest the preferable geometrical plates shapes.

3.6.3 Plates Shapes

Details of a flat plate chopper have been reported by (Gopinath and Hill 1977). In discussing design and construction of the curved plates (cylindrical plates) as shown in Figures 3.30 and 3.31, a two dimensional model of parallel plates is presented for comparison with flat plates.

Curved plates were found to work with a small gap between the plates which can be controlled by using screws, the same arrangement has been developed for flat plates(see Figure 3.31) so that the plates gap can be fixed precisely. A central field is considered as a source of electron beam deflection.

Thick and thin film capacitors may be used for electron beam-chopping with small plates gap. But these were not used, due to the complexity of design and construction of these plates and incompatibility in fitting these plates with the chopping assembly and present electron beam column in the SEM. It was decided to use a simple parallel plate capacitor as a chopper, which is found adequate for present electron beam switching applications. Both types of flat and curved plates were used in the SEM, have been designed and constructed to perform stroboscopy and sampling modes by pulsing the primary electron beam.

Experimentally curved plates were found more useful than the flat type for solving the electron beam non-alignment problem in the present SEM machine. Flat plates of 5 and 10 mm lengths, and curved plates with different curvatures were developed to perform chopping of the electron beam at high speed switching.

3.6.4 Electronic Circuitry for Beam Switch

The circuitry developed for the electron beam switch is a simple

(A)

- fixing screws
- chopping plates
- brass body
- insulator

Ø50mm
20mm
Ø26mm
Ø44mm

(B)

- 100μm top aperture
- insulator
- chopping plates
- blanking plates
- aluminium body

Ø50mm
Ø8mm
60mm
8mm
Ø34mm
Ø38mm
Ø42mm

(C)

- rounded end
- flat end
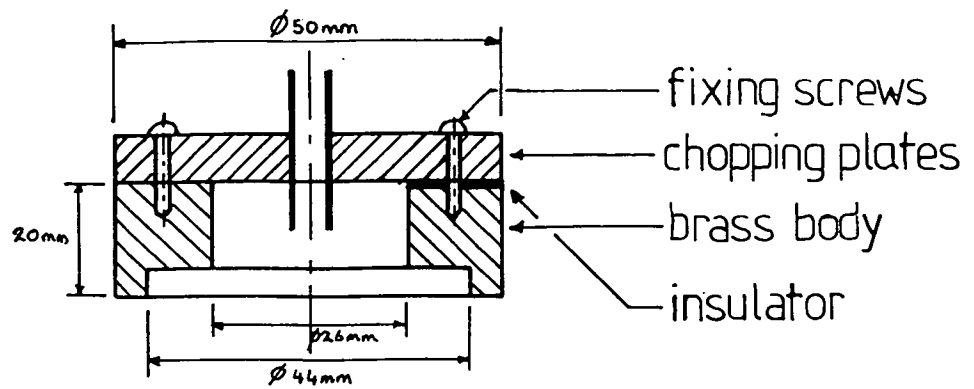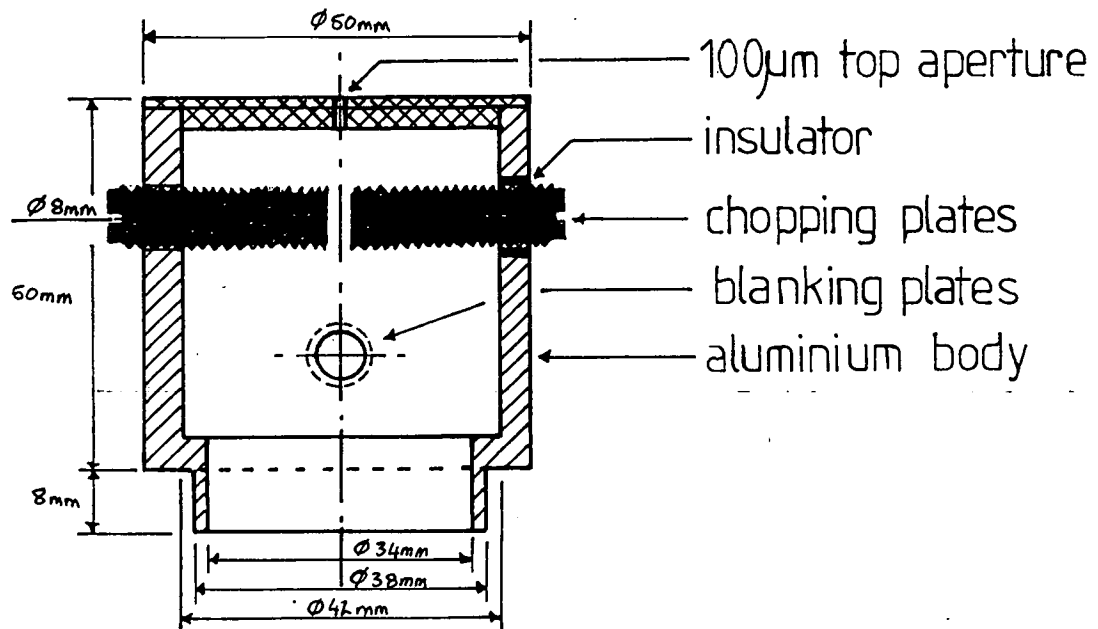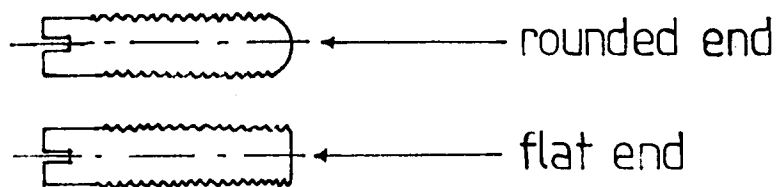
Figure 3.31: Shows chopping plates assembly. (A) ordinary parallel plates (B) present plates assembly (C) screw thread of flat and curved plates.

electronic switch and is shown in Figures 3.32, and 3.35; it is adequate for the present chopping speeds.

Gopinathan and Gopinath (1978) have used a high voltage pulse with a fixed delay with respect to the chopping pulse which is applied to blanking plates for the entire fly back period which corresponds to the falling edge of the chopping pulse. The plates required more than 40v to blank the beam. They used a regenerative switching circuit using complementary bipolar devices to produce a 60v output pulse across the blanking plates with a rise time of 5 ns (see Figure 3.10).

For the present work a similar technique has been used, but it is found that 15v is enough for both chopping and blanking plates to chop off the electron beam (see Figures 3.33, 3.34). The positive-going edge of the delay unit signal is shaped by the electronic beam switch (pulse shaper). The beam switch is fitted close to the SEM column, to reduce the time delay error and the capacitive load. The output signal from the beam switch with fast rise time allows the deflection voltage to achieve the specified electron beam pulse width; this signal overcomes a d.c bias which is normally on the plates and turns the beam on for 1 ns.

The pulse width is determined either by measuring the video pulse rise time, or by measuring the chopping pulse rise time.

Feuerbaum and Otto (1982) have suggested a method of measuring the electron beam pulse width by the ratio of the average pulse current to the original unchopped beam current which is not reliable.

Double plates are used, one for chopping to deflect the beam across an aperture, the other for blanking during fly back time to avoid there being two beam pulses per cycle (see Figure 3.33). Two plates ly-
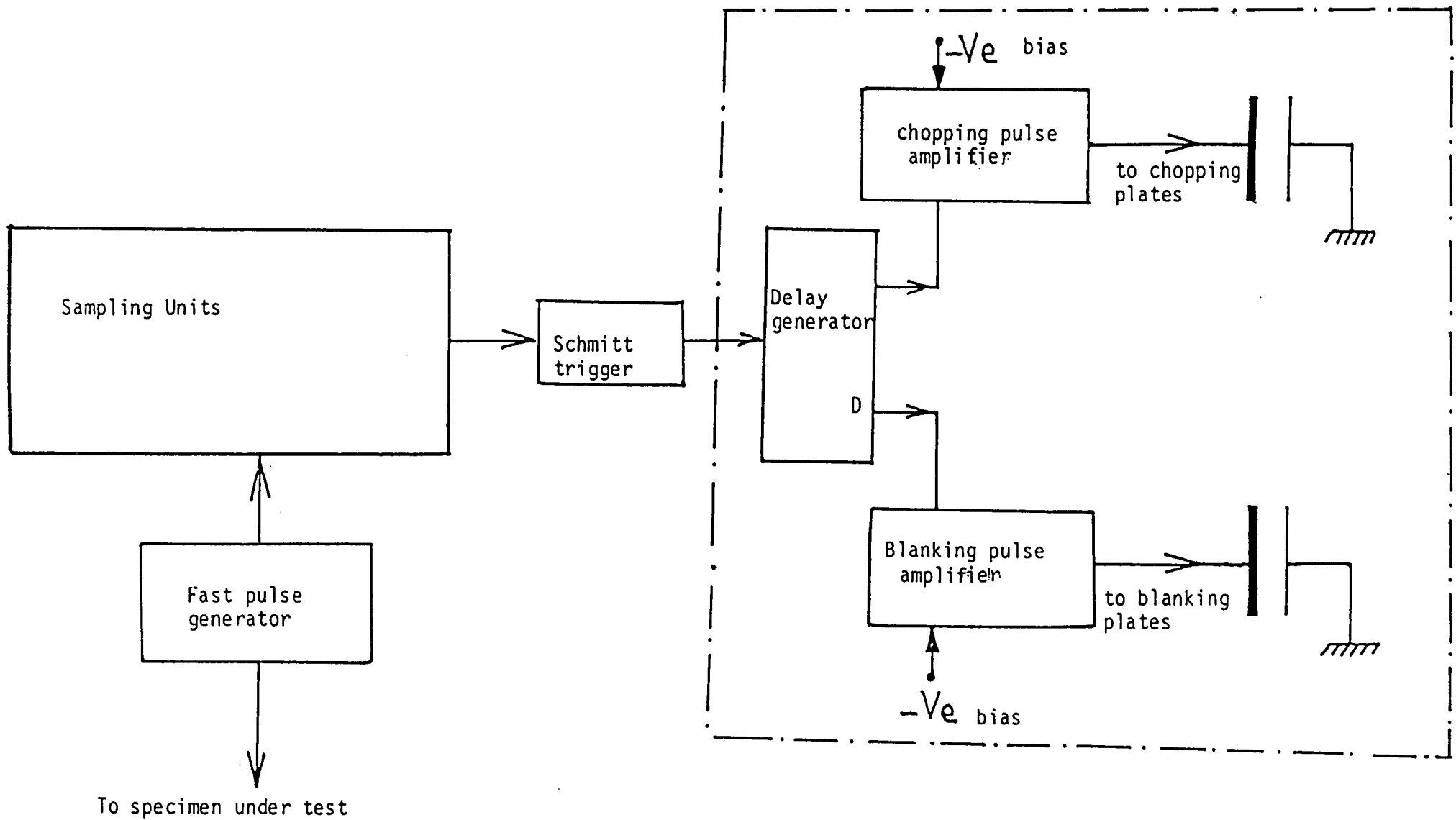
Figure 3.32: Shows beam switch unit.

(A) Two video pulses/ period problem solution.

o/p from amplifier

+15V

0V

chopping pulse

+7.5V

blanking pulse

'ON' window

-ve bias

-7.5V

Beam pulses

wanted
pulse

unwanted
pulse

0 ve

bias

-15V

o/p

AMP

aperture

blanking plates
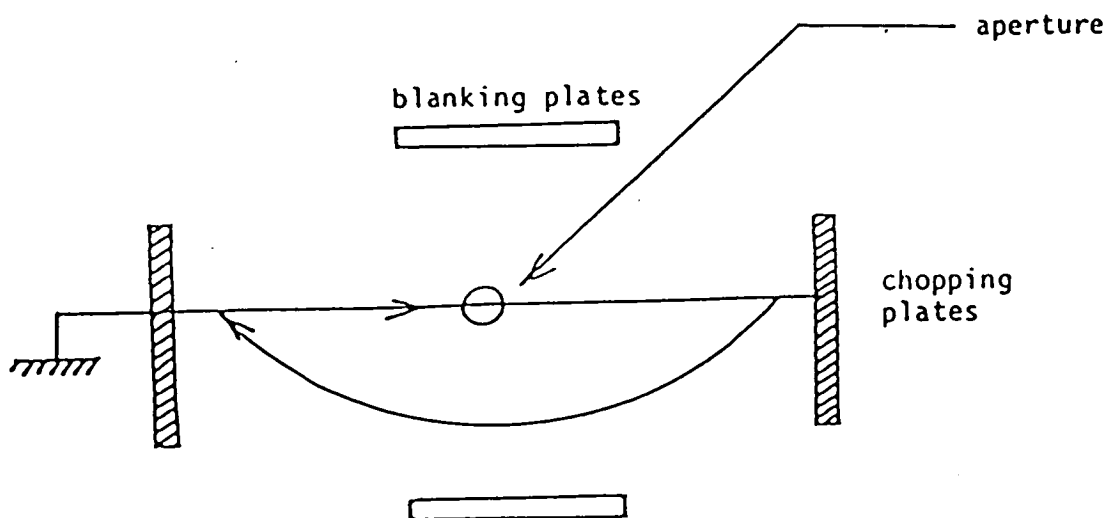
chopping
plates

Figure 3.33 : (B)   Beam chopping trajectory

screw blanking plates

-Ve

electron beam throu
100μm top aperture

-Ve
screw chopping
plates

Blanking system layout

Figure 3.34: Shows a schematic diagram of present chopping and
blanking plates of beam switch.

ing perpendicularly to each other have been developed to achieve fast electron beam switching pulse with a time of 1 ns which indicated the time resolution of the chopping system. These plates are connected to the beam switch (see Figure 3.32). The d.c bias to the **chopping and blanking plates must produce the conditions shown in Figure 3.33(A). and gives results as in Figure 3.37.**

In the stroboscopic mode the output from TTL devices is fed directly to the plates to produce fast rise time pulse (for fast electron beam switching of 2 to 5ns speed). An electron beam pulse of 1ns width is achieved, mainly by the use of a variable switching time (see Figure 3.36). Push pull amplifiers were also used to produce a very fast switching of the chopping pulse(See Figure 3.35). **Figure 3.37 shows the two pulses/period problem is overcome at present.**
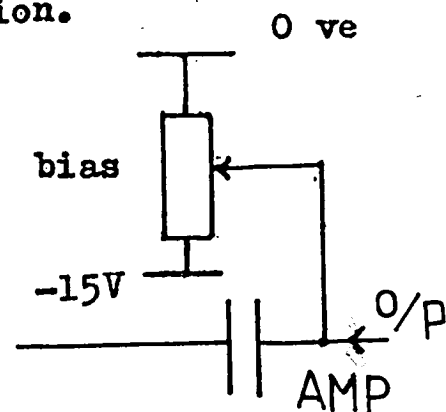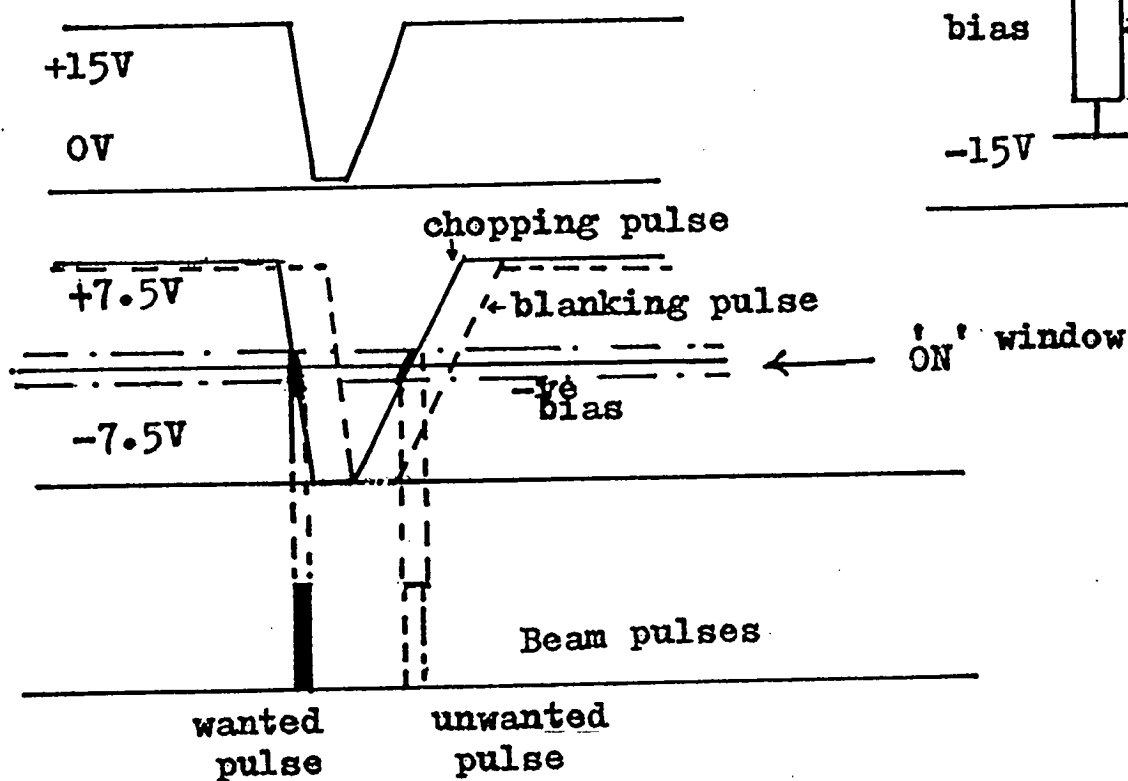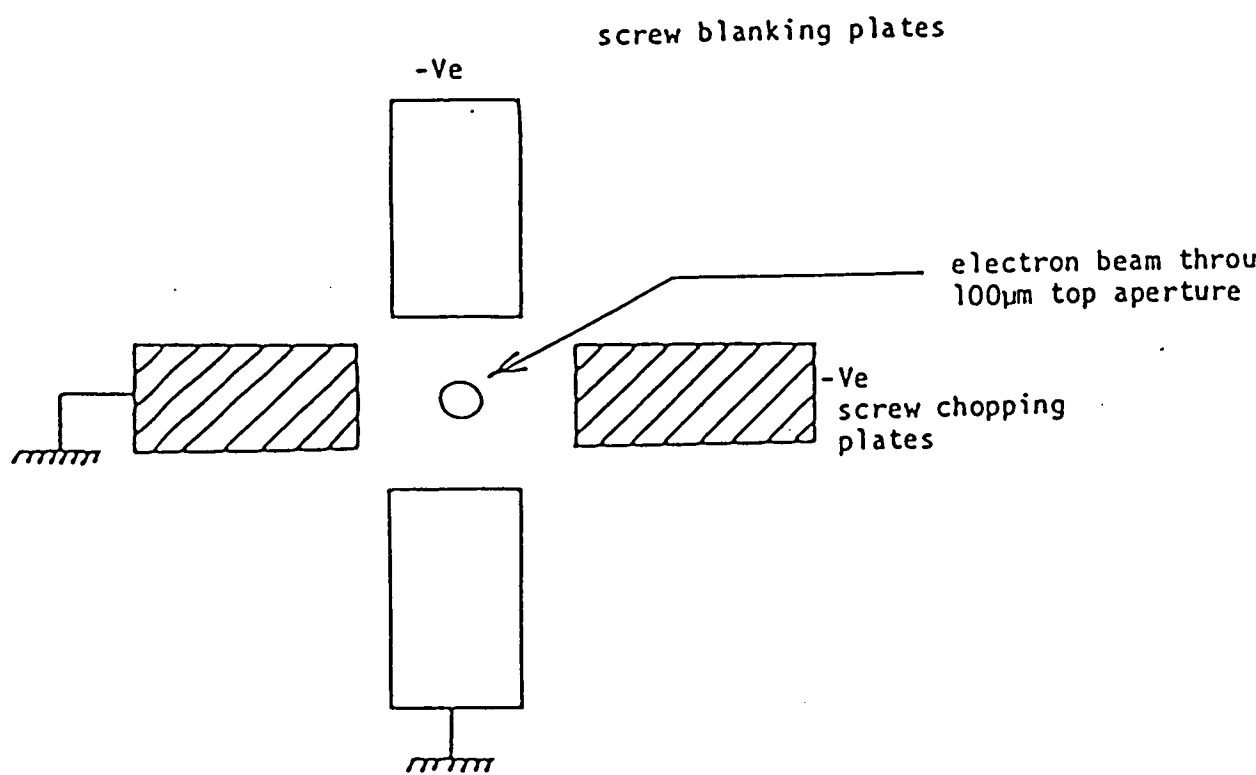
Thomas et al (1976) have reported using a step recovery diode (S.R.D) to give very fast speed switching (see Figure 3.10) to study emitter coupled logic (ECL) devices, which is not essential for the present applications.

3.7 CHOPPING SYSTEM PERFORMANCE

3.7.1 Beam Switch Position

The present chopping assembly is positioned between the gun and the first lens for the following reasons:

It is possible to fit the electron chopping assembly at any place in the electron optical column of the SEM, but above and below the first lens offers the opportunity of using the final aperture image (FAI) as a small chopping aperture. With the chopping assembly above the first lens, a large deflection angle is needed as the divergent beam has to be deflected across the FAI (see Figure 3.6), with a large field of view
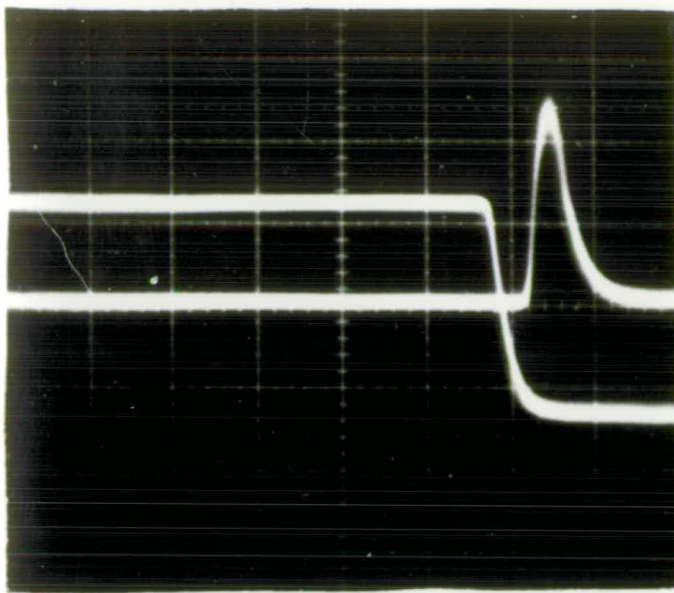
(a) upper trace is SEM
video pulse o/p

lower trace is chopping
pulse

H = 2μs/cm
V = 2V/cm
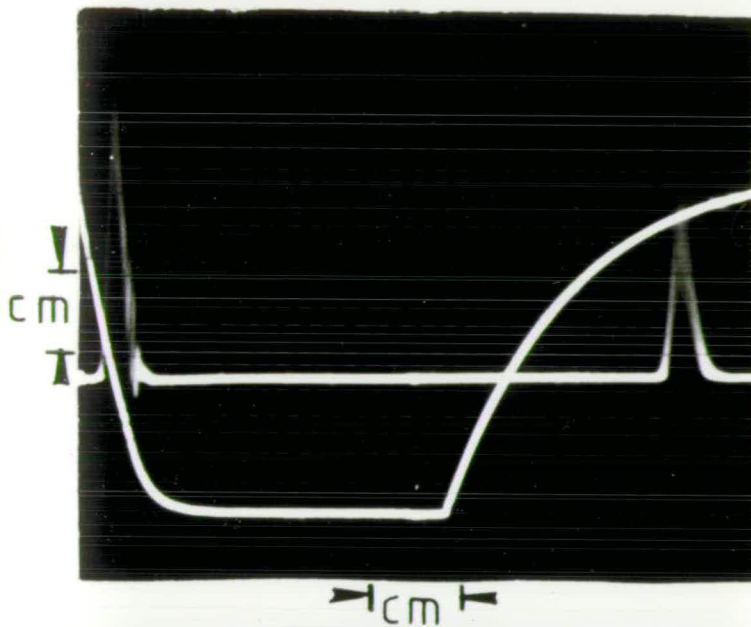
(b) bright trace is
chopping pulse

dark trace is SEM
video pulse (two
pulses per period)

H = 1μs/cm
V = 0.5V/cm (dark)
    2V/cm   (bright)

without dc bias
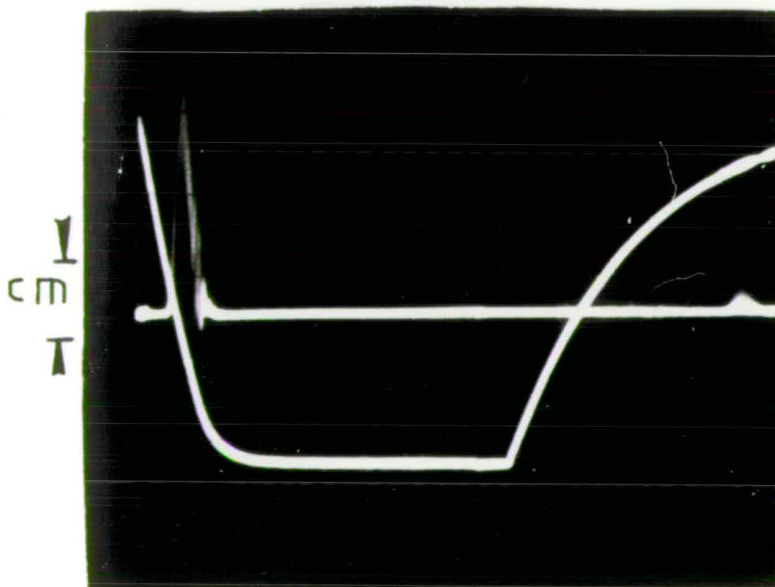
(c) same but with dc
bias

Figure 3.37: Shows two pulses per period problem
in beam switch.

causing severe degrad ation (Gopinath and Hill (1974).

A100 µm aperture has been used at present for reducing deg rad a-
tion to a certain limit, it is also the simplest set up, and causes the
least change in the electron optical column. If the deflection angle
has to be kept to a modest value, the crossover is brought as near to
the FAI as is compatible with the column demagnification, and the chop-
ping degrad ation may be kept to a small value by limiting the field of
view with an appropriate choice of top aperture.

3.7.2 Beam Switch Efficiency

Feuerbaum and Otto (1982) have reported a primary electron leak-
age current flows in the pauses between pulses which means that the
electron beam is not blanked completely when potential difference is ap-
plied to the plates. This leakage current is considered as a constant
amplitude and as a part of the full beam current for present. Figure
3.38 shows beam switch devices developed at present.

To test the efficiency of the present chopping plates, the follow-
ing procedure is required:

1. The effectiveness of electron beam cut-off

- This is achieved by looking at any point on the specimen and measuring
the signal level for:

   - full beam current where the plates are earthed, I_B

   - chopped beam current when voltage v_{off} is on the plates, I_C
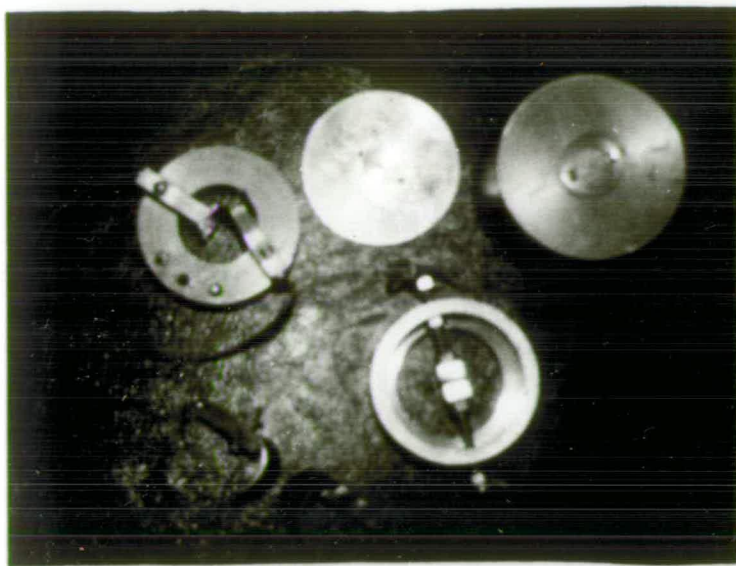
(a) Different types of beam switch devices.
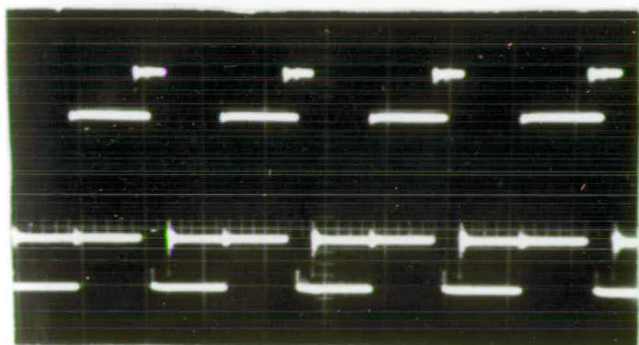
(b) upper trace is blanking pulse

lower trace is chopping pulse

H = 2μs/cm
V = 1V/cm
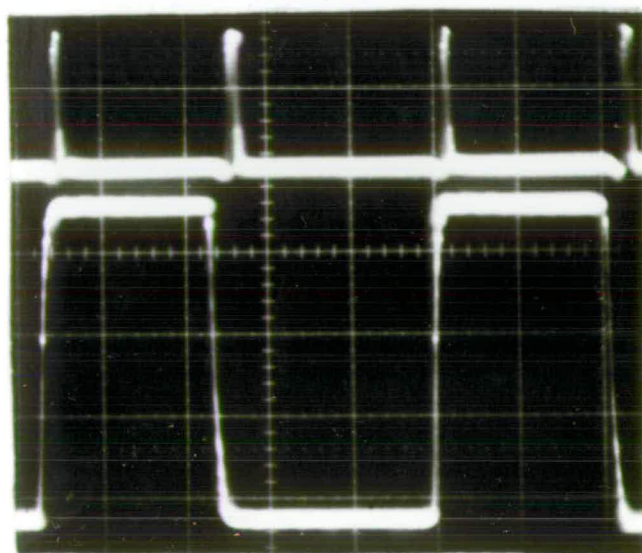
(c) upper trace is SEM video pulse

lower trace is chopping pulse

H = 2μs/cm
V = 5V/cm upper
    1V/cm lower

Figure 3.38: Snows present beam switched as tools for stroboscopy and sampling techniques.

Chopping efficiency of beam switch = $\dfrac{I_B - I_C}{I_B}$ * 100%   (3.1?)

2. Degrad ation of resolution

Occurs due to movement of the spot before it cuts off. This is actually more difficult to measure, but by viewing at a high magnification, some effectw as noticed and an estimate made of its magnitude.

3. The limiting speed of the electron beam switch

A direct measurement of switching is difficult, but measuring the change in the rise time of the voltage at the chopping plates (see Figure 3.36) can give an indication of how fast the beam switch is working, which was measured for the present. The maximum frequency at which stroboscopy works will give an indirect measurement of the switching time.

The electron beam switch has been tested with different types of waveforms, sinusoidal, rectangular, triangle. These show the linearity of the chopping system assembly as depicted in Figures 3.39 & 3.40, indicating a significant performance of the present chopping plates. But due to bandwidth restriction of the SEM collector which shows video sig-
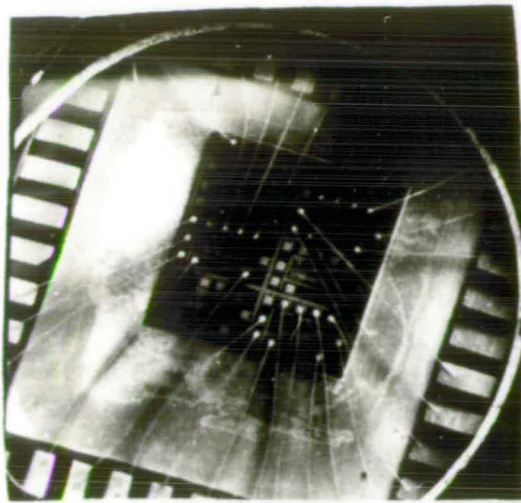
X20

(a) Topographical micro-
    graphy with beam
    switch is earthed
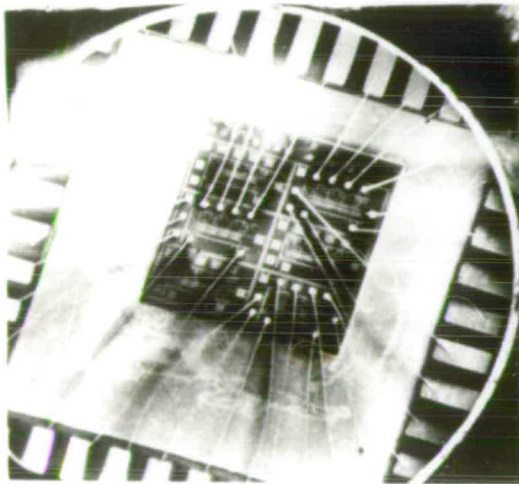
X20

(b) Topographical micro-
    graphy with beam
    switch with dc bias,
    with beam voltage of
    2keV.
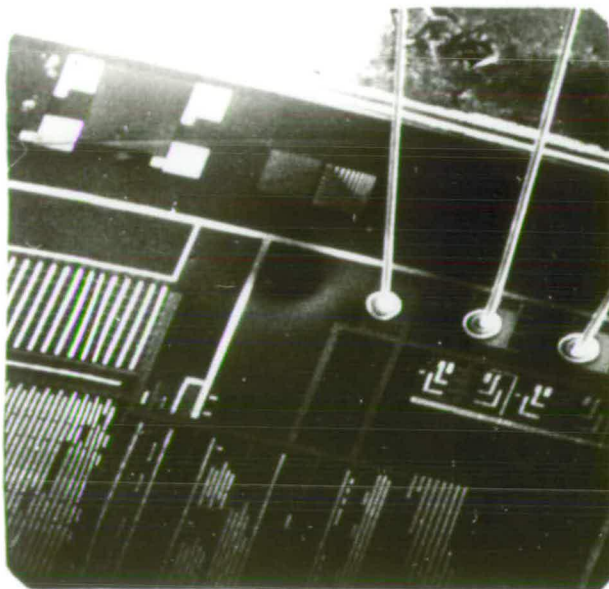
X500

(c) Topographical micro-
    graphy with beam
    switch with dc bias,
    with beam voltage of
    15keV.

Figure 3.39: Shows the performance of beam switch.

(A)
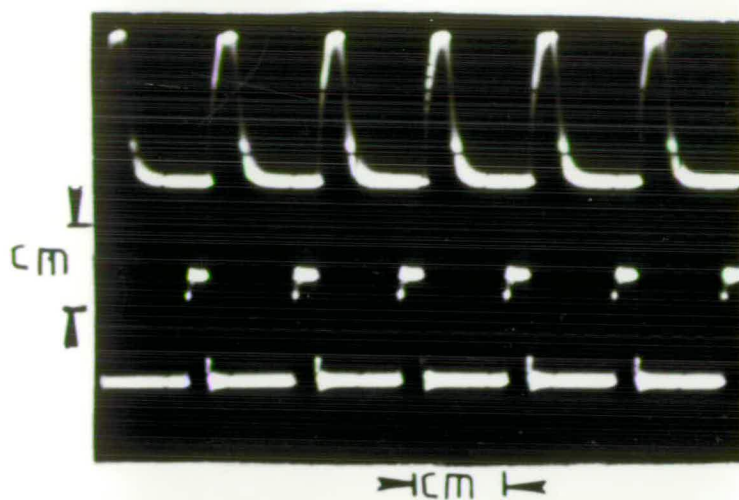
V = 0.5V/cm.
H = 0.5μs/cm
f = 1MHZ

upper trace is video o/p
lower is i/p pulse
using deflection coils
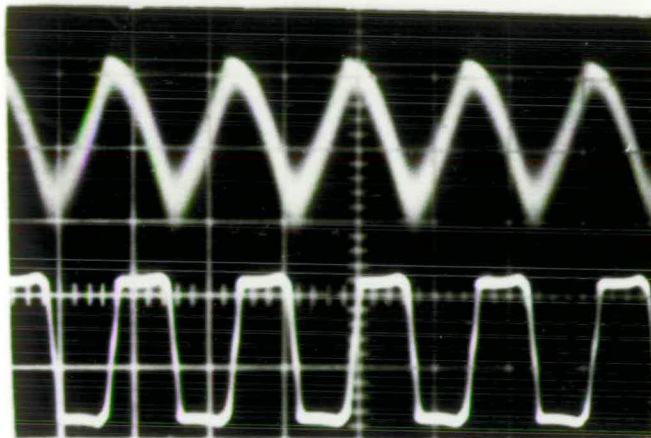
(B)

upper trace is SEM
collector output.

lower trace is square
pulse voltage on plates

V = 1V/cm
H = 0.1μs/cm
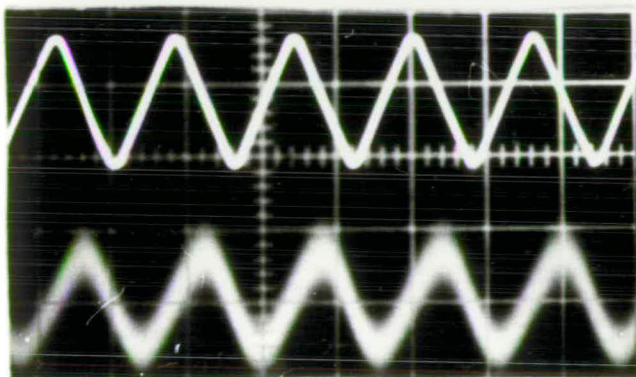
(C)

upper trace is triangle
pulse to the plates.

lower SEM collector
output

V = 1V/cm
H = 0.1μs/cm
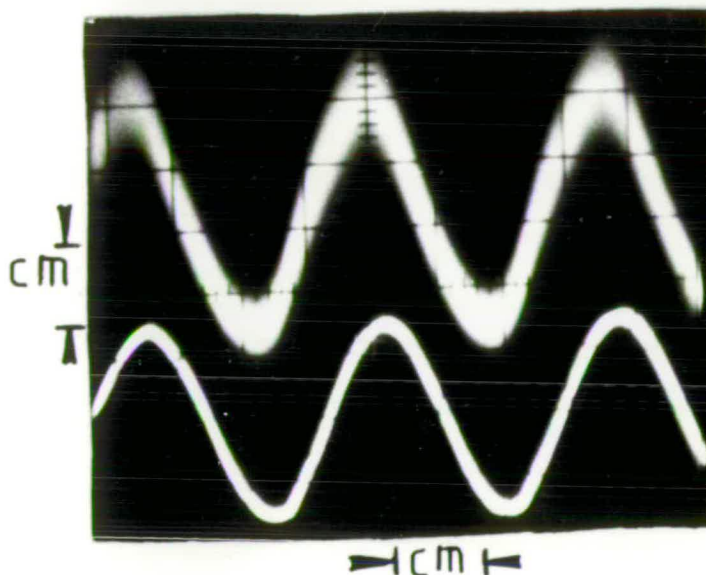
(D)

upper trace is SEM
collector output

lower is sine voltage
on plates

V = 3V/cm
H = 1μs/cm

Figure 3.40: Shows present beam switch linearity checking

nal output with time delay (see Figure 3.40) in respect to the input signal to the beam switch, stroboscopy must be used to perform and display high frequency signal up to 10 MHz. The plate length which limits the electron transit time through the plates is found as an important factor to limit the electron beam switching, but only at much higher frequencies than are used in the present work.

3.7.3 Plates Performance At Different Frequencies :

Figure 3.36 shows the chopping system performance at different frequencies as follow :

In (a), the video pulse is undistorted because of the slow edges on the chopping pulses.

In (b), the pulse on the trailing edge of the chopping pulse is only slightly distorted , but the one at the leading edge has lost amplitude

In (o), both pulses are severely affected, with loss of height and with pronounced decay effects on the trailing edges. There is a delay of = 200 ns.

The above effects are due principally to the restricted bandwidth of the head amplifier and the scintillator.

3.8   DISCUSSION

The performance of the recently designed chopping plates appears to be quite satisfactory, as shown by the results of Figures 3.39 & 3.40. The rise time and part of the delay on the output signal is caused by the restricted performance of the SEM video head amplifier, which has a limited bandwidth.

Chopping by magnetic deflection has advantages so far as contamination problems are concerned but at high frequencies it becomes inefficient. It is found to produce a time delay of about 250 ns to the input signal. However, as shown in Figure 3.28 and 3.40, it can be used effectively at low frequencies.

The transit time (flight time) of the electrons down the column is a significant factor, and has contributed to delays present in Figure 3.40. At very high frequency the transit time of electrons through the chopping plates is also significant and leads to a loss of efficiency. This problem can be overcome by the use of travelling wave deflection structures. But this problem does not arise with pulse widths around 1 ns which is the concern of this present work.

The problem of two pulses per cycle has been overcome by using chopping and blanking plates. Blanking pulse which is produced to chop -off the electron beam during the fly back period of the chopping pulse as shown in Figure 3.38. A -ve d.c bias up to 15V is used, and found to solve the problem of being double pulses so that only one pulse is produced per cycle (see Figure 3.37). For high speed switching of electron beams double plates were developed(see Figure 3.31). Similar electronic circuits have been used as beam switches (pulse shaper), for both chopping and blanking plates, where blanking pulse has fixed delays of about 20 ns from the chopping pulse (coaxial cable of about 4 m

length is used).

Curved plates are suggested for large deflection angles, and to solve the problem of electron beam non-alignment which is important for the present machine(see Figure 3.30). For the present study of MOS devices, ordinary parallel plates were found to be suitable to test these devices under dynamic operation.

CHAPTER FOUR

OBSERVATION OF HIGH FREQUENCY SIGNALS

USING ANALOGUE CIRCUITRY

4.1 INTRODUCTION

This chapter describes a system, using analogue circuits, which was developed in order to measure a high frequency waveform at any point on a specimen under test, using the chopped electron beam as the circuit probe. Figure 4.1 shows the analogue sampling system built at present.

The techniques used were based on the type of circuits which are used in sampling oscilloscopes, and a survey of such work which has been previously carried out by other workers is included. A requirement imposed on the new system was that it should be fully controllable by computer via the IEEE 488 bus, in view of the fact that in any system to be used with present and future IC's, it is essential that most measurement and control functions should be co-ordinated and controlled by computer.

4.2 WAVEFORM MEASUREMENTS

4.2.1 Introduction

The methods are to measure high frequency voltage changes in the waveforms at a particular specimen node. The measurement consists of two sections
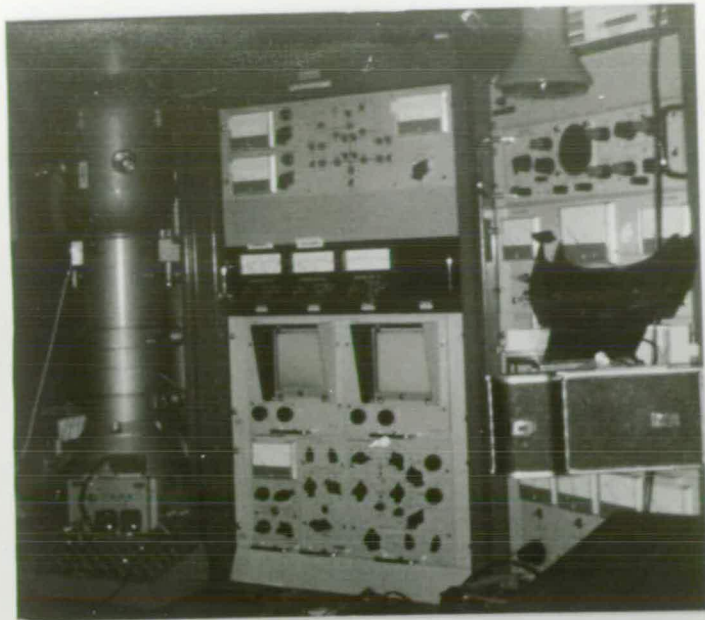
(A)
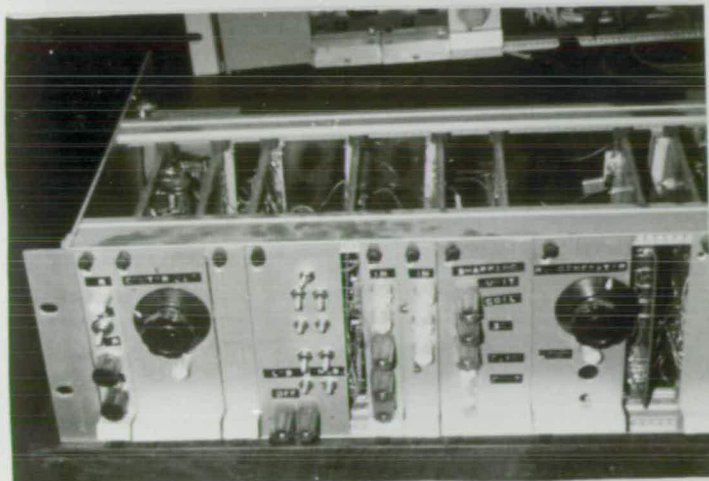
(B)
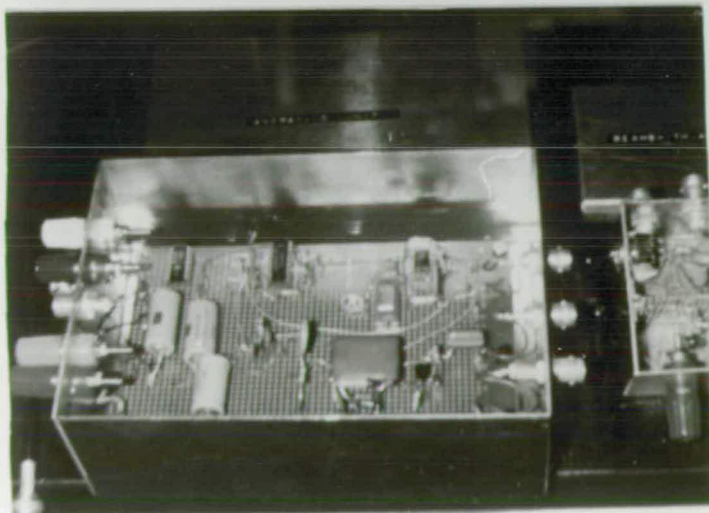
(C)

Figure 4.1 : (A) shows machine of scanning electron microscope (SEM-S$_2$), (B) present analogue sampling system (C) Averaging unit.

(a) phase definition

(b) signal processing unit

The electron beam is pulsed in such a way that it only strikes the measurement point at one particular phase of the waveform. The voltage at the measurement point is determined quantitatively by the signal processing using the secondary electrons which have been generated at that phase. To measure the entire waveform the phase of the primary electron pulses and the phase of the gate are shifted relative to the waveform from Balk et al(1976) ,Thomas et al (1976), and Feuerbaum (1983).

4.2.2 Electron-beam Testing Methods

These are :-

(a) voltage contrast

(b) voltage coding

(c) stroboscopic voltage contrast

(d) logic state mapping

(e) timing diagram

(f) real time voltage contrast

(g) waveform measurement

(h) quantitative voltage measurement

For more detail see Feuerbaum(1983);the present work is mainly

concerned with (c) and (g) only.

4.2.3 Stroboscopic Voltage Contrast

Stroboscopic voltage contrast allows the local distribution of periodic voltage changes to be visualised at a certain time window "Feuerbaum 1983". The time window is expressed as t, with time period T. The duty cycle is :

$$C = t/T \qquad\qquad (4.1)$$

where C is duty cycle

and t = phase (time window).

The duty cycle is a measure of the accuracy with which the stroboscopic voltage contrast technique can resolve the period of a voltage change in time.

There are three methods of producing stroboscopic voltage contrast micrographs:

1.   Video gating (Oatley and Everhart(1969)).

2.   Beam pulsing (Plows and Nixon(1968)).

3.   Box car averaging (Feuerbaum and Otto(1981)).

4.3 ANALOGUE SAMPLING SYSTEM REVIEW

This survey is on the work of the Bangor group, who were the first
to deal comprehensively with an analogue system to produce the sampling
SEM technique by using analogue electronic circuitry. In addition
the reported systems which displayed oscillographs of high
speed signals were mentioned in chapter two.

Thomas et al (1976) have reported using analogue circuitry
to show the stroboscopic mode on devices placed in the SEM.
A complete system is shown in Figure 2.7,
and circuitry in Figure 2.8 b (chapter two). It was therefore decided
to cover and concentrate on this work as a reference in this field.
Basically this group had interfaced the SEM with sampling circuitry as
shown in Figure 2.8b, on the lines of a sampling oscilloscope .

" The electron beam, held on a spot on the semiconductor device, was
turned "on" for the sampling period fulfilling the role of the
usual sampling diodes.

The sampling circuitry could operate up to a maximum frequency of 1 MHz
and periodic signals up to 18 MHz were sampled and measured at
some subharmonic at or below 1 MHz frequency.

Synchronisation was achieved by the trigger circuitry which is like
that used by a sampling oscilloscope. The time base circuitry
for stepping the phase and displaying the signal was also
retained except that the number of samples taken at each phase or time delay
position is variable, with beam sampling pulse widths down to 100 ps."
(from Thomas et al(1976)).

They built a delayed trigger pulse generator as shown in Figure 2.8b
which was built around the time base circuitry of the Hewlett Packard

(H.P) sampling oscilloscope time base unit of type (1811A).

They described how this circuitry works. The
trigger circuit block was capable of responding to the signal
waveform at the input with a step voltage which initiates a timing voltage
ramp(See Figure 2.8 b). They used a precision comparator to produce
a trigger pulse every time the ramp voltage reaches a d.c reference voltage.

The trigger pulse was amplified by the strobe driver before being applied
to the beam switch.

They reported that the reference voltage level determined the
delay between signal recognition by the trigger circuit and the
production of a trigger pulse. The reference voltage is derived
from a digital to analogue converter
(DAC)and advanced by the control logic. The signal waveform on the device
was sampled over its entire phase by varying the reference voltage and
thereby delaying the occurrence of the beam pulse. Since the sampling
frequency of the type (1811A) circuit is limited to a maximum of 150 KHz,
modifications were made to increase this frequency to 1 MHz. The areas
shown cross-hatched in Figure 2.8b[p 11]indicate the parts of the circuit that
required modification.

They reported that these alterations have not produced any noticeable
degradation of the circuit performance. They described the work of
control of multiple sampling as the triggered beam switching
system was operated in the normal sampling oscilloscope
mode with one sample being taken at each discrete time point. However,
since the measurement time with the chopped electron beam was many
seconds, it necessary to hold the phase of the sample constant for
a larger number of the 1 MHz sampling pulses than they suggested.
The delay was controlled, in the sampling oscilloscope time base,

which steps at each trigger pulse.

The trigger delay control unit, with its schematic shown in Figure 4.2, produced a staircase ramp which was triggered at a frequency much lower than the trigger pulses emerging from the time-base. This frequency was derived by digital decade division.

They mentioned that a good stability of the ramp steps was assured by the use of an 8-bit binary divider and a D to A converter supplied with a reference diode.

They used an x-y recorder which was swept by the staircase output of the control unit and the decade counter output operated the pen to record the settled voltage measurement. All measurements were made on a metal stub with the electron beam held on spot. They reported an effective system rise time of about 3.5 ns.

Gopinathan and Gopinath (1978) have suggested the same set up for the samplin SEM as shown in Figure 4.2. They added to their first report of 1976 , a circuit to block the initiation of a new ramp before full recovery of the previous one by using a hold-off circuit, using a monostable circuit, which, when triggered, inhibited further triggering until it had returned to its stable state. The output pulse width was reduced to obtain smaller hold-off periods and a minimum hold-off time of 800 ns had been obtained. They developed the sampling SEM for the study of high-speed bipolar logic circuits of emitter coupled logic (ECL) using these ideas.

Most of reported sampling systems are basically analogue type depending on the conventional sampling oscilloscpe principle, which produces a timing jitter problem in the reconstructed waveform.

The Bangor group work is incompatible with the present work purposes. Because they used electron beam accelerating energy of 25 keV with operating
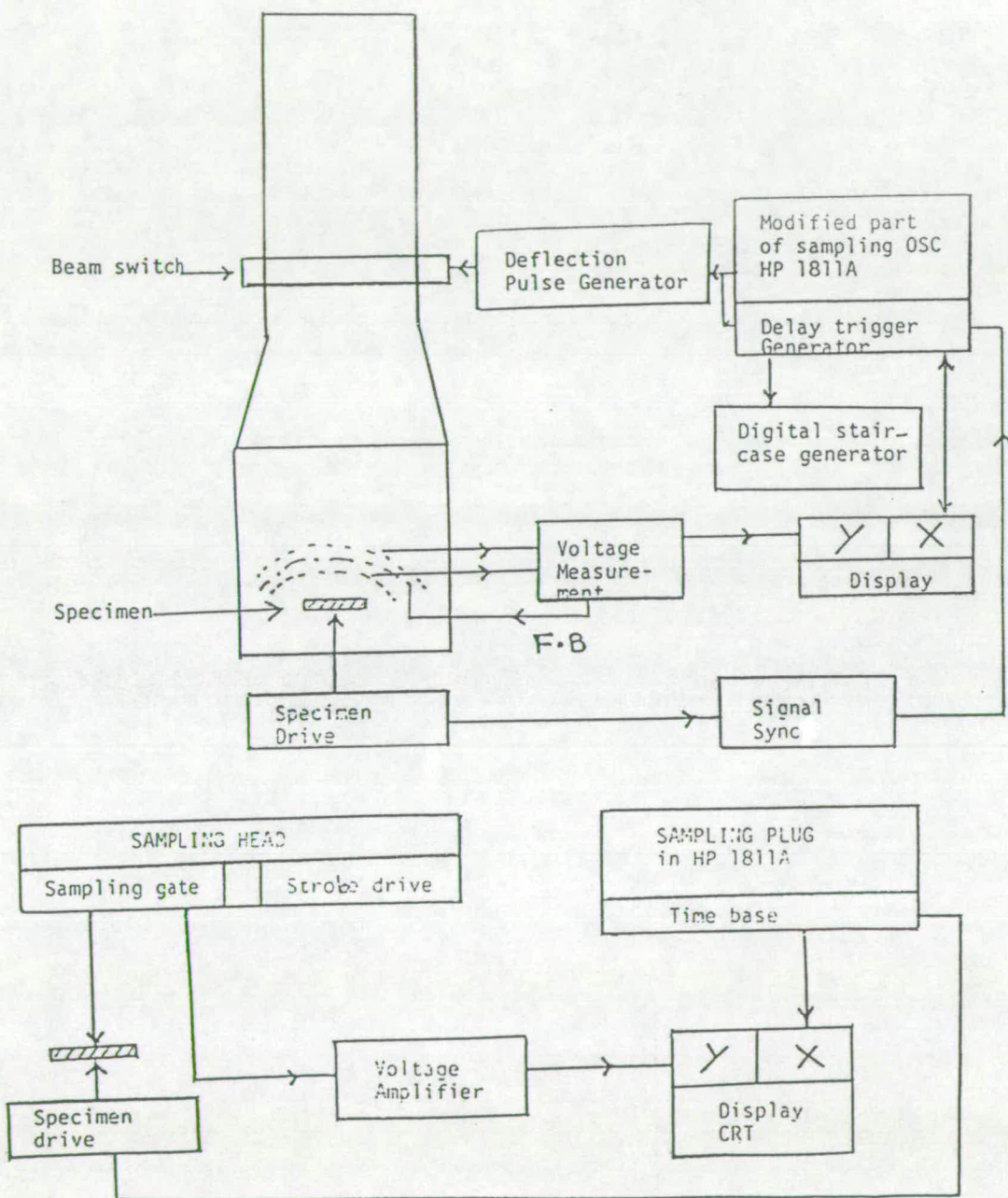
FIGURE 4.2: Comparison between the SEM Sampling System and Commercial Sampling Oscilloscope (From Gopinathan and Gopinath 1978)

frequency up to 1 GHz to test ECL devices. Their reported techniques

of analogue sampling circuitry and beam switching were considered for comparison

with analogue circuit design.

4.4 SAMPLING SEM

4.4.1 Using the Sampling Technique in the SEM

The design of analogue circuitry for sampling is based on the princi-
ple of the sampling oscilloscope. It is desired to reconstruct and
measure a high frequency waveform on a specimen under dynamic operation,
with time resolution of about 1 ns, and with repetitive signal frequency up
to 10 MHz.

Voltage measurement in the SEM requires the linearisation of the
voltage contrast phenomenon, most systems of linearisation are slow, be-
sides the limited bandwidth of the SEM collector. The main aim of this
work is to let the SEM collector respond to the collected signal and to
display data dots on the display to produce a reconstructed waveform.

In a sampling SEM, the electron beam is on the point of interest
where the high frequency signal is and many sampled are taken from the
waveform under test (see Figure 23). The sampling signal waveform is
applied to the chopping assembly which was mentioned in Chapter Three to
chop the electron beam "off" and "on", in synchronisation with the sig-
nal applied to the specimen under test. The sampling unit fixes the
phase position of the beam, depending on the required number of samples
needed at each phase position, also the number of phases to be sampled
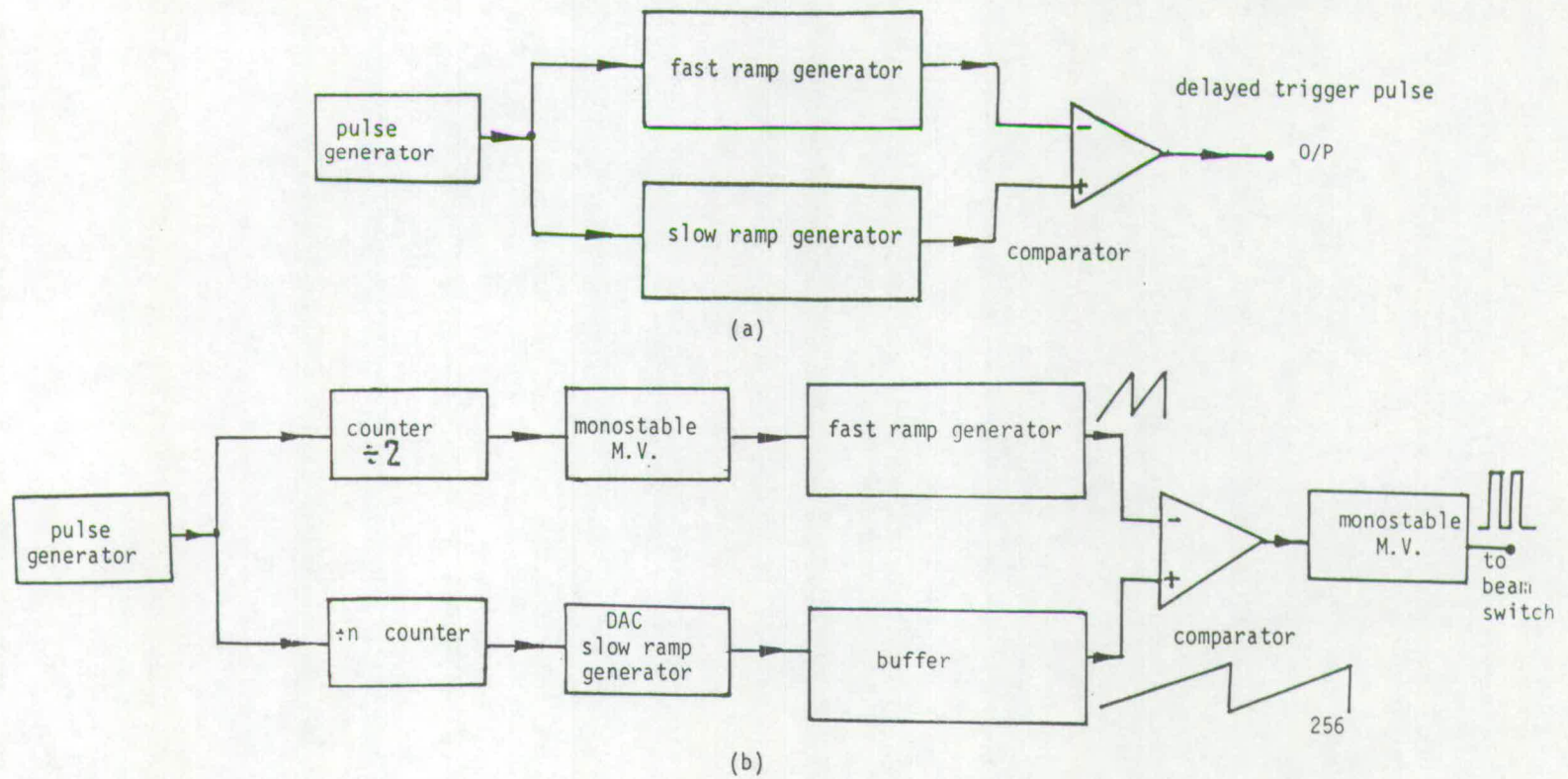
Figure 4.3: Basic analogue sampling system (a) simple block diagram (b) detail of block diagram

over the waveform.

4.4.2 Sampling SEM Requirements

In the stroboscopic SEM, the sampling phase was fixed and the electron beam scanned over the specimen.   The delay between the sampling pulse to the beam switch and the   input signal fed to the specimen under test ∧ In this equipment, toggle switches are used to
was fixed
change the phase manually or remotely by computer control as required.

In the sampling SEM, variable phase is used and the electron beam is fixed on one point of the specimen. The waveforms of voltages at nodes in the specimen are traced by developing a programmable delay gen- erator, where the phase is continuously varied. One measurement of the waveform is obtained after n pulses, the phase is then shifted and the same procedure repeated until the whole cycle has been completed. The phase is controlled by using programmable counters.

4.4.3 Incompatibility of Sampling Oscilloscope

To record the waveform at the specimen, under dynamic operation, it was at first suggested that the SEM could interface with a sampling oscilloscope, such as the   time base plug-in unit of a Tektronix (S711) sampling oscilloscope (7000) series. From simple practical experiments performed to investigate whether it could be used as SEM sampling tool, it was found that the sampling oscilloscope time base was inconvenient to use and required hardware modifications to operate at the frequencies required.

Therefore it was decided to start from scratch, designing simple

analogue circuitry for sampling and delay units on the lines of a sam-
                        This circuit was required
pling oscilloscope. to produce a fast ramp signal (using a current

source, electronic switch and capacitor), to be compared with the refer-

ence slowly varying d.c level (the "slow ramp"). This was produced by

using programmable counters and a digital to analogue converter (DAC),
                        as
in such a way to produce a delayed trigger pulse per phase.

The d.c level of the slow ramp for each step, determined the time

delay between the input trigger pulse to the sampling system and the

comparator output delayed pulse to the beam switch.

4.5 THE PRINCIPLE OF THE PRESENT SAMPLING SYSTEM

4.5.1 Introduction

                    circuit
The basic of the present analogue system is shown in Figure 4.3.

The integrator is used as a useful source of the linear ramp waveform.

The principle details are given elsewhere (Horowitz and Hill (1980)).

The fast ramp is produced by using a current source and capacitor with

an electronic switch shunted across it. The speed of the ramp is deter-

mined by the capacitor.

For the slow ramp a programmable counter is connected to a digital

to analogue converter through an open collector gate. The resulting slow

ramp signal, is considered as a d.c reference voltage (see Fig-

ures 4.4 & 4.5). Both fast and slow ramp signals are used to produce an

analogue sampling system as shown in Figure 4.6. Figure 4.7 shows a
                    the   the
block diagram of sampling apparatus with analogue ramp delay generators

used for the present work.

+V$_{CC}$

56K

100K

22K

C

1N

(A)

+V$_{CC}$ = 15V

2.7K

+15V

A

+

−

−15V

from
pulse
generator

in

÷2

counter

(B)

+V$_{CC}$ = 15V
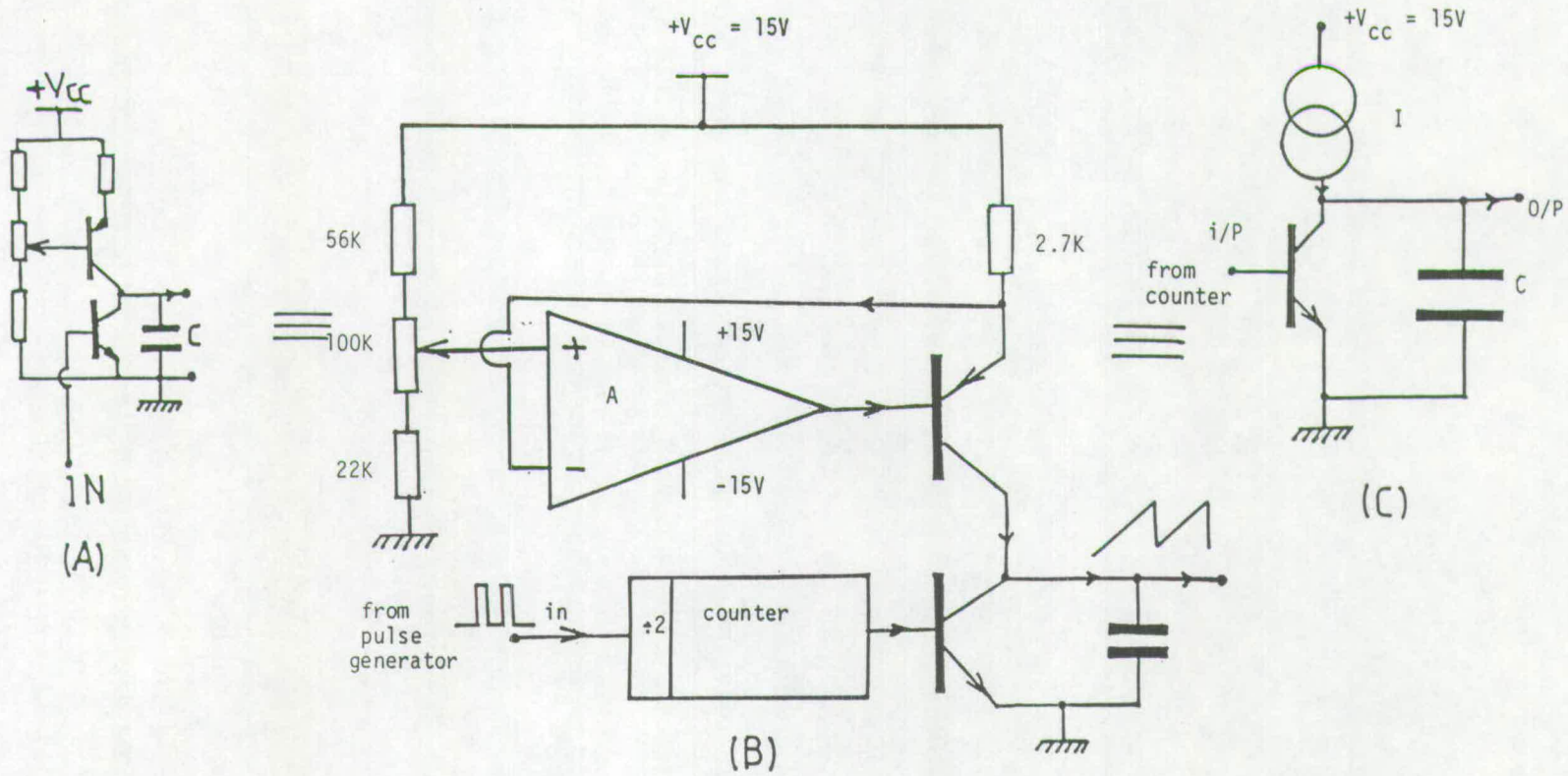
I

i/P

from
counter

O/P

C

(C)

Figure 4.4 : Shows fast ramp generator
            (A) discrete circuit (B) circuit with op amp (C) basic circuit.
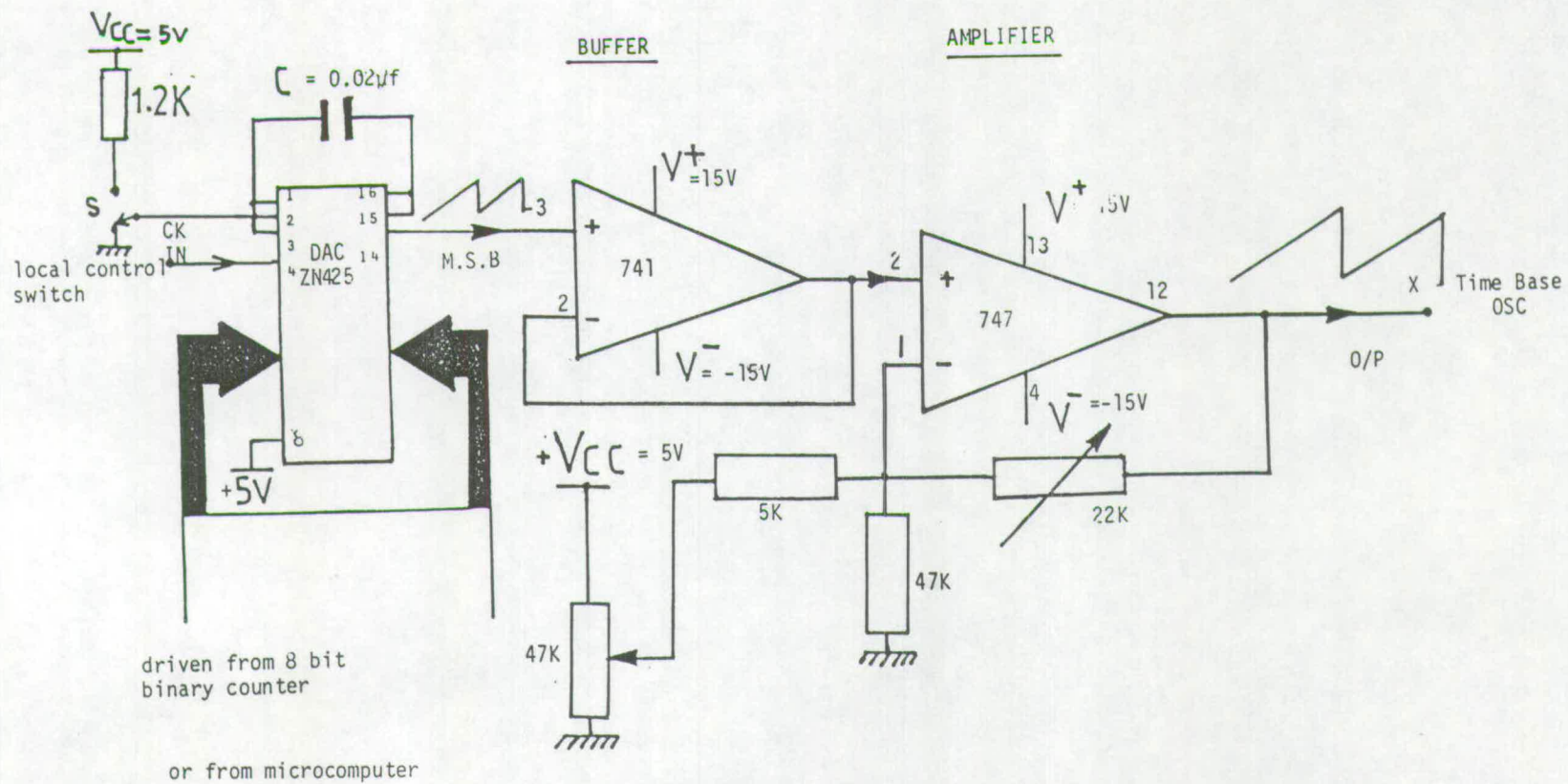
Fig 4.5 : Shows circuit for variable gain and offset of DAC - slow ramp generator
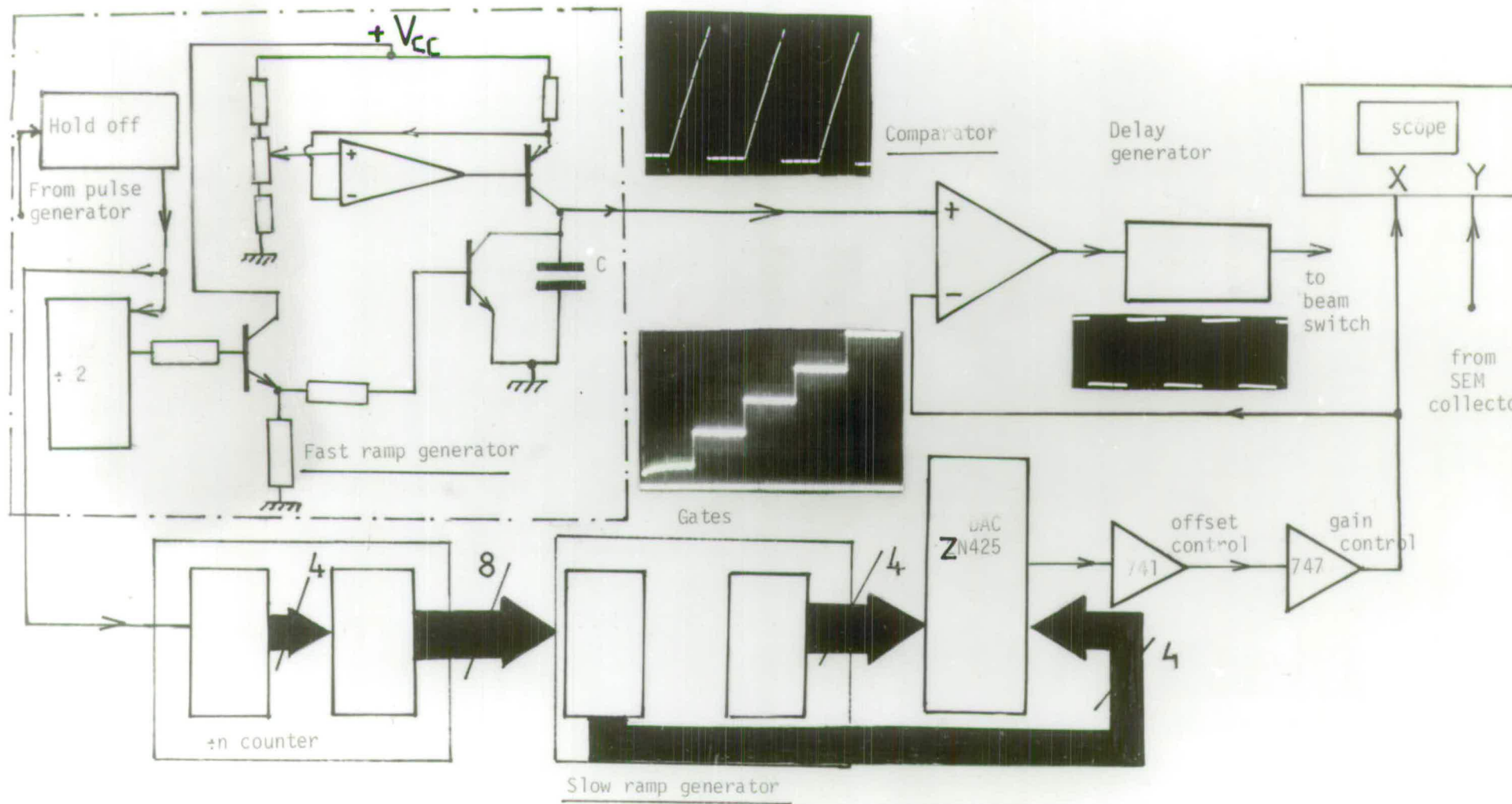
Figure 4.6 : Snows present analogue sampling system circuitry.
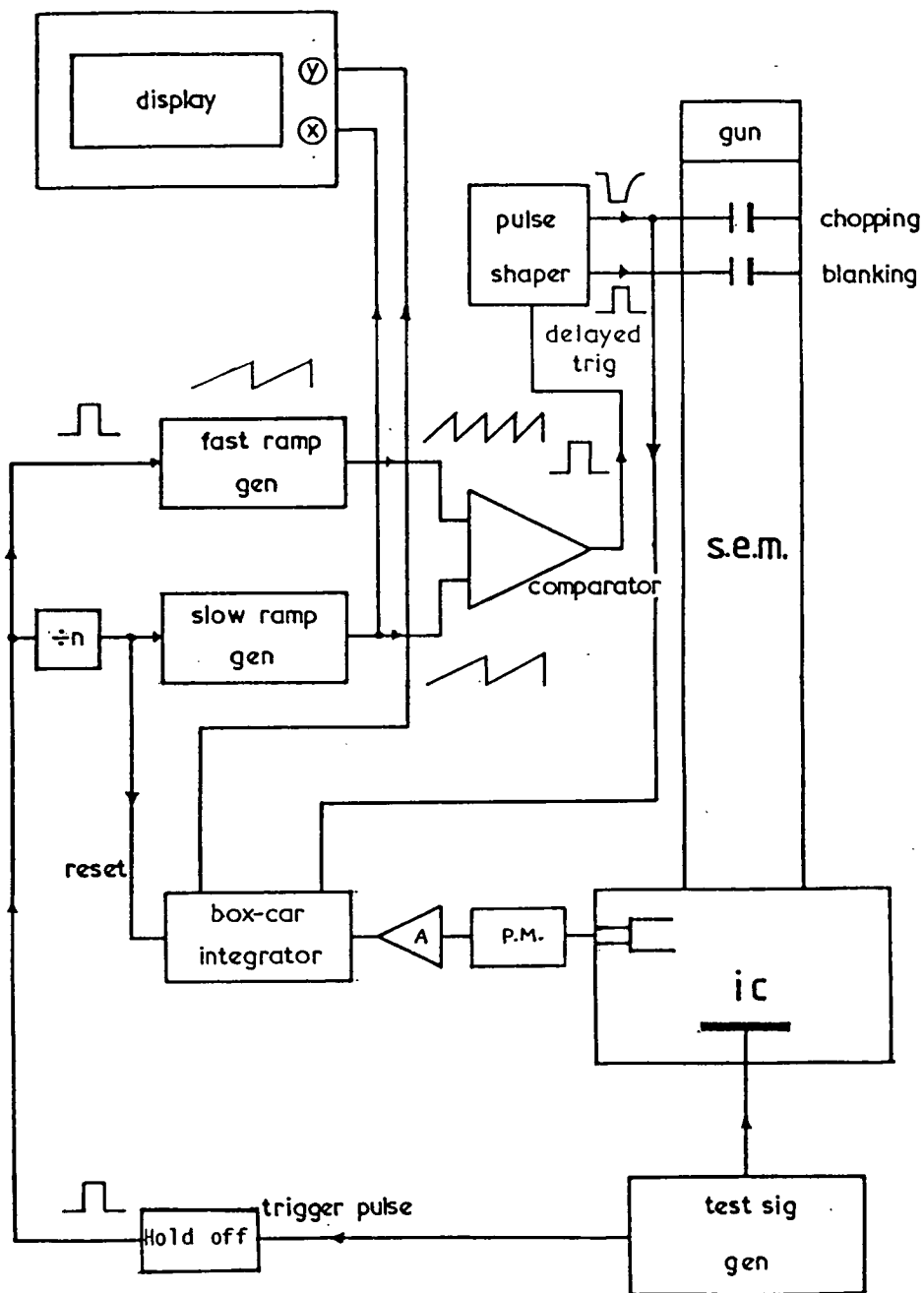
Figure 4.7: Sampling apparatus with analogue ramp delay generator.

4.5.2 A Design for Stroboscopy and Sampling of the SEM

(a) Fast ramp generator design

This basically works in the same way as the commonly used ramp genera-tor. The circuit involves a constant current source, electronic switch and capacitor (see Figure 4.4). The capacitor charges and discharges to produce a ramp waveform according to:

$$Q = C.V \tag{4.2}$$

and by differentiation with respect to time

$$dQ/dt = C \, dv/dt, \quad \text{and since } i = dQ/dt$$

therefore

$$i = C \, dv/dt \tag{4.3}$$

which shows how the voltage changes with respect to the time in the capacitor. Equation 4.2 is used to design the fast ramp.

Determining the speed of the ramp signal depends on values of capacitor (C) e.g. if V = 2 V, t= 10 us, i= 1mA, C = 5 nf, so if t, V and i are proposed, capacitor can be found.

Two types of current sources have been developed as shown in Fig-ure 4.4; one designed and built from discrete components for the high speed ramp signal up to 10 MHz frequency, the other with operational am-plifier, to control the current through the switch work up to 1 MHz fre-quency. From experiment work the capacitor value is found as an impor-

tant factor in limiting the fast ramp generators' speed. Different ramp signal speeds have been used at present as shown in Figure 4.8.

(b) Slow Ramp Generator Design

This actually involves a programmable counter (divide by N counter) with digital to analogue converter, so as to produce steps to achieve a phase difference each time the ramp generator signal changes its amplitude. This ramp can be controlled manually or remotely.

Counters are employed to ensure the waveform of interest is investigated once in every two cycles or once in every eight cycles or whatever is required. Details of how the DAC produces ramps is given elsewhere (Hnatek 1976). Buffers are used in such a way as to control the d.c offset, and the amplitude of the ramp signal as required (see Figure 4.5).

4.5.3 Principle Of Analogue System Operation

The analogue sampling system basically depends on the conventional sampling oscilloscope principle (see Figure 2.4), as follows:

(1) The input trigger signal from the fast signal generator is fed to both fast and slow ramp generators through the hold_off unit, it is fed also to the specimen under test. This initiates two ramp voltages.

(2) When the fast ramp reaches the quasi d.c level reference corresponding to the slow ramp, then the comparator produces a delayed trigger pulse, which is fed to a monostable multivibra-
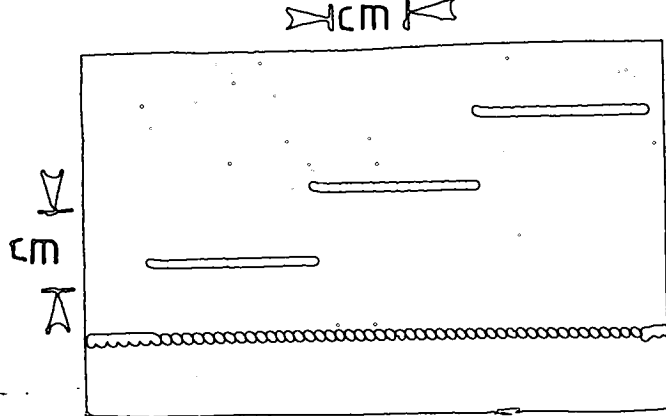
H = 0.2 ms/cm
V = 1 V/cm
slow ramp   + fast ramp signals.
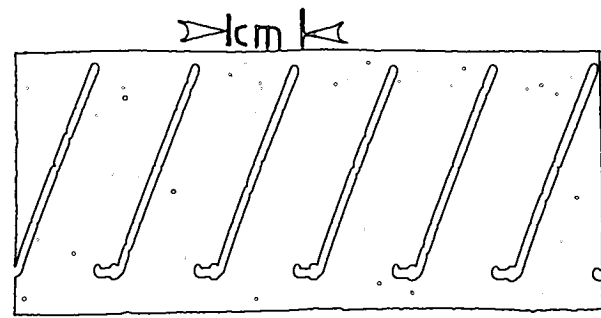
H = 50µs/cm
V = 1V/cm
fast ramp
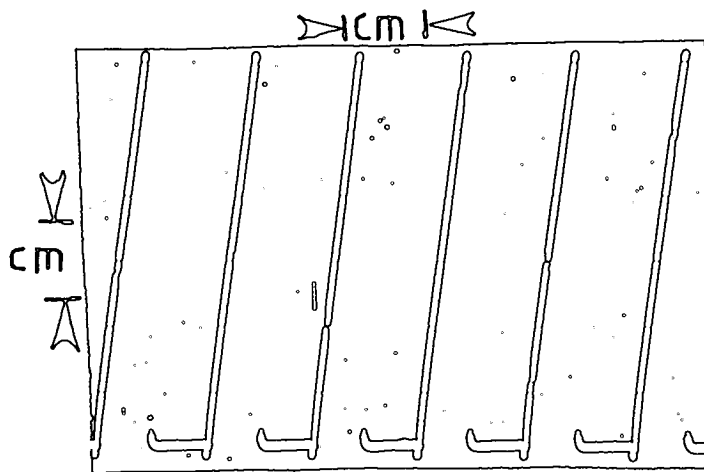
H = 5µs/cm
V = 50 mV/cm
fast ramp
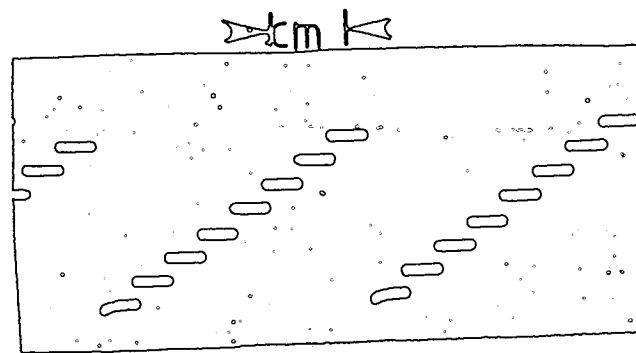
H = 6.2 ms/cm
V = 1V/cm
slow ramp
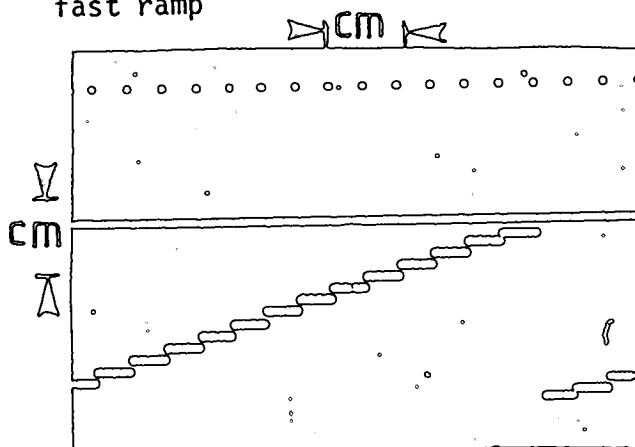
H = 50µs/cm
V = 2V/cm
upper trace is comparator O/P
lower trace is slow ramp
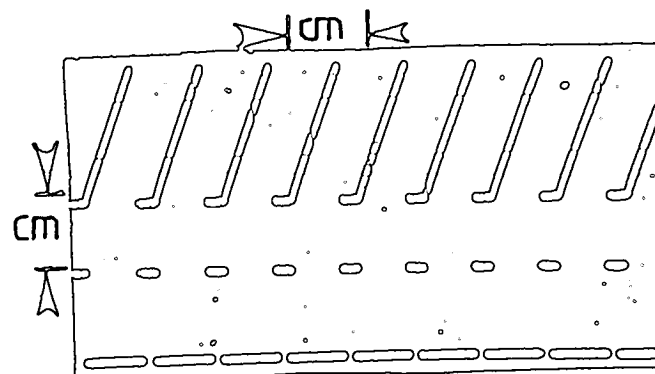
H = 20µs/cm
V = 2V/cm
upper trace is fast ramp
lower trace is ÷ 2 counter
pulse i/p

Figure 4.8: Shows different ramp waveforms with different speeds developed
in analogue sampling systems

tor to produce a short pulse (see Figure 4.6). The time constant of this multivibrator corresponds to the sampling pulse width (switching time). The delayed pulses are then fed to the beam switch amplifiers after shaping by a Schmitt trigger for electron beam pulsing by pulse shaper which turns the electron beam "on" for the sampling period.

(3) The slow ramp signal (quasi d.c level) at the comparator determines the delay between the input signal to the sampling system and the comparator output delayed signal. The slow ramp can be operated manually or remotely to change the sampling phase as required (see Figure 4.9).

(4) Increasing the slow ramps' amplitude leads to delay of the sampling pulses, so that the waveform on the specimen may be resolved over its repetition period.

(5) The hold-off unit is produced by using a monostable multivibrator circuit which inhibits further trigger input signal until it is returned to its stable state.

(6) Beam switch amplifiers built with sufficiently fast speed switching to generate a fast rise time of the sampling pulse to produce a pulse width of 1 ns which is the switching time of the electron beam (see Figure 3.35). Figure 4.10 shows the overall circuitry of the analogue sampling system developed at present.

4.6   SAMPLING - STROBOSCOPIC   ANALOGUE   SYSTEM

4.6.1 System Description

To make the analogue sampling system more flexible to work in
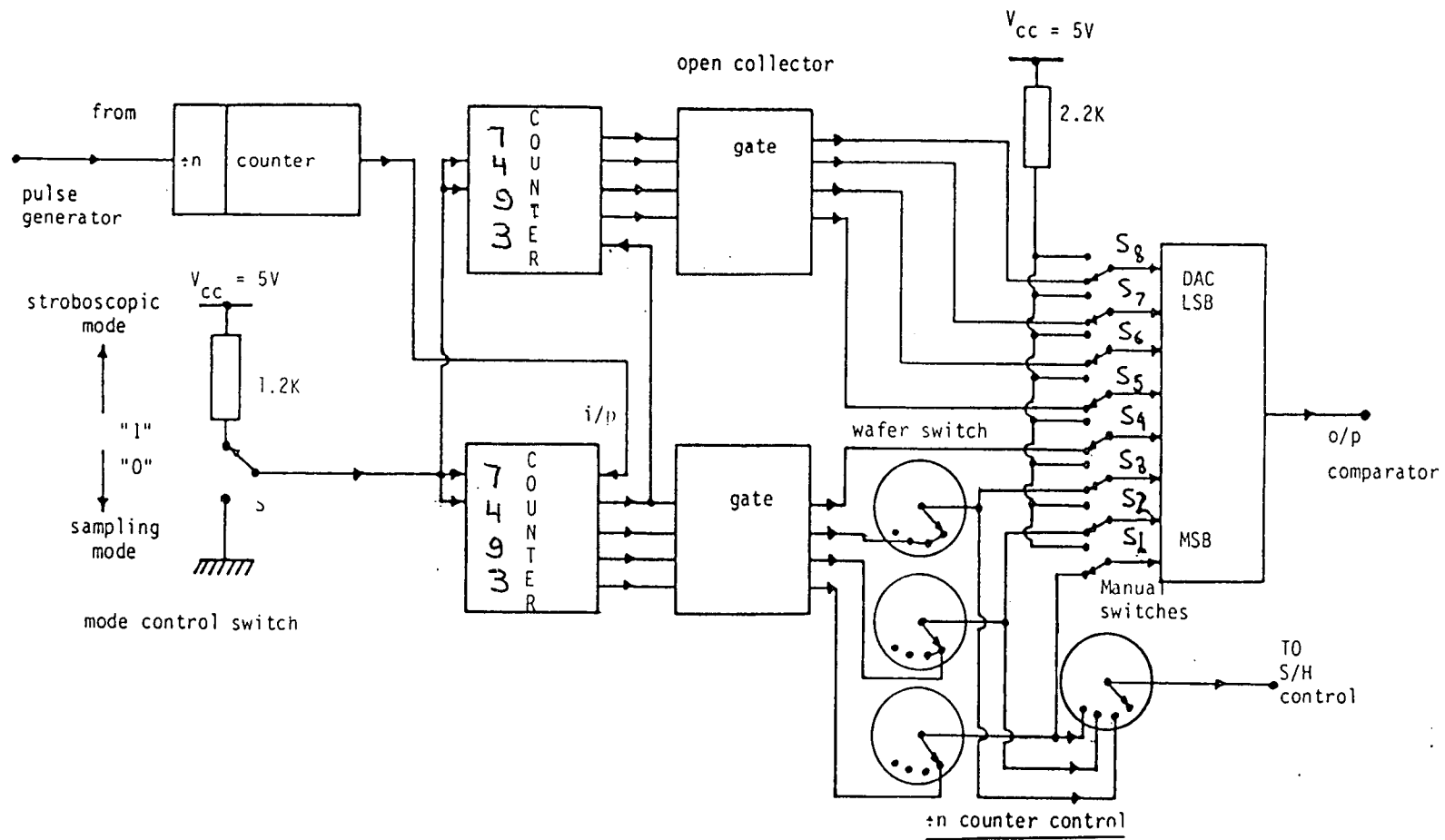
Figure 4.9 : Shows sampling/stroboscopic modes circuitry controlled by local switches (Programmable slow ramp).
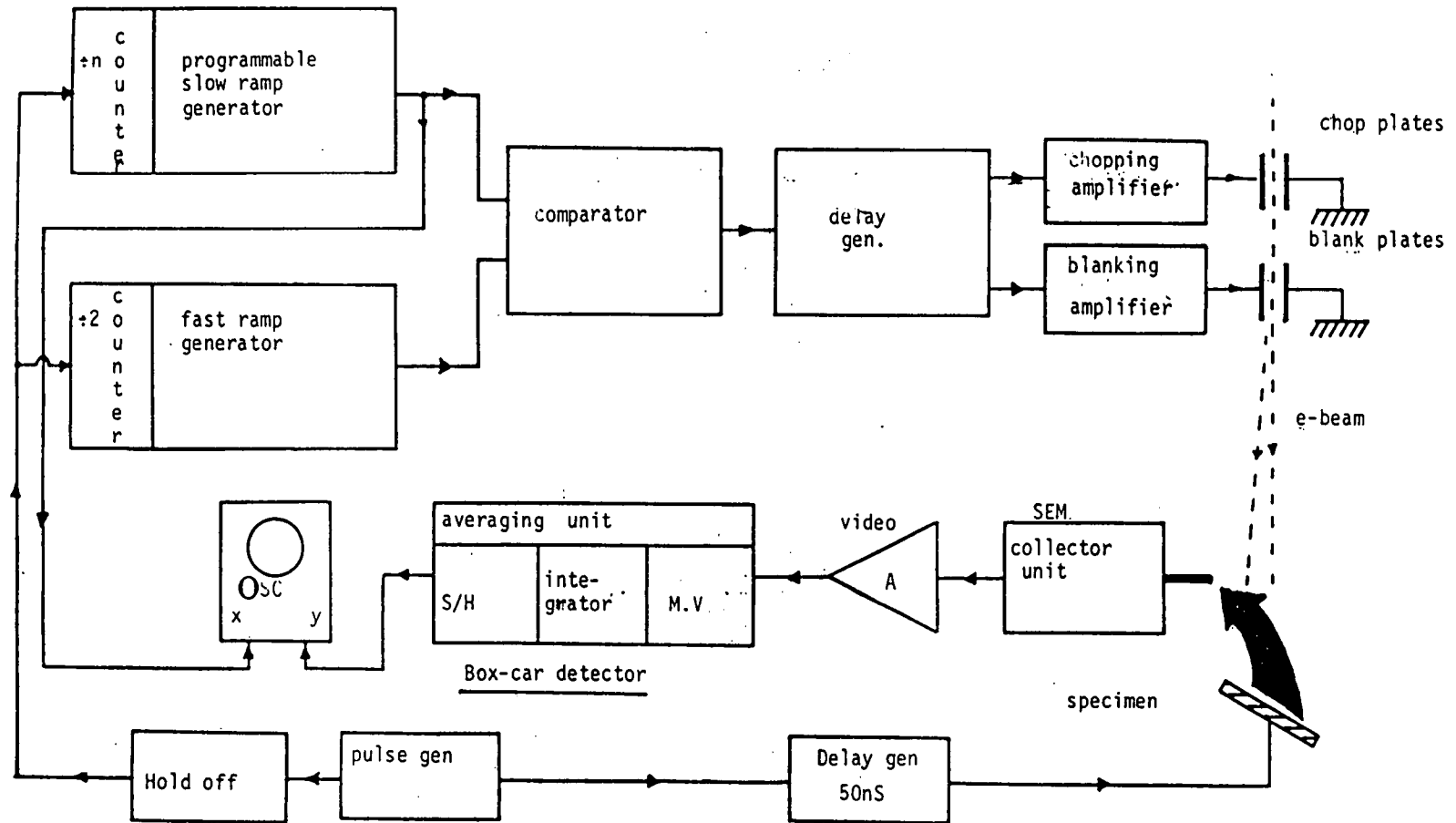
Figure 4.10: A block diagram for analogue sampling SEM.

both stroboscopic and sampling modes, it was necessary to develop a pro-
grammable slow ramp generator, in such a way to produce a variable
number of samples per phase; this is made by:

(1)   Changing the trigger input signal frequency fed to the
slow ramp generator (using separate signal generator).

(2)   Using divide by N counter (8 bit counter is used), where
the DAC internal counter is disabled.

(3)   Controlling the slow ramp output digitally by program-
ming the DAC (ZN425) manually or remotely.

Manual (stroboscopic mode) is achieved by using eight toggle
switches connected to high d.c supply, to control the DAC
counter. (If counter is connected to earth it is disabled, if
it is at high d.c level it is enabled).

Remotely the DAC can be controlled by computer or wafer switches
(sampling mode), to produce different quasi d.c levels (see Fig-
ure 4.9), where the phase changes automatically. The comparator
responds in sequence to the corresponding phase changes, produc-
ing output trigger signal which are delayed with respect to the
input trigger signal to the sampling system and to the specimen
under test.

The circuit for the programmable slow ramp generator was developed
by using wafer switches as shown in Figure 4.9. As a first step in the
development of the circuit control of the delay in the sampling work was
made by selecting 3 bits of M.S.B of the DAC internal counter which is

controlled by wafer switches which were connected in watches form as shown in Figure 4.9, where any number of samples per phase are chosen and performed in sequence.

In stroboscopic mode, the DAC counter is disabled and 256 steps of DAC may be selected to show fixed phase while letting the electron beam scan over the specimen. The slow ramp signal is developed to trigger the time base of the display unit which was an oscilloscope to display the measured voltage against phase change (time delay).

The time resolution of the sampling system is determined and specified by the fraction of switching time (rise time) of the sampling signal or by the rise time of the periodic pulses which are fed to the specimen under test.

The experimental results show the time resolution by both ways is relatively comparable of 1 ns. Time resolution measurement was not possible by the reconstructed waveform because of the timing jitter problem which disturbed the measurement.

4.6.2 Control of the Analogue Sampling System

The main control switch which is used to set the working mode has two states of logic. These are either:

(a) When switch S is at low voltage level at logic "0", it means the counter (7493) is enabled and is counting ordinarily (sampling mode).

or

(b)   When switch S is at high voltage level at logic "1", the counter is disabled and switches

(S 1 to S 8) to work separately (stroboscopic mode).   (See Figure 4.9).   In both cases the DAC internal counter is dis-abled.

To make the system work in the stroboscopic mode all toggle switches (from S 1 to S 8) should be "on" and connected to the DAC (ZN425) through d.c voltage of 5v (see Figure 4.9). By this mode, 2 to 256 steps are produced, by showing any d.c level as a reference voltage to the comparator of the sampling unit by means of manual control.   In sampling mode, the programmable slow ramp generator produces different d.c voltage levels for different phases automatically.

The output delayed signal of the wafer switches shown in Figure 4.9 is used to control the monostable multivibrator of the averaging unit (box-car averager), in order to reset the integrator each time the phase is changed. Three wafer switches are used to control the output performance (see Figure 4.9) of data resolution(dots/phase).   The hold-off circuit of multivibrator is used to stop the ramp before the full recovery of the previous one.

The suggested table relating operating signal frequency with chop-ping pulse rise time for sampling system is :

Frequency	Beam pulse width	Chopping pulse rise time	Fast ramp period
10 MHz	1 ns	4 ns	200 ns
5 MHz	2 ns	8 ns	400 ns

2 MHz	5 ns	20 ns	1 us
1 MHz	10 ns	80 ns	4 us
500 KHz	20 ns	80 ns	4 us
200 KHz	50 ns	200 ns	10 us
100 KHz	100 ns	400 ns	20 us
50 KHz	200 ns	800 ns	40 us

A variable switching time of the fast ramp generator and chopping pulse are produced with reed relays and capacitors as shown in Figures 4.11 and 4.12 to produce different ramp signal speeds with different time constants.

The delay generator after the comparator in the sampling unit, which is used to produce delay for blanking pulse from chopping pulse has a variable time constant using reed relays, to work in accordance to any change in fast ramp speed.

Reed relays are arranged in such a way that they may be controlled locally or remotely by computer interfacing, to produce any phase required . The fast ramp was found to work at repetitive signal frequency up to 10 MHz.
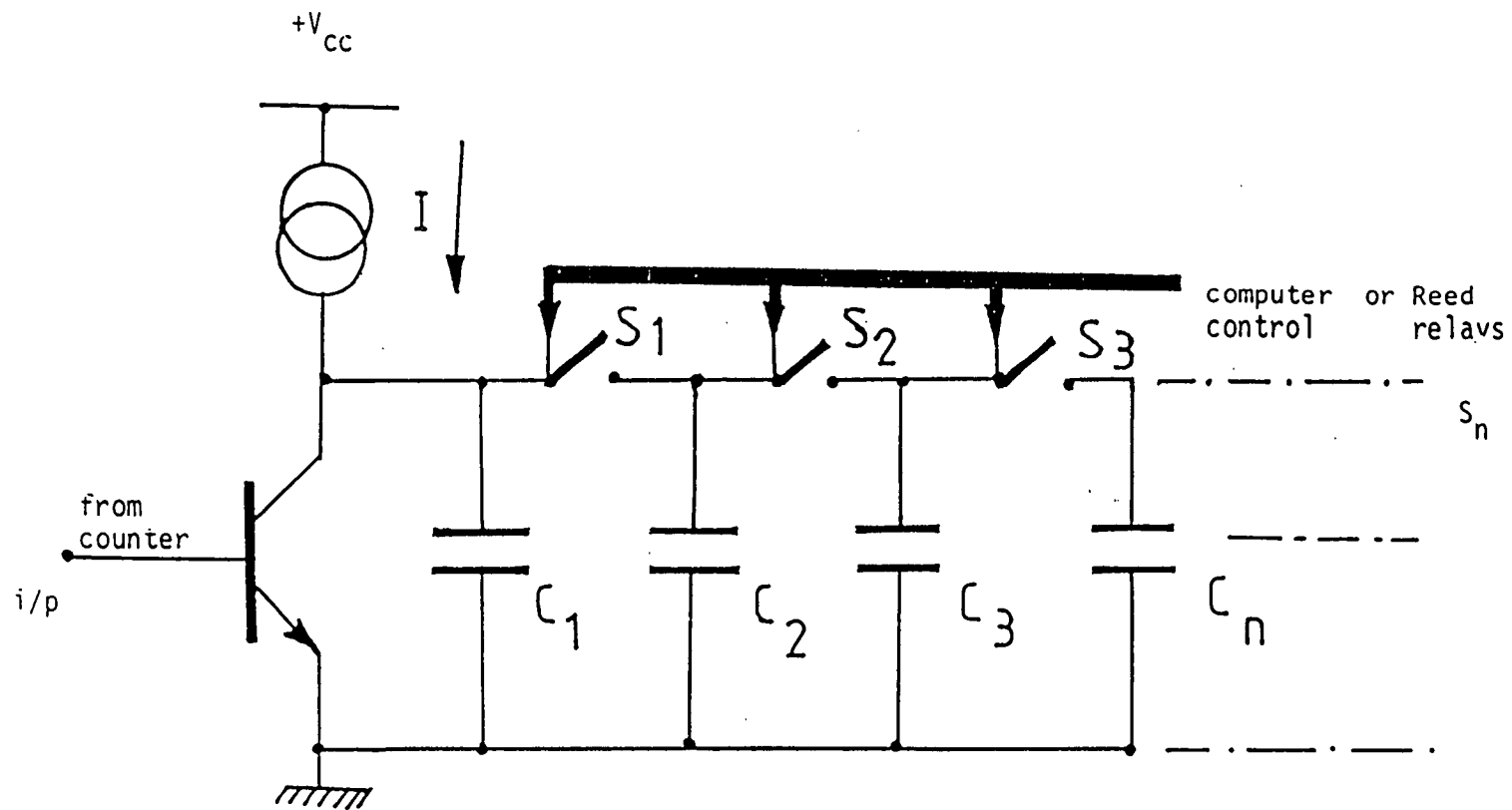
Figure 4,11:Programmable fast ramp generator
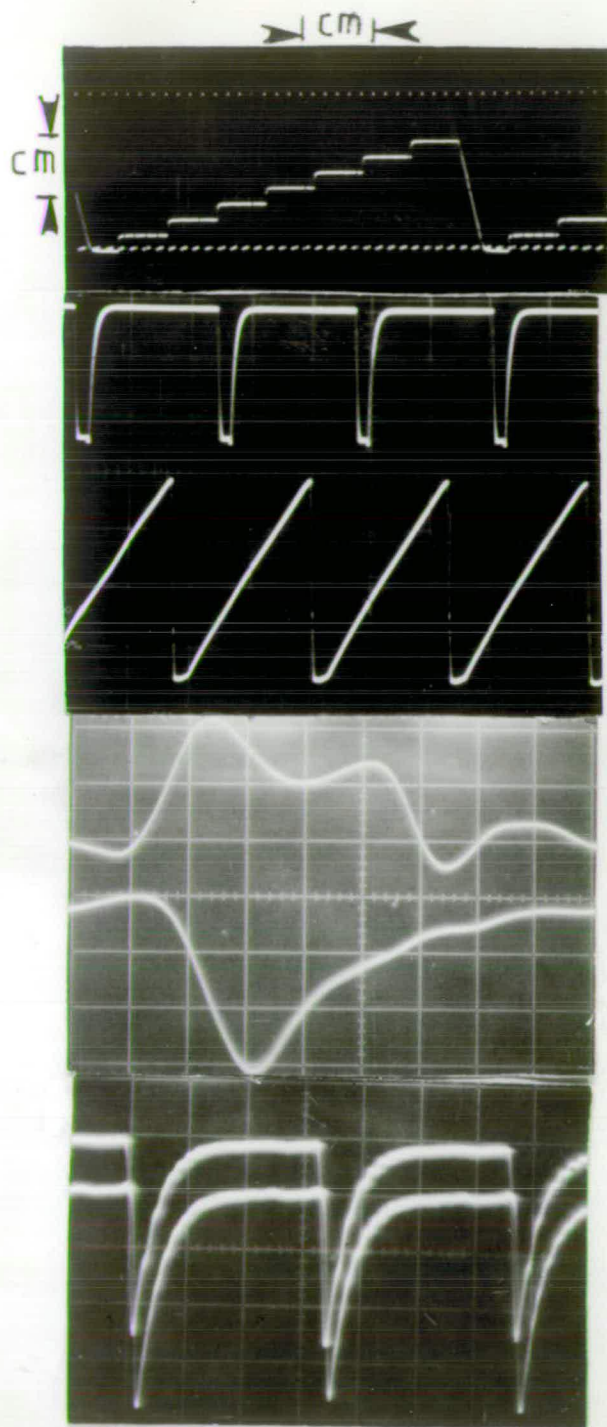
(A)

fast ramp in dots
with slow ramp

H = 0.5 ms/cm
V = 2V/cm

(B)
upper trace is
chopping pulse O/P

lower trace is fast
ramp

H = 20µs/cm
V = upper 10V/cm
    lower 2V/cm

(C)
upper trace is input
trigger pulse O/P

lower trace is O/P
delayed trigger pulse

H = 10ns/cm
V = upper 2V/cm
    lower 5V/cm

(D)
upper trace is
blanking pulse

lower trace is
chopping pulse

H = 20ns/cm
V = 5V/cm

Figure 4.12 Shows generation of delayed trigger pulse by
analogue sampling system.

4.7   NOISE PROBLEMS

The analogue sampling system noise problems can be classified into:

(a) Amplifier Noise

Real fluctuations in the quantity being measured, overcome only with signal averaging and bandwidth (B.W) narrowing. Noise was reduced by filtering and careful attention to configuration and parts location.   Noise in the amplification process has been reduced by using low noise amplifiers. It was decided therefore to start with devices that are free of preventable interference and that possess the lowest amplifier noise.

Filtering capacitors, low pass filters and Schmitt triggers have been used to reduce noise. A terminated transmission line with 50 Ohm impedance is used between the sampling system and beam switch to prevent the problem of reflections, and a short coaxial cable is used.

(b) Interference and Pick Up Noise

The analogue sampling system using slow and fast ramp generators was found to produce a problem of noise as shown in Figure 4.13. This noise started at the fast ramp generator circuit but also affected the slow ramp waveform. Noise, which existed at the negative going edge of the comparator output pulse and was fed to the delay generator (monostable multivibrator 74123), appeared to produce an extra short delayed pulse beside the original one which produced unexpected video pulses as
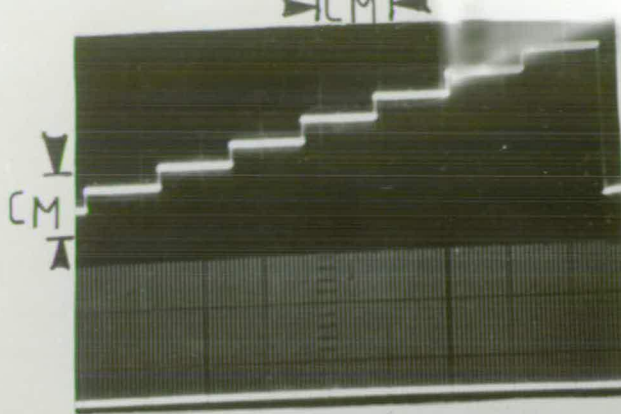
(A)

upper trace is slow ramp
lower trace is fast ramp

H = 0.1 ms/cm
V = 1V/cm

noise in fast ramp
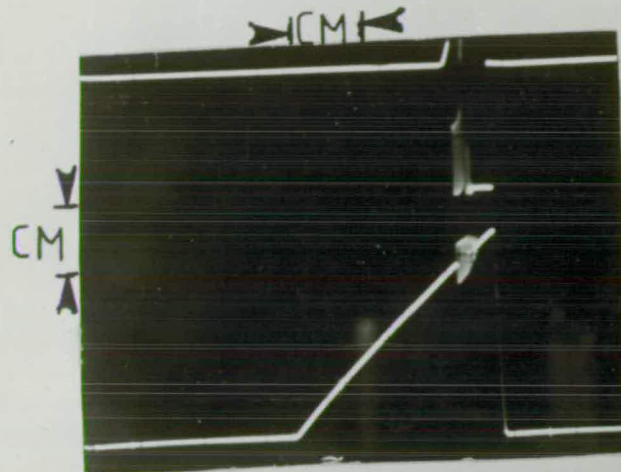
(B)

upper trace is comparator O/P pulse
lower is fast ramp

H = 10μs/cm
V = 2V/cm

noise is in fast ramp
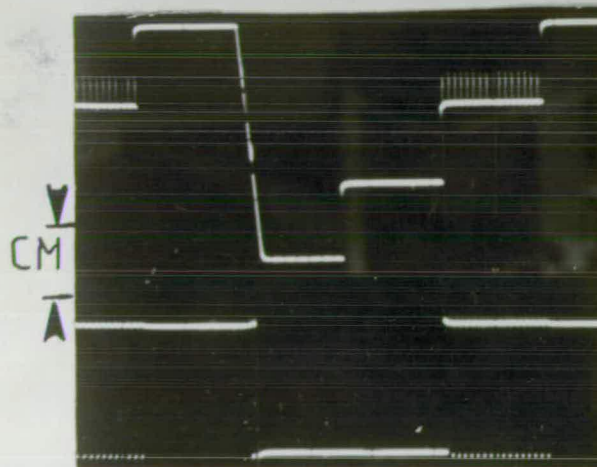
(C)

upper trace is slow ramp
lower is comparator pulse O/P
H = 1 ms/cm
V = 2V/cm

noise appears in slow ramp
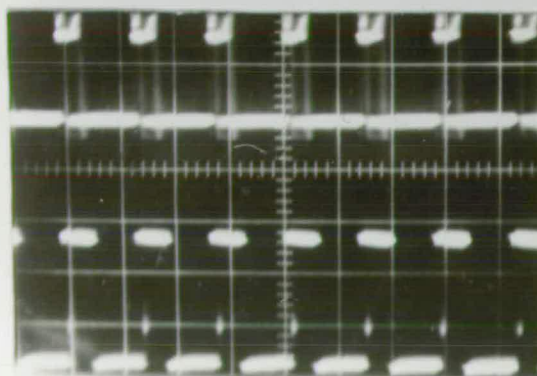
(D)

upper trace is comparator O/P pulse
lower is monostable O/P pulse with noise problem.

Figure 4.13: Shows noise problem in analogue sampling system.

a result.

The way to minimise this noise was by using buffers immediately after the slow and fast ramp generators for perfect matching, which was found to be effective. Improper biasing of the slow ramp generator shown in the circuit of Figure 4.5 as well as control of the ramp signal amplitude were found to be important factors leading to noise which was the cause of the comparator output pulse phase instability problem.

Correct adjustment of the potentiometer controlling the amplitude and d.c offset of the slow and fast ramp amplifiers input were essential to avoid saturation and timing jitter (instability effects). Interference noise also entered by the power lines and through input and output signal leads; decoupling filtering capacitors were found to help in stopping this noise.

To reduce interference noise the following are required:

1. perfect contact to avoid voltage drops,

2. proper layout of electronic components,

3. correctly designed printed circuit boards

4. moving wires close to the ground plane for
   reducing fringing field "coupling".

Pick-up noise from the units' layout and from its surroundings was mainly due to the irregular arrangement of current paths which may lead to interaction of electromagnetic fields; "floating fields", especially with high frequency signals. To reduce this noise, shielding between delay units and surrounding was required, especially with low frequency

signals at high impedance levels. To produce better performance of the analogue system, it was recommended to use printed circuit boards with double copper layers, to prevent any pick up noise from the surroundings.

4.8 POST HEAD AMPLIFIER SAMPLING

4.8.1 Basics of the Box-Car Averager

Box car averagers are sometimes placed at the output of the video head amplifier. These may be used in two modes:

(i)   To perform stroboscopy and improve S/N ratio
        without beam chopping.

(ii)   To improve S/N ratio with beam chopping.

In both cases the frequency of operation will be restricted by the bandwidth of the video chain up to the averager unit. In case (i), the signal has to pass through the system without serious distortion, but will have noise added to it.

By sampling and averaging, the noise contribution can be reduced. In case (ii), the pulses through the head amplifier may be attenuated by the finite bandwidth of the video chain and will also have noise added. For comparison see Figure 4.14. By opening the box car gate (see Figure 4.15) only when the signal pulses are expected, the noise during the rest of the cycle is eliminated. This can obviously be highly advantageous when a low duty cycle is necessary.

(i) without beam chopping

(ii) with beam chopping
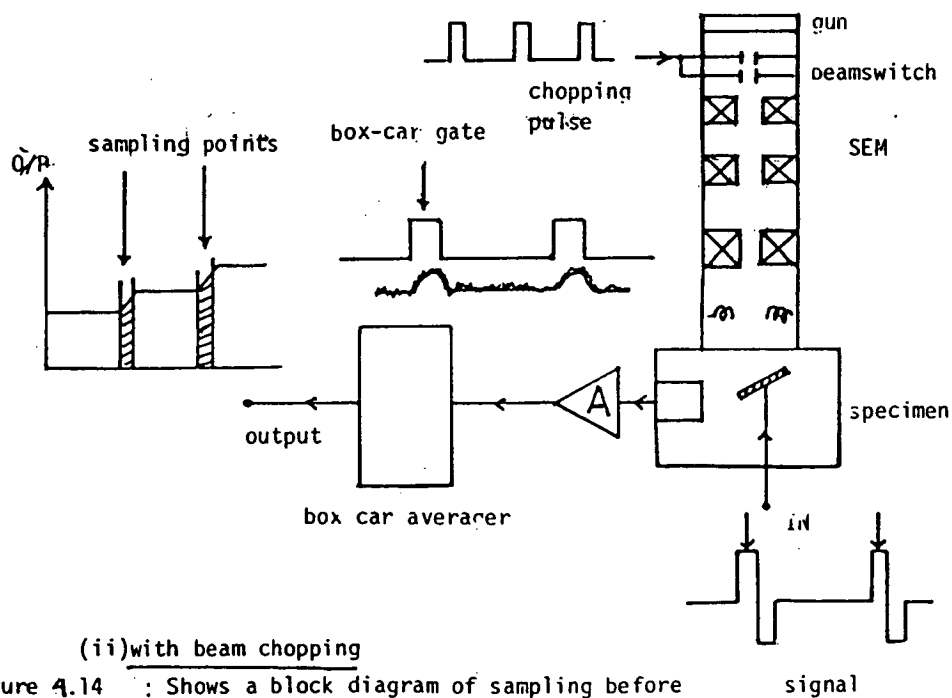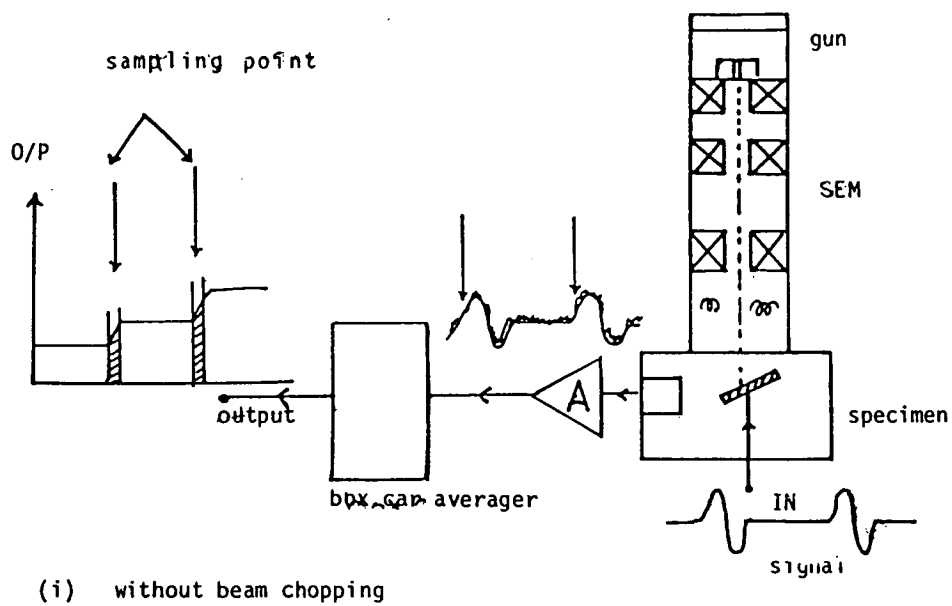
Figure 4.14 : Shows a block diagram of sampling before
and after SEM video amplifier as the basic
principle.
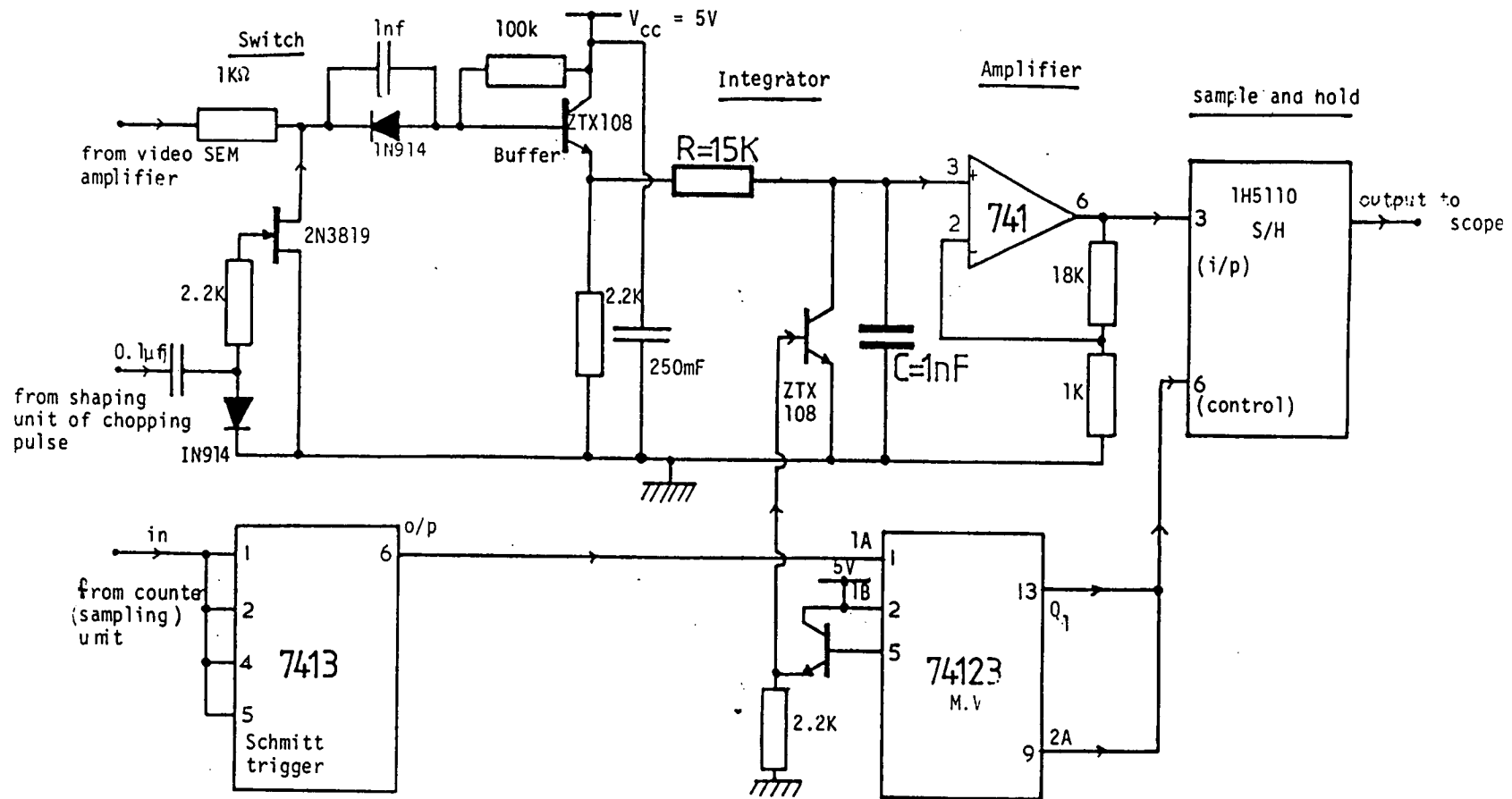
Figure 4.15 : Shows circuitry of averaging unit (box-car detector).

Feuerbaum and Otto(1980), and (1982) described a box - car integrator to measure electron beam waveforms: "A box-car averager is an integrator which measures a noisy periodic signal using a sampling gate. By integrating the signal measured at the gate the S/N ratio is improved. The averager is a combination of beam pulsing and video gating. The primary electrons are pulsed in synchronism with the periodic changes in voltage as in the beam pulsing method. The secondary electron signal is only amplified in the video gain - a process similar to video gating and shows local voltages and the advantages of beam pulsing and video gating" (from Feuerbaum and Otto 1980)).

The averaging unit is used as an exponential averaging R.C integrator, with variable time constant, which responds to any change of input signal frequency in a succession of sampled voltages. If the averaging time is long enough, the output will stabilise to the average value of input, then the number of samples after integration is:

$$n = \frac{2 R.c}{\pi} \cdot \omega_s \qquad (4.4)$$

where $\omega_s = 2\pi/t_g$ = bandwidth of the sample waveform

$$\omega_s = 2\pi f_s \qquad (4.5)$$

where f_s = sampling frequency

t_g = chopping pulse width

More detail is given elsewhere (de Sa 1981).

4.8.2 Design of an Averaging Unit

Figure 4.15 shows a circuit designed for an averaging unit, where a FET (2N3819) is used as a gate together with a buffer, integrator, sample and hold, amplifier, and electronic switches. The voltage on (C) of the integrator only changes while the gate is open, for t_0 seconds out of every (T). Design of (C) will determine the time constant of the integrator; the effective value of RC is obtained:

$$n = \frac{2RC}{\pi} \cdot \frac{T}{t_o} \cdot \omega_s \qquad (4.6)$$

When multiple samples/sweep are taken an improvement in S/N ratio is achieved. The resolution of this detector can increase by increasing the sweep time up to a limit set by the width of the sampling pulse. This technique is used to perform sampling in repetitive frequencies up to 1 MHz, which is one of the disadvantages for the time being, of this sort of sampling system.

4.8.3 Averaging Unit Circuit Details

The delayed trigger signal from the sampling system is fed to the n-channel FET gate, to trigger the switch by using a clamp diode circuit as shown in Figure 4.15 . Video pulses are fed to the integrator through a buffer. The pulse width is controlled by the divide by N counter in the sampling units. Pulses from the control counter are fed to the multivibrator to control the input to the sample and hold (S/H - 1H5100). A 741 amplifier is used to amplify the signal after the integrator which is controlled by a transistor switch to reset it every

time the input signal goes high. Since the aperture time for sample and hold is limited to 150 ns, then it does not respond to a chopping pulse less in width than indicated.

The overall sampling system with the averaging unit is shown in Figure 4.10. The stroboscopic mode is performed by both analogue sampling systems and by using post head amplifier sampling technique (averaging unit) , for S/N ratio improvement as shown in Figure 4.15. Above 1 MHz frequency, a low pass filter (L.P.F) is used as the integrator after the head amplifier instead of the averaging unit, with variable time constant, to average over video signal noise, due to electron beam and other noise.

Timing jitter has been found in the reconstructed waveform, due to the present analogue sampling system. It is due to the phase instability of the analogue type of delay generator. One of the reasons is due to interference noise superimposed on a slow ramp signal and mistriggering of the time base of the display is found, and other reasons were discussed before. Figure 4.17 shows the timing jitter is appearing clearly.

4.9 ANALOGUE SYSTEM CIRCUITS ANALYSIS

The reliability of the present analogue sampling system mainly depends on the design of the ramp generators which consist of discrete components, also on the precision comparator and the layouts of the electronic components used. The accuracy and stability of the resistors used in the network are an important factor to decide the degree of precision of reference voltage at the comparator, current source and am-

plifier gain of the sampling unit. The accuracy and linearity of the fast ramp generator depend on the properties of the capacitors used (dielectric absorption in capacitors causes non-linearity), as shown in Figure 4.12.

In the Bangor work, a strobe driver as shown in Figure 3.10 with step recovery diode (S.R.D) was used with modification to the time base circuitry of type (HP1811A) sampling oscilloscope. A similar requirement has been met at present, by building a new analogue sampling system with different design of beam switch amplifiers developed as in Figure 3.35 (chapter three) with beam switching around 1 ns.

A monostable multivibrator is used as a hold-off circuit at the input of the present systems, in such a way as to block off a new ramp before full recovery of the previous one, so when the multivibrator is triggered, it inhibits further triggering until it has returned to its stable state.

The performance of the slow ramp was found to be adequate by developing an 8-bit counter and DAC (see Figures 4.5 & 4.9). The divide by N counter is used to produce better resolution in the sampling mode.

In the stroboscopic mode, results have been found to be satisfactory as shown in Figure 4.16 on an MOS Arithmetic averager specimen under test which shows a specimens' pad with a rectangular strip dark and bright, when the phase (time delay) is changed respectively with repetitive signal of 2.5 MHz frequency.

The main comparison between sampling before and after the head amplifier is that infinite bandwidth can be used for the first technique, while the second case is mostly used to average over the noise of the SEM output waveform instead of using an ordinary integrator which is not stable and with limited bandwidth of the video chain.
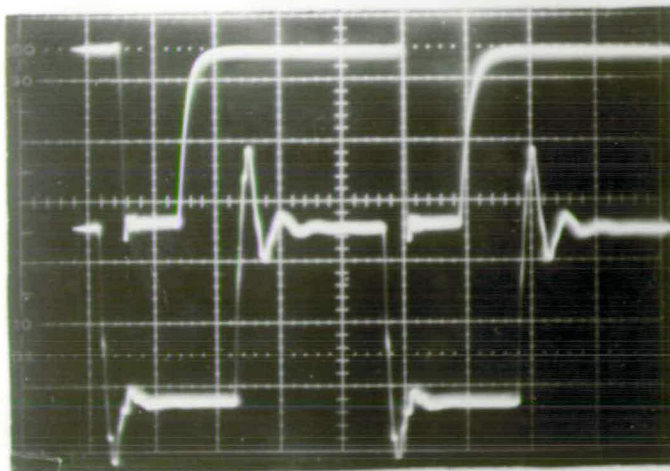
(A)
upper trace is chopping pulse,
lower is i/p pulse
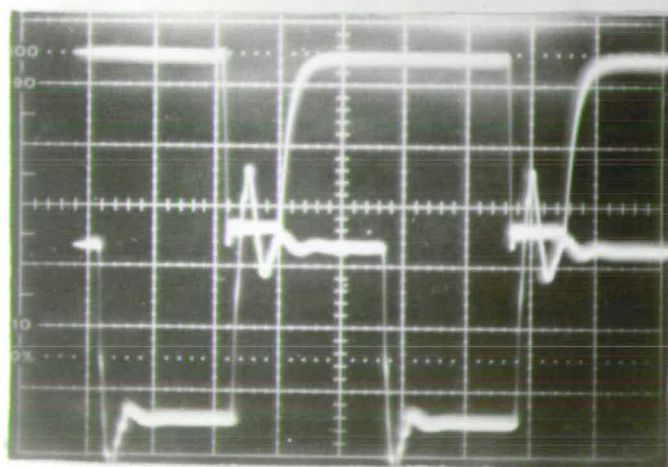
H = 100 ns/cm
V = upper trace is 5V/cm
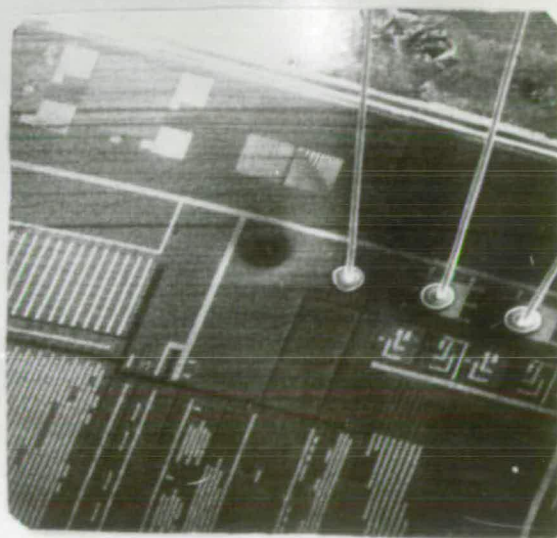   lower trace is 1V/cm

Both are low level voltage

X200 BRIGHT pad of arithmetic
      averager specimen

(B) Same scale as above but

Both are high level voltage

X200

DARK pad of arithmetic
averager specimen

Figure 4.16 : Shows stroboscopic SEM
             by analogue system.

For the present system, reed relays were needed in many places in the sampling units:

1.   To control the electron -beam chopping pulse width.

2.   To change the switching time of the chopping pulse by controlling the rise time (see Figure 4.11).

3.   To change the time constant of the integrator in the box-car averager.

4.   To interface analogue sampling systems with a micro-computer for remote control.

These were found to complicate the circuitry.

Interference and pick up noise were reduced by using box-car averagers up to 1 MHz frequency, and by an integrator (L.P.F) for fre-quency up to 10 MHz as shown in Figure 4.17 which shows a reconstructed waveform with timing jitter problem and improved S/N ratio.

The modified box-car averager is recommended for better perfor-mance; as well as designing a digital programmable filter with narrow bandwidth and high resolution, which is thought to be more stable than present integrators and can be easily tuned and controlled by microcom-puter.

Software design is required to control the digital filter for im-proving S/N ratio of the video signal output, for sampling system flexi-bility, and to make the filter more flexible. This can be done for the time being using ready made A/D converters cards of the HP multiprogrammer. It can be used for further signal processing. A frame store system with software facility for reducing noise would be useful to smooth high frequency

(A)
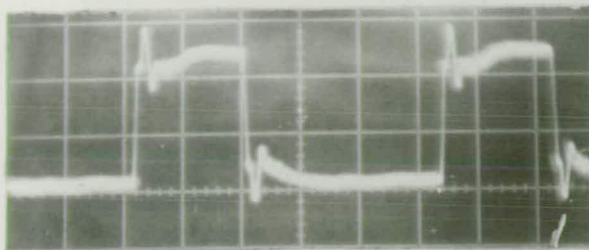
V = 2V/cm
H = 0.1μs/cm

(B)
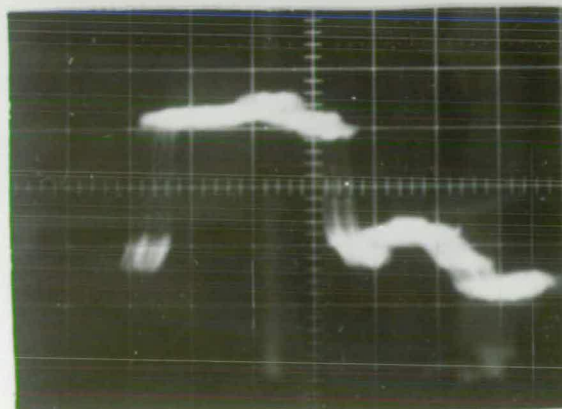
V = 20 mV/cm

Figure 4.17: Shows reconstructed waveform
by sampling system with timing jitter problem
in (B). In (A) shows input pulse to specimen
under test.

noise in the picture. These are not available and not being used for the present work.

4.10   DISCUSSION OF RESULTS

The work so far involved the development of a new analogue system design outlined in block diagrams, and resulted in a practical analogue circuit design based on the principle of the conventional sampling oscilloscope, to see whether these principles of analogue instruments could be adopted to the present purposes. In the event, it was concluded that it needed too many modifications and auxiliary units to be worthwhile in comparison with building a fairly simple piece of special purpose equipment. Therefore a system was constructed as outlined in Figure 4.7, using the conventional way of generating a delayed sampling pulse by ramp generators.

The analogue sampling system was found to work reasonably satisfactorily at fast ramp frequencies up to 10 MHz, and would produce beam pulses which were assumed to be in the nanosecond system. From the measurement, it was found that there was excessive jitter in the timing of the reconstructed waveform (see Figure 4.17). Some degree of jitter had also been mentioned by Plows and Nixon (1971), Gopinath and Hill (1977), and Fujioka etal (1978) displayed timing jitter in the reconstructed waveform.

Feuerbaum and Otto (1980 and 1982) have preferred using a box car averager instead of using the sampling the electron - beam technique, because of the primary electron leakage current flows in the pauses between pulses and to avoid the sensitivity to repetition rate of primary electron pulse. They measured a jitter of 100ps in the reconstructed waveform test.

Timing jitter in the reconstructed waveform is due to phase instability in the timing of the analogue circuitry which has been discussed extensively by the author. A simple box- car averager is used here to average the signal over several sampling pulses at each phase, to reduce noise and to produce different d.c levels of the reconstructed waveform on specimen under test. Serious consideration should be given to the construction of the analogue circuitry to minimise noise.

Furthermore, arrangements to permit the remote digital control of the functions of the system were becoming rather difficult. It was decided that the system should be simplified by developing a new digital sampling system to produce precise time delays with better performance to study devices under dynamic operation.

CHAPTER FIVE

DEVELOPMENT OF AN AUTOMATED HIGH FREQUENCY

SIGNAL MEASURING SYSTEM

5.1 INTRODUCTION

Chapter Four has demonstrated the analogue sampling approach. The aim of this Chapter is to produce a digitally switched time delay by using a digital technique for sampling systems in the SEM.

This chapter consists of two parts. The first part describes a design of electronic circuitry (hardware), which was developed to perform stroboscopic and sampling SEM. New models of delay lines for producing time delays to the input signal at different frequencies are presented. The second part deals with software design and computer interfacing to the digital sampling system. A review of the past work on controlling functions of the SEM by computer is given.

5.2 REVIEW ON THE SEM FUNCTIONS CONTROL

Up to date, there is no reported paper on using a digital sampling system for high frequency signal measurements in the SEM. References to be mentioned in this chapter are on controlling functions of the SEM by using a computer.

Jones and Unitt (1980) have reported on computers in the scanning microscope. They clarified the principle on-line computer systems, laying particular stress on the hardware aspects such as interfacing.

They mentioned that a recent development is the use of microprocessors in scanning microscopes. They also reported on image processing systems as shown in Figure 5.1 using a computer, as well as the basics of interfacing the computer to the SEM. They produced a technique for a digital scan generator and they mentioned software for different purposes, for storing image information.

Smith (1981) has also reported on-line digital computer techniques in electron microscopy as shown in Figure 5.2, which were used to display image acquisition. He discussed on-line hardware as in the same Figure above, how TV image signals from the SEM or video tape recorder were used as input directly to the frame store. Slow scan image signals are also fed to the frame store, directly to the computer.

Analogue to digital converter (ADCs) are used in all input signal lines. He preferred to use a separate digital scan generator rather than the microscope's internal scan generator, alternatively the computer itself may be used to generate the scanning waveforms. A similar facility of digital scan generator is used in the present work.

Dinnis et al (1981) have reported using a microcomputer to control all elements of the SEM (see Figure 5.3). They used a "Superbrain" microcomputer as the centre of the system, which connected to the many functions of the SEM using the IEEE 488 General purpose interface bus (GPIB). The Superbrain was also used to control the X and Y direction of stepper motors for specimen stage position. They also developed a digital scan generator which allows very flexible control of the scanning or positioning of the electron beam either from the front panel or remotely via the GPIB. This too has its own microprocessor which allows "spot", "line", record or visual scans.
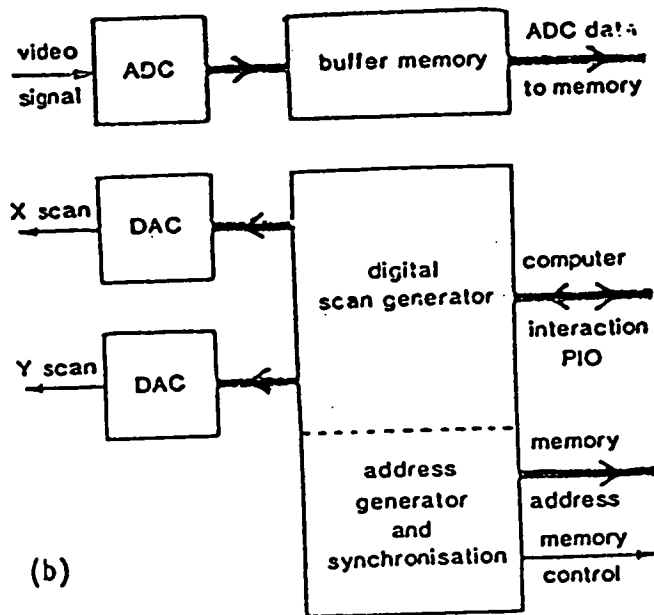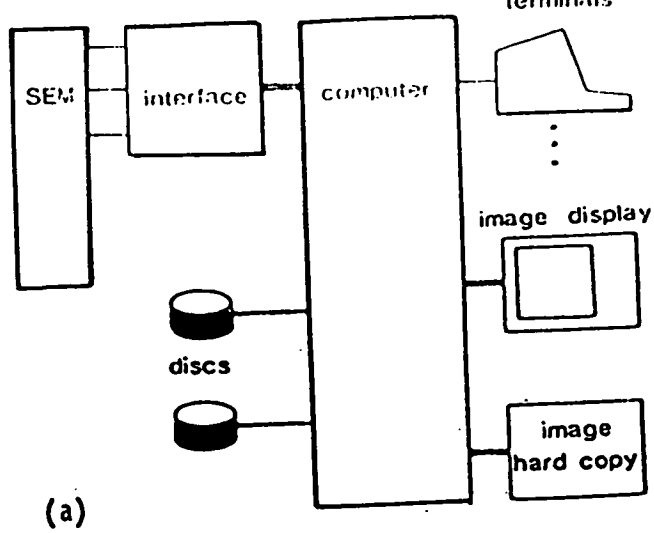
(a)

(b)

Figure 5.1: Shows SEM image processing system
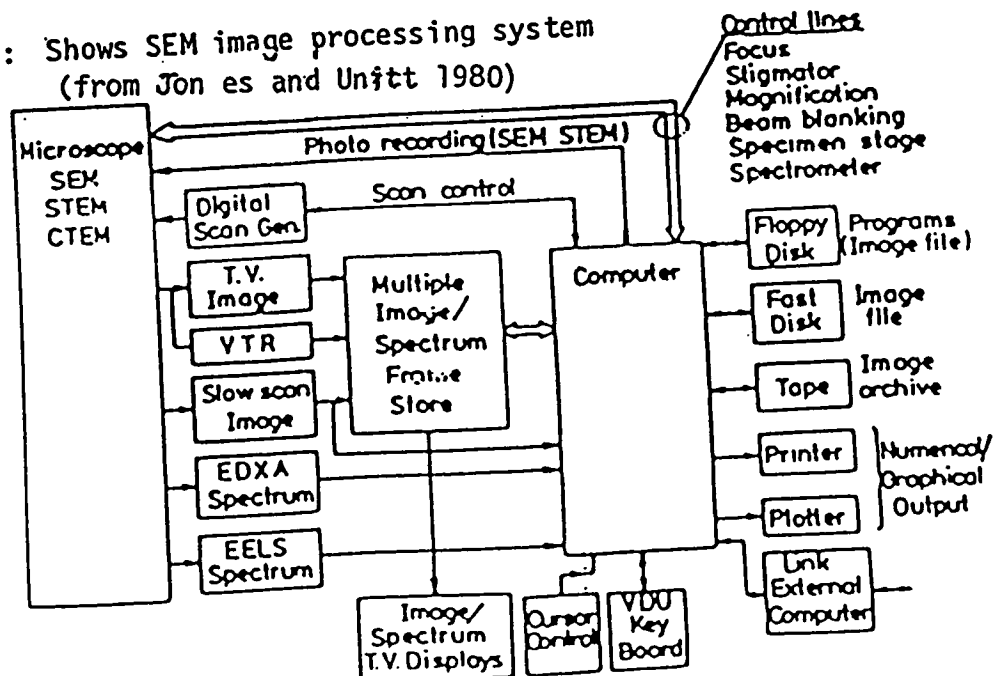(from Jones and Unitt 1980)

Figure 5.2: Shows a schematic diagram of an on-line computer system
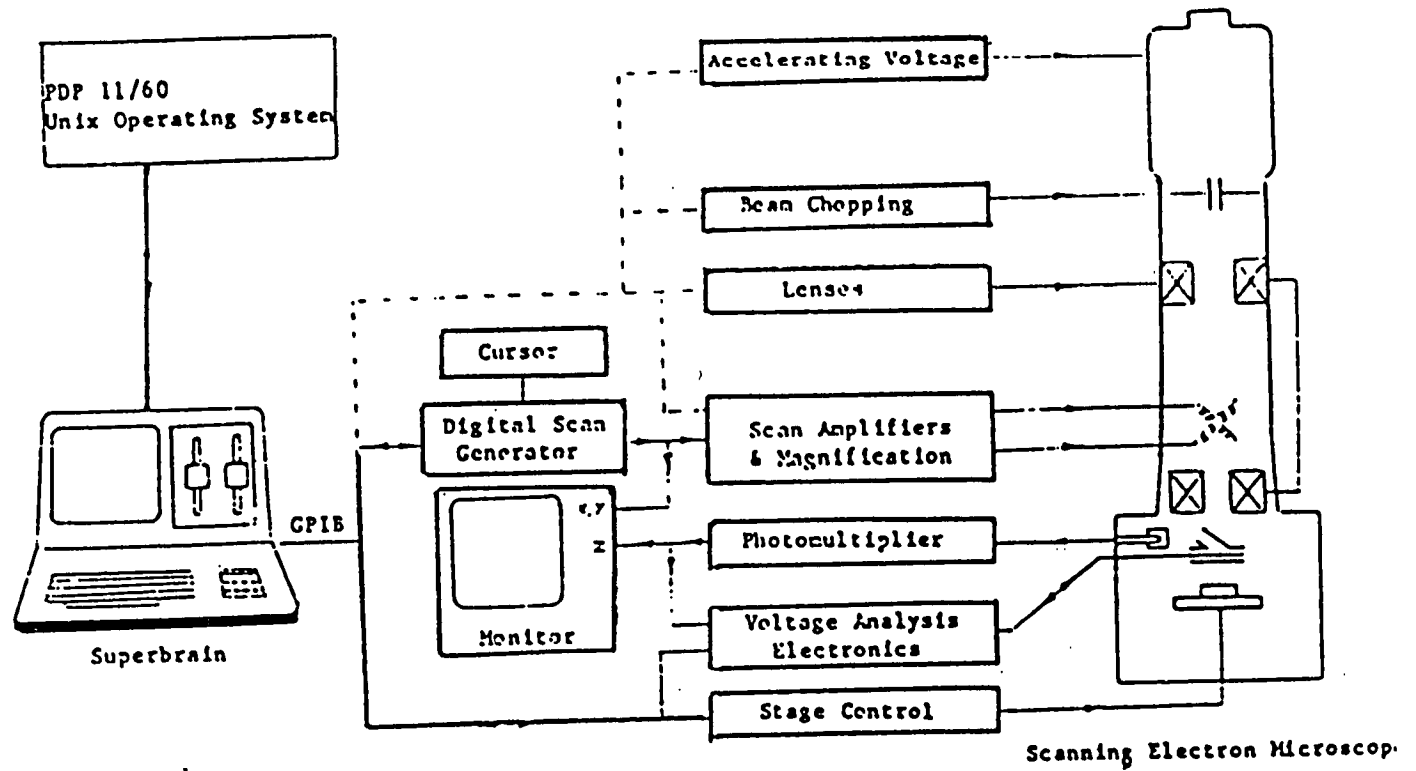for the electron microscope. (from Smith 1981)

Figure 5.3: Shows control system for SEM (Dinnis et al) 1981

They employed this system for measuring quantitative voltage contrast in the SEM. This facility is used at present for SEM function automation.

Fujioka et al (1981) have reported on interfacing a microcomputer to the SEM, for functional testing of bipolar and MOS LSI circuits, which is shown in Figure 2.16. The microcomputer has a central processing unit (CPU) which has 24K, 16 bit words of RAM and two floppy disc drives. Communication between computer and operator is made through a CRT character display. The computer interface consists of a low pass filter (low frequency), a successive approximation analogue to digital converter (ADC), a counter, five digital to analogue convertors (DACs) and necessary control logic. This was developed to convert the signal from the detector into an 8 bit binary number which is read into the computer. The time constant of the low frequency **filter is made programmable.**

A set of DACs was used to control the magnification of the SEM, the signals from the DAC were used to control horizontal and vertical positions of the electron beam. Another set of DACs controls the positions of the spot on a CRT screen where sampled waveforms are displayed. The waveform data stored in the RAM or a floppy disk are sent through an 8 bit DAC to the CRT display.

The procedure of waveform measurement is shown in Figure 5.4. The sampling phase is shifted after the signal averaging operation is performed at each phase point. They suggested a formula for the total sampling time per position, t :
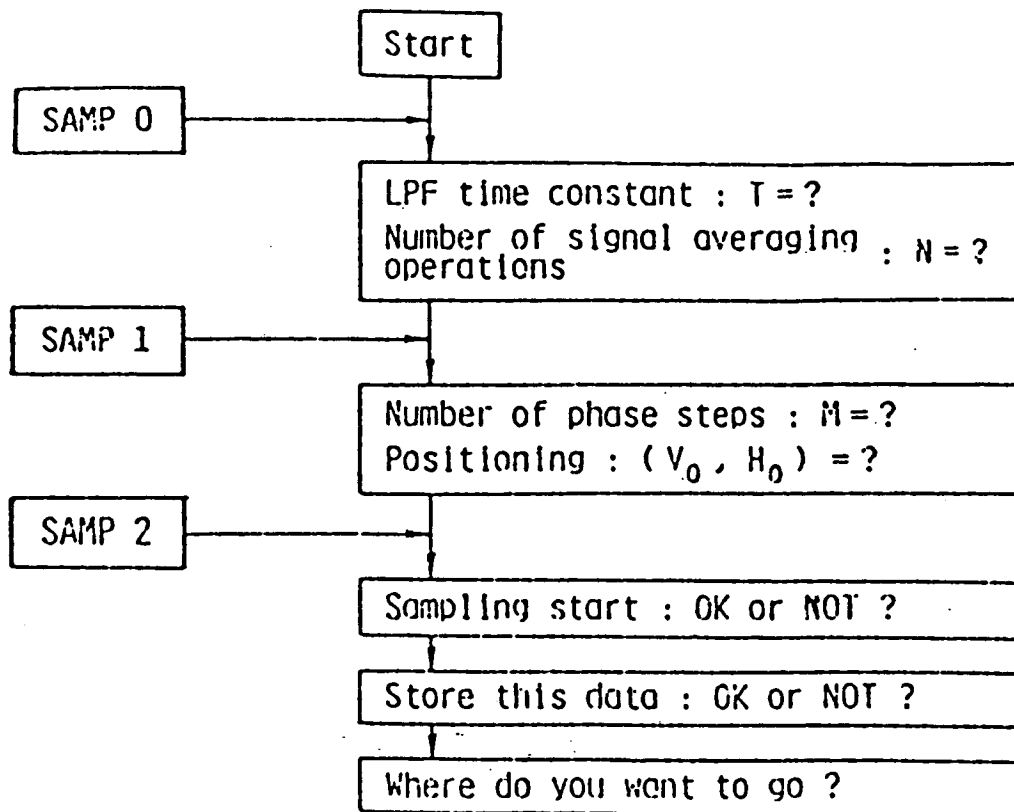
$$t = (191N - 112)M \qquad (5.1)$$

```
                    ┌─────────┐
                    │  Start  │
                    └────┬────┘
┌──────────┐             │
│ SAMP 0   │─────────────┤
└──────────┘             │
              ┌──────────▼──────────────────────────────┐
              │ LPF time constant : T = ?               │
              │ Number of signal averaging  : N = ?     │
              │ operations                              │
              └──────────┬──────────────────────────────┘
┌──────────┐             │
│ SAMP 1   │─────────────┤
└──────────┘             │
              ┌──────────▼──────────────────────────────┐
              │ Number of phase steps : M = ?           │
              │ Positioning : ( V_0 , H_0 ) = ?         │
              └──────────┬──────────────────────────────┘
┌──────────┐             │
│ SAMP 2   │─────────────┤
└──────────┘             │
              ┌──────────▼──────────────────────────────┐
              │ Sampling start : OK or NOT ?            │
              └──────────┬──────────────────────────────┘
              ┌──────────▼──────────────────────────────┐
              │ Store this data : OK or NOT ?           │
              └──────────┬──────────────────────────────┘
              ┌──────────▼──────────────────────────────┐
              │ Where do you want to go ?               │
              └─────────────────────────────────────────┘
```

Figure 5.4 : Shows a blook diagram of software system
for waveform measurements
(From Fujioka et al 1981)

Where t is in μs, N is the number of repetitions of signal averaging and M is the number of phase steps. 191 μs is the time required for sampling the data and 112 μs for stepping the phase, these figures are for this particular microcomputer and come from the operation time. This technique is flexible in controlling sampling phase required by using microcomputer, and is similar to Dinnis et al (1981) work.

JEOL Ltd (1982) produced a commercial stroboscopic SEM, by adopting the principle of Fujioka et al (1981), as shown in Figure 2.6 (chapter two).

Plows and Lintech Instruments Ltd(1981) have reported controlling the sampling system by computer (detail is given by their manual of a sampling electron beam system in circuit testing of integrated circuits). The system block diagram is as shown in Figure 5.5, which included hardware and software for VLSI design and failure analysis on the lines of the Plows and Nixon(1968) principle (which has been discussed in chapters three and four).

They have also reported on a computer interface to the SEM, for storage and processing. An automated way of triggering the sampling phase sweep, and a box-car signal averager working to a repetition rate of 40MHz is required to enable the display of more than one cycle of the specimen waveform were also reported.
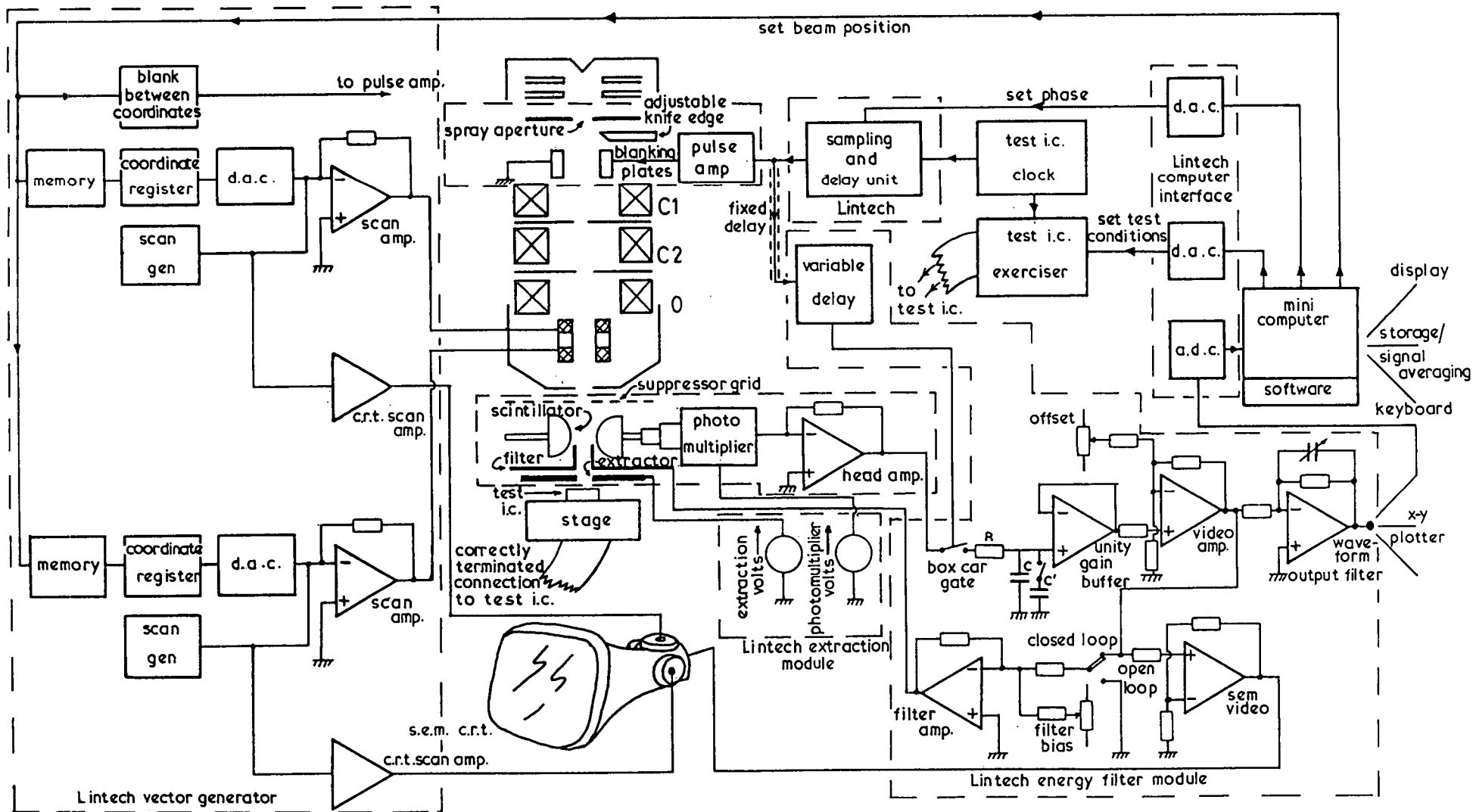
set beam position

blank
between
coordinates

to pulse amp.

memory | coordinate register | d.a.c. | scan amp.

scan gen

c.r.t. scan amp.

spray aperture

adjustable knife edge

blanking plates

pulse amp

C1

C2

0

suppressor grid

fixed delay

variable delay

sampling and delay unit

Lintech

test i.c. clock

test i.c. exerciser

to test i.c.

set phase

set test conditions

d.a.c.

d.a.c.

Lintech computer interface

a.d.c.

mini computer

software

display

storage/ signal averaging

keyboard

scintillator

filter

extractor

photo multiplier

head amp.

test i.c.

stage

correctly terminated connection to test i.c.

extraction volts

photomultiplier volts

Lintech extraction module

box car gate

R

c

c'

unity gain buffer

offset

video amp.

closed loop

open loop

filter amp.

filter bias

sem video

wave-form

output filter

x-y plotter

Lintech energy filter module

memory | coordinate register | d.a.c. | scan amp.

scan gen

s.e.m. c.r.t.

c.r.t.scan amp.

Lintech vector generator

Figure 5·5 shows a block diagram of Lintech sampling system

PART ONE

DIGITAL SAMPLING SYSTEM CIRCUITRY

5.3 DIGITAL SYSTEM PRINCIPLE

Figure 5.6 shows the circuit diagram of the overall present system, which is developed to perform stroboscopic and sampling SEM. The system consists of three main "blocks" of electronics. These are: the control boards, delay lines and display unit. The circuitry (hardware) is largely digital for operational flexibility and since most measuring systems require computer control. All logic circuitry is TTL with control and output signals TTL compatible.

The system uses a series of discrete switchable time delays. The shortest delays (1.5ns to 640ns) are implemented with tapped delay lines, made up from sections of miniature coaxial cable or from lumped inductors and capacitors. Time delays longer than 640 ns are produced by using presettable counters to count down the oscillations of a delay-line oscillator which is normally quiescent but is triggered by the incoming pulse (see Figure 5.7).

The time delay is variable over the range 1.5 ns to about 2ms (plus a fixed delay), by the bit pattern on the 21 delay selector inputs, these should be controllable from the "Superbrain" or alternatively controlled by a manual system implemented by means of another set of presettable counters (see Figures 5.8, 5.9). In the stroboscopic mode, these control counters are used simply as latches to connect 21 manual

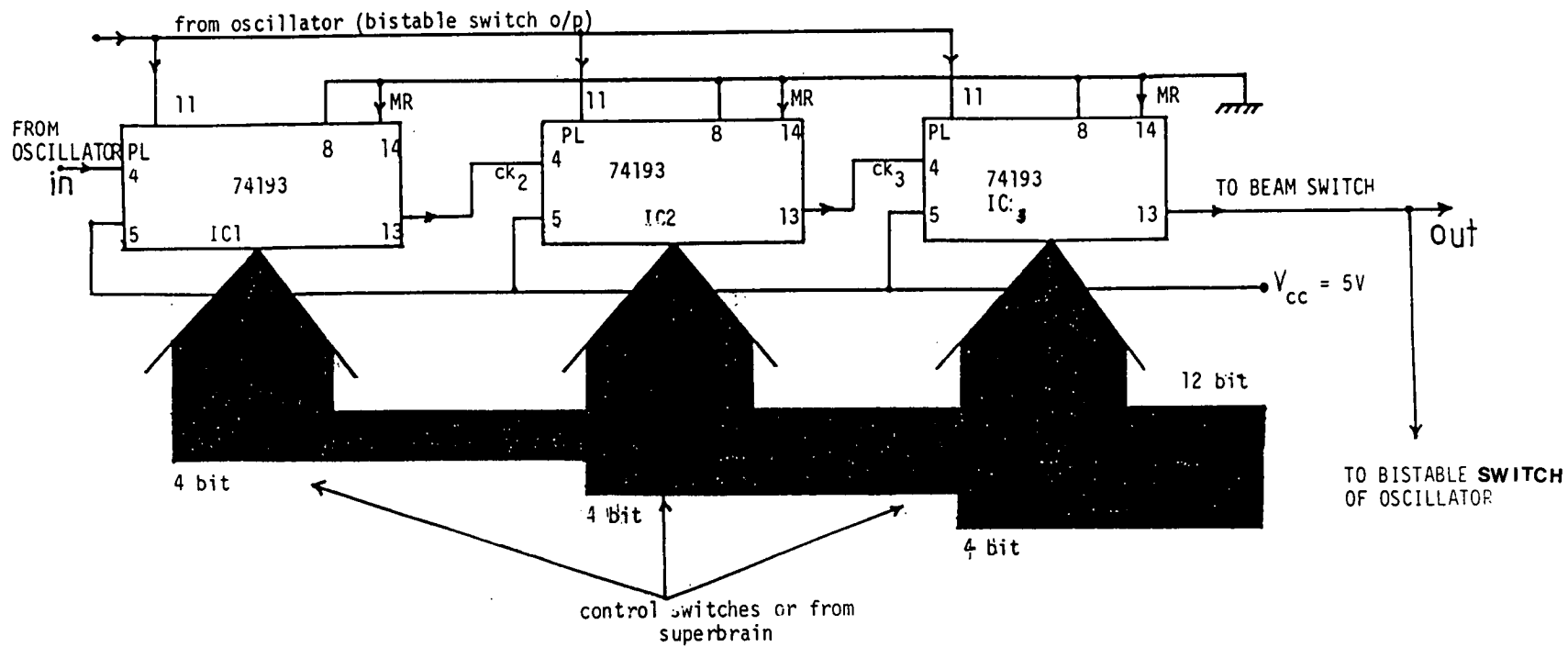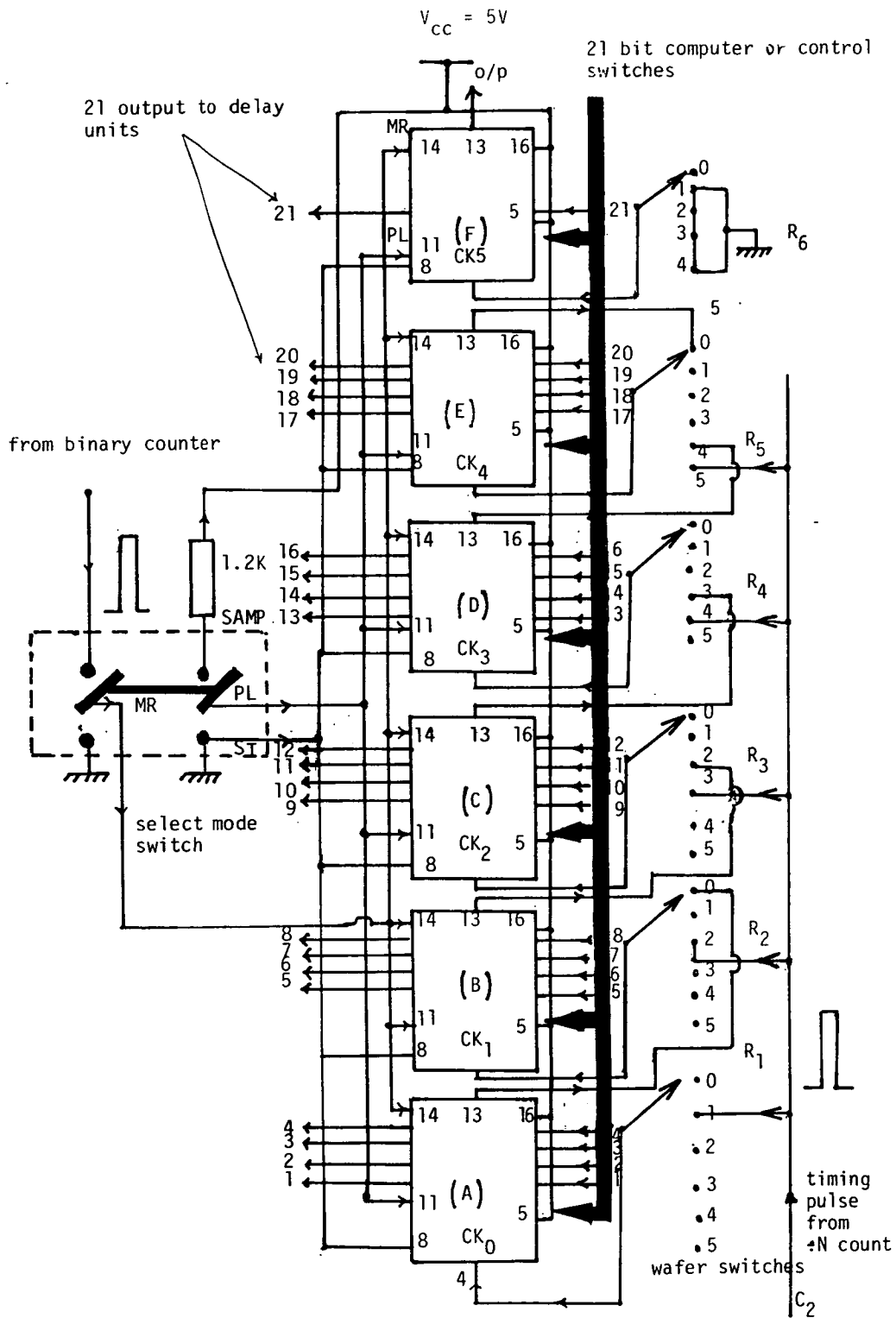FIG 5·6 SHOWS CIRCUIT DIAGRAM FOR PRESENT DIGITAL SAMPLING SYSTEM
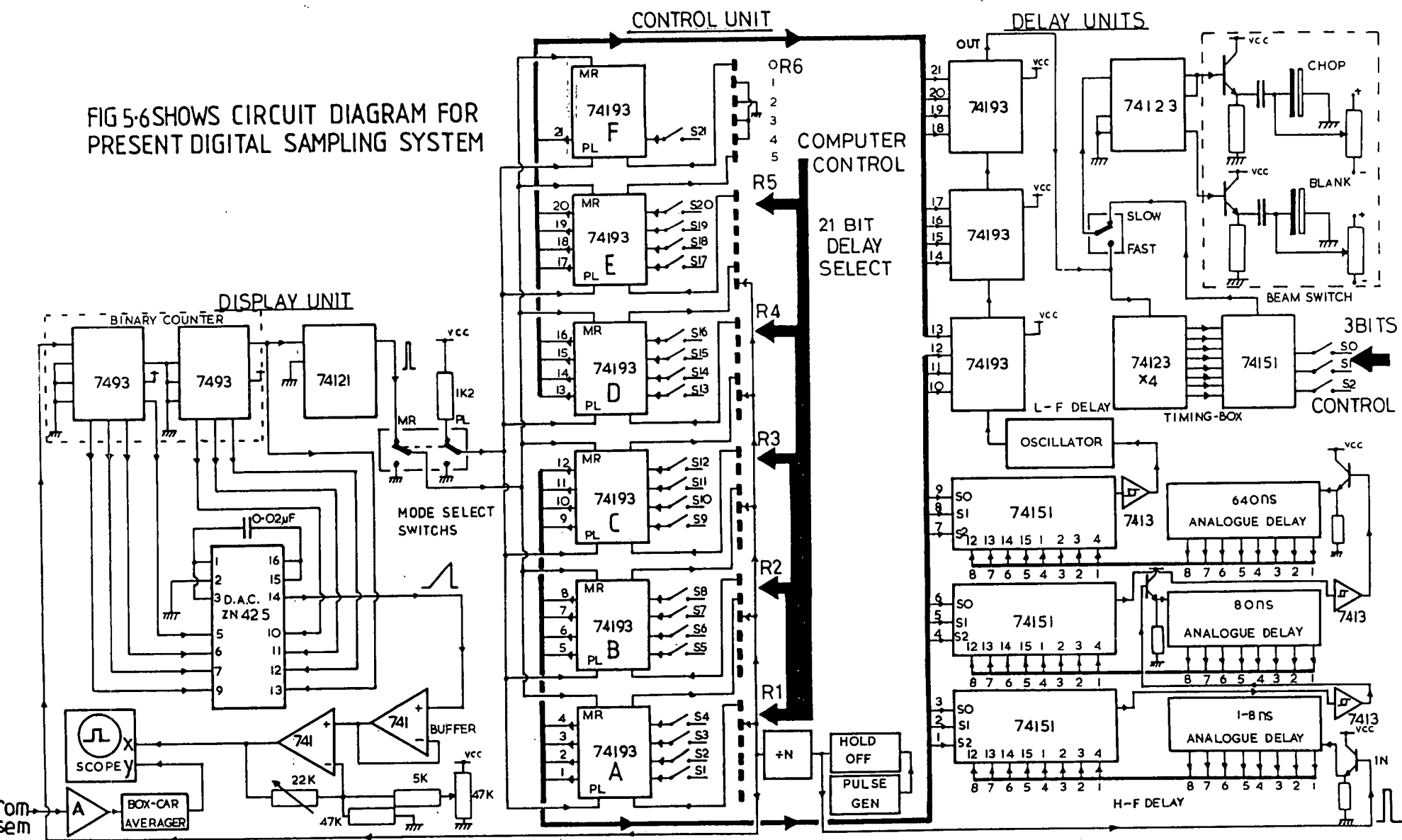
Figure 5.7 : Shows a block diagram for L.F delay using presettable counter in cascaded form.

All counters used are 74193 (A, B, C, D, E, F).

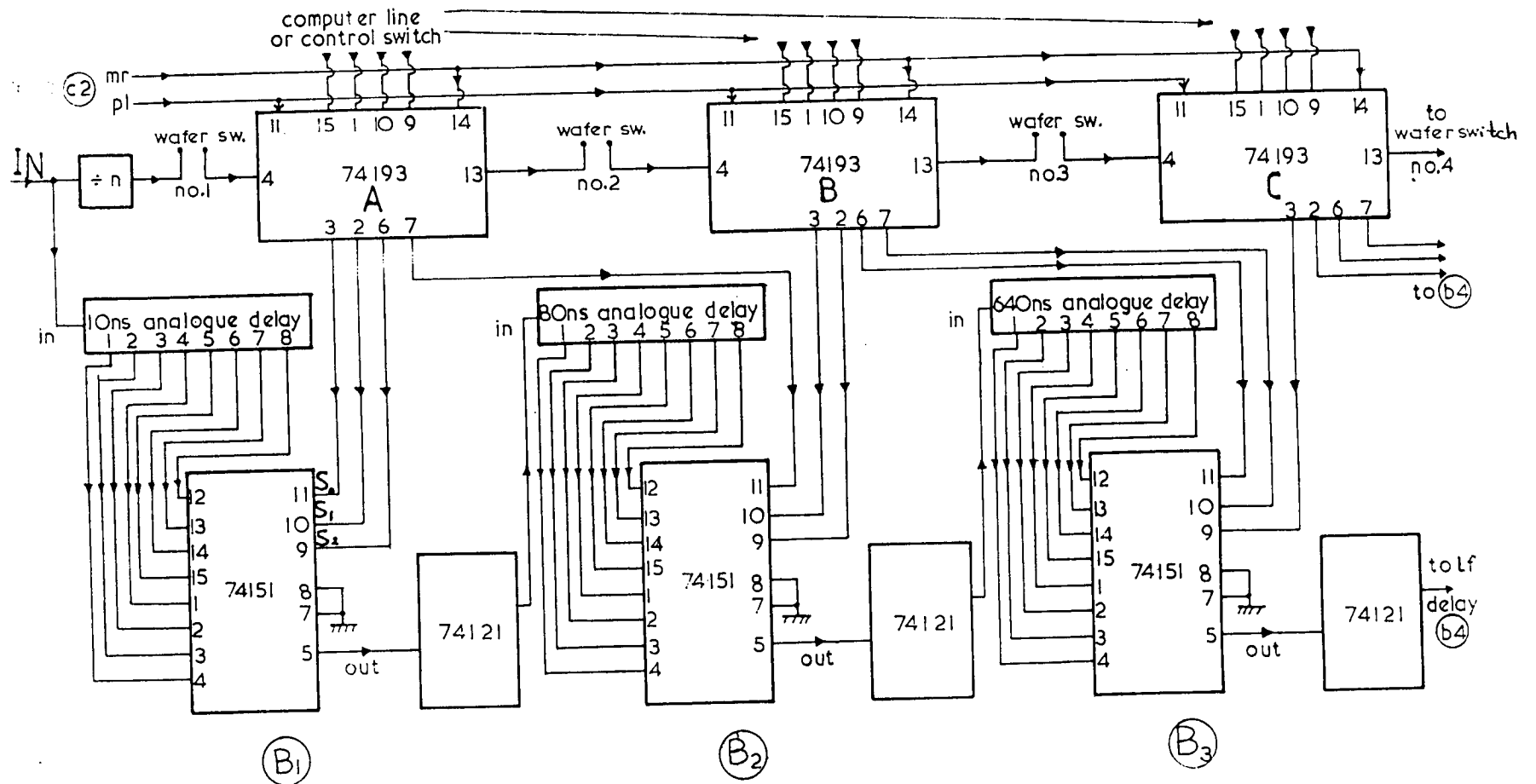Figure 5.8: Shows block diagram of digital sampling system control

Figure 5.9: Shows a block diagram for HF delay line units (B_1, B_2, B_3) with control board.

switches to the 21 delay selector inputs, so that the delay between the input trigger pulse and the electron beam pulse can be varied over the range 1.5 ns to 2 ms. In the sampling mode, however, the counters are fed by pulses which are counted down from the input trigger pulse (see Figures 5.9, 5.10), so that there are "n" electron beam pulses for each sampling dot on the display. The number of the sampling dots is normally 256, so that 8 successive bits of the 21 delay control bits are activated. In the manual control mode (see Figure 5.8), the appropriate 8 bits are chosen by a wafer switch, which has five ranges.

5.4   DELAY UNITS DESIGN

5.4.1 Analogue High Frequency Delay Lines Design

Currently available commercial delay lines were unsuited for the present system , due to limited bandwidth (BW) and high cost, so it was decided to build new delay lines for the present work.

Coaxial cable is used for producing a delay of 1 ns to 7 ns, in such a way that 200 mm cable length produces 1 ns delay, the layout as shown in Figure 5.11. For delays of 8 ns to 640 ns, lumped element L-C delay lines were used.

The following formulas are used for their design:

$$t_s \cong 1/\pi f_c = \sqrt{LC} \qquad\qquad (5.2)$$

where t_s is time delay for a single T-section (see Figure 5.12, 5.13) and f_c is the cut off frequency of low pass filter and the line terminat-
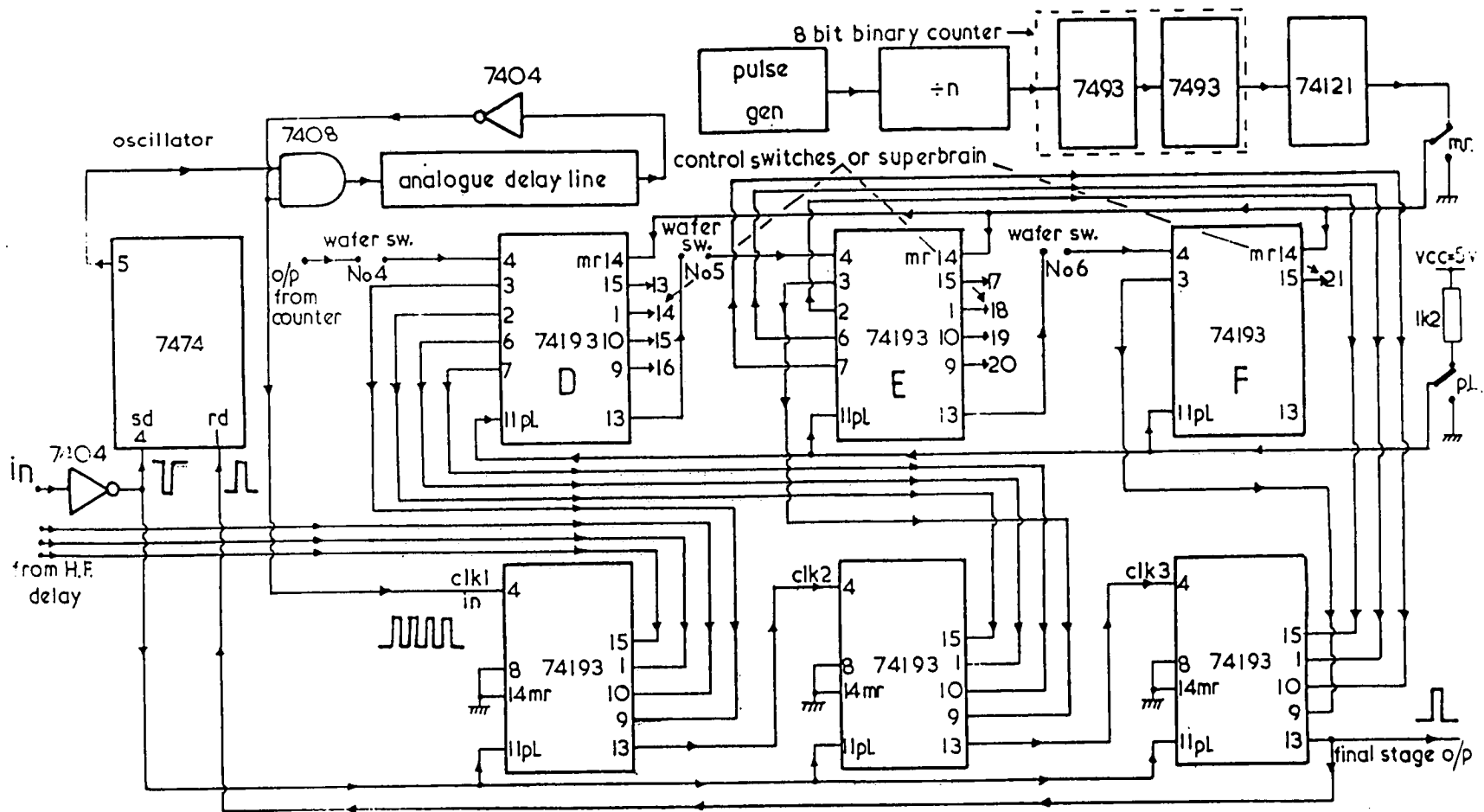
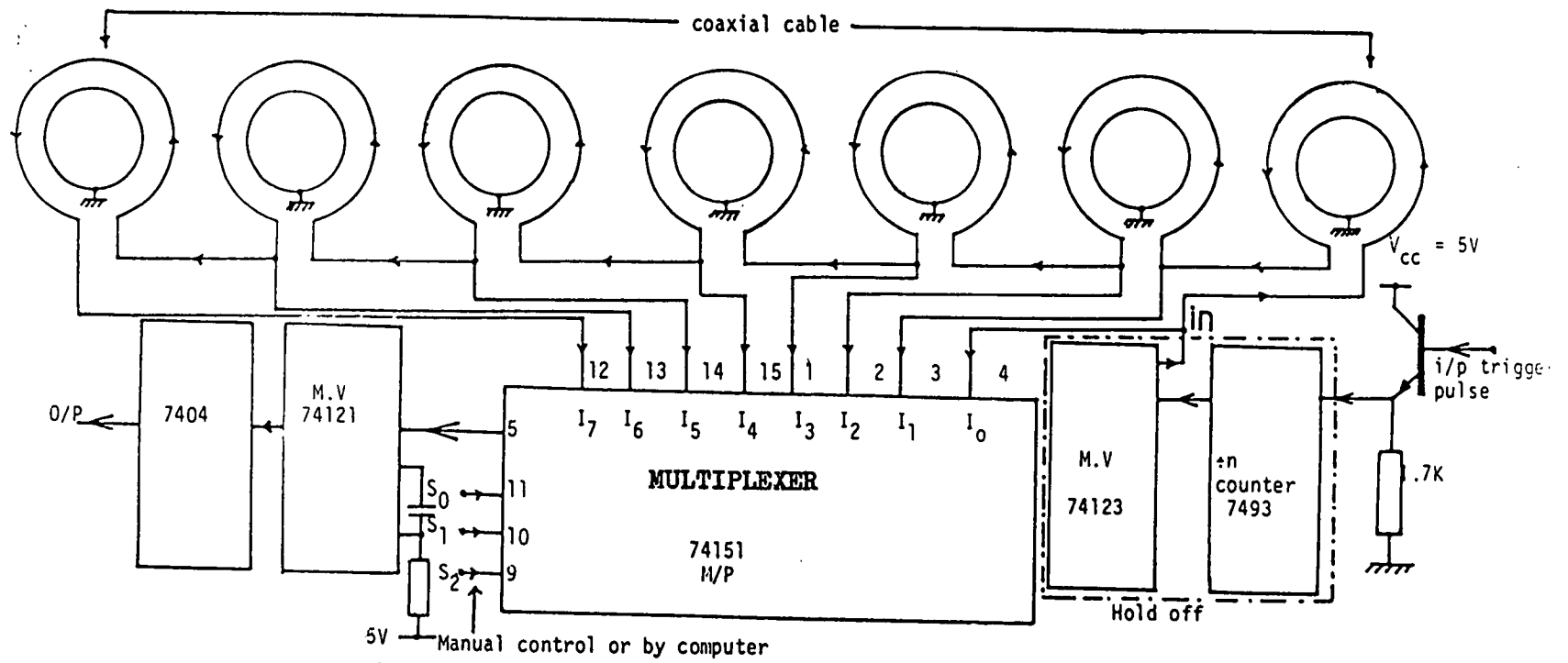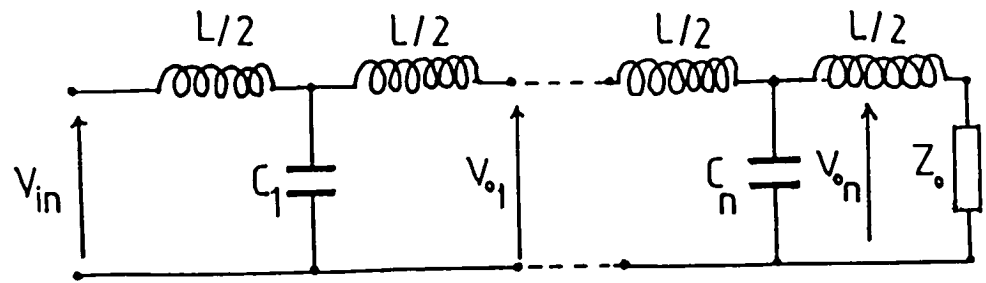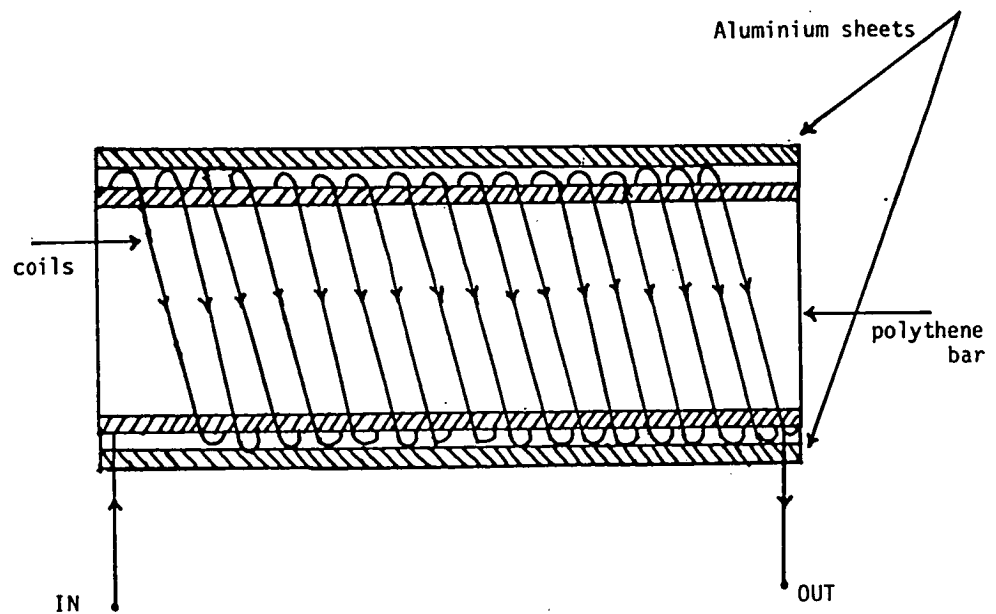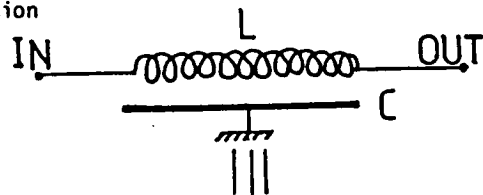Figure 5.10: Shows a block diagram for L.F delay unit with control board.

Figure 5.11: Snows a block diagram for H.F delay line to generate delay of 1 - 8 ns.

(A) T-section

(B)   Construction of double aluminium sheet layer used to produce 640 ns delay.

Figure 5.12 : Shows high frequency delay lines developed in sampling system.
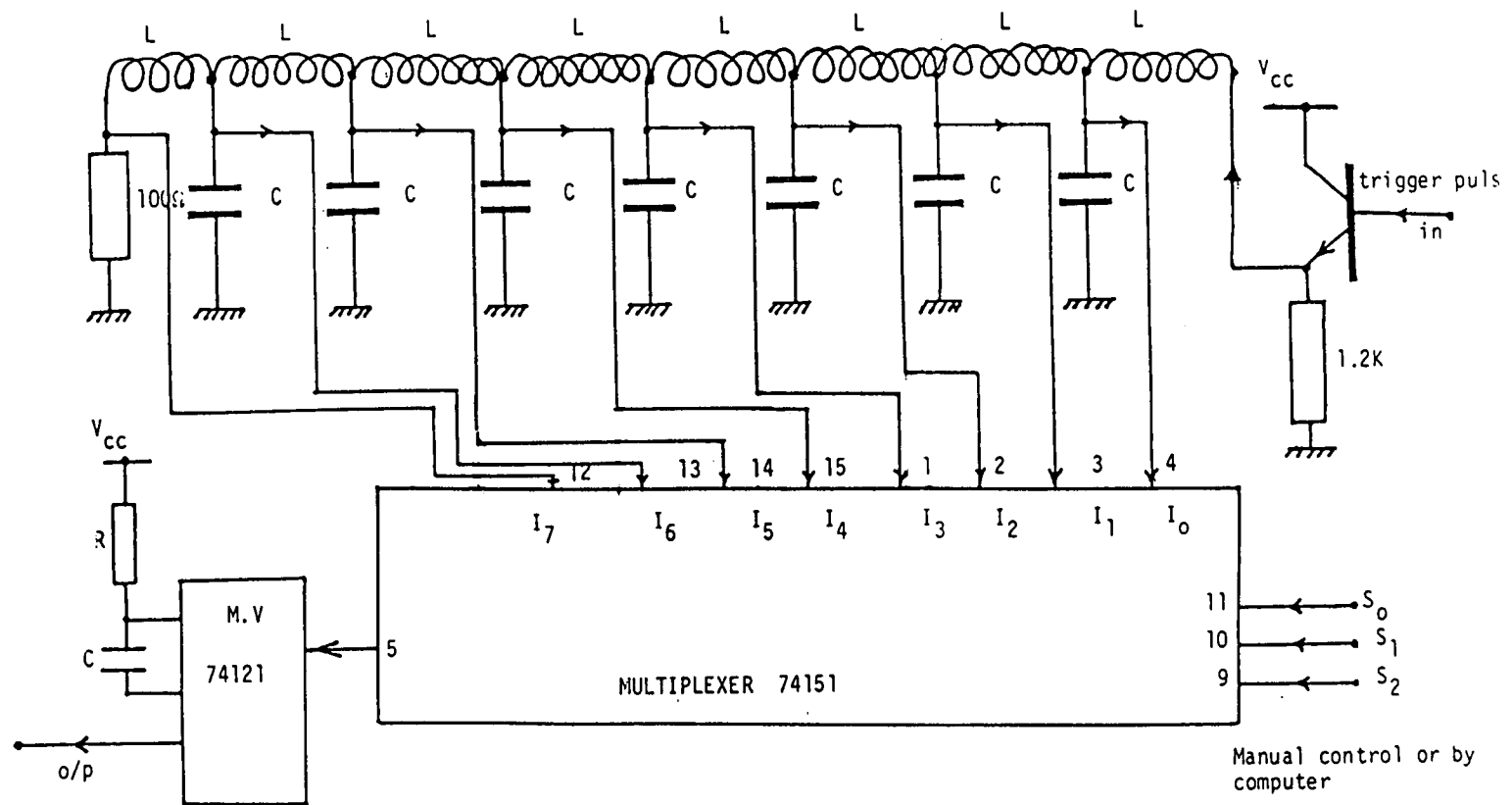
Figure 5.13: Shows a block diagram for H.F delay using L-C transmission line to generate 80 ns

ed impedance (characteristic impedance) Z_o is expressed as:

$$Z_o = \sqrt{L / C} \tag{5.3}$$

This T-section is a low pass filter (L.P.F) whose attenuation and phase shift are a function of frequency. If the frequency of $V_{in} \ll f_c$, $V_{(output)}$ will be a reproduction of $V_{(input)}$ but delayed. A number of T-sections (See Figure 5.13) cascaded into a so called "Lumped parameter delay line" increases the total time delay:

$$t \text{ (delay)} = n \cdot t \text{ (single)} \tag{5.4}$$

where n = number of cascaded T sections.

Because of the sharp cut off frequency of lumped parameter delay lines, amplitude and phase distortion becomes a problem when the frequency of the input signal increases. Overshoot and ringing problems of the output delayed pulse are expected. Wire of SWG 30 was used in winding the coils for the delay lines. Termination by the impedance of the line is employed to stop pulse reflections. Emitter followers and drivers are used for matching between delay lines.

5.4.2 Digital Low Frequency Delay Line Design

Initially, shift registers were used to simulate low frequency delay lines but there was a clock triggering difficulty, due to no synchronisation between the input delayed pulse and shift register clock. For this reason, it was decided to use presettable counters, to count

down the number of triggered oscillator pulses. Three counters (74193) are used in cascaded form as the low frequency delay generator (see Figure 5.7). These counters are preset by another set of counters (see Figure 5.14), by either manual (local) control using wafer switches or automatically (remotely) by the "Superbrain" through the GPIB. The unit produces a delay of 640 ns to 2 ms. This model of digital principle was developed with significant results.

5.4.3 Oscillator Unit Design

The circuit of the oscillator works on the same principle as the gated counter(for gated counter principle see Malvino and Leach(1975)) where the output of the high frequency delay line (see Figure 5.15) is used to start the oscillation and control the parallel load (PL) of the presettable counters (74193), which are utilised to produce the low frequency delay. The oscillator output pulses are employed as clock input pulses to the counters to be counted down. The present oscillator circuit consists of a bistable switch (7474) with an analogue delay line (L-C transmission line type is used), AND & NOT gates.

The bistable switch is used to control the number of delayed pulses from the high frequency delay unit, to count down the number of oscillations. The switch resets by the output pulse from the presettable counter. The condition for synchronisation of high frequency delay with low frequency delay generators is as shown in Figure 5.16.

5.4.4 Local Delay Control

Figures 5.8, 5.14 show block diagrams of the manual way to control the delay lines (high frequency and low frequency signal delay).
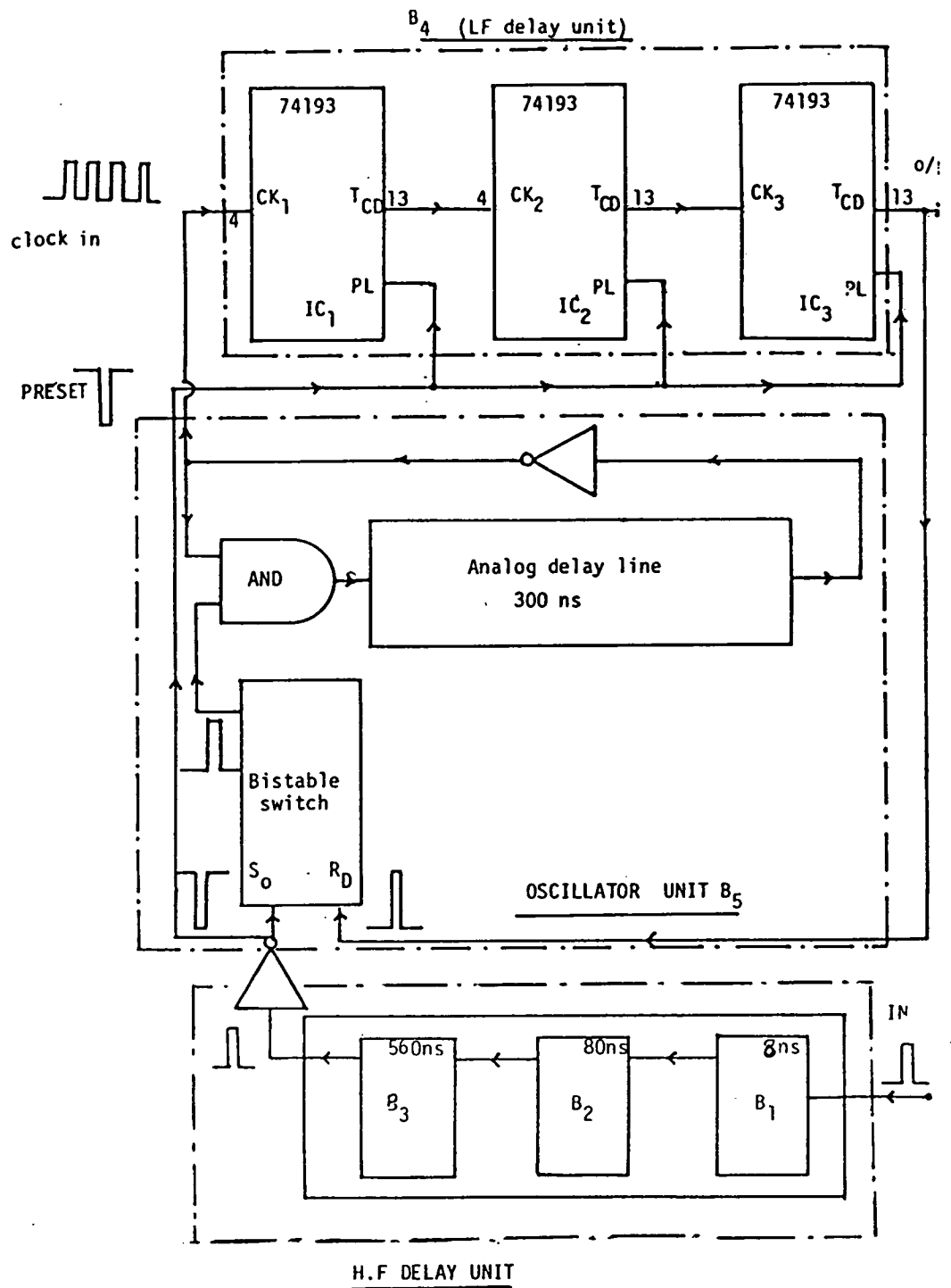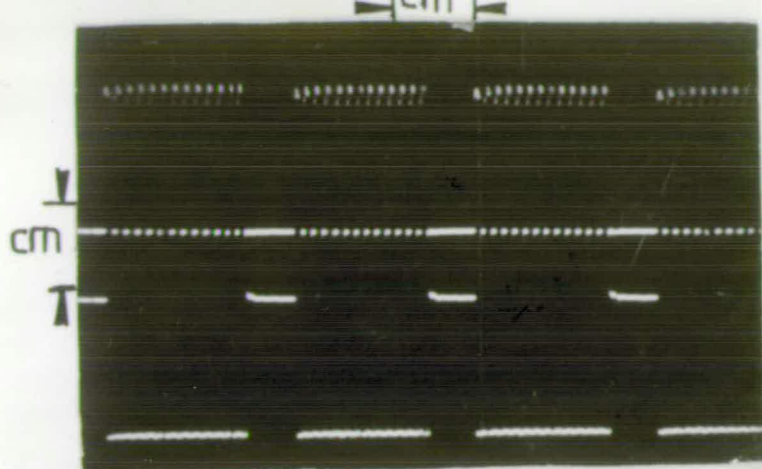
Figure 5.14 : Shows a block diagram for manual control of delay units

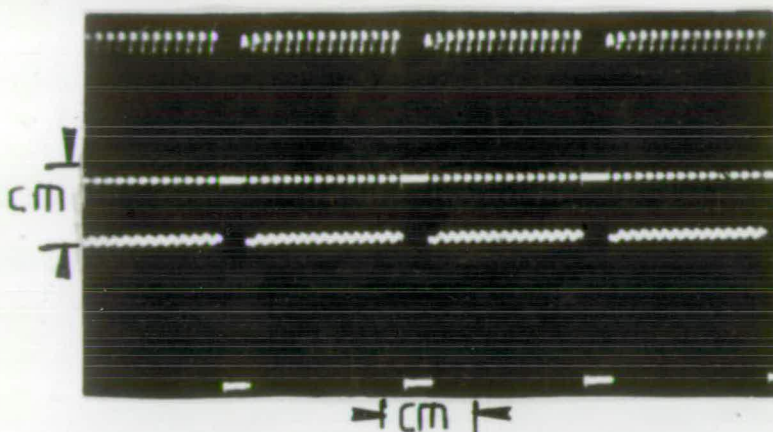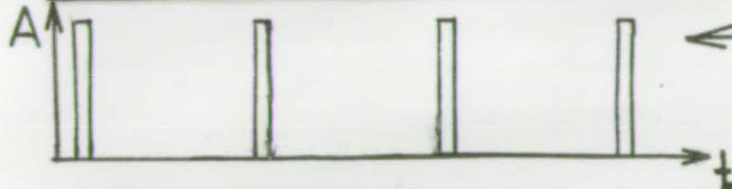Figure 5.15: Shows a block diagram for delay units and oscillator circuit for digital sampling system.

(A)

upper trace is trigger
pulse to L.F delay
generator

lower trace is o/p
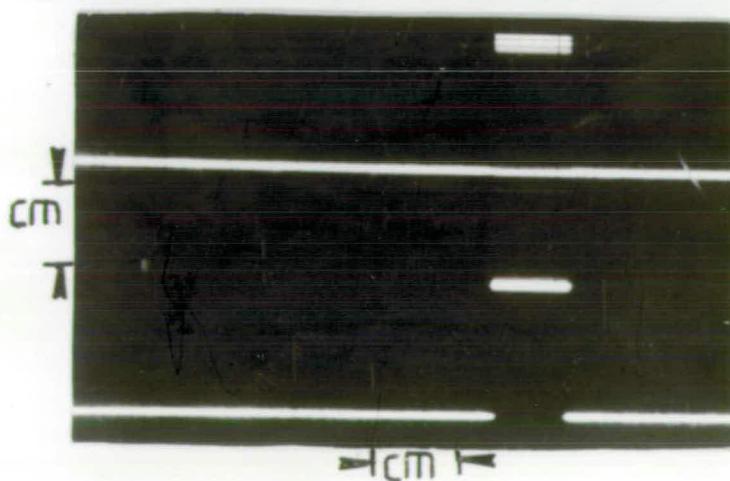from digital counters
to RD of bistable
switch

$H = 2\,\mu s/cm$
$V = 2V/cm$

To s_o of bistable
i/p from analogue
stage

(B)

upper trace is trigger
pulse to L.F delay
generator — i/p clock

lower trace is control
pulse of PL of
digital counter

(C)

upper trace is i/p
trigger pulse to L.F
delay generator

lower trace is o/p
of L.F delay generator

$H = 1\,ms/cm$
$V = 2V/cm$

Figure 5.16: Shows synchronization of H.F delay
with L.F delay generators.

21 toggle switches are used to control phase change in the stroboscopic mode.

Wafer switches provide a manually- programmable phase change control, by means of five ranges of operation in the sampling mode. Another wafer switch is used to control the number of samples per phase to control divide by N counter (3 sets of binary counters in series are used).

The mode select switch is employed, to decide the type of operation to carry out (stroboscopic or sampling modes). All switches are in the control panel board of the sampling system. Computer control can replace all the control switches.

5.4.5 The Band Width Limitation Problem

Figure 5.17 shows the discontinuity problem of time delay (non-uniform time delays distributions) in the sampling pulses. The delay line of 560 ns was found experimentally to have a serious bandwidth limitation, which causes the irregularity problem affecting the performance of the sampling system at high frequency. It was decided therefore to build a new type of delay line as shown in Figure 5.12b with a construction of double aluminium sheet layers, which forms a distributed capacitor.

The advantage of this sort of construction is the distributed capacitor and inductor which gives wide bandwidth. 10 mm length of the line produces a measured 10 ns delay. The reflection problem is stopped by termination resistors at each line. Inverter and driver gates are used to provide a good match between lines and provide regeneration. Each line produces a delay of 60 ns, plus a delay of 20 ns
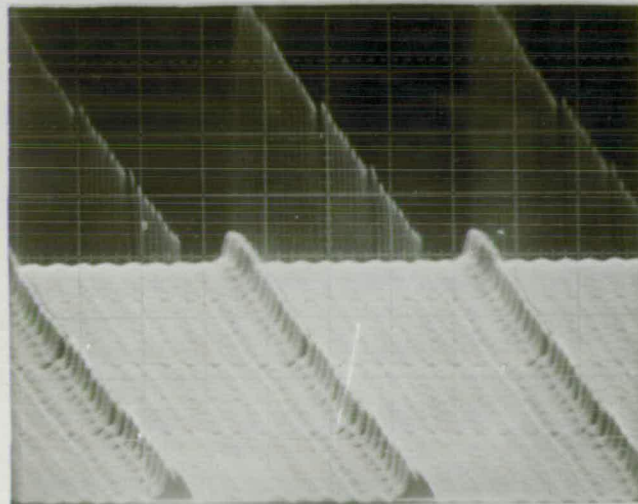
(A)
upper trace is i/p
trigger pulse
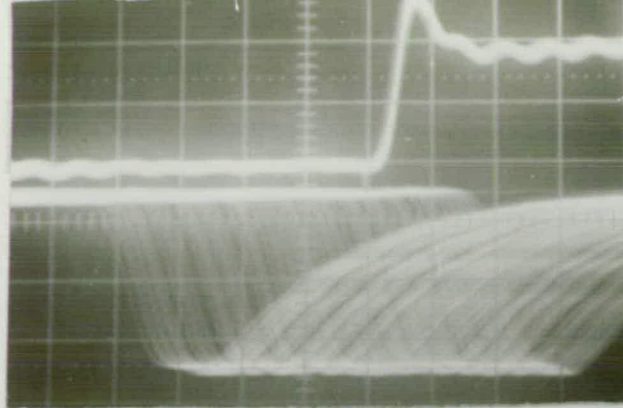
lower trace is
sampling pulse with
time delay irregularity
problems.

H = 20 ns/cm
V = upper 2V/cm
    lower 5V/cm

(B)
Same as above
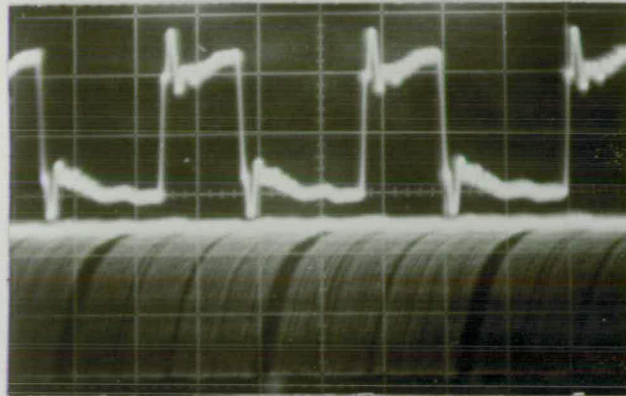
H = 0.1µs/cm

with time delay
problems

amplitude

(time)

delay

(C)
time irregularity
3-D picture ramp +
delayed pulse.

delay time
discontinuity problems
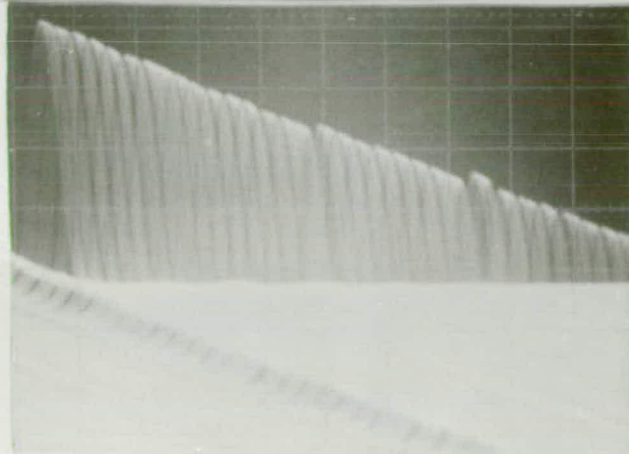
(D)
Same as above

Figure 5.17 : Shows testing regularity of time delay
              problem in digital sampling system.

produced by the gates used. 560 ns is the total time delay produced by seven delay lines which work with a satisfactory performance. The overall high frequency delay unit is shown in Figures 5.18 & 5.19, where a new zig - zag layout of delay lines is created and recommended for this sort of time delay in analogue form.

The performance of the high frequency delay line was found to be reliable and repeatable in generating time delays (see Figure 5.20). After the modifications of the recent design of the delay lines, the experimental evaluation indicates that serious consideration should be given to the construction of the high frequency delay lines.

5.5 SAMPLING SYSTEM CIRCUIT DESIGN

5.5.1 Description of Circuitry

The signal from the pulse generator is fed through the hold‑off circuit to both of the delay units and to the divide by N counter (see Figure 5.6). A switch for selecting the mode of the system operation is used to control the master reset ($\overline{MR}$) and the parallel load ($\overline{PL}$) of the presettable counters (six counters of type 74193 are used in cascaded form to control the sampling phase change). The output of the 8 bit binary counter is fed to a monostable multivibrator to produce a short pulse, to reset the presettable counters in the control board each time 256 samples (pulses) are counted down.

The switch position allocates the type of mode operation in the sampling system as follows:

1. If $\overline{MR}$ and $\overline{PL}$ are at earth position, then the operation is in

Figure 5.1& Shows analogue zig-zag model for H.F delay to generate 560 ns.

Hint 1 to 8 is o/p to multiplexer (M/P)

Figure 5.19 : Shows a block diagram for H.F delay unit generating 560ns delay.

(A)
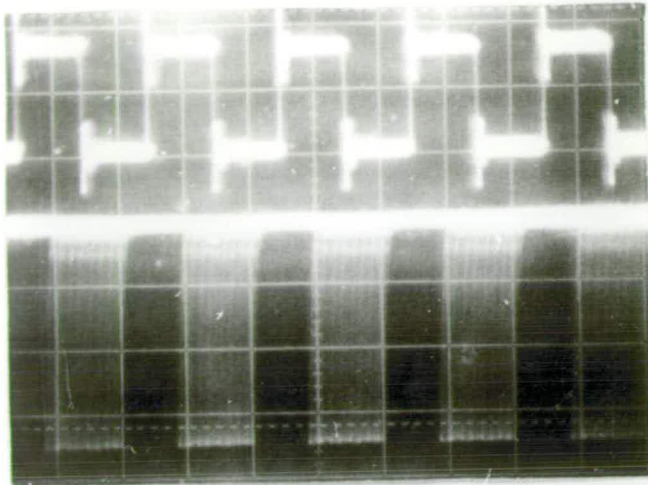
upper trace is i/p
trigger pulse
lower trace is samp-
ling pulse.

Time delay regularity
distribution solving
B.W. limitation of
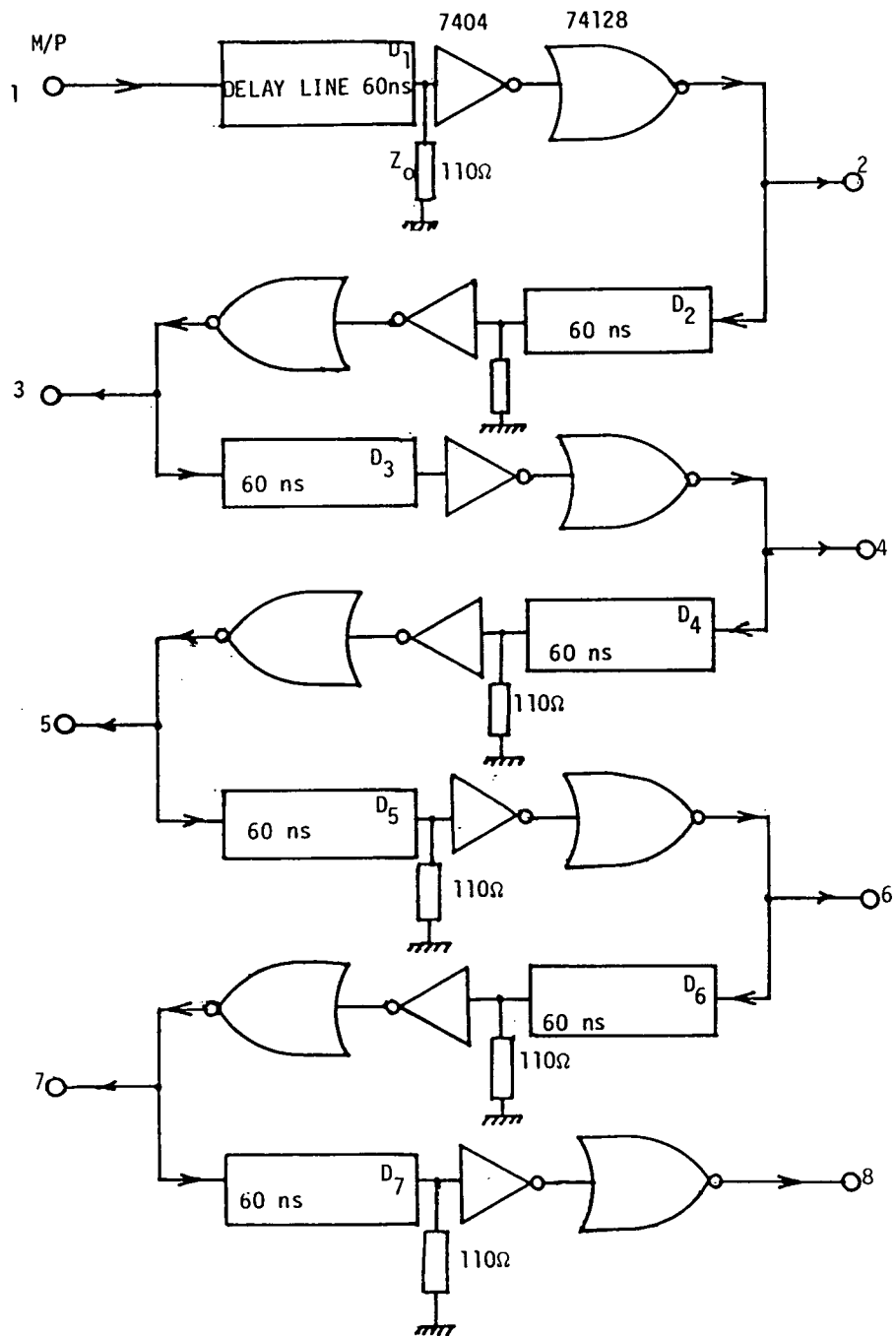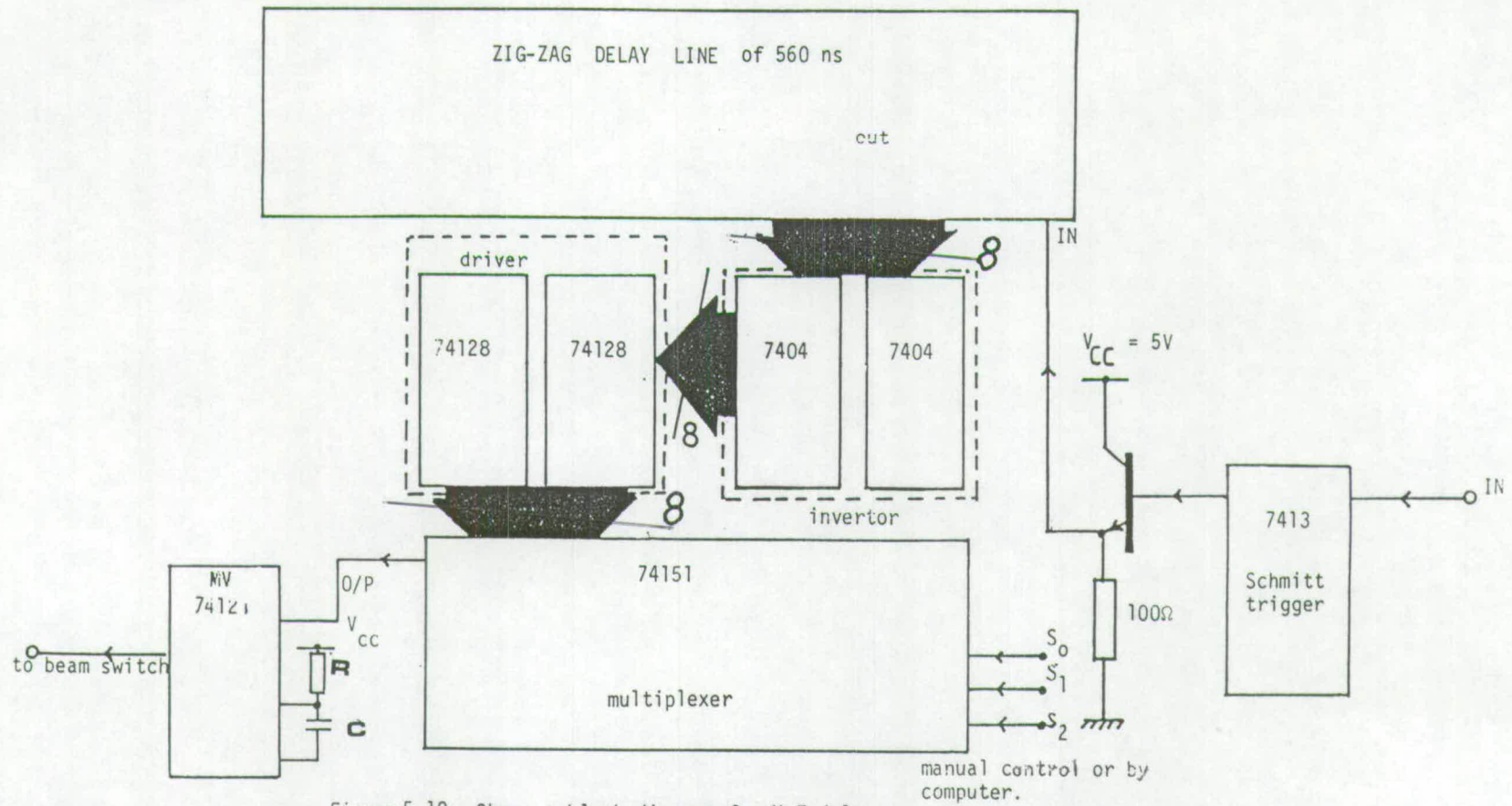H.F delay generator

H = 0.5μs/cm
V = upper 2V/cm
    lower 5V/cm
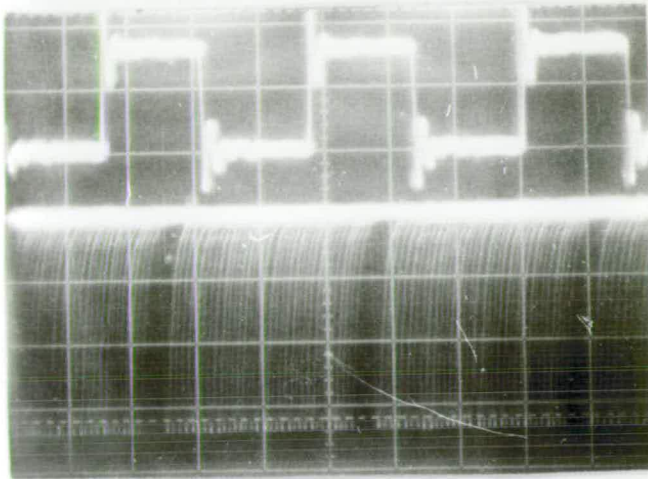
(B)

Same as above but
H = 0.1μs/cm
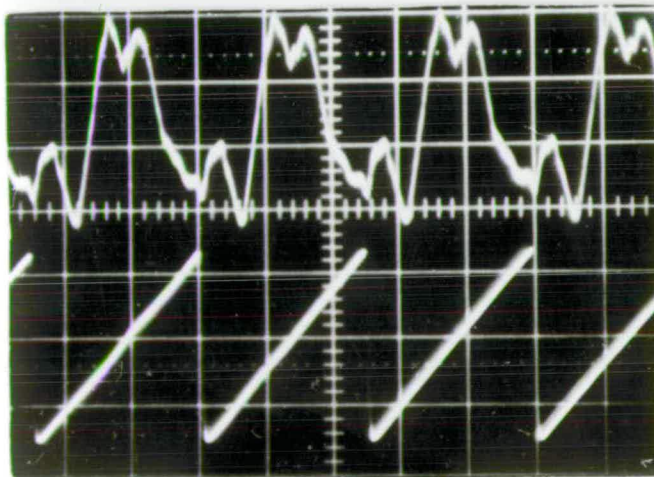
(C)

upper trace is
reconstructed wave-
form
lower trace is ramp
signal to the scope

H = 2 ms/cm
V = upper 20 mV/cm
    lower 2V/cm
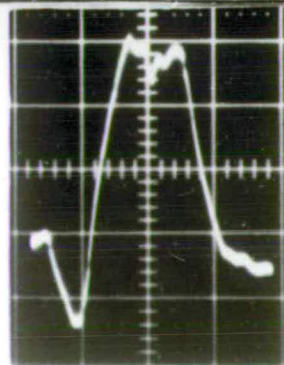
(D)

reconstructed wave-
form without ramp

V = 20 mV/cm
f = 3.5 MHz

Figure 5.20: Shows time delay regularity with reconstructed
            waveform.

the stroboscopic mode (Image Mode).

2. If $\overline{MR}$ and $\overline{PL}$ are at the high voltage position, it is then in sampling mode (waveform mode).

Wafer switches are used as a manually programmable control of sampling phase and also used for the range select (see Figures 5.8 & 5.14). Two of the presettable counters of 8 bits run each time in sequence, to count down from the input signal (there are actually five ranges of operation, the first two are for high frequency signal time delay). The output of the presettable counters which are used to control phase change in the sampling mode are connected to 21 tapping points of the delay units (9 points for high frequency delay units, 12 points for low frequency delay unit). The overall circuit design was developed to produce any delay for any signal frequency from 10 KHz to 10 MHz. If the operator wants to produce a delay, a main toggle switch is employed to decide the operation speed as:

1. To produce time delay of a high frequency input signal, the switch should be at the fast position, where the input signal only propagates and progresses through high frequency delay lines, and then passes directly to the beam switch amplifiers and does not pass through the rest of the delay circuit to avoid time delay error of the delay units.

2. A long time delay is achieved by selecting the slow speed position, then the input signal to the sampling system propagates through all delay units.

Error in the time delay is produced by the signal progressing and

propagating through devices in the present system, and is measured as 70 ns time delay for high frequency delay lines and 700 ns for the overall sampling circuitry. 50 ns delay is also measured as a delay error for electrons to transit from the chopping plates to the display unit. All these delays should be considered as a constant delay of the system. Figure 5.22 shows the block diagram of the digital system set up. (For more details of other circuitry see sampling system and delay unit manual by the author).

5.5.2 Variable Pulse Width generator Design

Figure 5.21 shows a circuit designed in such a way as to generate different pulse widths (observation windows) of the delayed input signal (chopping and blanking signals), to provide better picture resolution in the stroboscopic SEM (image mode).

This circuit is made of a cascade of monostable multivibrators with different time constants, with multiplexer, which is controlled by three toggle switches (local), or by computer(remote) by three bits(a programme is written to control this unit), to produce pulse widths of 35 ns to 3 μs of eight different sampling pulse widths. This generator is found useful in slow speed condition in repetitive signal frequency up to 1 MHz. It is worth while to indicate here that it is necessary to choose an electron beam pulse that is small compared to the time period of the signal to be analysed.

5.5.3 The Hold - Off Circuit Design

Figure 5.11 shows the hold-off circuit which has been developed to meet the requirement that only one pulse should be travelling through the delay system at any instant i.e. the repetition period should be
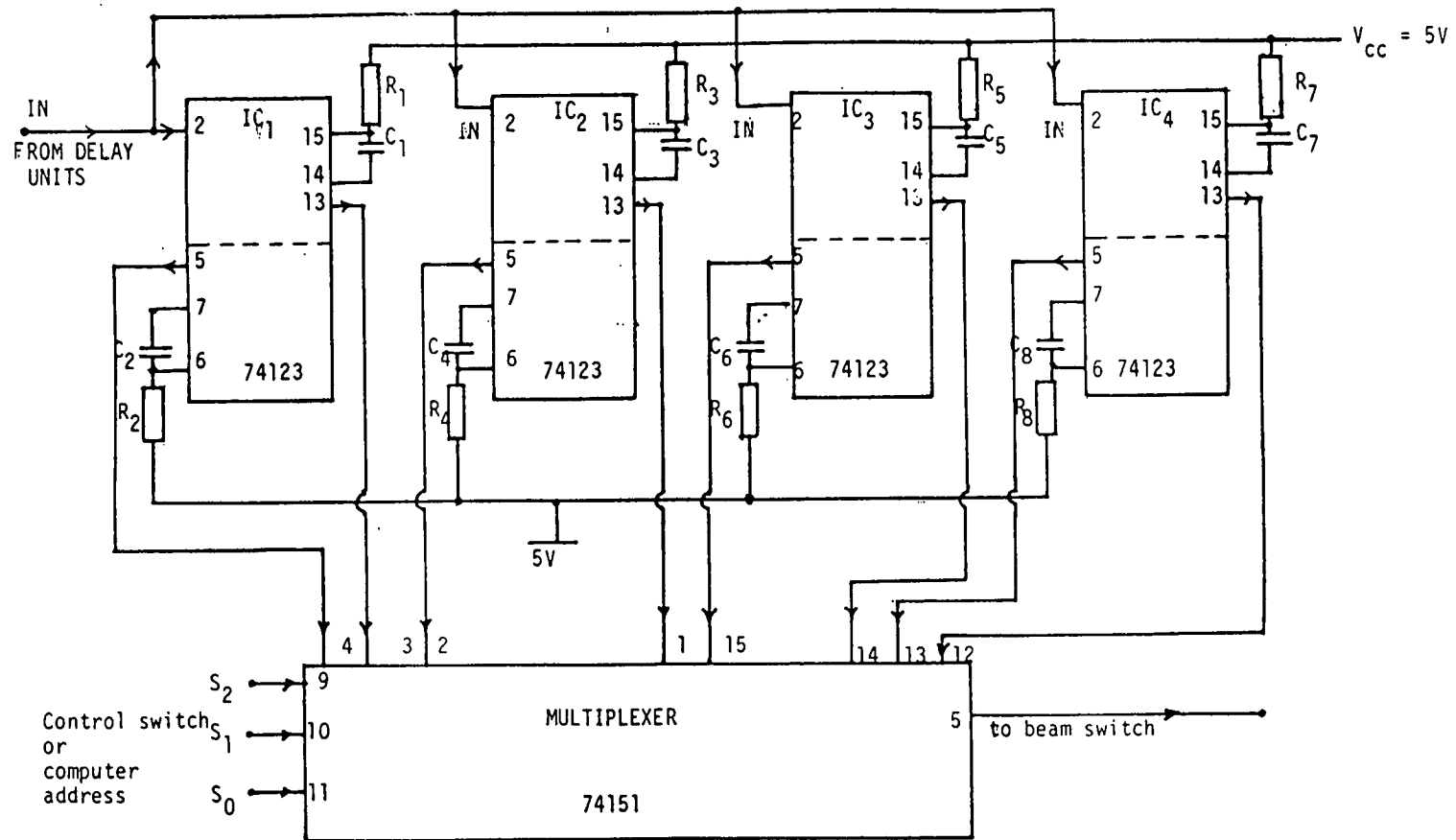
Figure 5.21: Shows a block diagram for a timing unit to produce different pulsewidths. (observation window)
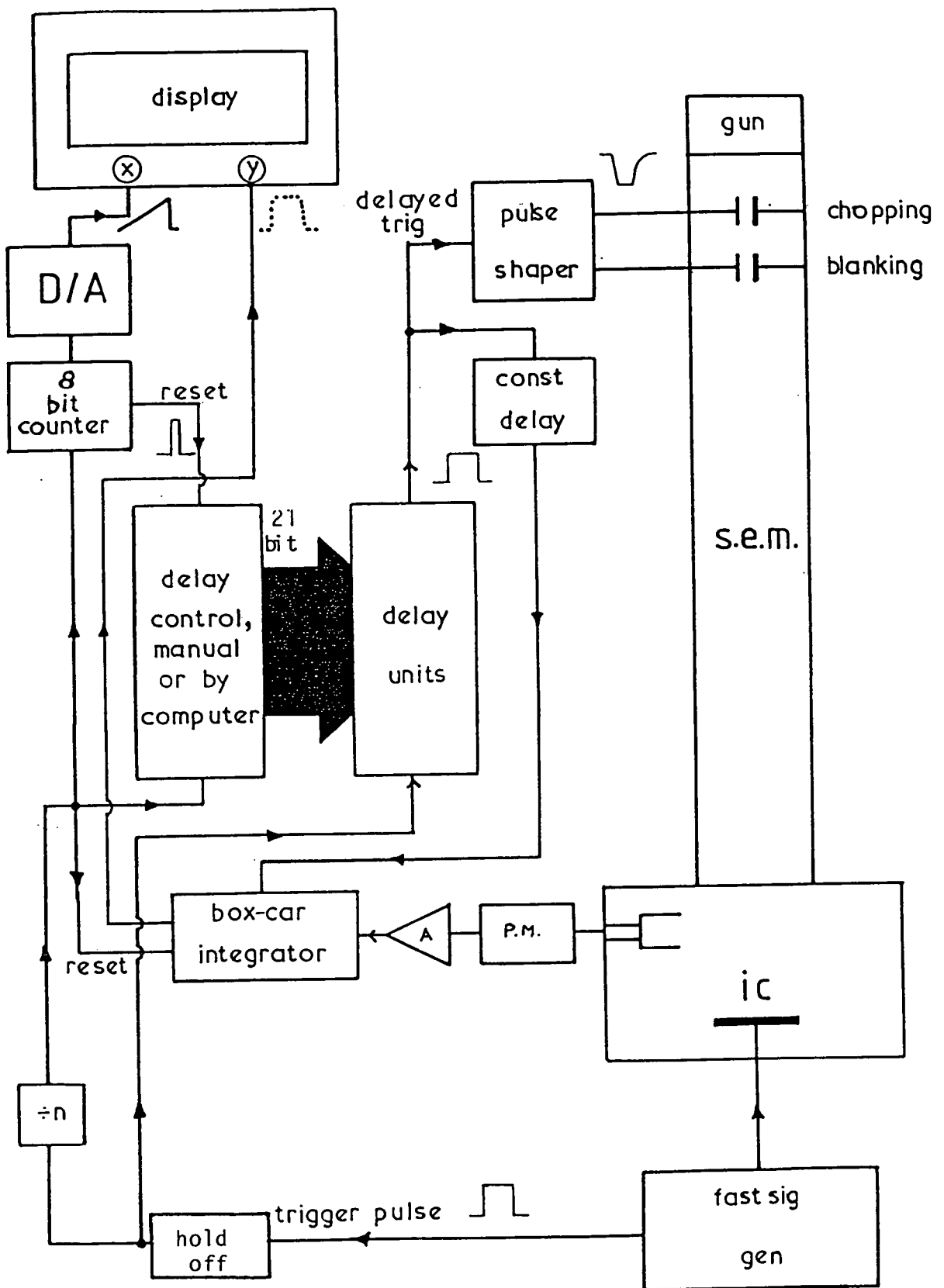
Figure 5.22 : Shows a block diagram of sampling apparatus with direct digital control of e-beam pulse delay.

longer than the delay.

This circuit consists of a monostable multivibrator and binary counters, to inhibit further trigger pulses to the system until it returns to its stable state. The time constant of the multivibrator is decided to be 30 ns, in such a way to allow the shortest input signal to pass to the delay units. This circuit is found useful above 1 MHz frequency, it also could be used to control the number of sampling pulses per input signal to perform sampling mode (allows one electron beam pulse for every nth trigger input pulse)

5.5.4 Digital Sampling and Delay Unit Specification

Operating Modes	Sampling - Stroboscopy
Delay	1.5ns to 2 ms
8-different pulse widths	35 ns, 300 ns, 450 ns, 1 µs, 8 µs, 2.5 µs, 3.2 µs.
(Time Unit)	To 5V(f.s.d) 256 steps
X-deflection O/P	To 5V(f.s.d) 256 steps
Number of dots/trace (sampling resolution)	256 (manually) unlimited (remotely)
Number of samples/phase	2, 4 , 8, 16, 32, 64, 128, 256 up to 2048.
Trigger rates	10 KHz to 10 MHz
Trigger amplitude	100 mV up to 3V
Stroboscopic Mode	Full manual control (1.5nto 2ms in

1.5 ns steps)

Sampling Range   Five ranges (R1, R2, R3, R4, R5)

R1 ,R2 - high frequency delay (1.5 -640ns).

R3 , R4 ,R5 - low frequency delay -
                 (640n- 2 ms).

Computer Interface

Computer interface via IEEE 488 bus and
multiprogrammer.

Hold Off   At trigger input rates **at any frequency.**
one electron beam pulse results from
one trigger input pulse. At higher
frequency trigger input rates,
hold off allows one electron beam pulse
for every nth trigger input pulse.

5.5.5 Noise Problem

Two types of noise are considered at present; these are

(a) Interference noise

(b) Beam noise

Interference noise which, appears especially at the high frequency
delay generators, is mainly due to reasons which were mentioned in
Chapter Four. Also this noise does exist in the digital delay unit. and
it becomes worse as the operating frequency of the input signal is in-
creased above 5 MHz (see Figure 5.23).
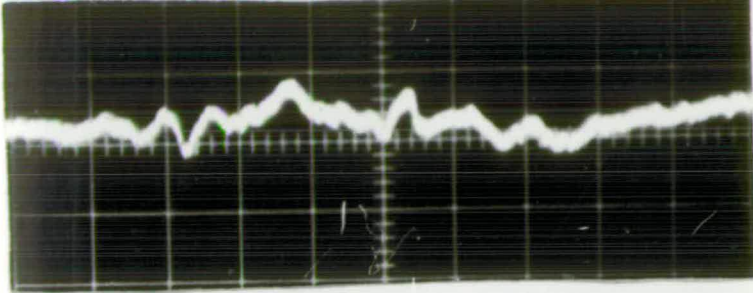
(A)

noise level

V = 10mV/cm
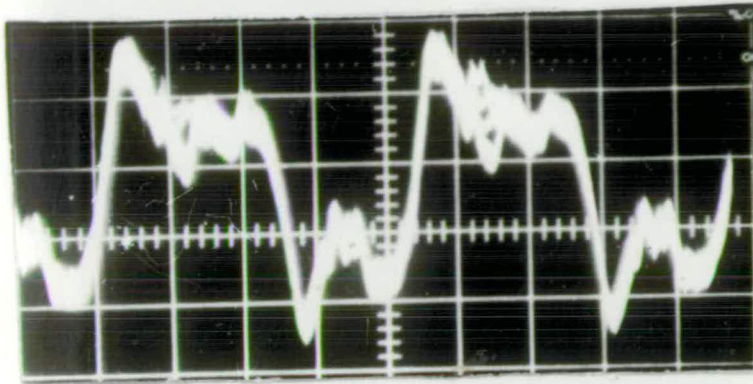
(B)

reconstructed
waveform with noise

H = 5 ms/cm
V = 20 mV/cm
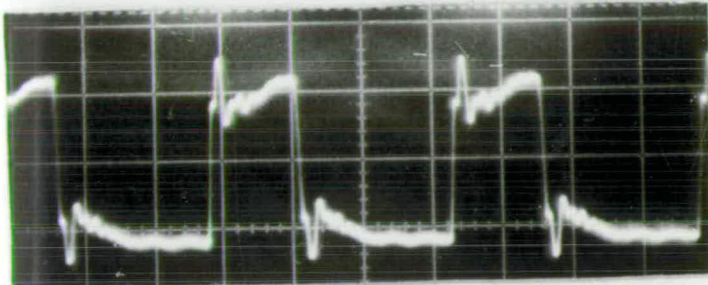
(C)

input signal waveforms
fed to specimen

H = 0.1μs/cm
V = 2V/cm
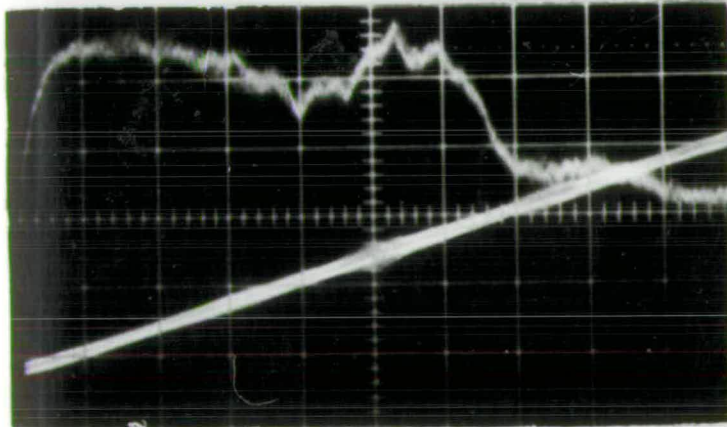
(D)

upper trace is re-
constructed waveform
with noise

lower trace is ramp
with noise

H = 5 m/cm
V = upper 20 mV
    lower 5V/cm
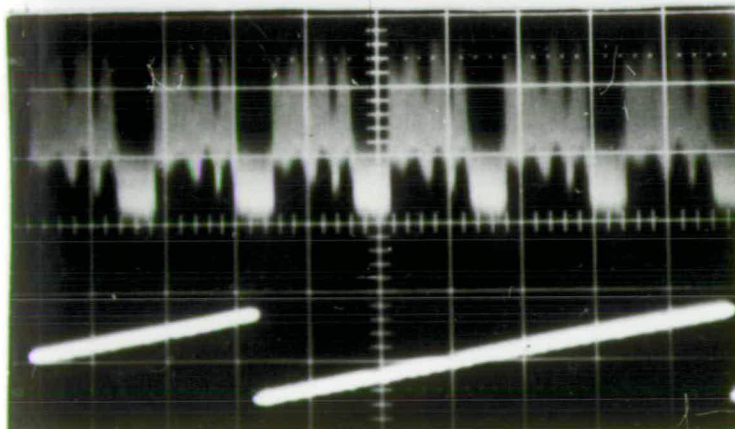
(E)

upper trace is a
reconstructed waveform
with beam noise

lower is ramp

H = 2 ms/cm
V = upper 50 mV/cm
    lower 5V/cm

Figure 5.23: Shows noise problem in digital sampling system
in reconstructed waveform on specimen under test.

Interference noise enters with the input signal and is superimposed on the ramp signal (which is used to drive the X-plates of the display unit) and increases the difficulty of measuring the rise time of the reconstructed waveform. This noise is minimised by proper circuit layout, and by using a low pass filter with variable time constant, also used to smooth other high frequency noise. The box-car averager has been found to improve S/N ratio and reduce noise at operating frequencies up to 1 MHz.

Beam noise still appears in the reconstructed waveform as shown in Figure 5.23 . This noise could be further reduced by taking more samples per phase point and longer time constant of the filter or by developing a programmable digital filter unit after the SEM head amplifier. This filter is more stable than the analogue type.

5.5.6 Testing the Reliability of the Digital System

Two methods are developed to test the digital sampling system by:

1. Analysing the reconstructed waveform.

2. Production of regular time delays of the sampling pulses in the delay lines.
Figure 5.24 shows stroboscopic SEM using the digital system. Digital sampling system as shown in Figure 5.25 has performed a repetitive signal frequency of 10 MHz stroboscopic SEM.

The linearity performance of the sampling system is shown in Figure 5.26 and is found to work with high speed electron beam switching.
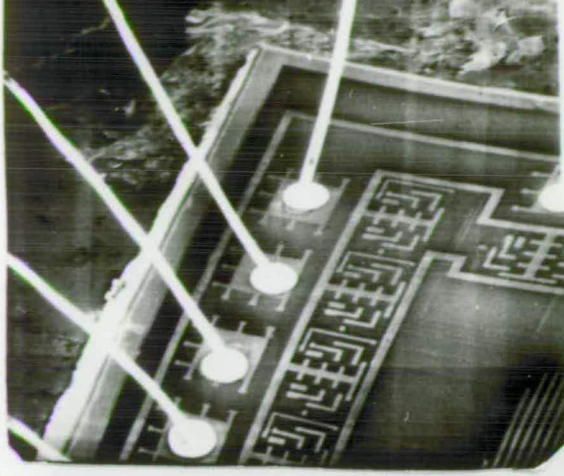
X500
(a)
micrograph with
bright pad (top)
at 5 MHz frequency
of i/p trigger
pulse to specimen
of arithmetic
averager
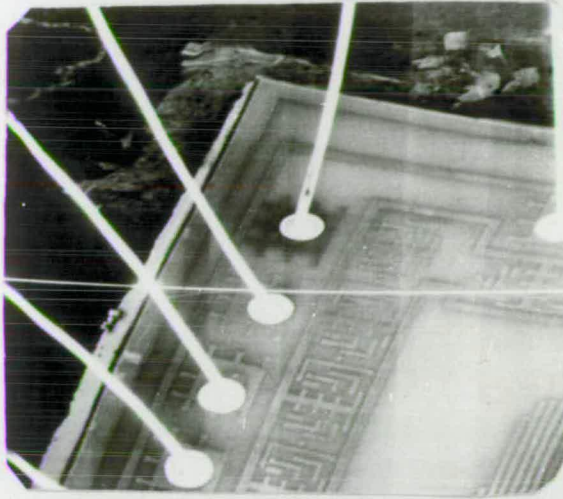
X500
(b) same as above
micrograph with dark
pad (top)
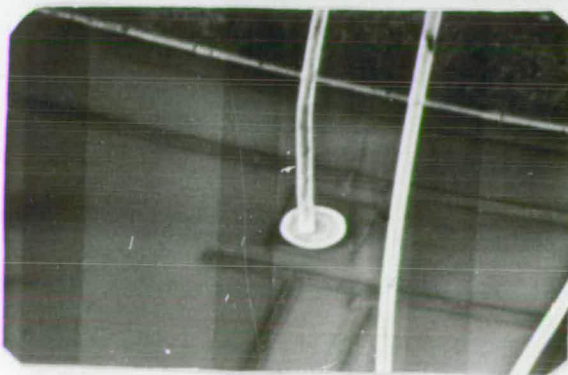
X1000
micrograph with
bright pad at 10 MHz
frequency of i/p
pulse to specimen

x1000
micrograph with dark
pad at 10 MHz freq-
uency of i/p pulse
to specimen

Figure 5.24 : Shows stroboscopic SEM using digital system.
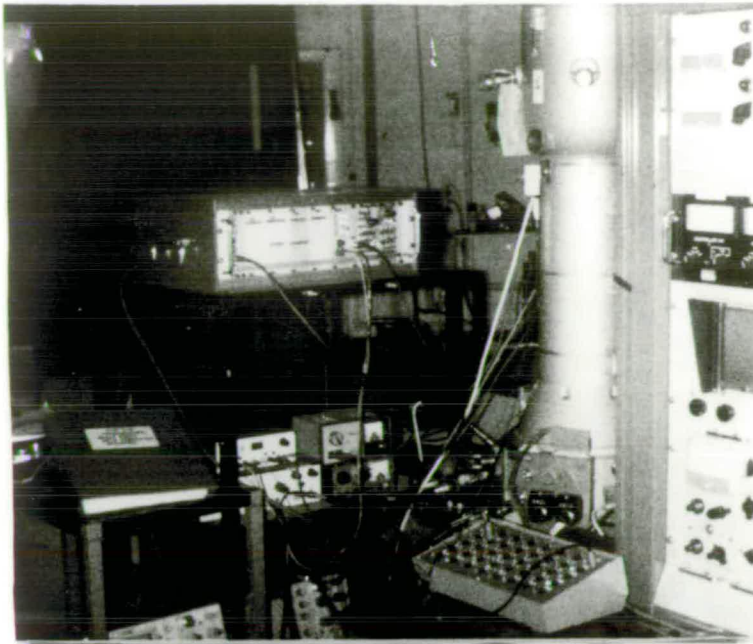
(A)
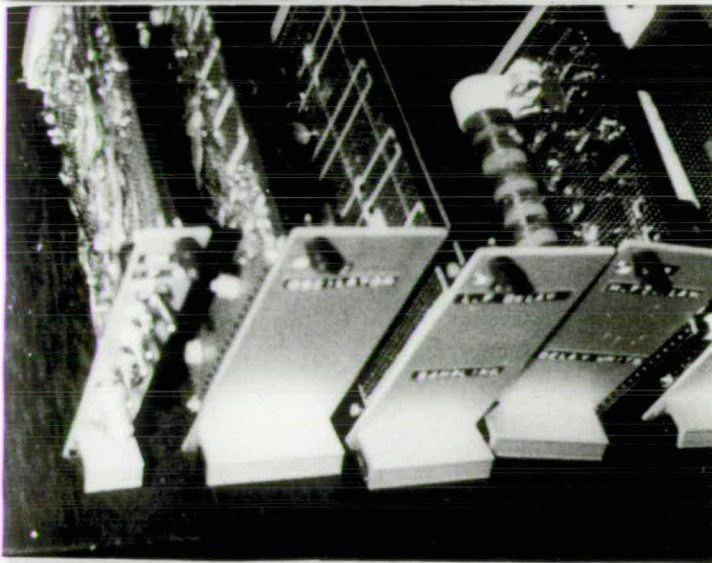
(B)
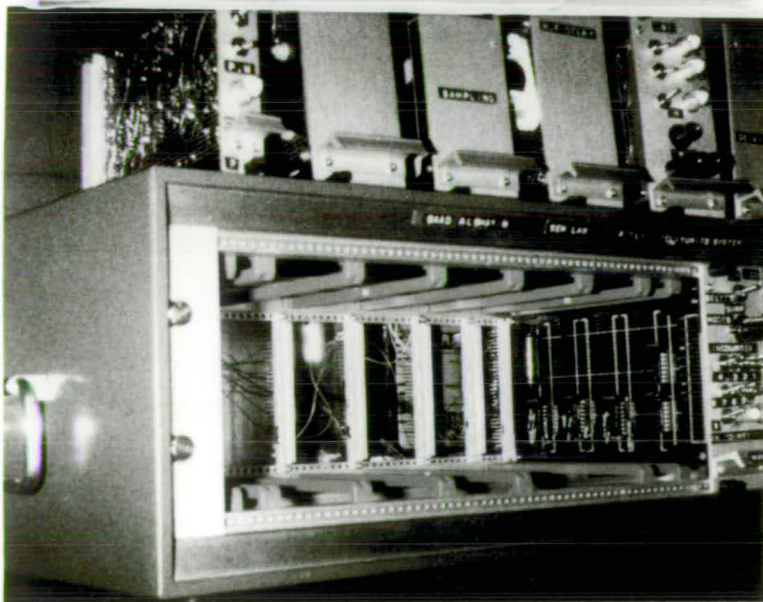
(C)

Figure 525 : Shows present digital sampling system with
experimental set up. In A, B shows
delay units and C shows subrack.

(A)
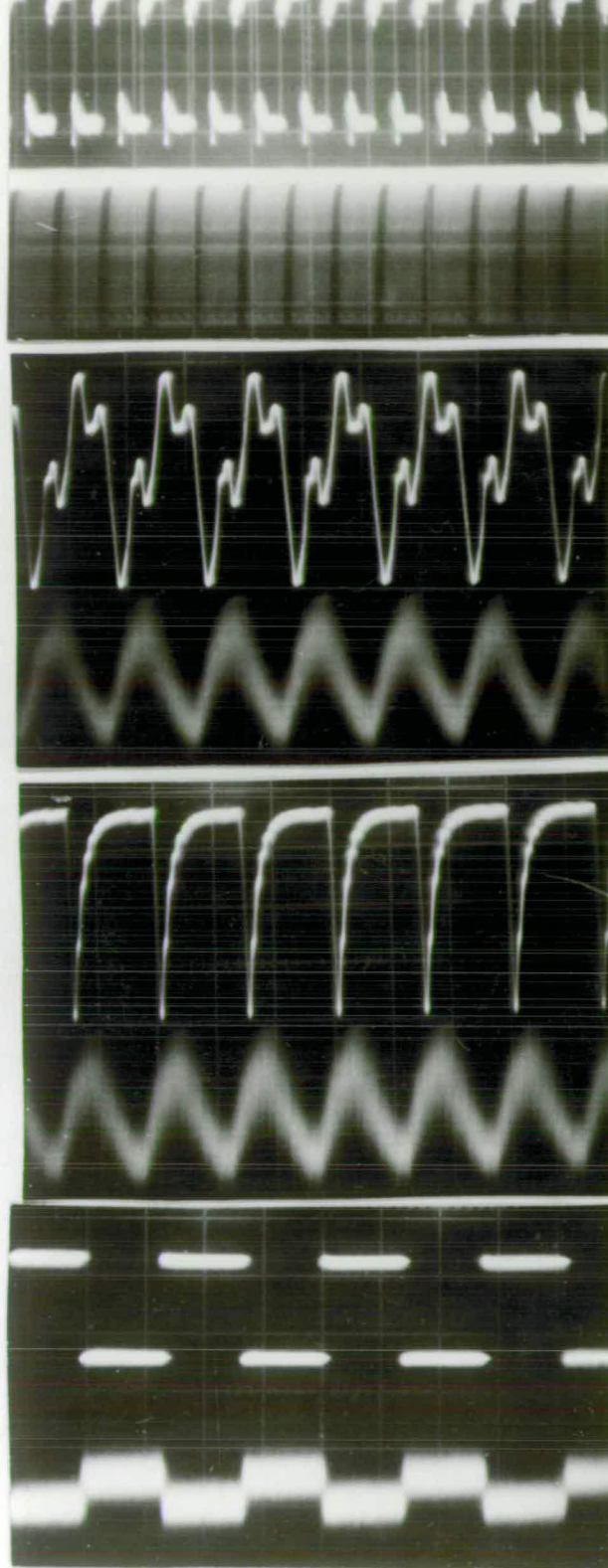
upper trace is i/p
trigger pulse

lower is sampling
pulse to the plates

H = 1µs/cm
V = upper 2V/cm
    lower 5V/cm

(B)

upper trace is i/p
trigger pulse
lower is video o/p
pulse

H = 200 ns/cm
V = upper 2V/cm
    lower 1V/cm

(C)

upper trace is
sampling pulse

lower trace is
video o/p pulse

H = 200 ns/cm
V = upper 5V/cm
    lower 1V/cm

(D)

upper trace is
i/p trigger pulse

lower trace is
video pulse

H = 50µs/cm
V = upper 2V/cm
    lower 50mV/cm

Figure 5.26 : Shows digital sampling system performance.

The system has been tested as a start with an aluminium stub specimen which is connected to a fast pulse generator through a coaxial cable terminated with a resistor , to prevent any reflection of the transmitted signal. This technique was developed to measure the time resolution of the system, by measuring the input waveform rise time which was fed to the specimen under test, to be compared and confirmed the rise time of the reconstructed waveform with that of the input signal under test.

Two other specimens of MOS devices were also tested, these were an arithmetic averager and 4 bit dynamic binary counter. The original input signal on specimen under dynamic operation has been reconstructed as shown in Figures 5.27, 5.28 & 5.29 with some ringing and noise.

Figure 5.30 shows a production of a regular distribution of sampling pulse by the digital system.

Testing the production of regular time delays of the sampling pulses at different operating frequencies is shown in Figure 5.17. At start an experimental results show some missing or overlapping sampling pulses, this has been mentioned in this chapter (5.4.5 - non-uniform time delays distribution of sampling pulses). To discuss and analyse this problem, a three dimensional picture of the delayed input signal is developed to show this problem. The picture comes out of adding the ramp signal (which is used to trigger the display unit) and the delayed input signal. By this method the time discontinuity problem was investigated.

Trimming the length of the separate delay lines was used to produce regular time delays and the discontinuity problem has been overcome. It is worth while to mention that changing any time delay, to generate uniform time delays through delay line should be according to the formula ($t_s = \sqrt{LC}$). After the recent modifications on the present sampling system, it is found to work in a satisfactory manner as shown
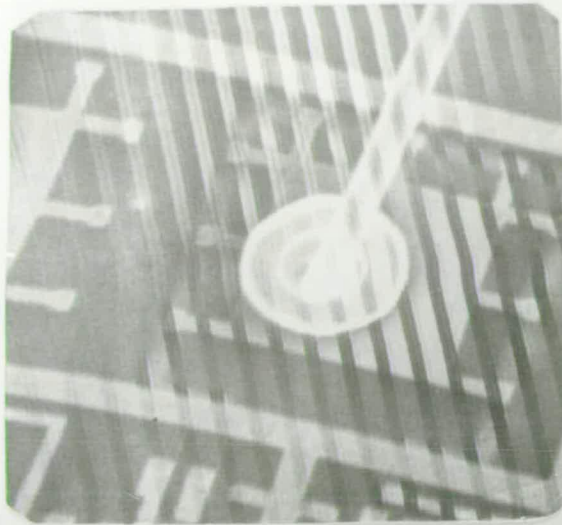
(A)
micrograph with sampling mode at frequency of 2 MHz at specimen under test of 4 bit MOS dynamic binary counter,

which shows a waveform on the specimen under dynamic operation.
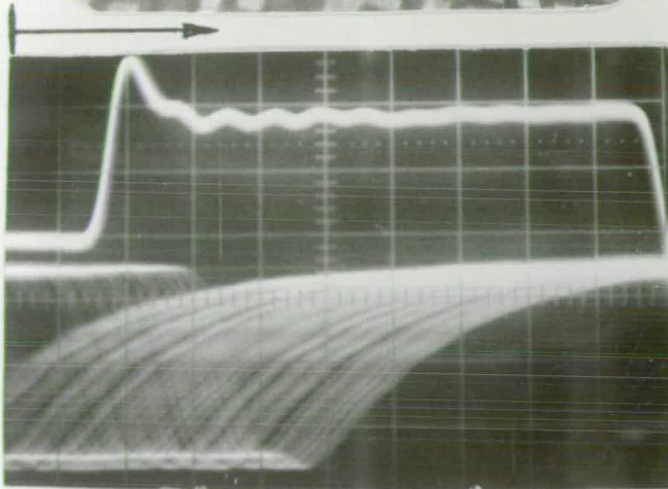
(B)
upper trace is i/p trigger pulse

lower trace is sampling pulse.

H = 20 ns/cm
V = upper 2V/cm
lower 5V/cm
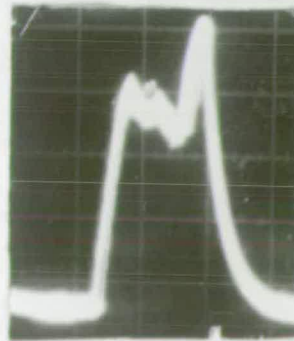
(C)

shows reconstructed pulse

H = 20 ns/cm
V = 20mV/cm

(time axis is reversed in reconstructed waveform)

Figure 5.27: Shows digital sampling system performance.

(A)
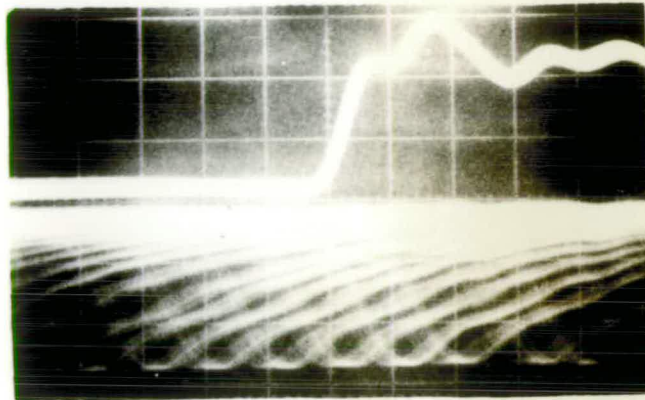
upper trace is i/p
trigger pulse to
specimen

lower trace is
sampling pulse

H = 10 ns/cm
V = 2V/cm upper
    5V/cm lower

(B)
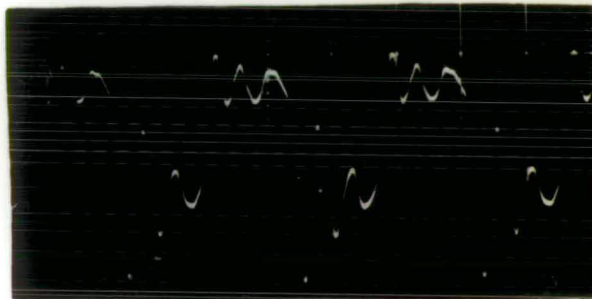
i/p trigger pulse
to specimen
H = 200 ns/cm
V = 2V/cm

(C)
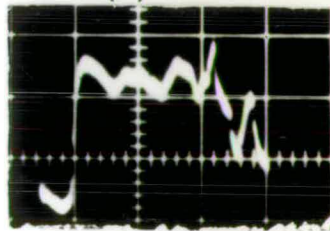
reconstructed pulse
with
low pass filter

V = 20 mV/cm
H = 20 ns/cm

Figure 5.28 : Shows reconstructed pulse with risetime measurement
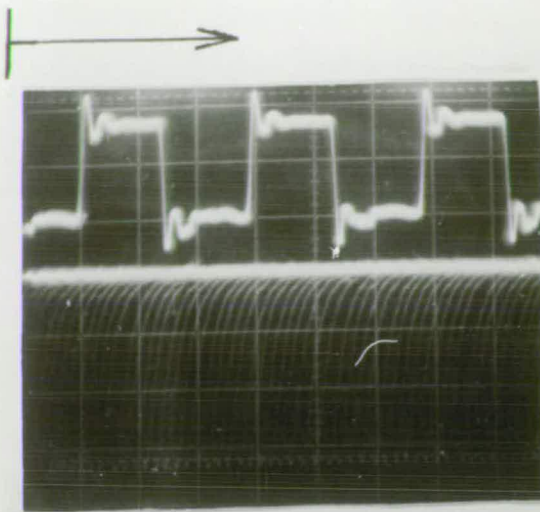
(A)

upper trace is 2V/cm
lower trace is 5V/cm
H = 0.1µs/cm
upper trace is i/p wave-
form to specimen.

lower trace is sampling
pulse
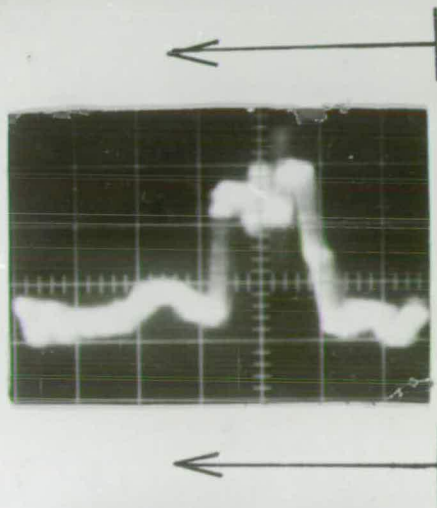
(B)

reconstructed pulse
V = 20 mV/cm
H = 20 ns/cm
without integrator
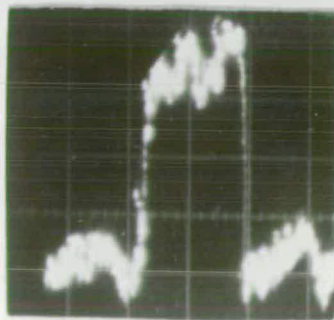
(C)

with integrator
H = 10 mV/cm

Figure 5.29: Shows reconstructed waveform of specimen under test
using digital sampling system.
Note reversal of the axis on reconstructed waveform
due to down-counting.
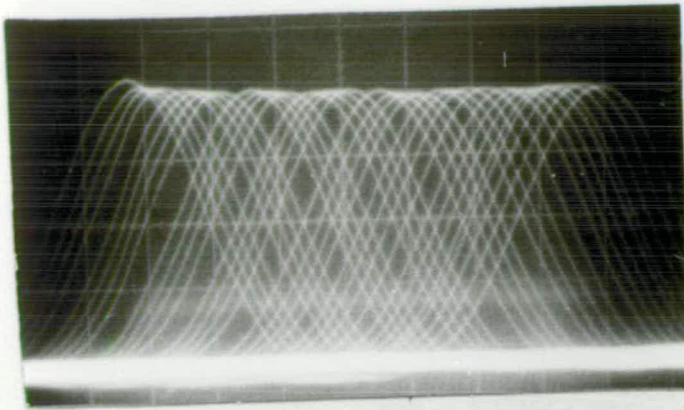
(A)

Sampling pulse

H = 10 ns/cm
V = 5V/cm

(B)
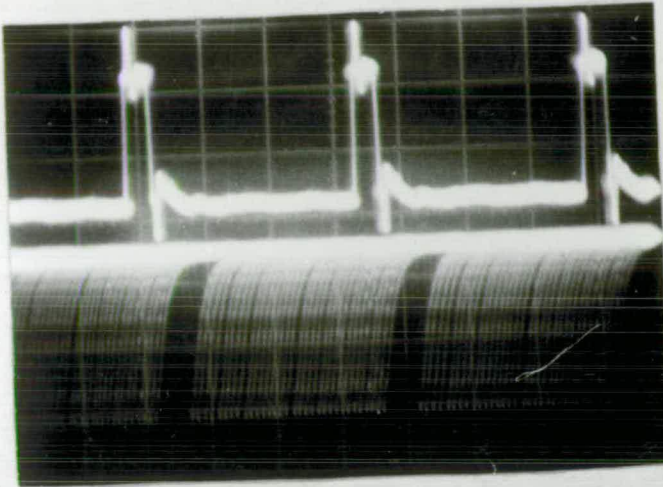
upper trace is i/p
trigger pulse

lower is sampling
pulse

H = 20 ns/cm
V = upper 2V/cm
    lower 5V/cm

(C)
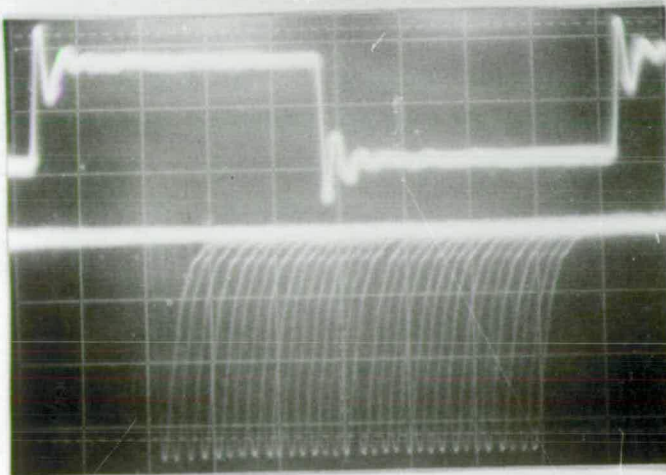
upper trace is i/p
trigger pulse

lower is sampling
pulse

H = 100 ns/cm
V = upper 2V/cm
    lower 5V/cm

(D)
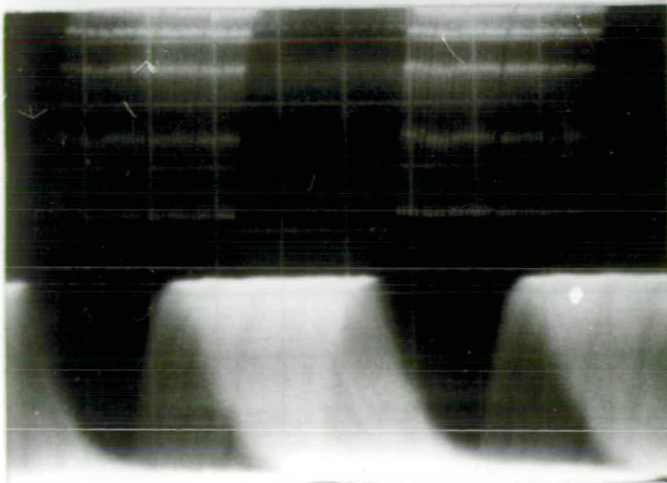
upper trace is
sampling pulse

lower trace is video
pulse o/p

H = 20 ns/cm
V = upper 5V/cm
    lower 1V/cm

Figure 5.30: Shows sampling pulse developed to reconstruct waveform
on specimen undertest in dynamic operation

in Figures 5.26,and 5.30.

5.6 Calibration of time delay,electron beam pulse width,and rise time

5.6.1 Calibration of time delay :

The time delay produced by the sampling system and delay units between the electron beam pulse and the signal fed to the specimen under test, this time represents the time axis of the reconstructed waveform on the display unit is measured with an accuracy of 1ns . When the slow ramp signal is used to show time delay (phase change) on the oscilloscope in the x-axis,an inaccuracy of about 2% in time delay is measured, due to non - linearity problem of the ramp signals. This is so far for analogue sampling system. Menzel and Kubalek (1983) have reported inaccuracies of 0.2 to 1%.

In the digital sampling system precise time delay is produced (see Figure 5 .31a). Time delay of 12 ns is for electron beam to transit from chopping plates to the specimen(flight time), and 50 ns is the total delay up to the display unit. A calibration of time delay error should be considered when measuring the time delay of the signal under test.

5.6.2 Calibration of electron beam pulse width

Robinson (1971) has reported measuring the pulse width of the electron beam by concentrating the electron beam on a PIN - diode connected to a sampling oscilloscope for an electron pulse width of 0.5ns . For the present work a -ve d.c bias is used to produce an accurate electron beam pulse width by producing a fraction of the chopping pulse rise time in such a way as to have a pulse width of 1ns (Linear slope of
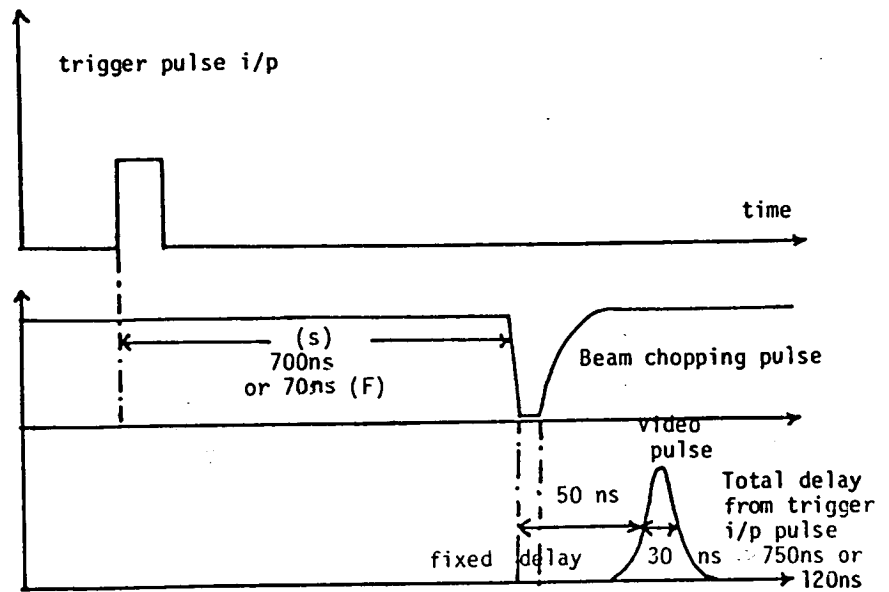
Figure 5.31(A) : Shows the sampling system time delay error measurement.
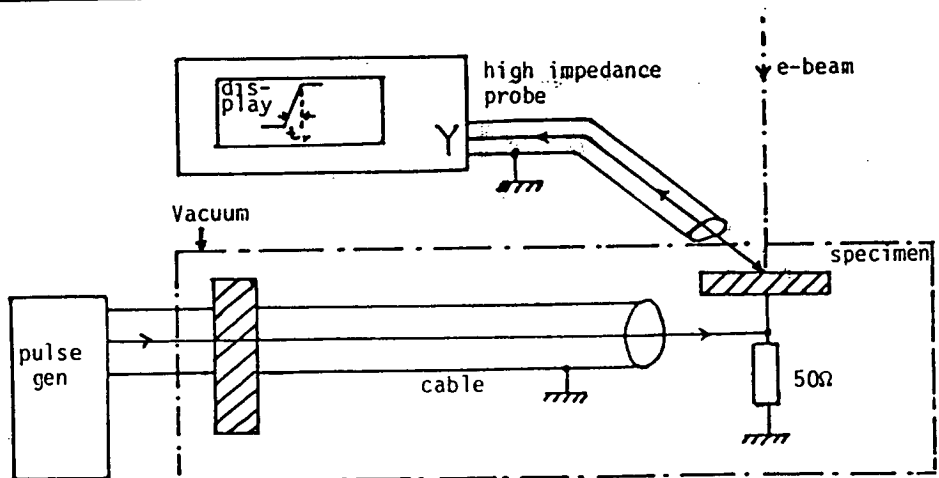
Figure 5.31(B): Shows the set up used for input trigger pulse risetime measurement.

chopping pulse rise time is allocated in mid way of this time).

A calibration can be achieved by controlling the slope of the chopping pulse rise time, and -ve d.c bias to the plates which were assumed to be linear. This measurement is compared with the video signal rise time.

Ratio of chopped and un chopped electron beam is suggested by Feuerbaum and Otto (1982) to measure electron beam pulse width as discussed in chapter three. This mainly depends on the chopping efficiency of the plates. Leakage current has been reported by Feuerbaum(1982) as due to chopping the primary electron beam, and is considered at present as a fraction of full electron beam (un chopped beam). This shows one of the disadvantages of using this method of measuring electron beam pulse width. It is concluded that this method is not reliable. Present method provided an accurate way of measuring electron beam pulse width which indicates the speed of switching of the electron beam.

5.6.3 Calibration of the rise time

The technique of Figure 5.31b is used to measure the rise time of the input waveform on the specimen under test, to be compared and confirmed with the reconstructed waveform rise time. In the analogue system a difficulty was found in measuring the rise time due to timing jitter in the reconstructed waveform (see Figure 4.17).

In the digital system a difficulty is faced due to beam noise and other noise which is superimposed on the reconstructed waveform, and found also some what to disturb the rise time measurement. The recon-

structed waveforms' rise time is measured by the sampling system and compared with the input signal rise time which is measured by the technique shown in Figure 5.31b, with comparable results.

Error is found in measuring the reconstructed waveforms' rise time due to noise indicated; it is considered here to be negligible and irrelevant for the present.

5.7 PERFORMANCE OF THE DIGITAL SAMPLING SYSTEM

Figures 5.24, 5.27, 5.28 & 5.29 show the efficiency of the present system in both stroboscopic and sampling modes. To run the system for testing devices under dynamic operation, it is first required to check the beam switching capability, by stopping the electron beam on line scan, and then to produce the largest amplitude of the video signal by adjusting the -ve d.c. biases to the chopping and blanking plates (see Figures 5.26 & 5.30).

In the stroboscopic mode (image mode), the system was found to work satisfactorily with repetitive signal up to 10 MHz frequency, in which phase is controlled by local and computer control, and time delay is generated by specified delay lines (see Figure 5.24). In the sampling mode (waveform mode) adjustment should be the same as for the stroboscopic and sampling modes , the SEM scan is stopped at one point of interest, and - ve d.c bias to the plates should be adjusted to produce only one video pulse per one cycle (See Figure 5.26). The phase is held constant, and integration over the video signal is carried out by the averager, for improved S/N ratio. One measurement of the signal is recorded after (n) pulses (see Figures 5.27 & 5.28), the phase is then changed, and the same procedure repeated until the whole cycle has been completed (the phase can be changed and controlled manually or remotely).

Feuerbaum and Otto (1980) have reported signal processing for electron beam waveform measurements using a box-car averager (modified type), to measure periodic noisy signals by shifting the phase of the gate in accordance with the sampling principle (a similar technique has been developed in the present work). They mentioned that normally the photomultiplier voltage needed adjustment when changing the repetition rate, but with their method the continual adjustment of this voltage is eliminated. The present work averages the overall noise by using a box-car averager or by ordinary integrator (L.P.F) to show a reconstructed waveform of the voltage waveform on the specimen under test without a necessity of adjusting the photomultiplier voltage.

The tested waveform is displayed on an oscilloscope with respect to the ramp signal, as shown in Figure 5.23. A variable time constant integrator was developed to minimise the high frequency signal and interference noise, which appeared in the reconstructed waveform,this was found experimentally making some signal detail to disappear, especially at frequency up to 5 MHz. It was decided at present to ignore further processing high frequency noise at this frequency, to keep the waveform shape detail as shown in Figure 5.23.

The use of the computer is recommended to improve S/N ratio, by producing as many samples per phase as is found necessary in each case. The present box-car averager works up to 1 MHz frequency of input signal, due to a limited aperture time of the present sample and hold(S/H) of 0.1 us. Therefore to let the averager work up to 10 MHz, a modified integrator with S/H device of aperture time of 50 ps should be developed.

The time resolution of the present system is 1 ns at a repetition signal frequency of 10 MHz. The reconstructed waveform on an MOS-4 bit dynamic binary counter is produced as shown in Figure 5.28, with pulse

overshoot shown to the right of the picture. The time axis is reversed in the reconstructed waveform. This could be easily rectified by inverting the output from the DAC ,due to the set up of counters which are designed in such a way to count down oscillations from the input signal to the system as discussed before.

Little noise in the reconstructed waveform is also produced by the present system. This noise is originated by noise on the time base signal(slow ramp signal), and this has been treated by smoothing the noise using a low pass filter.

An increase in noise superimposed on the reconstructed waveform has been recognised experimentally; especially when the electron beam spot is left on the specimen under test (in sampling mode) for half an hour. This is due to possibly charging up of the specimen area under test which creates a floating field around the specimen and may produce this noise. This is believed to be due to contamination layers on specimen generated by the polymerisation of hydrocarbons by the electron beam (Miller 1978).

5.8 COMPARISON BETWEEN ANALOGUE AND DIGITAL SYSTEM

(A) In analogue sampling system :

The present analogue sampling system and delay unit is found to have the following problems:

1.   Difficulty of interfacing the analogue system
        (depending on conventional ramp signal generator
        principle), to the computer for remote control.

2. Difficulty of producing variable pulse width of delayed trigger pulse.

3. Analogue circuitry complication in design and construction.

4. ، Timing jitter problem due to phase instability of the analogue systems. This has been reported also by other workers (Plows and Nixon (1971), Fujioka et al(1978), Gopinath et al (1976)).

5. It required a continual manual adjustment.

(<u>B</u>) <u>In digital sampling system</u> :

1. Reliable design
2. Easy to be used and understood.
3. Control by local (manual) or remote.
4. Basically digital principle of operation.
5. Insignificant timing jitter.

<u>PART TWO</u>

<u>REMOTE CONTROL OF THE DIGITAL SAMPLING SYSTEM - COMPUTER CONTROL</u>

<u>5.9 COMPUTER INTERFACING TO DIGITAL SYSTEM</u>

<u>AIM</u>

To automate

1. Delay control

2. Range selection

3. Pulse width selection

4. Allowing storage of waveforms, sampling, etc.

5. Colour stroboscopy

5.9.1 Introduction

Dinnis et al(1981) have reported the instrumentation facility of the SEM functions control mentioned in the review. It has been used for the present work. The computer (such as Superbrain) is used to control the sampling phase, by advancing the sampling phase through the cycle of operation, by setting the delay in stroboscopic mode and storing information for later display and analysis. Colour stroboscopy can then be implemented by software techniques.

Programmes were written in the Pascal language, and designed as shown in Figure 5.32 to control both stroboscopic and sampling modes. The (HP 6940 B) multiprogrammer is connected to the general purpose interface bus (GPIB) of (HP 59500 A) to provide very simple interfacing between the computer, the various functions of the microscope and of the sampling system and delay units (see Figures 5.33, 5.34) by use of ready built plug-in cards.

Three bits are provided to control the pulse width of the delayed trigger pulse or to control the colour coding unit, to produce eight different colours(see colour stroboscopy in chapter six). 21 bits are provided to control the delay units replacing the manual control (9 bits for high frequency units, 12 bits for low frequency unit). The software is arranged to produce an easy to operate system, where little computer

How to define sampling?

$$D = \tau \times n + I \quad \text{where } I = \text{phase, } n = \text{index}$$
$$D = \text{delay, } \tau = \text{delay steps (increment)}$$

Delay = delay steps X index + phase
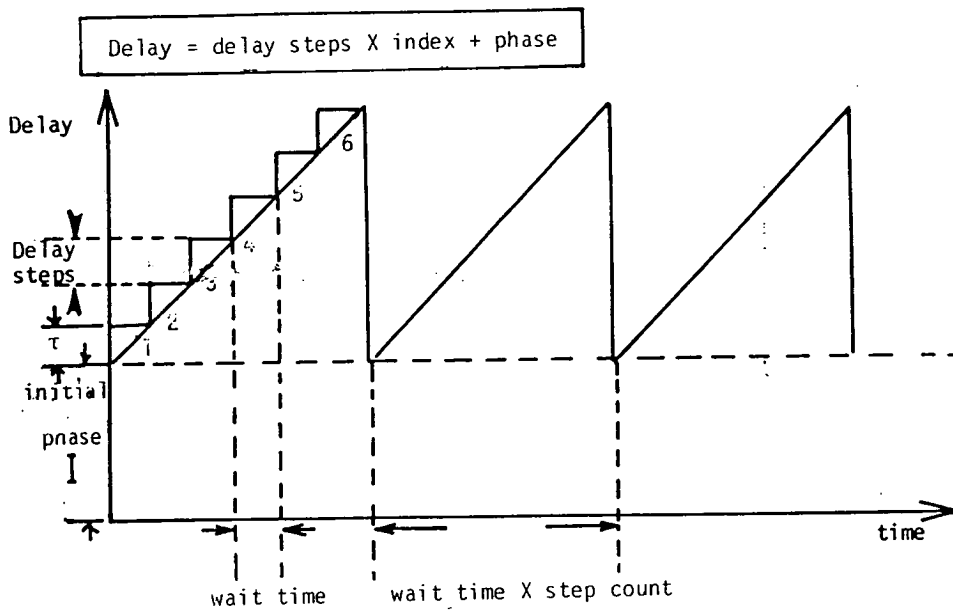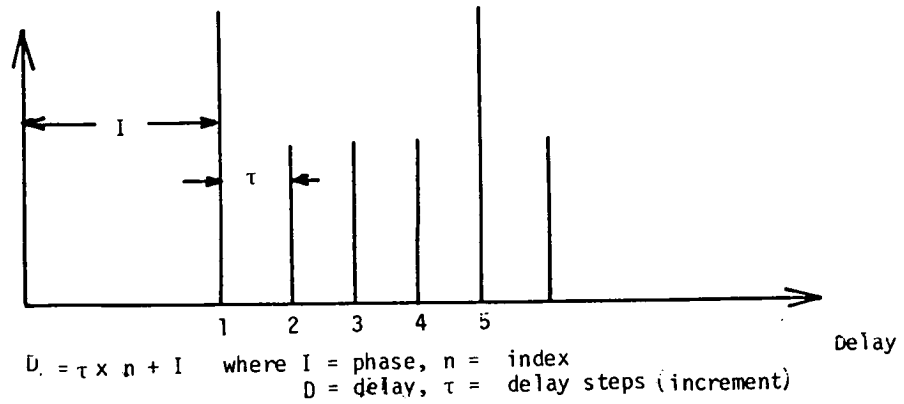
Figure 5.32: Shows Principle of Sampling Program
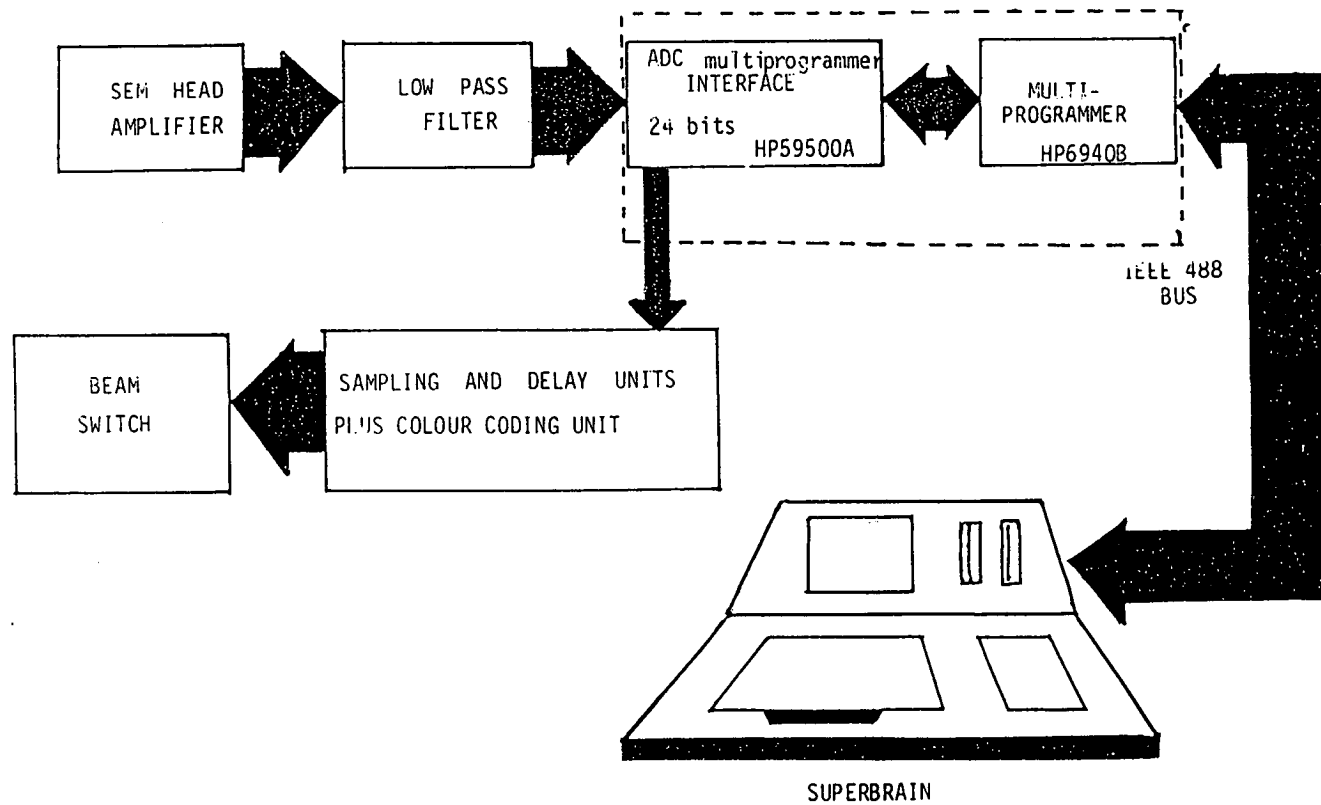
Figure 5.33 : Block diagram of remote (computer) controlled system
interfacting to digital sampling system
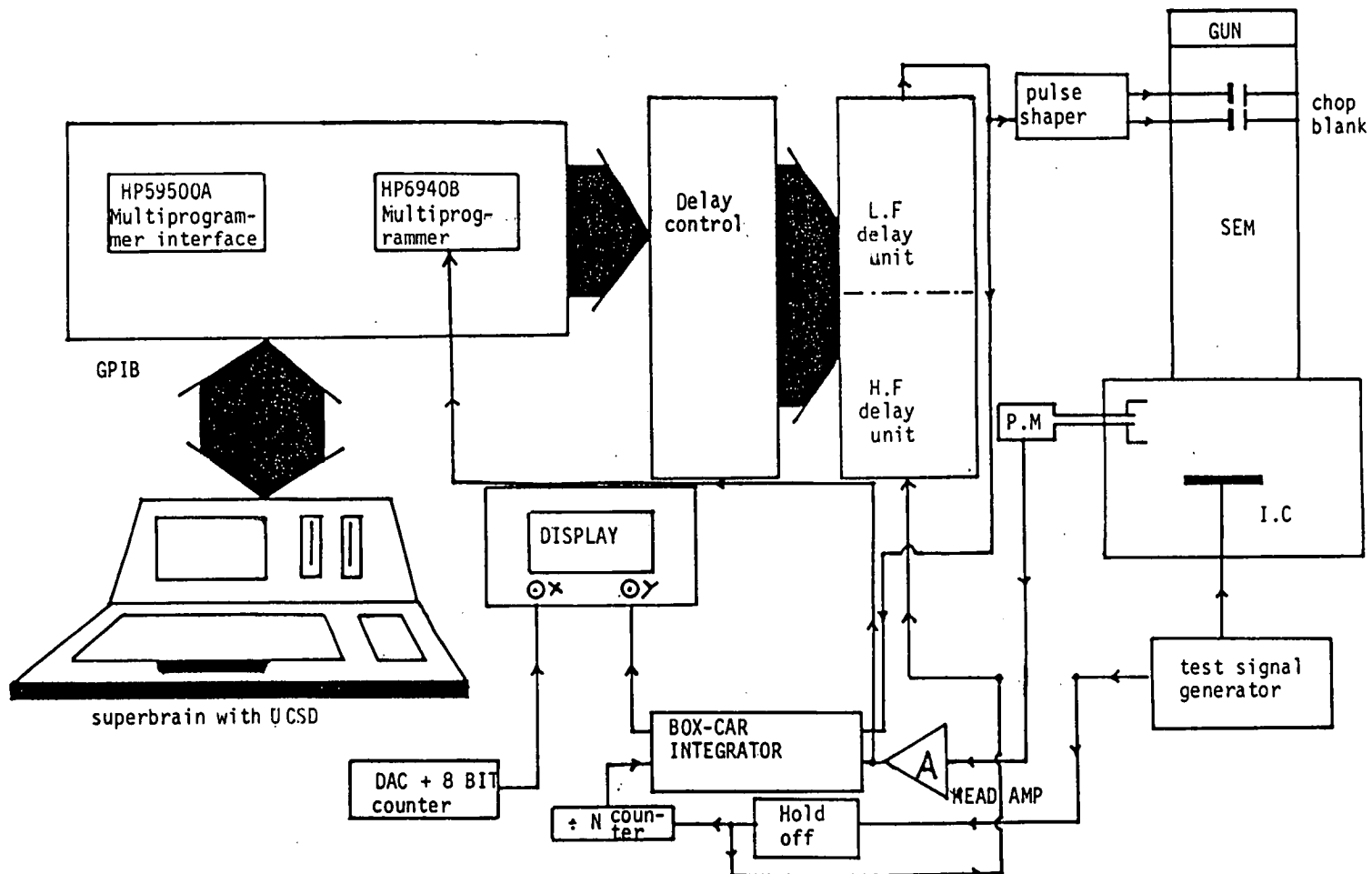
Figure 5.34: Shows automated delay control for digital sampling system

experience is required to perform stroboscopic and sampling SEM.

NOTE: Since the present H.P multiprogrammer is limited with 24 bits therefore 21 bits were used for time delay control and 3 bits for either control of colour stroboscopy or the sampling pulse widths.

5.9.2 Principle of Sampling Programmes

Figure 5.32 shows the principle adopted at present as follows:

1. Initial delay (Initial phase)

2. Delay increment (Delay steps)

3. Number of steps (Increments)

4. Number of cycles

In stroboscopic mode, the operator can select any static time delay as desired. The mode of operation can be changed at any time with one programme (stroboscopic and sampling modes). Storage of waveform information by computer is achieved by feeding the head amplifier output as input to the multiprogrammer by the analogue to digital converter(ADC).

5.9.3 Computer Program Design Detail

To produce a time delay of 1.5 ns to 2 ms as designed for the sampling system since delay is limited:

For delay   0 ns $<$ T $<$ 2000000 ns

where T is delay required.

it was decided to accommodate 9 and 12 bits into two words of two integers as follows:

A 1   is chosen to be 9 bits (for high frequency delay control)

A 2   is chosen to be 12 bits (for low frequency delay control)

Two words of MP WORD 1 , MPWORD 2   which represent 12 and 9 bits respectively as:
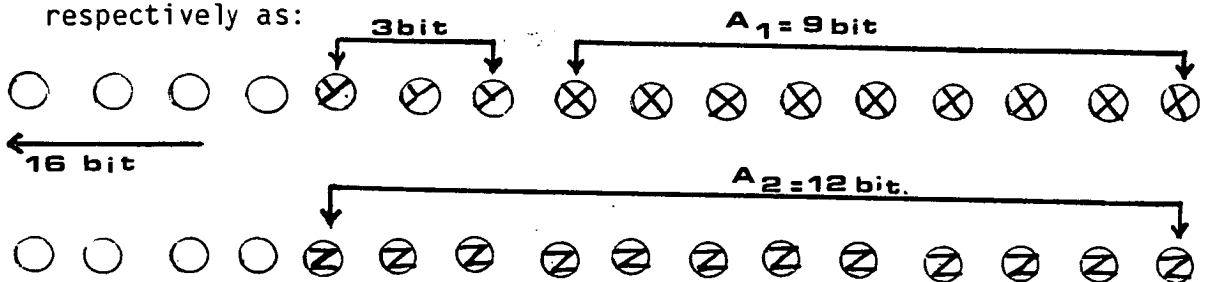
12 bits   of 0 - 4095

9 bits   of 0 - 511

N.B

MP = multiprogrammer.

3 bits are used either to produce variable pulse width of delayed trigger pulse or for controlling colour stroboscopy in the SEM.

There are two slots of MP used:

$$A\ 1 = MP\ WARD\ 1 = Trunc(Delay/4096) \qquad (5.5)$$

$$A\ 2 = MP\ WARD\ 2 = ROUND(Delay-MPWARD1*4096). \qquad (5.6)$$

$$A\ 1 = MP\ WARD\ 1 = 512(colour-1)+MPWARD1) \qquad (5.7)$$
$$\|\|\|$$
or (pulse width)

In order to estimate the constant scale factor for translation of time delay into binary as follows:

$$T = A.K \qquad (5.8)$$

where T = delay required

     A = delay in binary

     K = constant scale factor

One of the variables should be known. K is constant between step delays starting from minimum time delay of 1.5 ns to maximum time delay of T = 2 ms, so that transformation of an order from the computer via the multiprogrammer to the sampling system could be accomplished by binary equivalent number.   K factor is measured experimentally and found:

$$K = T/A = 0.76923 \qquad (5.9)$$

It is worthwhile to mention here that computers (such as the Su-

perbrain), do not work as in hardware (to select number of samples per phase e.g. divide by N counter) but it stops for a short time interval (wait for short time delay), to produce a time delay, which is useful in both stroboscopic and sampling modes in the SEM, by selecting any number of samples per number of cycles (5 cycles or 10, or 100 and so on), phase should change in sequence to reconstruct the whole waveform on the specimen under test.

Using computer control is found more flexible to select a greater number of samples per phase for better resolution, rather than in hardware which requires a large number of counters with complicated circuitry, to perform the same time resolution of the reconstructed waveform. The Superbrain is also used to store different time delays by floppy disc memory for more signal processing .

5.10 COMPUTER PROGRAMMES

In developing computer programmes to represent a physical situation, a noticeable question arises of how much the application of the programme is restricted to the particular purpose it was written for. That is, the physical system could be slightly modified without completely rewriting the programme. Therefore it was decided to develop very general programmes for the above purposes to save time.

The programmes in the present work are written in the Pascal language, and used to perform stroboscopic, and sampling SEM, also colour stroboscopy. Different types of statements were used (e.g. CASE, IF, STATEMENTS). The main programmes are given in appendix (I) with simplified flow charts.

Two types of programmes are mainly presented for the present system.

These are :

1. Chopping control programmes, to describe time delay, the sampling procedure, variable sampling pulse width (or colour).

2. Colour stroboscopy programmes are to perform colour stroboscopy in the SEM.

5.11 DISCUSSION

The results which have been presented in this Chapter show clearly the performance and characteristics of the digital sampling system developed at present.

These are:

1.   A bility to give accurate digitally switched time delays by
      local and remote control.

2.   Relatively linear time delay of sampling pulses at
      different frequency signals.

3.   No significant timing jitter problem.

4.   No bandwidth limitation problem in delay lines.

These characteristics are demonstrated as shown in Figures 5.22, 5.26 which show the improvement in performance of the digital system with respect to others work described previously by the Bangor group, Lintech Lt, JEOL Ltd., Fujioka et al, and others.

A new principle and design of the sampling system depending on digital principles employing switched delay lines has been developed at present. It is of interest to examine whether or not further improvement would require redesign of circuits. The experimental results show that the system works surprisingly well.

In the stroboscopic mode it allows detection of the faulty part in an integrated circuit. Changing the phase in steps by local or computer control can show signal progresses in a circuit.

These modes have a wide applications such as fault diagnosis of circuit functions.

Gopinathan and Gopinath (1978) have developed the analogue sampling system with a copper stub, as the test specimen to check the linearity of the system. They used an ECL device to measure the time resolution of the system. They reported a difficulty in placing fast edges on the specimen pad because of long leads from the drive unit via the electrical vacuum feed through to the device in the chamber, high capacitive line loads may influence the proper functioning of the device under test. Package parasitic impedance also exists, Menzel Kubalek (1981). The same problem is faced at present in testing MOS devices at operating signal frequency up to 10 MHz.

From experimental study of delay lines characteristics, a delay line of high frequency signal was found with serious bandwidth limitation problems associated with the construction of the line; this problem was overcome by investigation of suitable techniques for the construction of high frequency delay lines (see Figures 5.12 & 5.18).

Gopinath and Hill (1974) have reported about timing jitter (phase instability) of the analogue system. Fujioka et al (1980) have also reported the timing jitter as a main factor of disturbing the time resolu-

tion measurement in the analogue sampling system.

In the present work no significant timing jitter exists in the digital system, since a digitally switched time delay which is generated by recent digital sampling system, is developed at present.

Aluminuim stub and two MOS devices were used, for reliability test of the digital system by measuring the rise time of the waveform on specimen under test and was found to be 1ns by a technique shown in Figure 5.31b, to confirm the recorded rise time of the reconstructed waveform as in Figure 5.27. The system works with repetitive signal frequency up to 10 MHz, and if the hold-off circuit is used where one electron beam pulse is produced for every nth trigger input signal, then the system could work up to 20 MHz as requested.

Improving the resolution of the reconstructed waveform (S/N ratio)can be done either by choosing a large number of samples/phase and by using long integration time of the averager, or by using a noise reducing frame-store system for sophistication, or using a long exposure time for recording the picture. Software can replace any local control in the digital sampling system. The function of the computer is to make operation much easier and more convenient by programmes given in Appendix I, to control the sampling system.

Software design replaces hardware in many places of digital systems for better performance and for partial or complete automation of the system with programming option and this is easily controlled by microcomputers .

Digital sampling system is found to produce an accurate time delay between 1.5 ns to 2 ms, by digitally switched time delay. This is eventually useful for study and analysis of high frequency signals in the

SEM, especially for displaying the timing of the signal propagated in the integrated circuit under test in colour as well as monitoring digital signal rise time.

These investigations of limitations and operating characteristics of the digital system, have shown it to be a successful measurement system. Its operation indicates its ability to meet the requirement presented for study of the MOS devices under dynamic operation.

CHAPTER SIX

COLOUR STROBOSCOPY

6.1   INTRODUCTION

This chapter describes techniques which were developed to produce colour stroboscopy in the SEM. A review of past work in this field is given. The digital sampling system was developed to produce digitally switched time delays required for colour coding in the time domain. A colour stroboscopic technique was used to display timing and delay information throughout the specimen.

The colour mapping method was utilised to analyse repetitive signals on a specimen with repetitive signal frequencies up to 10 MHz which is a significant improvement on the frequency limits of past work in colour stroboscopy. A new simple and fast diagnostic analysis of functioning of MOS devices by colour stroboscopy is presented.

6.2 COLOUR STROBOSCOPY REVIEW

Dinnis (1980) has reported on colour stroboscopy developed for colour display of voltage contrast in the SEM. The basic principle is shown in Figure 6.1a and is summarised as follows:

" If a signal which varies with time is applied to a circuit, then colour can be used to denote the time dimension. If a particular digital pulse is chosen to correspond with a given colour, then the appropriate gun in the display tube is switched in synchronism with the pulse so all conductors carrying that particular repetitive pulse will be readily identified " (from Dinnis (1980)).

Shadow-mask CRT

Primary beam

Electron detector

R G B

i.c. specimen

(a) Arrangement for simple colour stroboscopy. The conductor on the right will appear red.

Square wave generator

SEM column

Scan generator

4 k RAM

4 k RAM

4 k RAM

4 k RAM

Encoder

Decoder

R
G
B

Colour TV monitor

Voltage measurement system

Power supply for i.c.

Address

Composite monochrome video

Video

Controller

TV sync. pulse generator

Insert TV sync. pulses
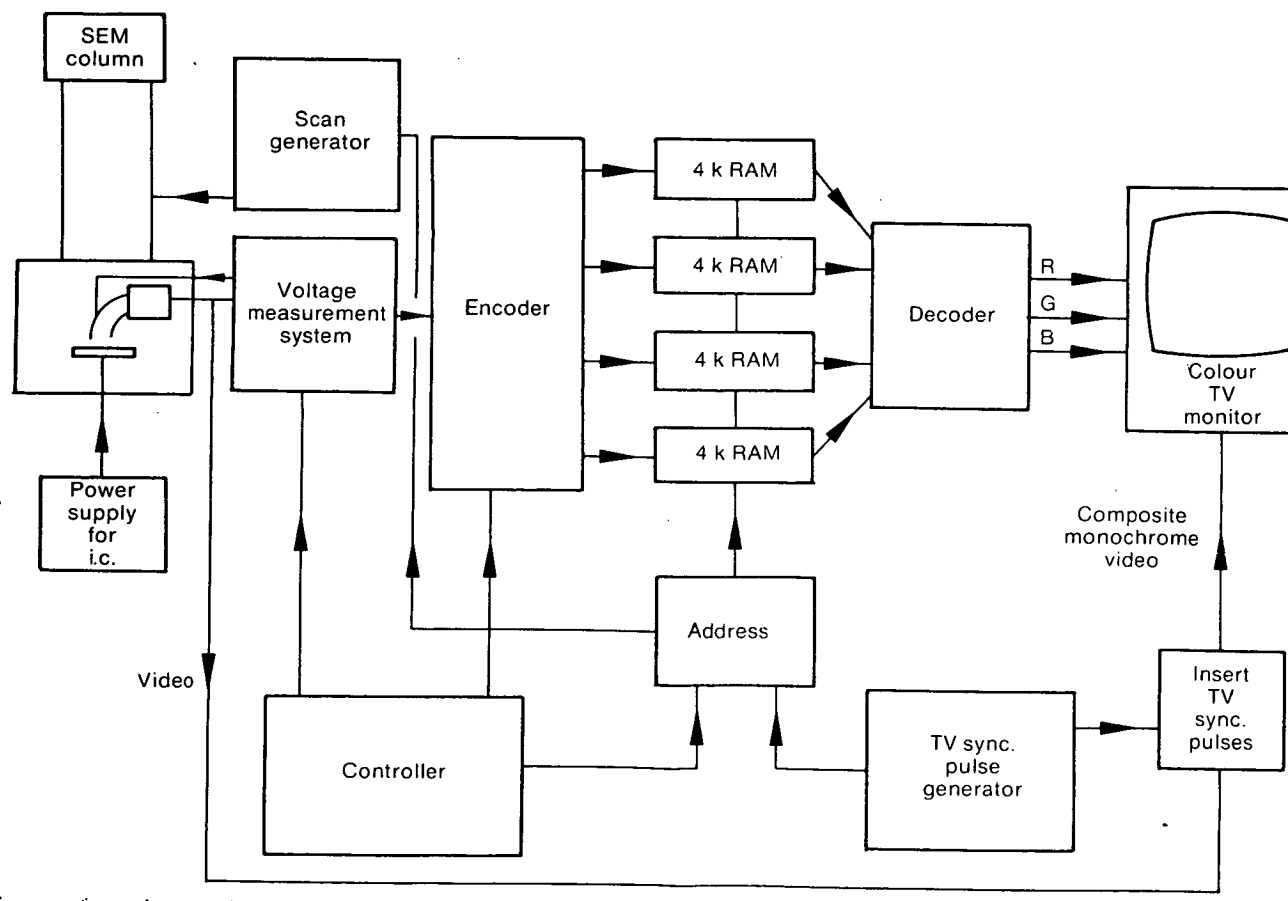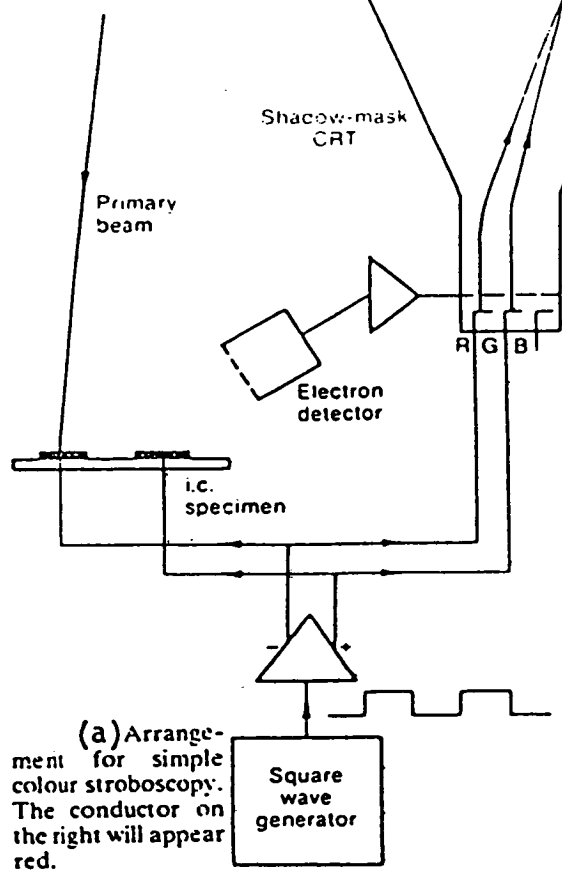
(b) System for colour-coded voltage mapping

Figure 6.1: Shows a colour stroboscopy demonstration in [a].
(from Dinnis 1980)

An implementation of this principle was shown in Figure 6.1 where a square wave at T.V field frequency was used to switch the red and green guns alternately (two colours of red and green were used) while being simultaneously fed to the circuit. As the right-hand conductor is more negative when the red gun is on, it will appear red, while the left-hand conductor will correspondingly appear green as shown in Figure 6.2. All the rest of the circuit will appear in shades of yellow, d.c voltage levels are displayed in the normal way, i.e. negative region bright and positive ones dark. If the applied signal is at an integral multiple of the field or line frequency, then colour striations will appear, for similar reasons as in the monochrome case described by Feuerbaum and Hernaut (1978).

At higher frequencies ,Dinnis recommended the use of the stroboscopic technique developed by Plows and Nixon (1968) which involves chopping the electron beam at the frequency of the signal. The display would then, in effect, be an anaglyph made up of 2 or 3 pictures taken with different sampling phases. The system in Figure 6.1b is being developed to display potential in a colour-coded form overlaid on a topographical image of the specimen (see Figure 6.3). Dinnis suggested using a microcomputer for colour control, but he does not mention how to build and design the colour stroboscopy requirements. He demonstrated colour stroboscopy at low frequency of 50 Hz, using 10 ke electron beam accelerating energy.

6.3 AIM OF USING COLOUR STROBOSCOPY

The present work aims to give timing information in the form of colour on two dimensions image of the specimen. The colour is at present generated in a real - time analogue video system. In principle it could be
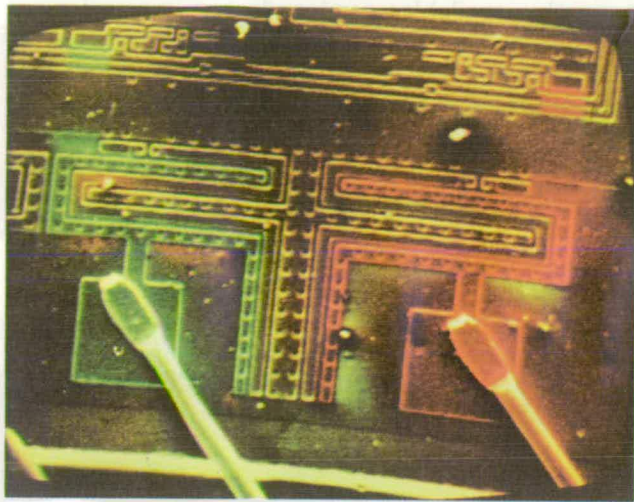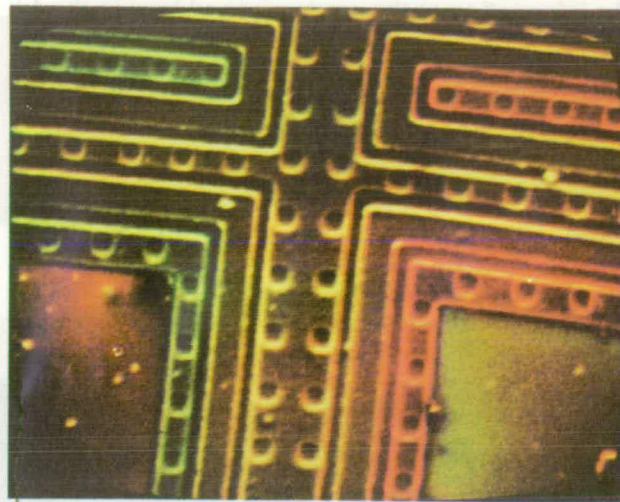
(a) (b)

Figure 6.2 Low frequency colour stroboscopy.10v,25Hz square wave applied toinput wires of silicon integrated circuit.Beam voltage 10kV.(from Dinnis 1980).
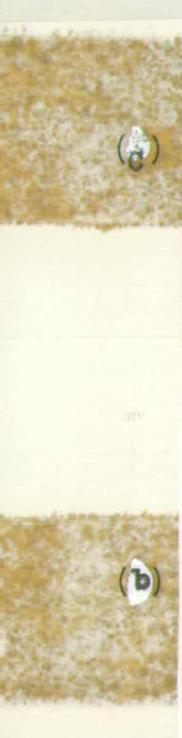
(c)
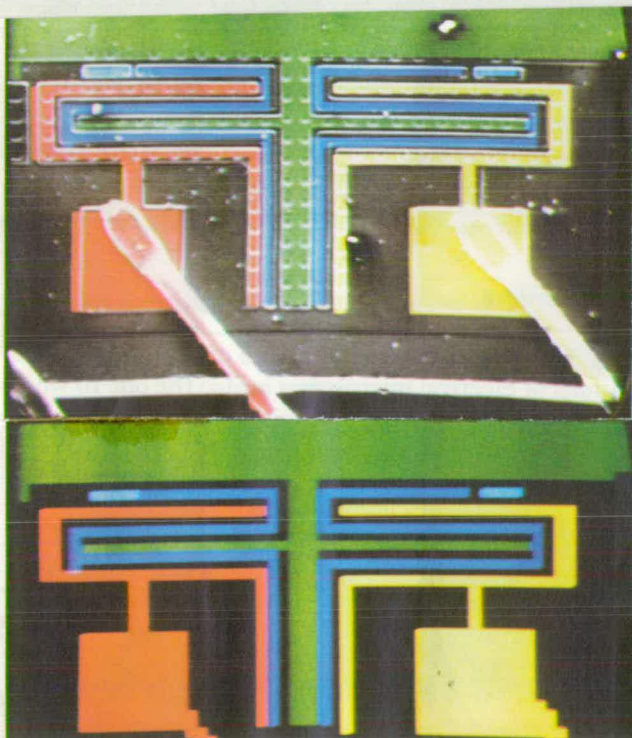
(b)
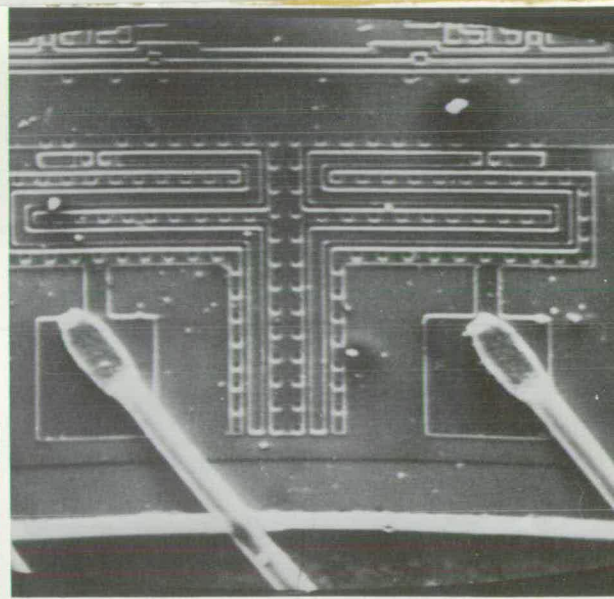
(a)

Figure 6.3: Colour overlay TV image formation. Field width=750 um.
a) Topographical image. b) Synthetic colour overlay.
c) Composite colour image. (from Dinnis 1980).

used with a computer- generated synthetic colour overlay of the type described by Dinnis(1980).

The diagnostic tool of colour stroboscopy is faster and simpler than the conventional methods of waveform analysis. The colour mapping method was used to analyse signals on the specimen under test in the SEM with repetitive signal frequencies up to 10 MHz.

Colour stroboscopy is used:

(1) To display the propagation time delay of digital signals as they progress through a long conductor on the specimen under test in colour.

(2) To display and measure the slowing down of the digital signal rise time, while the signal propagates through a long conductor on the specimen.

The changeable rise time will be displayed by different colours at each end of the conductor through the circuit. This is useful in monitoring the rise time of the digital waveform.

(3) Results are obtained very rapidly compared with the normal method of using waveform measurements at a number of points and those points suitable for more detailed probing and can quickly be identified.

(4) Measuring the transition time of the digital signal.

6.4 COLOUR STROBOSCOPY CIRCUIT DESIGN

6.4.1 Colour Stroboscopy Requirements

The Dinnis (1980) principle of colour stroboscopy in the SEM was adopted. In the first stage, therefore, the work was aimed at extending the frequency range of this method and extending the number of colours from the two colours used by Dinnis (1980) to a larger number of easily distinguishable colours.

The following instrumentation is required to work at TV rate frequency as a modified T.V receiver is used for the display :

1. Digital scan generator

2. Video head amplifier

3. Display

4. Scan amplifier

Also colour coding circuitry, hardware and software control, are implemented (see Figures 6.4, 6.5 ,6.6 , 6.8a , 6.8b). The digital scan generator was designed and built by Mr P. Nye (1981).

6.4.2 Colour Coding Circuit Design

Dinnis and McCarte (1980) have used 14 different colours (plus black and white) by using 4-bit number. They mentioned that these can be distinguished from one another if correct choice of primary com-
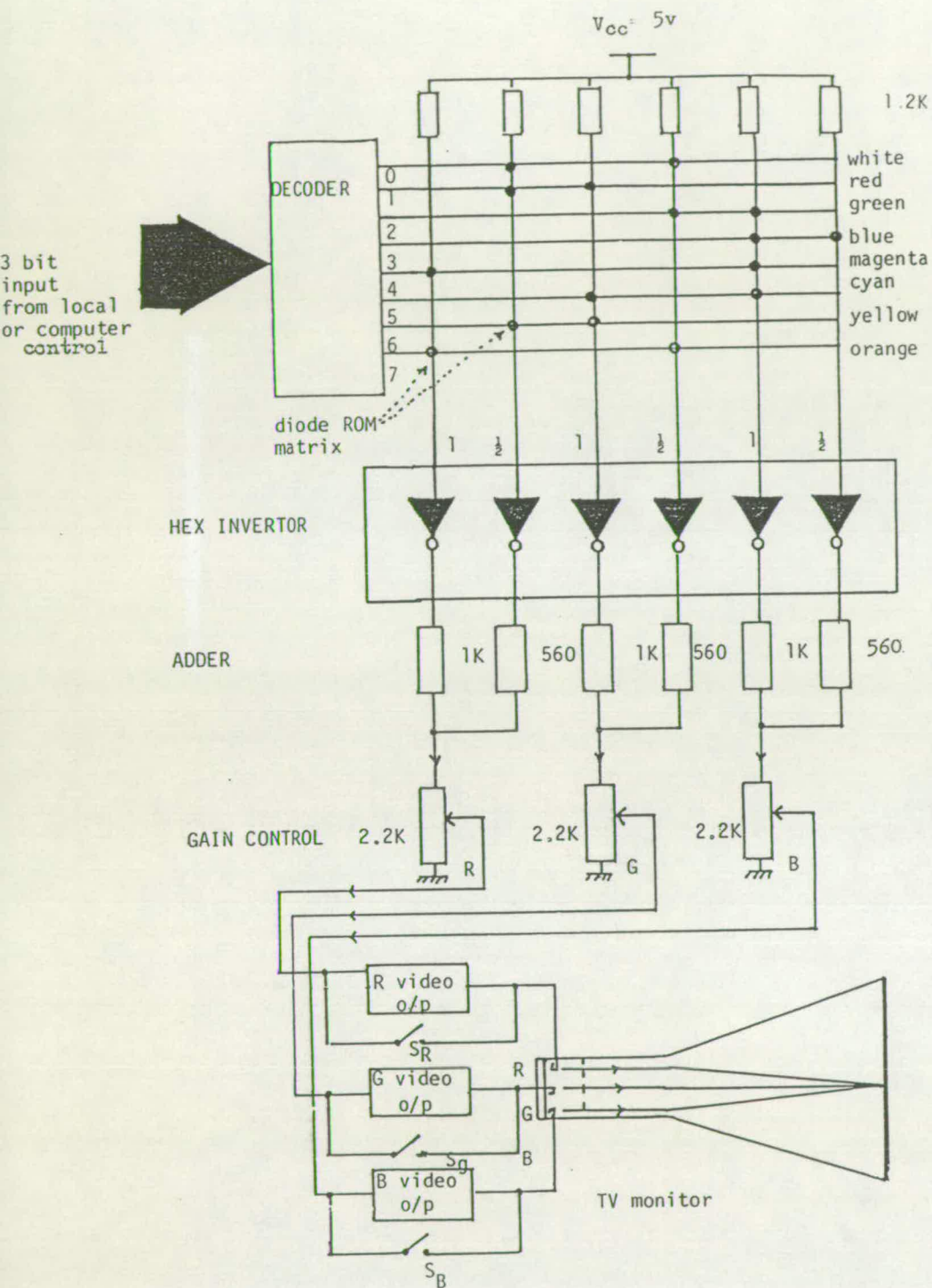
Figure 6 4: Shows practical circuit for colour coding
with colour TV monitor modification
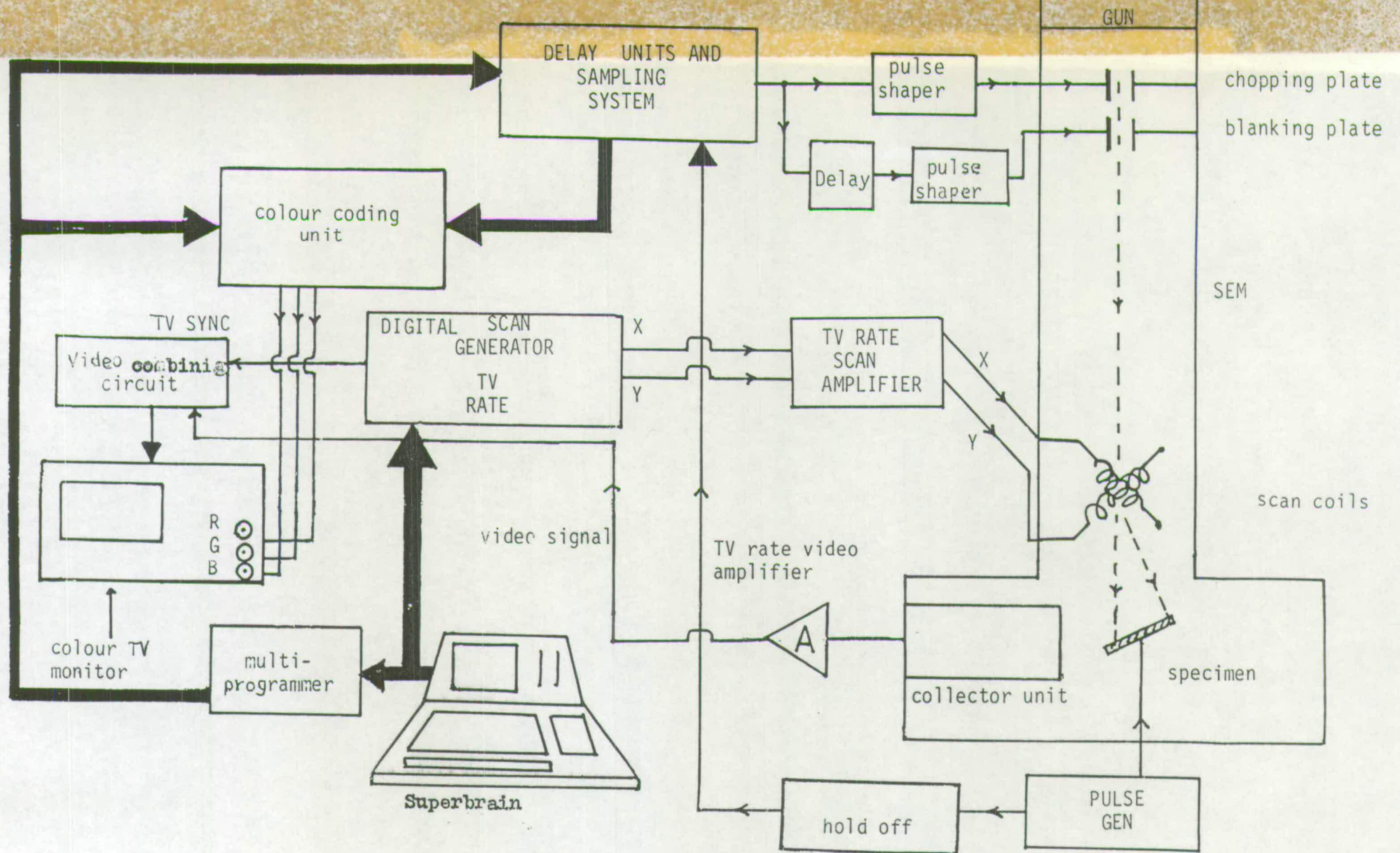
Figure 6.5   Shows a block diagram for colour stroboscopy instrumentation.

sampling and
delay unit

Multiprogrammer

colour TV
monitor
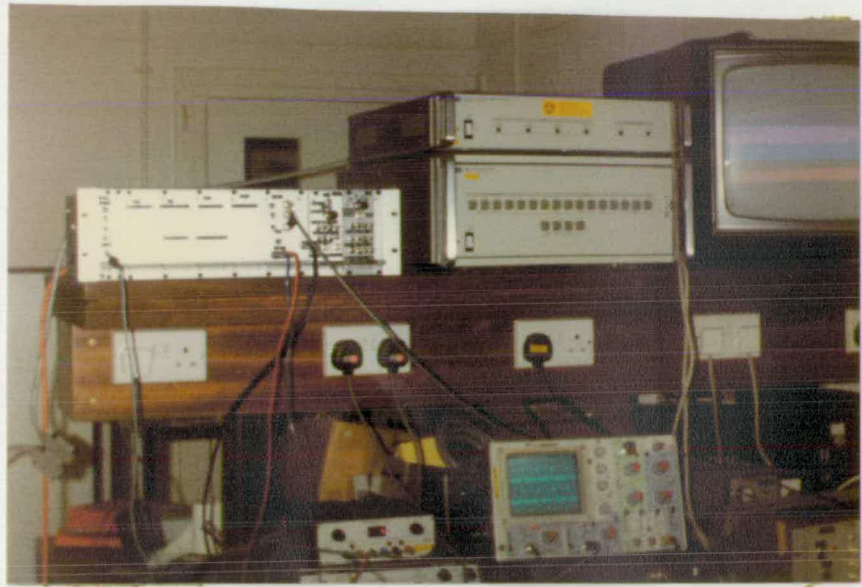
(A)

colour
monitor

scan
Amp

Digital
scan
generator

Multiprogrammer

(B)

Figure 6.6 : Shows instrumentation used to demonstrate colour
stroboscopy. (A) Experiment set-up, (B) remote
control.
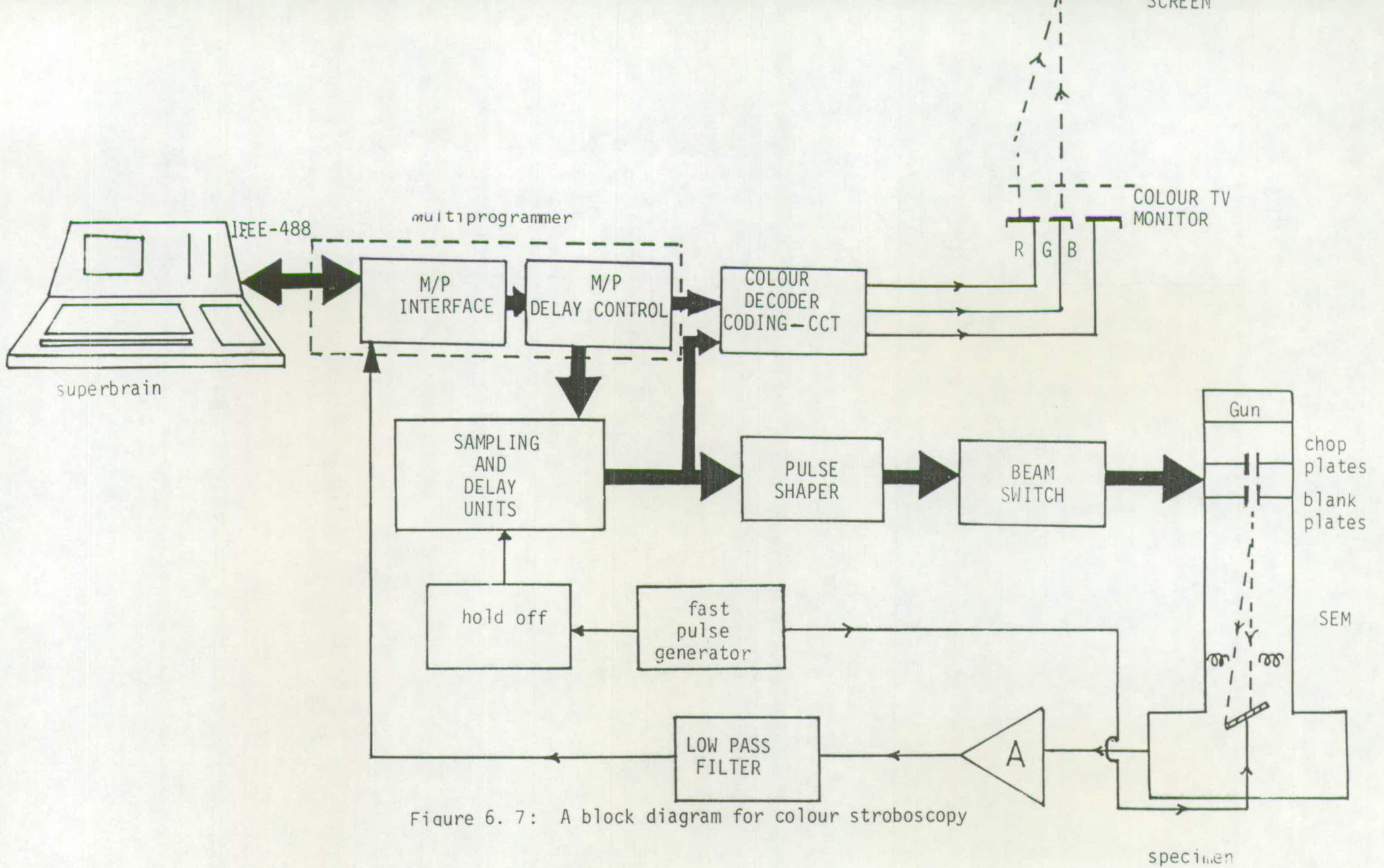
Figure 6. 7: A block diagram for colour stroboscopy
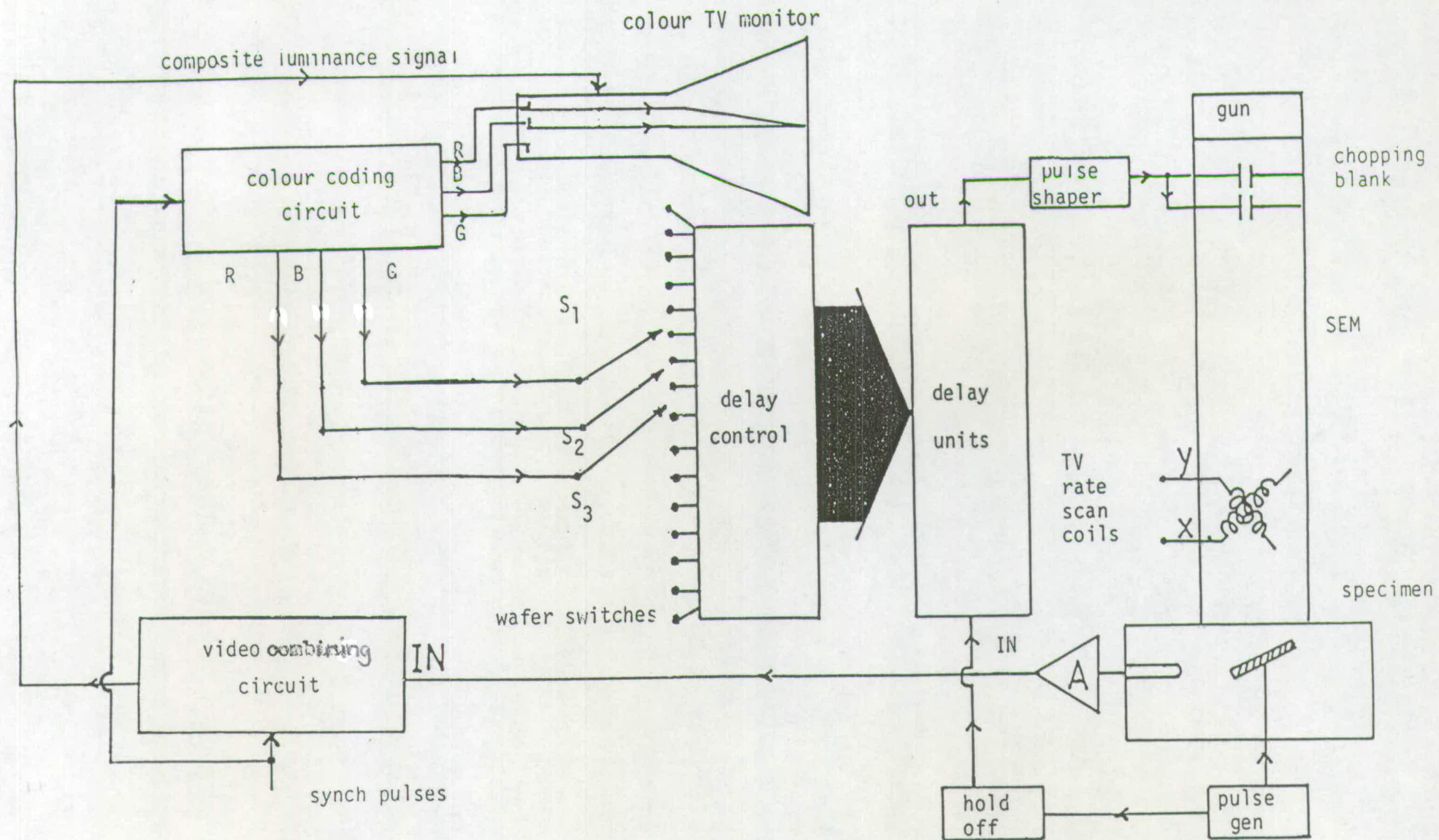
Figure 6. 8 a Shows a block diagram for hardware control of initial colour stroboscopy technique.
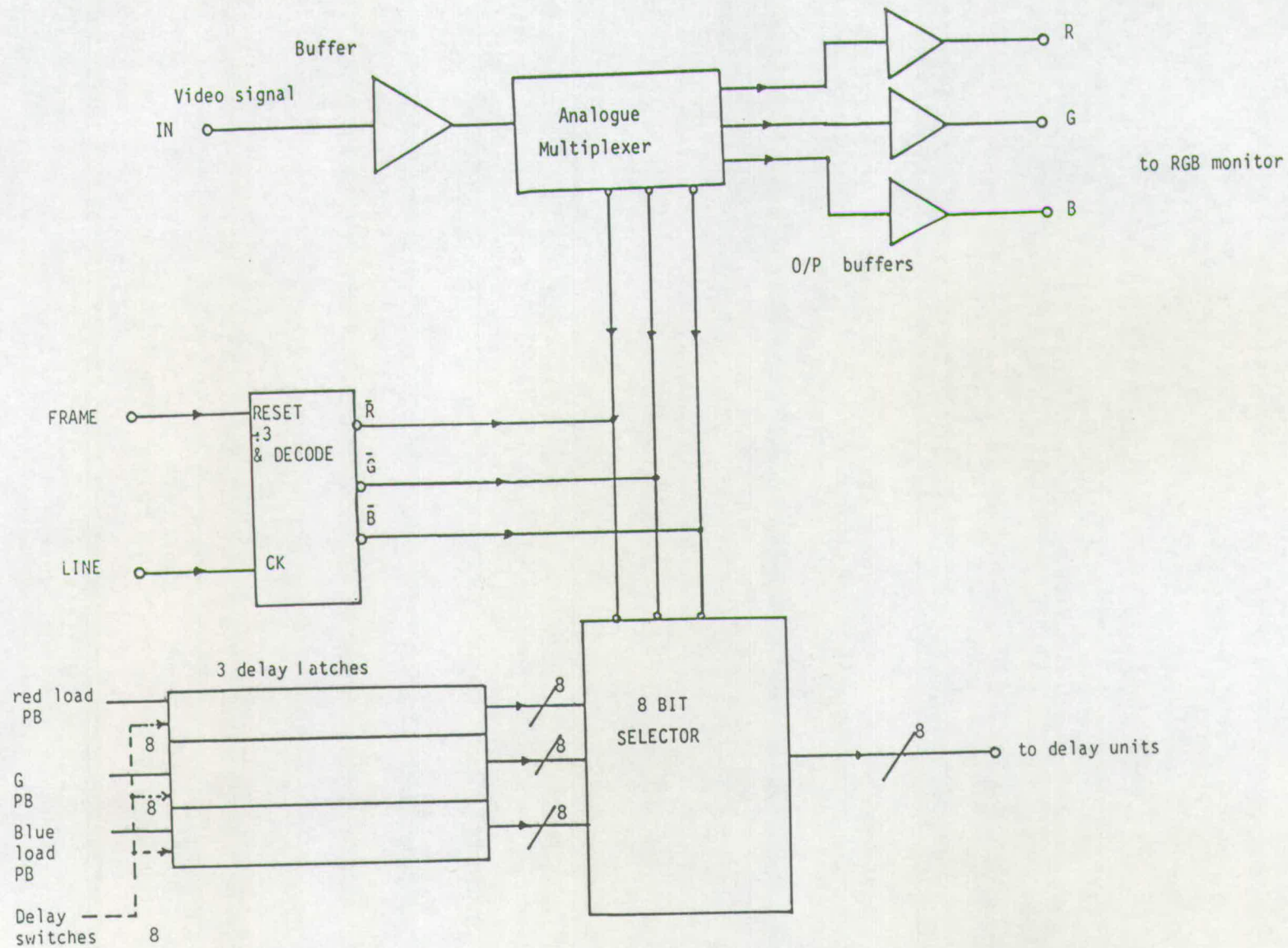
Figure 6.8 b : Shows hardware **control** for colour stroboscopy (modified circuit).

ponents is made for each time. Only sixteen colours could be displayed simultaneously, due to the limitations of the human eye. Therefore it was decided for the start to choose eight colours to produce precise distinguishable colours. These could be programmed by three toggle switches on the front panel of the sampling system for local control, or by three bits colour code for remote control of the colour stroboscopy by using a microcomputer. (see figure 6.7, which shows the automation of the colour stroboscopy).

The colour coding circuit was designed to produce different colours by using a diode ROM matrix (see Figure 6.4). The purpose of the ROM (read only memory) was to decode the three bit video word into three binary words, each relating to the relative proportions of a primary colour. The outputs from the gain stage of the colour coding circuit were used to switch the colour T.V monitor guns of the display.

Before deciding on a particular method of implementing colour stroboscopy, it was necessary to carry out preliminary experiments to find out how the human eye would respond to various ways of presenting the colour information.

Figure 6.8 a, shows a simple video counting circuit designed for this purpose. This used a 3 bit binary counter, where the field signal frequency is used as an input clock to the counter. The 3 bits of the counter output are fed to the monitor guns (R.G.B), they are also fed via a wafer switch to three successive bits of the 21-bits delay units control (see Figure 6.8a), to produce digitally switched time delays by digital sampling system and delay units of Figure 5.6 (chapter five). These eight time delays of the sampling pulses are shown in Figure 6.9 each corresponding to one of eight different colours The pulses are

(i) (ii)

G M B C R Y O W
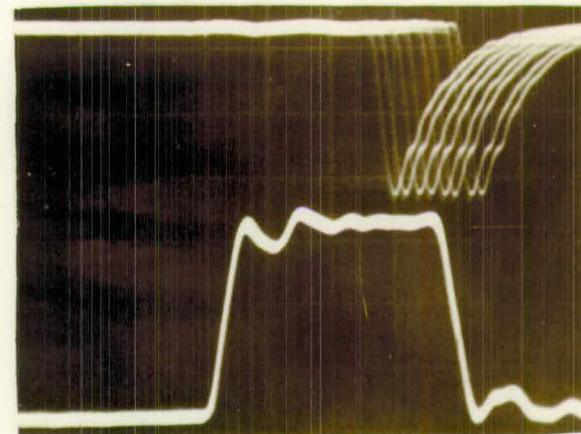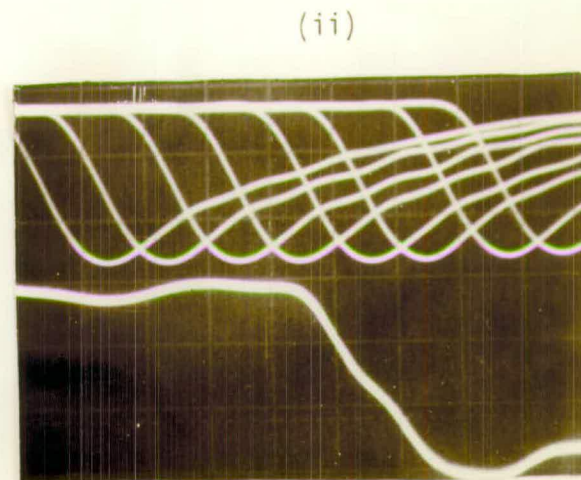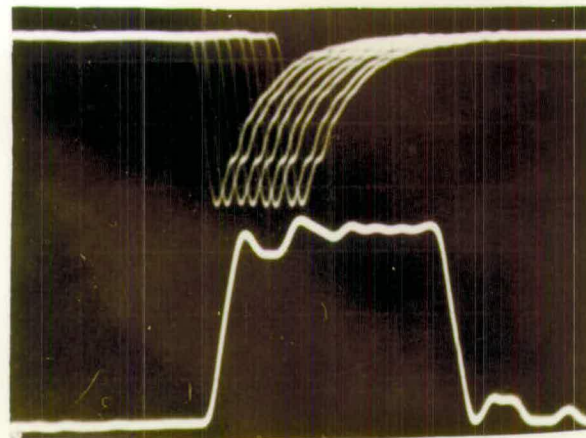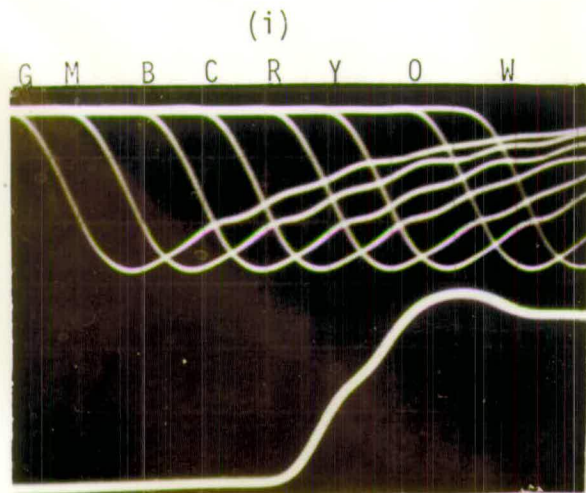
upper trace is
sampling pulses
lower trace is
i/p pulse to spec-
imen

H = 10 ns/cm
V = 5V/cm upper
    2V/cm lower

same as above but

H = 50 ns/cm

Figure 6.9 : Shows sampling pulse (delayed trigger pulse) to produce eight colours to study rise
and fall times of waveform on specimen under test by colour stroboscopy.
i, is for rise time, ii is for fall time.
Note: G = Green, M = Magnenta, B = Blue, C = Cyan, R = Red, Y = Yellow, O = Orange, W = White

shown positioned near the rising and falling edges of a pulse, in order
to produce some visualisation of these edges.

In practice the display was found to be unsatisfactory. One rea-
son for this was that the colours were switched at field frequency (50
Hz) so that there was obvious flickering at (50/8) 12.5 Hz. This could
be overcome by using line frequency to trigger the counter so that the
sequence of 8 colours occurred over each group of 8 lines of each field
of the display. (each then occupies 2 lines per frame of 2 fields).
However, even when this was done there were still difficulties with in-
terpretation of the picture. For example, in Figure 6.9(i), the first
(green) pulse is present when the signal is at its most negative
(brightest) while the second one (magenta) is present at about half the
pulse height. The other colours occur at the top of the pulse and so
will not appear on the image. The colours green and magenta will there-
fore superimpose on the conductor carrying this pulse.   These colours
will mix additively to produce a greenish white colour which is diffi-
cult to distinguish. By close examination of the screen it is just pos-
sible to see the separate 2 lines of green followed by 2 lines of magen-
ta, but because of the noisy picture this is unreliable. It was decided
therefore that further work on pulse edges would at first be done using
only two colours (red and green) so that there would be much more visi-
ble discrimination between phases.

A modified hardware control circuitry was designed and used for
colour mapping as shown in Figure 6.8b , where electronics circuitry is
developed to select any colour corresponding to time delay produced by
digital sampling system and delay units. Latch devices are used to
select any time delay required out of 21 - bits of control unit of the
sampling system, to make control of colour stroboscopy more flexible to
be controlled manually and by computer.

6.4.3 Colour TV Display

To display the colour stroboscopy in the SEM, a modified colour TV receiver was used as shown in Figure 6.4. The three guns of the monitor were fed separately with appropriate primary colour signals A separate voltage proportional to picture brightness was required at the display unit, which also incorporated the T.V synchronising pulses. The main modification in the receiver was at the video output stage, where the gun drive transistors were shunted by three electronic switches. The video signal from the SEM head amplifier was fed to the modified colour T.V receiver through the video combining circuit at the luminance point (see Figure 6.5). A capacitor was used to separate the TV circuitry from the display unit. The chassis of the receiver was isolated from the mains and connected to the earth of the SEM system.

6.5 BASICS OF SIGNAL ANALYSIS BY COLOUR STROBOSCOPY

The principle of colour stroboscopy is based upon the representation of different time delays, and the transition time by different colours.

Colour stroboscopy is used in two different modes:

(a) The time delay mode :
   Where different colours denote different time delays.

(b) The transition time mode :
   Where **different** colours denote the transition times of the digital signal.

Two basic colours of red and green are used and displayed on the TV monitor. Two sampling pulses with independently variable time delays are used corresponding to red and green colours. The changeable rise time of the waveform (slowing down) is often of interest in work on dynamic systems.

The principle adopted for displaying the time delay and the transition time information in colour is as follows (see Figure 6.10). The timing of the pulses is set so that the sampling pulse immediately preceding the edge of interest corresponds to the green gun being on, while the sampling pulse immediately after the edge corresponds to the red gun. The time delay between "green" and "red" sampling pulses is set to the expected transition time of the edge being examined (see Figure 6.11).

1. When green and red sampling pulses are on either side of the waveform leading edge. The TV monitor displays a green image of the specimens' pad, while the red colour is dark (absent) at this instant of time (see Figure 6.10 a and Figure 6.12), as it is sampling where the waveform is positive.

2. When both green and red sampling pulses are at the high level of the waveform (logic "1"), the image is dark (see Figure 6.10 b), which shows ordinary black and white voltage contrast.

3. When the phase changes in such a way that the red sampling pulses are on the other side of the waveforms' falling edge, the TV monitor displays a red image of the pad (see 6.10 c and Figure 6.13), while the green pulse is absent.

4. When both green and red sampling pulses are at the low level of the waveform (logic "0"), the pad image is bright yellow (see

(a) green image when the display is switched to green
    and red is dark.
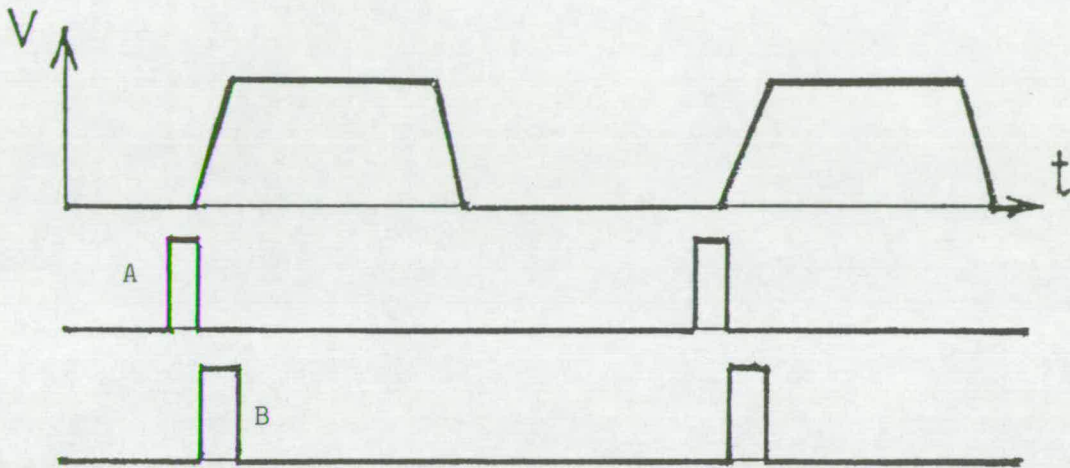
(b) dark image with ordinary voltage contrast.
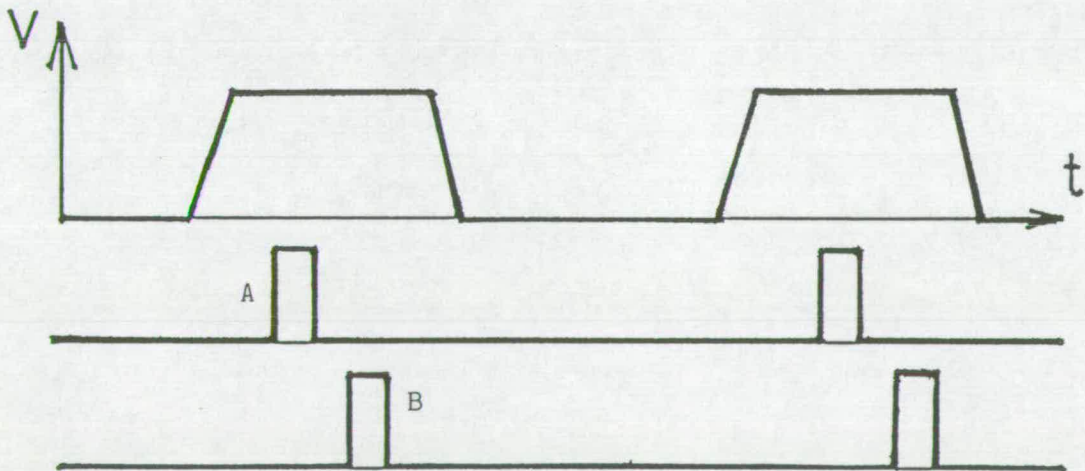
Figure 6.10(i): shows basic principle of colour stroboscopy
using two colours.

A: green sampling pulse when the display is switched to green.

B: red sampling pulse when the display is switched to red.

(c) red image when the display is switched to red and green
    is dark.
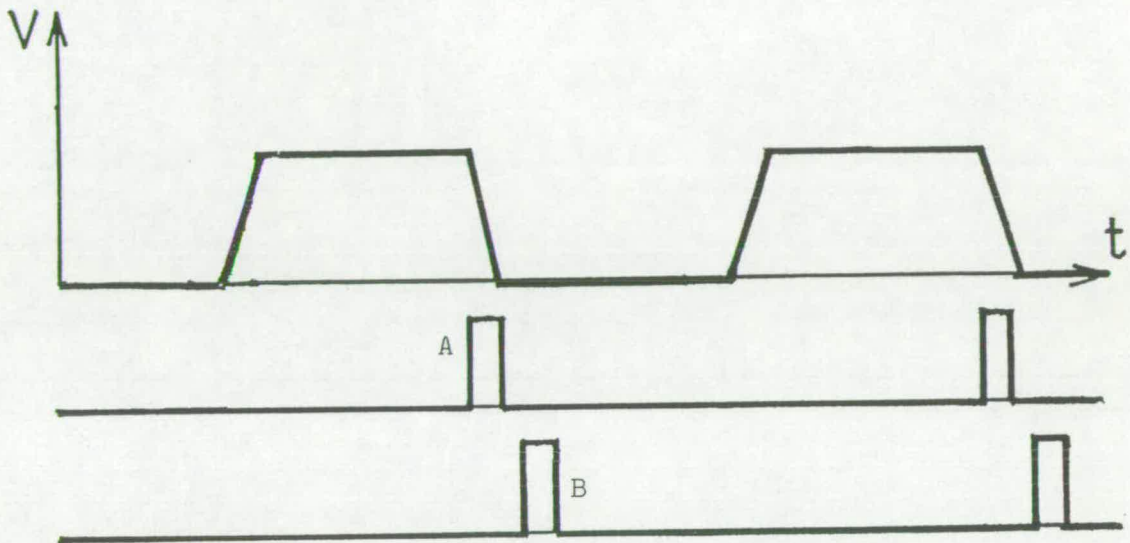
(d) bright yellow image when the display is switched off.
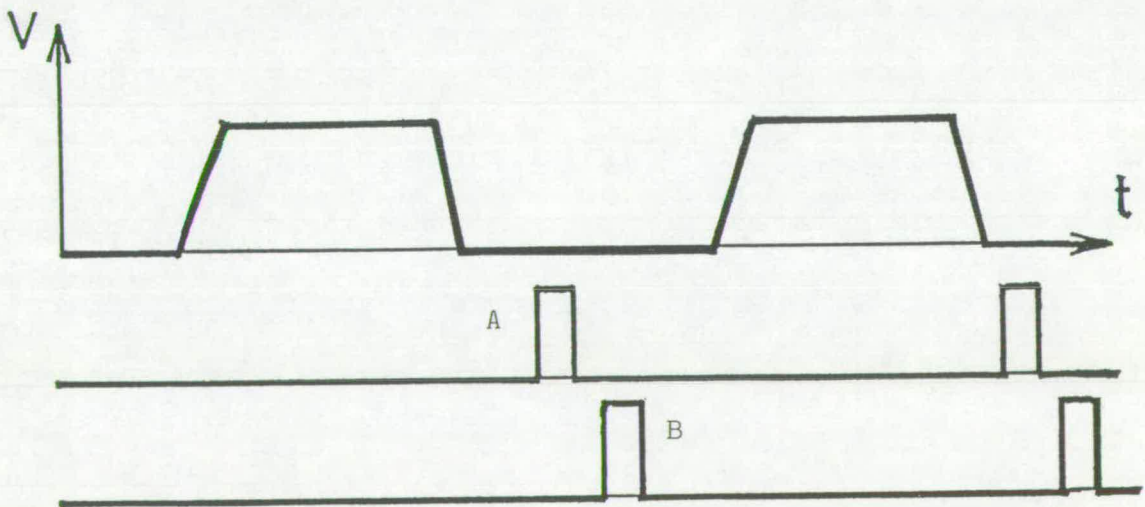
Figure 6.10(ii): shows basic principle of colour stroboscopy using
two colours.

A: green sampling pulse when the display is switched to green.

B: red sampling pulse when thedisplay is switched to red.

(e) yellow or orange image when display is switched to red and green

1. $t_d < t_r$ "orange image".

2. $t_d > t_r$ "saturated colour".

A

t_d

B
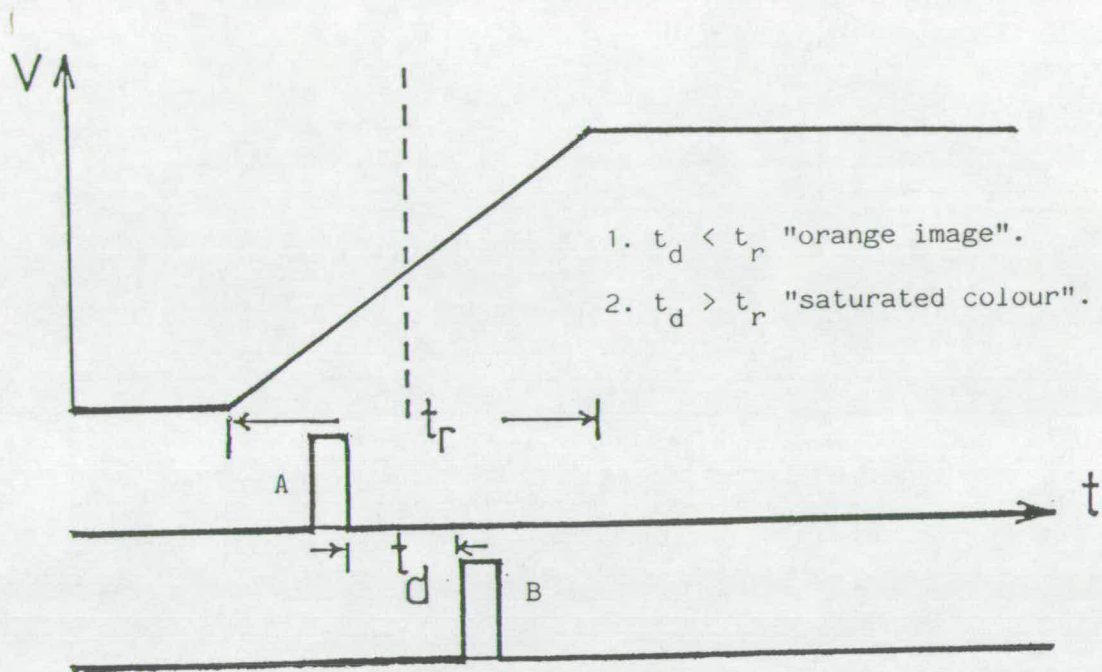
(f) green and red images

180° out of phase
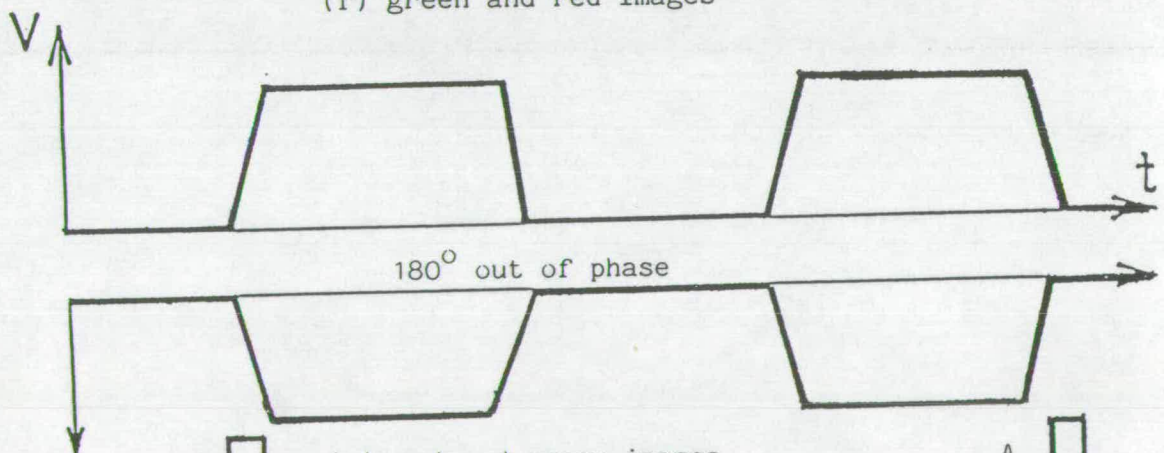
A   (g) red and green images   A

B   B
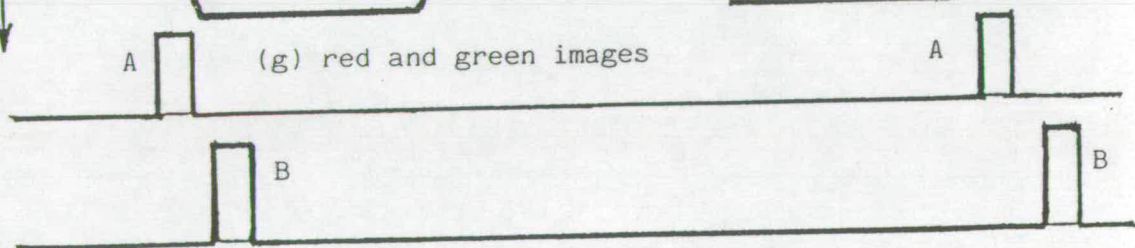
Figure 6.1 α(iii) shows basic principle of colour stroboscopy using two colours.

A: green sampling pulse when the display is switched to green.

B: red sampling pulse when the display is switched to red.
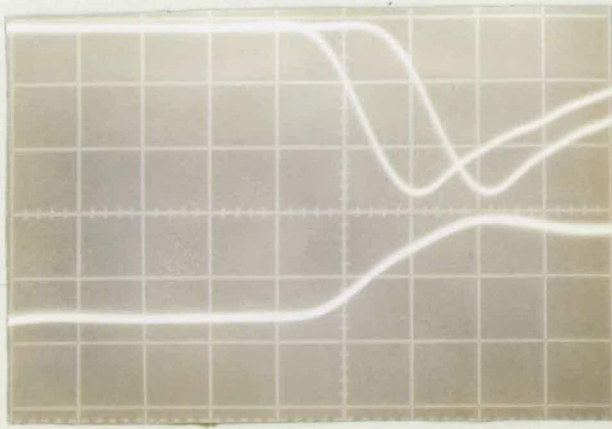
upper trace is sampling pulses
lower trace is signal on specimen
V = upper trace is 5V/cm
    lower trace is 2V/cm
H = 5ons/cm
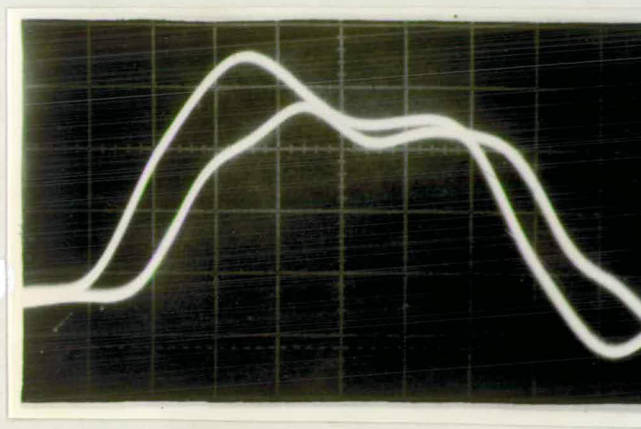
Two delay pulses
V = 2V/cm
H = 10ns/cm
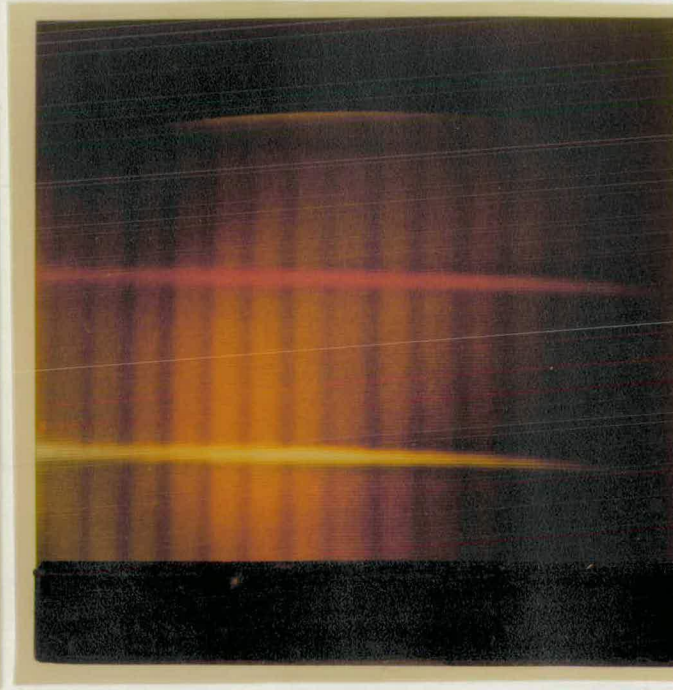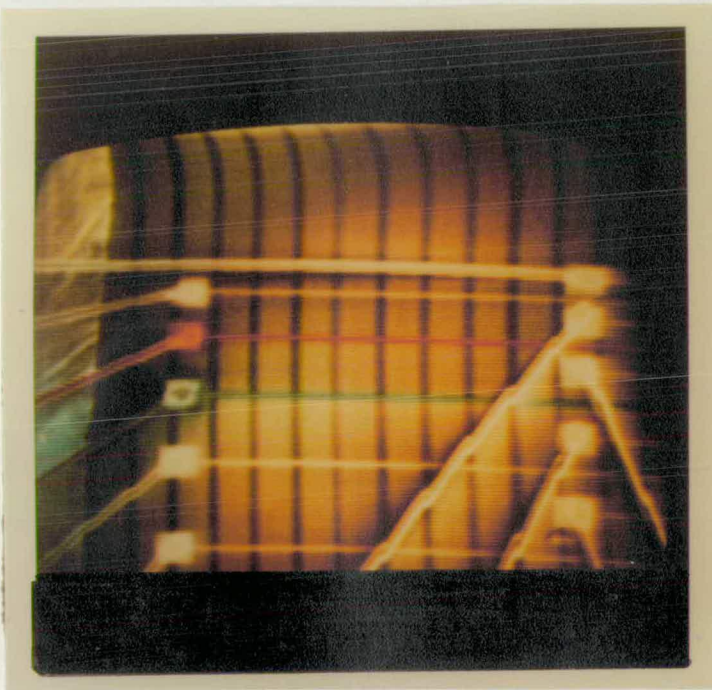
Figure 6.11: Shows the colour stroboscopy of two parallel
              aluminium strips with two delayed pulses of
              10 ns with two different colours to show
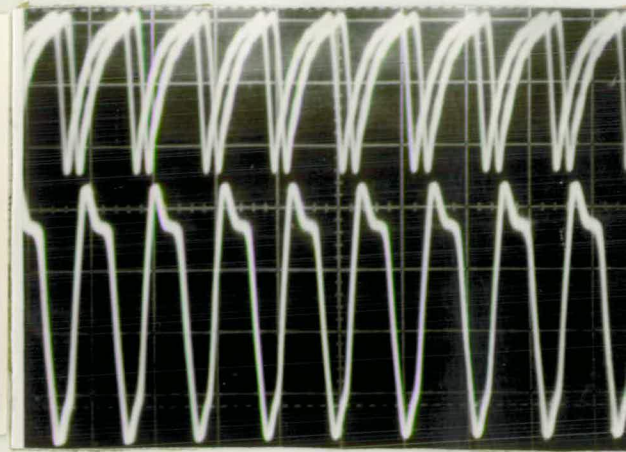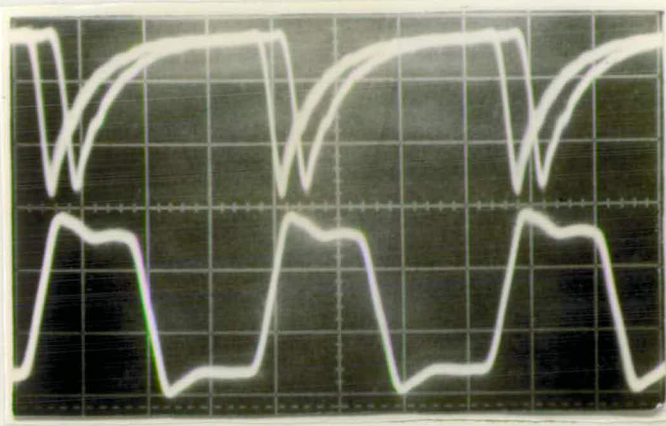
upper trace is sampling pulses
lower trace is signal on specimen
V = 5V/cm upper trace
    2V/cm lower trace
H = 5ons/cm

Same but H = 0.1µs/cm

Figure 6.12.   Shows colour stroboscopy of two parallel
                      aluminium strips with two delayed pulses
                      of 10 ns. Green and dark are shown, to

uppertrace is sampling pulses
lower trace is signal on
specimen
V = uppertrace is 5V/cm
    lowertrace is 2V/cm
H = 50ns/cm

Same but H = 0.1µs/cm
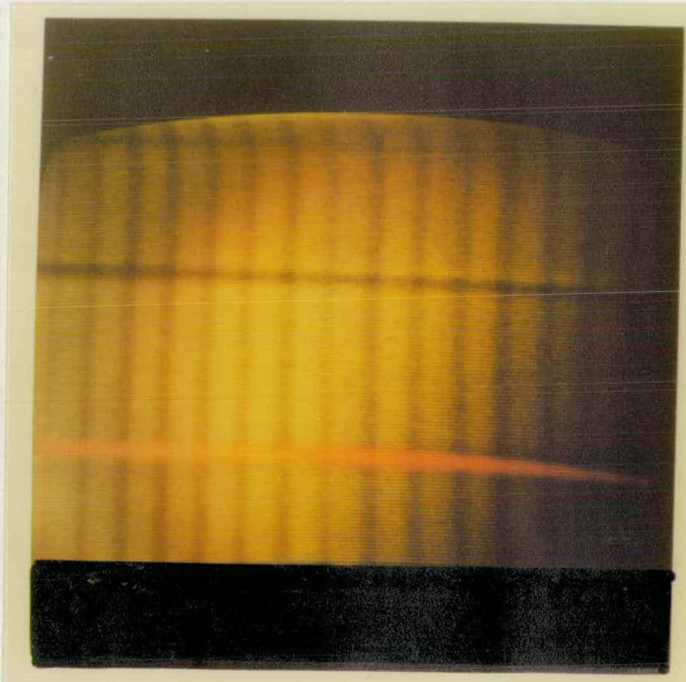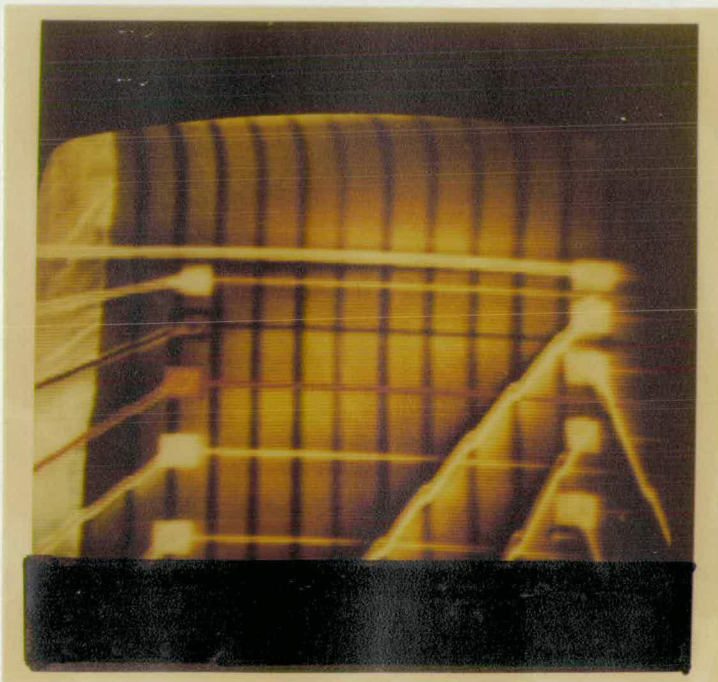
Figure 6.13: Shows colour stroboscopy of two
              parallel aluminium strips with two
              delayed pulses of 10 ns. Red and

Figure10 d).

5.   When the rise, or fall times are slowed down, a mixture of red and green colours is produced at mid way of the switching time of the waveform, where red and green sampling pulses combine to display a yellow or orange colour (see Figure 6.10 e).

6.   To display both colours of green and red at one instant of time (sampling phase) on different conductors, green and red sampling pulses should be on the leading edge of the waveforms on the specimens' pad under test (see Figures 6.10f and 6.14).

7. To display red and green colours on different conductors, there must be a falling edge on one conductor coincident with a rising edge on the other. (two waveforms of 180 out of phase were fed to an MOS 4 bit dynamic binary counter). This is shown in Figures 6.10 g and 6.14).

N●B: The exposure time for the photograph was approximately 5 seconds.

        The vertical dark bands are due to a temporary fault in the scan

        generator. Figure 6.14 shows a demonstration of two colours of two waveforms out of phase.

6.6   PROCEDURES FOR COLOUR DISPLAY OF TIME DELAY AND THE TRANSITION TIME

    The actual transition time may be measured by the minimum time delay between the two sampling pulses which is found necessary to pro-

upper trace is sampling pulses
lower trace is signal on specimen
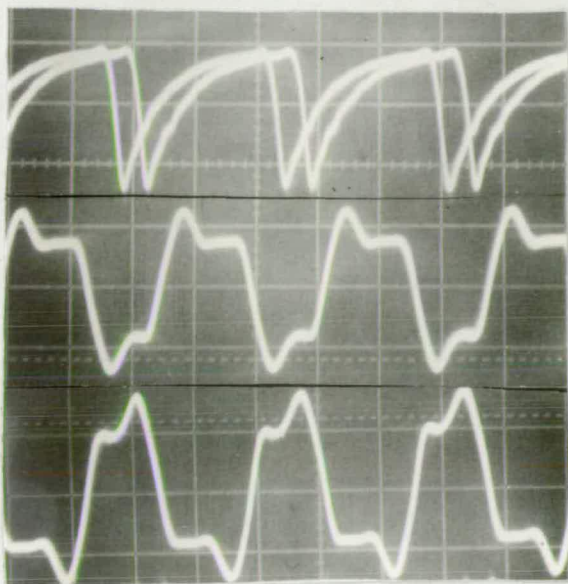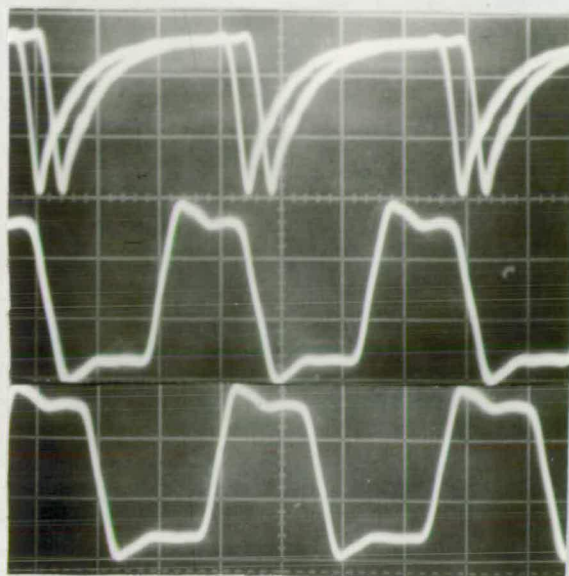
V = upper trace is 5V/cm
    lower trace is 2V/cm
H = 50 ns/cm
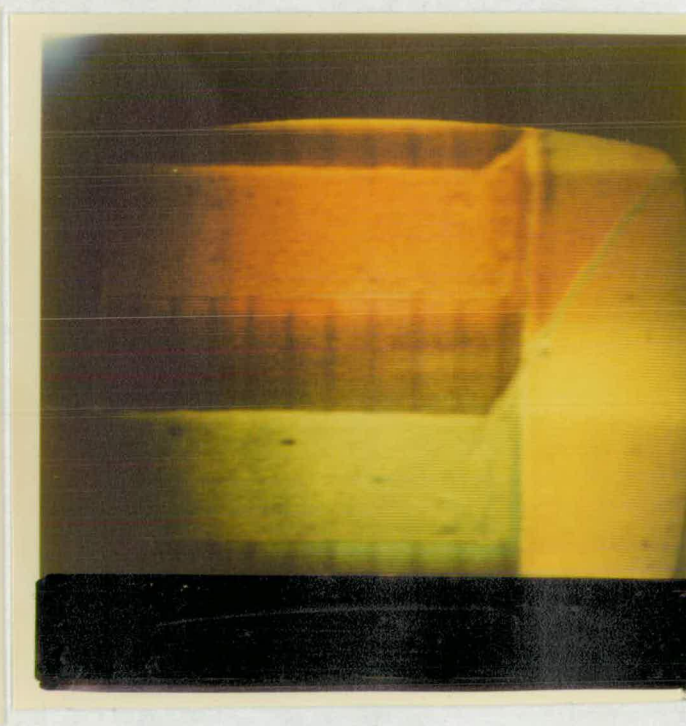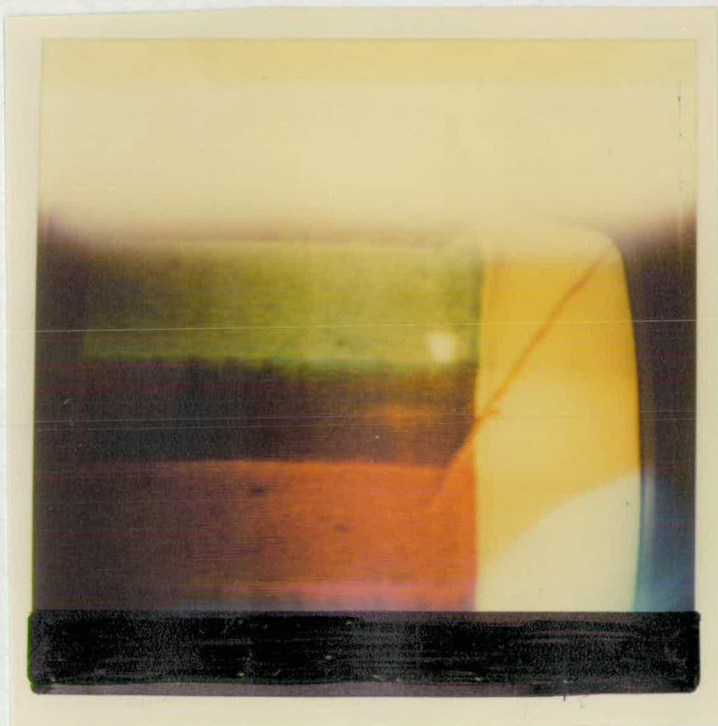
Figure 6.14:   Shows colour stroboscopy of two waveforms
               out of phase fed to 4 bit dynamic binary
               counters as (i) in leading edge (ii) in fall
               edge of the waveforms to show phase change
               principle.

duce a fully saturated colour at that edge. The digital sampling system and delay unit is used to produce any time delays between 1.5ns to 2ms.

When a long time delay is produced by the sampling system, then two different colours are produced for different time delays of the same specimens' pad under dynamic operation (same method if the phase of the signal on the pad is changed), or as simple as changing the phase of the two sampling pulses by using the pulse generator, as shown in Figure 6.15.

Thus the leading edge of the wave applied to one conductor makes that appear red while the coincident trailing edge on the conductor immediately below appears in green. The remainder of the conductors were held at earth potential (see Figure 6.11).

Figure 6.16 shows an aluminium test specimen pattern with long parallel strips , which is used for testing the reliability of the present colour stroboscopy technique. This specimen is a specially fabricated test circuit to which are applied two 5 MHz square waves in antiphase. The variation on this technique may be used to produce precise information about the timing of pulse edges. In its simplest form it uses only two colours,

say red and green, and two sampling phases; one positioned at each side of the edge of interest, as shown in Figure 6.10. If the time delay between the sampling pulses is set to be just greater than the transition time of the pulse edge , then the conductor will appear in one saturated colour(e.g red).

If the transition time is then lengthened for some reason (such as the slowing down of the signal due to loading etc), as shown in Figure 6.10 e, then the other colour (green) will begin to appear and the conductor will appear in orange or yellow. If a significant portion

(i)   (ii)
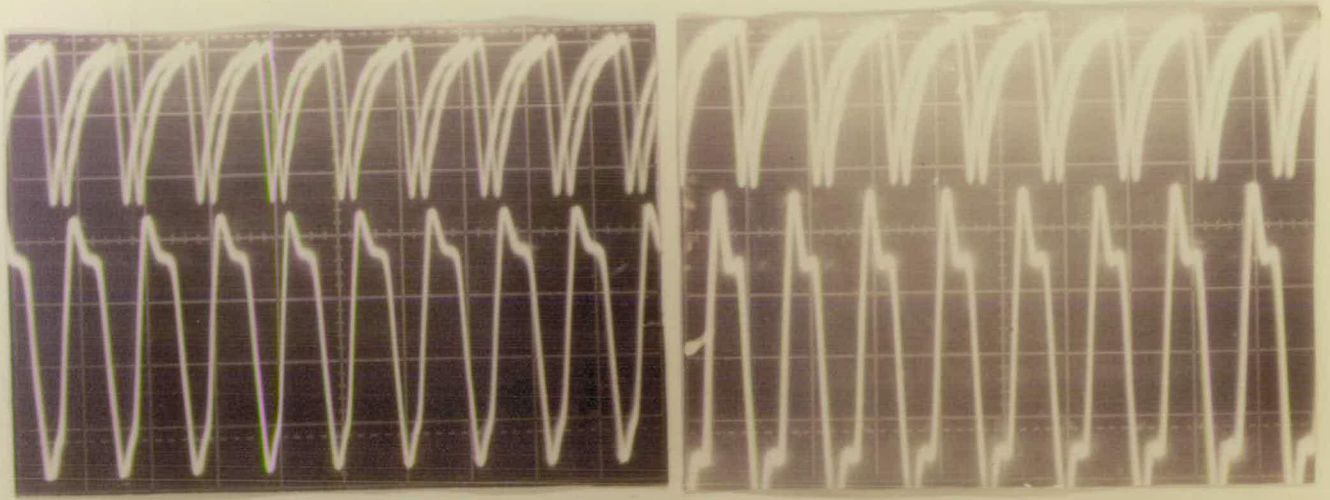
upper trace is sampling pulses
lower trace is signal on specimen
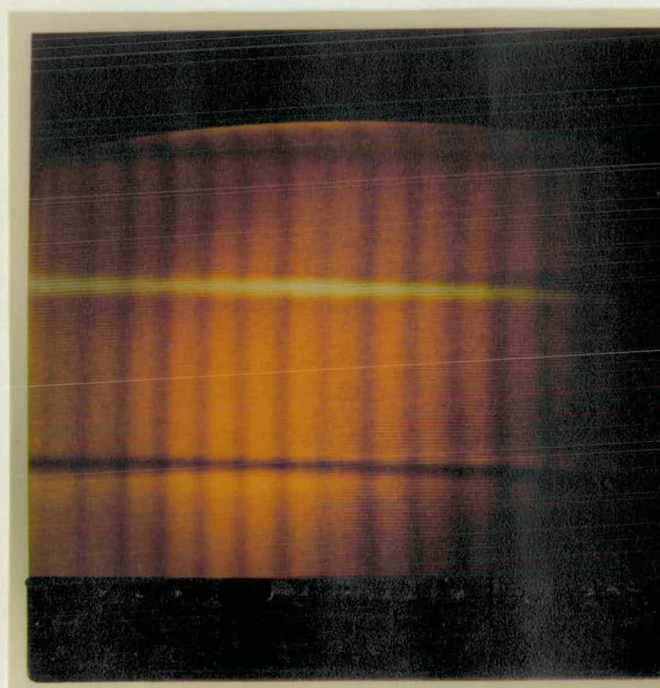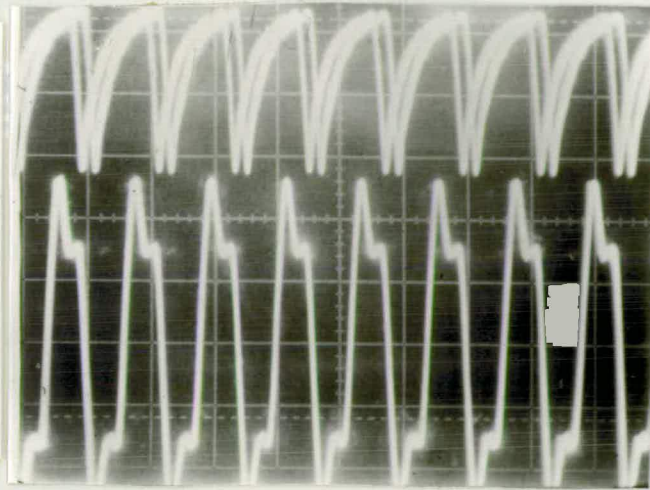V = 5V/cm upper trace
    2V/cm lower trace
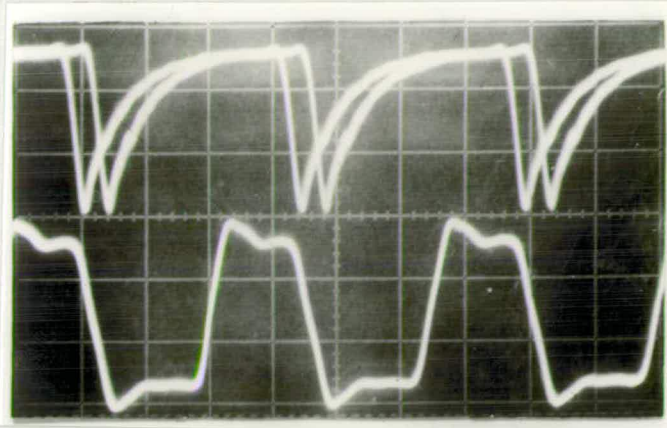H = 50 ns/cm
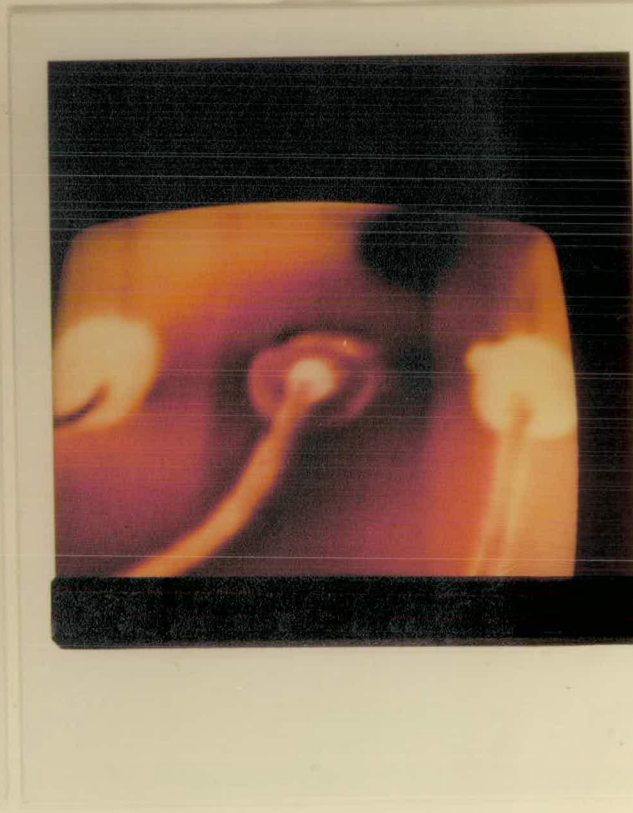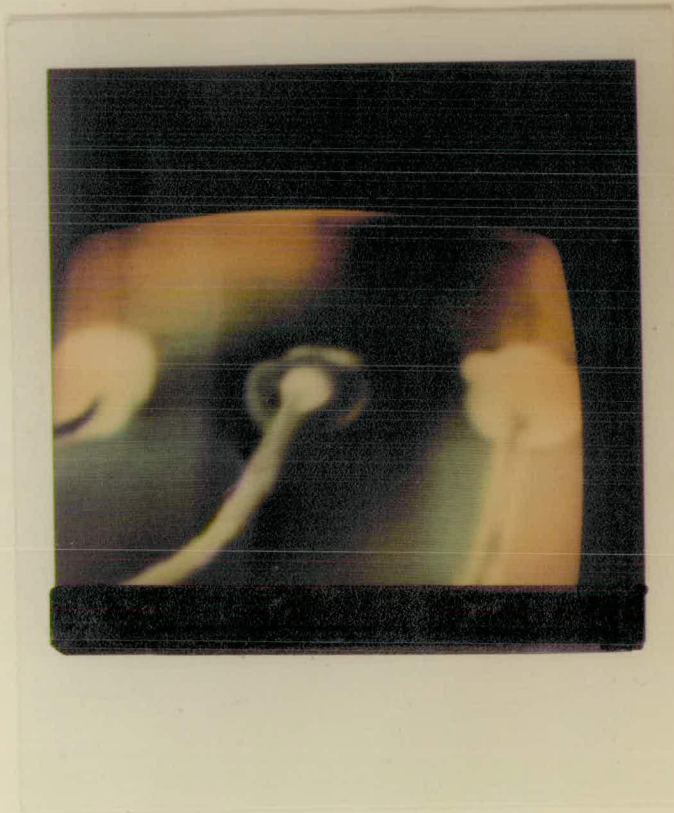
Figure 6.15: Shows colour stroboscopy on aluminium test
specimen work with frequency up to 10 MHz
of repetitive signal (i) Two sampling
pulses on rise time shows green pad (ii) on
fall edge shows red pad.
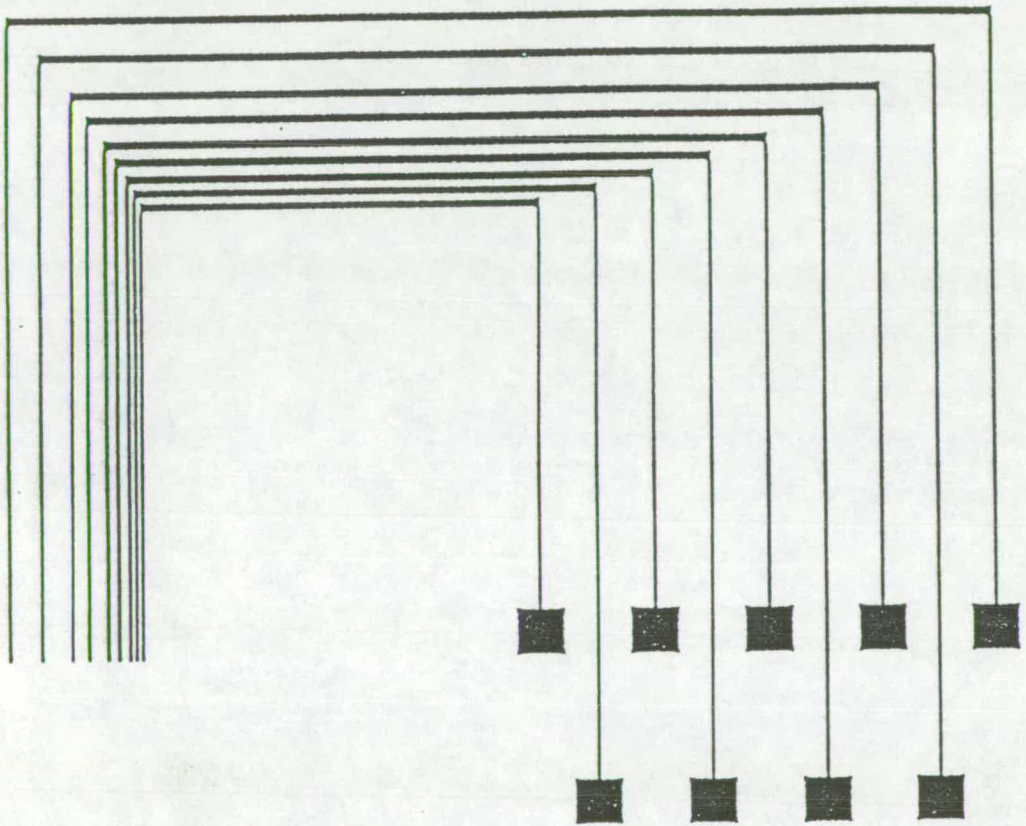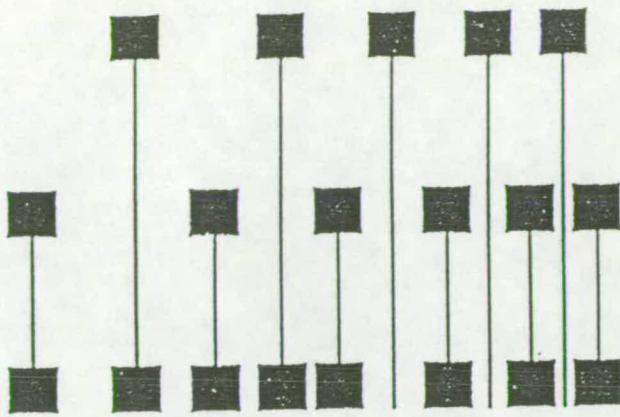
Scale: |⎯⎯⎯⎯⎯⎯⎯| 500 microns

Figure 6. 16 : Shows test specimen pattern of aluminium strips used
in colour stroboscopy

of the circuit is viewed in this mode, then it is easy to pick out where timing errors are occurring without having to take readings of actual waveforms at multiple points. Having established where any problems are appearing, then the waveforms at these particular points may be obtained by the usual beam- chopping sampling technique.

The experimental steps and conditions required to be used to perform the colour stroboscopy are :

1. The two sampling pulses are used to represent two colours of red and green. These pulses are made close to each other with a short time delay, is easy to be changed with respect to the phase of the tested signals. The time delays for the present work can be changed manually or automatically by using the sampling system and delay units.

2. Fix the time delays between the two sampling pulses and change the phase manually, it can be done by using the pulse generator.

The shortest time delay between the two sampling pulses produced by present sampling system is 1.5ns, which limits the transition time and time delay measurements.

3. Fix the phase of the sampling pulses and change the time delays between the two sampling pulses by using the sampling system and delay units.

4. Make adjustments to produce saturated colour to correspond with digital signal transition time, by selecting the precise time delay between the two sampling pulses and proper phases of the signal under test.

5. The transition time of the signal measured by colour stroboscopy is compared with the technique used as mentioned in Figure

5.31b (chapter five). The result was found comparable.

6. A time delay of a signal is measured when the colour is changed from one point at one end to another end on a long conductor. When propagating the signal along the conductor, the loading of the signal causes the slow down of the rise time, this produces an error of short time delay. It can be studied by this procedure and measured. The tested conductor is biased with -ve d.c voltage to display the colour image clearly.

6.7 DISCUSSION

This work has shown that colour stroboscopy at high frequency to give a real time TV display is both possible and useful. While there is clearly a need for development and sophistication of the technique, it has already been shown that it can very rapidly provide very precise timing information about pulses travelling through integrated circuit structures. Obtaining this information by other means would be laborious and time-consuming.

The work described by Dinnis (1980) was at very low frequency; a frequency which must be related to TV field or line frequencies. The present system has no restriction on frequency of operation other than that imposed by the chopping system. The type of delay unit employed using digitally switched delays, is particularly convenient in this application because the sampling pulse delay can be almost instantly switched as the colour display system demands. In alternate field switching, where there is lms between the end of one field and the

start of another, most methods of delay generation should be able to change to the new value and settle to a stable state. However, switching at line frequency requires that the time delay change within 12us, which is well within the capability of this system but could well cause problems in analogue-based systems. If vertical colour striation are required, then switching many times per line is needed and this, again, can be achieved with this system.

In viewing the image produced by this system, the most noticeable defect is the very poor signal-to-noise ratio. The spatial resolution is also somewhat degraded. The reason for these defects is the low duty cycle of the electron beam, which is necessary if good time resolution is to be achieved. In order to provide an image which is viewable at all at TV rate, it is necessary to use low demagnification of the gun crossover and large apertures, hence the poor spatial resolution. A brighter cathode is clearly one way to improve the situation. The other is to use a noise-reducing frame-store system. This should provide a very considerable improvement, as is demonstrated by the photographs taken of the display, which were taken with exposure times of about 5-10 seconds (i.e. 250-500 frames). No such system was available for the present work but it is clearly indispensable if the method is to become a standard tool for examination of ICs.

The straightforward method of direct computer control of colour stroboscopy was found to be incapable of the speed which the hard-wired system provided and was therefore not capable of giving the required form of display. However, the advantages of computer control are so obvious that the next step in the development of this system must be to provide a hard-wired computer-controlled system.

CHAPTER SEVEN

CONCLUSION

The survey of previous work in stroboscopy and sampling in the SEM given in Chapter two has shown their capabilities in testing integrated circuit devices under dynamic operation. These techniques are important for failure analysis and for displaying high frequency signals on a specimen under test. A short review of the conventional fashion of developing analogue circuitry to produce time delays by the method of ramp signals causes timing jitter in the reconstructed waveform on the specimen under test.

The performance of the most recently designed chopping plates appears to be quite satisfactory. From the experimental results, the transit time of the electrons down the SEM column is found to be a significant factor in contributing to the time delays present on the video signals and in the design of a chopping assembly.

The problem of two video pulses being produced per cycle has been overcome by using double plates for chopping the electron beam and blanking it at the fly back period of the chopping pulse. It was found that -ve d.c. bias on both blanking and chopping plates helped to eliminate the extra video pulse. Double plates are used also at present to produce high speed switching of the electron beam. A short electron beam pulse was produced by using a d.c bias to select a fraction of the chopping pulse rise time. Electron beam pulse widths of the order of 1 ns were achieved.

Curved plates are recommended for solving electron beam non-alignment problem which is important for the present machine. For study

of MOS devices, ordinary parallel plates are developed as a good chopper to test these devices under dynamic operation. An additional fourth lens in the optical column was used by Gopinath and Hill (1977) and Menzel and Kubalek (1979) to reduce the effect of crossover movement under the gun due to fast chopping of the electron beam, is found not necessary for the present work. A 100 um top aperture is used to let a limited number of electrons pass through the plates and not to accumulate around plates which leads to local floating fields due to contamination. This was found adequate to minimise the spot movement on the specimen under test, and it was not a serious problem at present.

In the analogue sampling system, a conventional way of generating a delayed sampling pulse has been develop using different speed of ramp signals. This was found to work reasonably satisfactorily at fast ramp signal frequencies up to 10 MHz, and would produce beam pulses which were assumed to be in the nanosecond region. However, there was a noticeable jitter in the timing, due to phase instability problems in the analogue circuitry as discussed in Chapter four.

Owing to timing jitter in the reconstructed waveform of the analogue sampling system, which has been reported by Plows and Nixon (1971) as a little shakiness in the stroboscopic waveform, Gopinath et al (1976), and Fujioka et al (1978). Further it was hoped that the present analogue system constitutes some improvement on previous systems which had sought to perform the same task with some deficiencies such as timing jitter. The conclusion from the survey is that none of the reported approaches studied the phase instability problem in the analogue systems.

Timing jitter is due to phase instability (timing problem) in the

analogue circuitry, especially in the comparator unit which does not always respond consistently to input ramp signals to be compared to give the moment of producing the delayed trigger pulse. Because it is found that when any change to the offset voltage to slow ramp is accomplished, less timing jitter appears in the reconstructed waveform.

It is therefore concluded on this occasion not to let the slow and fast ramp amplifiers work in the saturation region in producing ramp signals. Furthermore, arrangement to permit the remote digital control of the functions of the analogue system were becoming rather difficult. It was therefore concluded that the analogue system is not efficient to be used for present purposes.

From testing results, it is realised that the delay generation is found to be a most crucial aspect of the problem; so producing a new digital sampling system was essential to offer an attractive approaches to solve the problem.

For these deficiencies, it was decided therefore to develop a new digital sampling system of digital principle to be readily controllable by digital inputs to produce a digitally switched time delays with better performance; to study MOS devices under dynamic operation.

The digital sampling system which has been designed and constructed in this work was fully characterised and shown to be very suitable for observing and measuring high frequency signals on specimen. New models of time delay lines are produced. Different methods are adopted at present to test the performance and the reliability of the digital system. New technique is developed to calibrate time delay, electron beam pulse width and rise time of the signal on specimen. This system is found to be more efficient and reliable to perform sampling in the SEM over the analogue systems.

Full remote control by computer is used, with a certain amount of computing made by software design to meet the requirement of automating and sophisticating of the digital sampling system.

In colour stroboscopy basic technique, colours are allocated to various phases of a repetitive signal. The guns in the colour TV monitor are switched to display a fixed sequence of colour; switching at line frequency can produce a picture which may be viewed in real time, although it is noisy. As the display colours are switched, the phases of the sampling pulses are switched correspondingly by means of a digital sampling system develop at present. A variation on this technique may be used to produce precise information about the timing of pulse edges.

Colour stroboscopy is found to be a fast technique for signal analysis and to display time delays in colour. A significant improvement is achieved with respect to the frequency limitation of the previous work in colour stroboscopy, and is found to work up to 10 MHz in frequency of repetitive signal.

Two modes of colour stroboscopy were used to indicate timing through the specimen under test in colour. This technique is recommended as a new method of studying signals at high frequencies in the SEM. Colour stroboscopy is found significant in testing MOS devices under dynamic operation.

FUTURE WORK

There is a need to carry on designing the chopping plates with
proceed
different geometrical shapes (e.g curved plates) further work should by

finding a model of d.c and a.c excitation fields for the deflection an-gles of the electron beam with respect to, transit time, plates gap, plates lengths, frequency of deflection voltage, plates geometrical shapes, electron beam accelerating energy, and deflection voltage for better performance of the chopping system. study of the deflection in concern with, field strength, potential distribution, and the electron beam distribution pattern. This is useful in suggesting design and shapes of the chopping plates.

Improvements could be made to the present instrumentation using frame store system, which would enable the digital sampling system to minimise high frequency noise existing in the reconstructed waveform and improve S/N ratio in the picture.

For further work, it is recommended to design a digital programmable filter in such a way to trade a measurement time for accuracy, which adds a flexibility to the sampling system.

A computer can be used to store and release the colour information to produce a colour movie. This is useful in device reliability test as a diagnostic tool.

The next step in the development of the colour stroboscopy must provide a hard-wired computer-control system for sophistication of the system.

Areas requiring further investigation and development also in-clude design of circuitry to produce and display different coded vol-tage levels of voltage contrast in colour.

REFERENCES

N.B : SEM = Proceeding of the annual Scanning Electron Microscope symposium, Editor O Johari.

Ahmed, H, and Nixon, W.C. "Micro circuit engineering", Cambridge University Press, p 409-437, 1980.

Balk, L.J., et al. "Quantitative voltage contrast at high frequencies in the SEM",SEM,Vol IV, p 615-624, 1976.

Crewe, A.V. "Colour conversion in electron microscopy", Scanning, Vol 3, p 175-176, 1980.

Cooper, W.D. "Electronic instrumentation and measurement technique", Prentice-Hall,London, 1978.

Dinnis, A.R. "Voltage measurement on integrated circuits using the scanning electron microscope",Proc IEE, Solid-State and Electron Devices, Vol No 1, p25-28, 1979.

Dinnis, A.R. "Colour display of voltage contrast in the SEM". Scanning, Vol 3, pp 172-175, 1980.

Dinnis, A.R, and McCarte, J.T."Improved SEM voltage contrast measurements" , Microcircuit Engineering, Cambridge University Press, pp 465-477,1980.

Dinnis, A.R.,Nye,P, and Khursheed, A. "Quantitative voltage contrast in the SEM",Proc of Inst of Physics ,EMAG81,Conference No 61, Cambridge, pp 527-530, 1981.

Diefenderfer, A.J. "Principles of electronic instrumentation", W.B. Saunders , London,1979.

deSa, A. "Principle of electronic instrumentation", Arnold, pp 251-273, 1981.

Davidson, S.E. "Wehnelt modulation beam blanking in the scanning electron microscope", Inst. Phys. Conf. Ser. No. 61, Chapter 2, pp 39-42, 1981.

Edwards, D.F.A " Electronic measurement technique", Butterworths,London, 1971.

Feuerbaum, H.P., and Otto, J. "Beam chopper for subnanosecond pulses in scanning electron microscopy", J. Phys. E. Sci. Instrum., Vol 11, pp 529-532, 1978.

Feuerbaum, H.P. "VLSI testing using electron probe", SEM, Vol I, pp 285-318, 1979.

Feuerbaum, H.P. and Otto, J. "Signal processing for E-beam waveform measurements", Microcircuit Engineering, Cambridge University Press, pp 507-513, 1980.

Feuerbaum,H.P,J.Otto"Improved secondary electron signal processing for

waveform measurements" ,SEM,Vol IV,PP1501-15051,1982.

Feuerbaum, H.P, and Hernaut, K. "Application of electron beam measuring techniques for verification of computer simulations for LSI circuits", SEM, Vol I,PP 795-800, 1978.

Feuerbaum, H.P. "Quantitative measurement with high time resolution of internal waveforms on MOS RAMS using a modified SEM", IEEE, J. of Solid State Circuits, Vol SC-13, No 3, pp 319-325, 1978.

Feuerbaum, H.P, and Wolfgang, E. "Use of SEM for multi-channel-sampling oscillography", Proc. IEEE, 66, pp 984-985, 1978.

Feuerbaum, H.P." Electron Beam Testing : Methods and Applications", Scanning, Vol 4, pp 14 - 24, 1983.

Fujioka, H. et al. "Function testing of bipolar and MOS LSI circuits with a combined stroboscopic SEM - microcomputer system", The transactions of the IECE of Japan, Vol E 64, No 5, pp 295-301, 1981.

Fujioka, H. et al. "Submicron electron beam probe to measure signal waveform at arbitrarily specified position on MHz IC", SEM, Vol I, pp 755-762, 1978.

Fujioka, H, et al." Function Testing of Bipolar ICs and LSIs with the stroboscopy Scanning Electron Microscope", IEEE J.Solid - state circuits. Vol. SC15, No 2, 1980.

Fujioka, H. and Ura, K. "Electron beam blanking systems", Scanning, Vol 5, 1, pp 3-13, 1983.

Fazekas, P.et al. "Scanning electron beam probes VLSI chips", Electronics, 4, pp 105-112, 1981.

Floyd, T.L. "Digital fundamentals", Merrill Co,U.S.A, 1982.

Gopinath, A. and Hill, M.S. "Some aspects of the stroboscopic mode: A review", SEM, Vol I, pp 235-242, 1974.

Gopinath, A, and Tee, W.J."Theoretical limits on minimum voltage change detectiable in the SEM", SEM, Vol I, pp 604-608, 1976.

Gopinath, A. and Hill, M.S. "Deflection beam chopping in SEM", Journal of Physics E: Scientific Instruments, Vol 10, pp 229-236, 1977.

Gopinath, A, et al." voltage contrast : A review", SEM, Vol I, pp 375-380, 1978.

Gonzales, A.J. and Powell, M.W. "Internal waveform measurements of the MOS three transistor, dynamic RAM using SEM stroboscopic techniques", Technical Digest of IEDM, IEEE New York, pp 119-122, 1975.

Gonzales, A.J. and Powell, M.V. "Resolution of MOS one-transistor", J.Vac.Sci. Technol., Vol 5, No 3, pp 1043-1046, 1978.

Gonzales, A.J. and Powell, M.V. "Dynamic RAM using SEM stroboscopic technique", International Electron Device Meeting, pp 119-122, 1975.

Gopinathan, K.G. and Gopinath, A. "A sampling scanning electron microscope", J. Phys. E: Sci. Instrum, Vol 11, pp 229-233, 1978.

Gregory, B.A. "An introduction to electrical instrumentation and measurement systems", M publisher,London, 1981.

Grivet, P. "Electron optics", Pergamon Press, 1962.

Hill, M.S. and Gopinath, A. "Scanning electron microscope at 9GHz", SEM, Vol II, pp 198-204, 1973.

Hill, M.S. "Stroboscopic SEM", PhD thesis, University College of North Wales, 1974.

Hieke, E. et al. "Electrostatic deflection system in the SEM for blanking at high repetition rates and low deflection voltages", SEM, Vol I, pp 219-224, 1977.

Hosokawa, T. et al. "Giga hertz stroboscopy with the scanning electron microscope", Rev. Sci. Instrum. 49(9), pp 1293-1299, 1978.

Hosokawa, T. et al. "Generation and measurement of subpicosecond electron beam pulses", Rev. Sci. Instrum. 49(5). pp 624-628, 1978.

Hnatek, E.R. "A user handbook of D/A and A/D converters", Wiley interscience,U.S.A,1976.

Hearle, J.W.S. et al, "The use of the scanning electron microscope, Pergamon Press, 1972.

Horowitz, P. and Hill, W. "The art of electronics", Cambridge University Press, U.S.A, 1980.

Hannah, J.M. "Development of a technique for voltage measurement on I.Cs", Ph.D thesis, University of Edinburgh, 1974.

Hawkes, P.W. "Electron optics and electron microscopy" Taylor and Francis ,London,pp 163-209,1972.

Hutter, R.G.E. "Beam and wave electronics in microwave tubes", Van Nostrand,NewYork,1960.

Harada, X. et al. "Reduction of contamination in analytical electron microscopy", SEM, Vol II, pp 103-110, 1978.

JEOL Ltd. " manual of STROBO SEM ", U.S.A, 1982.

Jones, A.V. and Unitt, B.M. "Computers in scanning microscope", SEM, Vol I, pp 113-124, 1980.

Jones, M.H. "A practical introduction to electronic circuits", Cambridge University Press, 1977.

Jensen, K. and Writh, N. "Pascal user manual and report", Springer-Verlag,Berlin, 1975.

James, A.D. "Principle of electronic instrumentation", Saunders, 1979.

Koffman, E.B. "Problem solved and structured programming in Pascal", Addison Wesley,Canada, 1981.

Khursheed,A "Computer Aided Design of electron detector for scanning electron microscope",Ph.D thesis,university of Edinburgh,1983.

Lin, L.H., and Beauchamp, H.L. "High speed beam deflection and blanking for electron lithography", J. Vac. Sci. Technol, Vol 10, No 6, pp 987-991, 1973.

Lorrain, P. and Corson, D. "Electromagnetic field and waves", Freeman , pp 644-656, 1962.

Lee, G.M. "A three beam oscillograph for recording at frequencies up to 10000 MC/S", Proceedings of the IRE, Vol 34, No 3, sec 2, pp 121-127, 1946.

Laurence, C.F. "A rotationally symmetric electron beam chopper for picosecond pulses", J. Physics. E. Vol 9, pp 455-463, 1976.

MacDonald, N.C. et al. "Time resolved scanning electron microscopy and its application to bulk effect oscillator", Journal of Applied Physics, Vol 40, No 11, pp 4516-4528, 1969.

Masuda, M. et al. "Analysis of the high field domain dynamic in a planar gunn diode using a stroboscopic SEM", J. Appl. Phys., 50(1), pp 530-536, 1979.

Malvino, A.P. and Leach, D.P. "Digital principle and applications". TATA McGraw-Hill Publishing Ltd.,NewYork, 1975.

Menzel, E. and Kubalek, E. "Electron beam test system for VLSI circuit inspection ", SEM, Vol I, pp 297-304. 1979.

Menzel, E. and Kubalek, E. "Electron beam chopping system in the SEM", SEM, Vol I, pp 305-318, 1979.

Menzel, E. and Kubalek, E. "Electron beam test techniques for integrated circuit", SEM, Vol I, pp 305-322, 1981.

Miller, D.E. "SEM vacuum techniques and contamination management", SEM, Vol I, pp 513-528, 1978.

Obyden, S.K. et al. "New imaging technique and stroboscopy in colour scanning electron microscope", SEM, Vol IV, pp 41-48, 1980.

Ohiwa, H. "The design of deflection coils", J. Phys. D. Applied Phys, Vol 10, pp 1437-1449, 1977.

Oatley, C.W. "The scanning electron microscope", Part 1, The Instrument, Cambridge University Press, 1972.

Plows, G.S. and Nixon, W.C. "Stroboscopic scanning electron microscopy", J. Scientific Ins. (Journal of PhysicsE), Vol 1, Series 2, pp 595-600, 1968.

Plows, G.S. and Nixon, W.C. "Operational testing of LSI arrays by stroboscopic scanning electron microscopy", Microelectronics and Reliability, Vol 10, pp 317-323, 1971.

Plows, G.W. and Lintech Instruments ltd. "Lintech sampling e-beam systems in circuit testing of integrated circuit", Manual, 1981.

Pierce,J.R "Theory and design of electron beam", Van-Nostrand,NewYork, 1954.

Parry, M. and Domina, E.S. "Field theory for engineers", The Van-

Nostrand Series,NewYork,pp361-373,1961.

Peatman, J.B. "Microcomputer-based design", McGraw-Hill,NewYork, 1977.

Paszkowski, B. "Electron optics", Iliffe ,London, pp 264-272, 1968.

Robinson, G.Y. et al. "Probing of Gunn effect domains with scanning electron microscope", Applied Physics Letters, Vol 13, No 12, pp 407-408, 1968.

Robinson, G.Y. "Stroboscopic scanning electron microscopy at GHz frequencies", The Review of Scientific Instruments, Vol 42, No 2, pp 251-255, 1971.

Ranasinghe, D. and Proctor, G. "Failure analysis on custom LSI circuits of modified SEM to display voltage waveform", to be published.

Rau, E.I. et al. "Colour encoding of video signals in SEM", Scanning, Vol 3, 3, pp 242-248, 1980.

Ramo, W. "Fields and waves in modern Radio", Wiley,NewYork, pp 171-176, 1956.

Smith, K.C.A. " On - line digital Computer techniques in Electron Micrscope", Inst. Phys. Conf. Ser. No 61, EMAG, Cambridge, 1981.

Szentesi, O.I. "Stroboscopic electron mirror microscopy at frequencies up to 100 MHz", Journal of Physics E. Scientific Instrument, Vol 5, pp 563-567, 1972.

Stuart,R.D "Electromagnetic field theory", Addison Wesley,NewYork, pp 187-189, 1965.

Thomas, P.R. et al. "The observation of fast voltage waveforms in the SEM using sampling techniques", SEM, Vol IV, pp 609-614, 1976.

Thomas, P.R. et al. "Some aspects of quantitative voltage measurements in the SEM", Microcircuit Engineering, Cambridge University Press, pp 479-499, 1980.

Ura, K. et al. "Stroboscopic scanning electron microscope to observe two dimensional and dynamic potential distribution of semiconductor dev-ices", Int. Electron Device meeting,Osaka,Japan, pp 502-505, 1977.

Ura, K. et al. "Electron optical design of pico-second pulse stroboscop-ic SEM", SEM, Vol I, pp 747-752, 1978.

Ura, K. et al. "Stroboscopic observation of passivated microprocessor chips by scanning electron microscopy", to be published.

Ura, K. and Fujioka, H. "Picosecond pulse stroboscopic SEM", Oyobutsure (Japan), Vol 48, Part 9, pp 890-894, 1979.

Wolfgang, E. et al. "Stroboscopic voltage contrast of dynamic 4096 bit MOSRAMs: Failure analysis and function testing", SEM, Vol IV, pp 625-632, 1976.

Wolfgang, E. et al. "Electron-beam testing of VLSI circuits", IEEE, J. of Solid State Circuits, Vol SC14, No 2, pp 471-481, 1979.

Wolfgang, E. " Electron Beam Techniques for microcircuits Inspection",
Microcircuits Engineering, pp 409 - 430, Cambridge University Press,
1980.

Wilson, I.R. and Addyman, A.M. "A practical introduction to Pascal", M.
Publisher, London, 1978.

Weinfield, M. and Bouchoule, A. "Electron gun for generation of sub-
nanosecond electron packets at very high repetition rate", Rev. Sci.
Inst, Vol 47, No 4, pp 412-417, 1976.

Wells, O.S. and Bremer, C.G. "Voltage measurement in the SEM", J. of
Scientific Instrument (J. of Physics E), Series 2, Vol 1, 1968.

APPENDIX I

Flow diagrams and written programs:

1.   Chopping Control

2.   Colour stroboscopy

3.   Delay Control
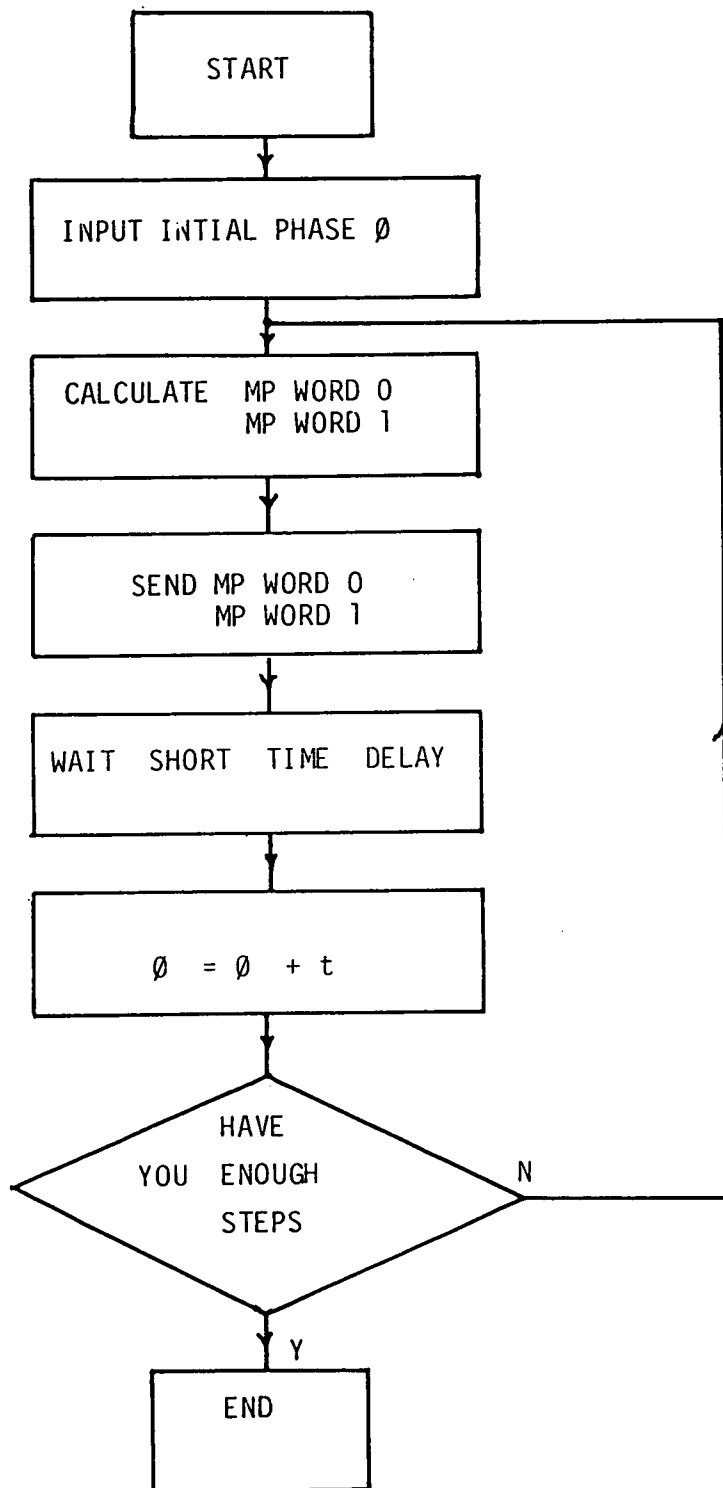
Figure   1 : Shows a Flowdiagram of Sampling
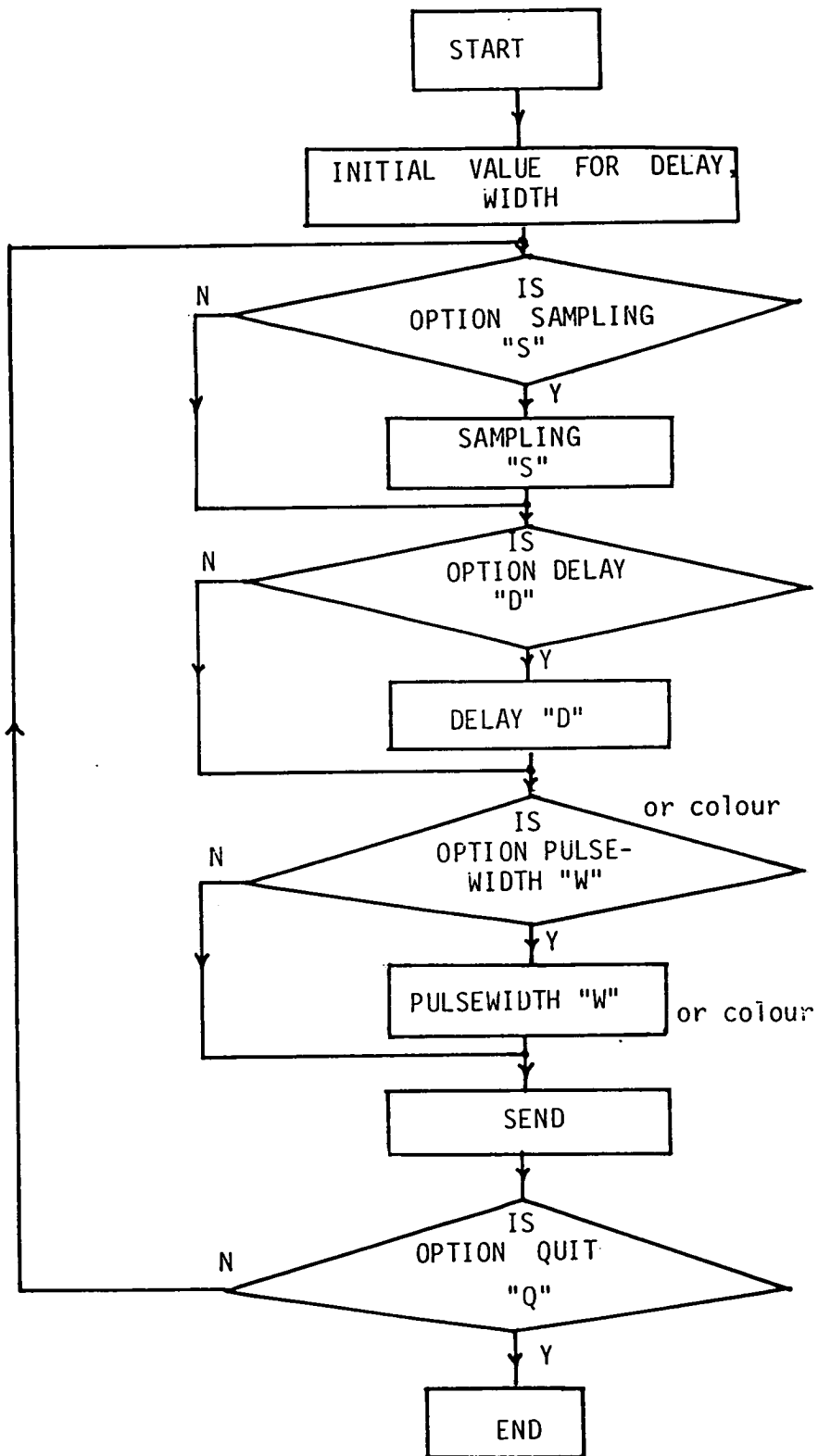
Figure 2 : Shows Computer Program Flow Diagram "IF STATEMENT" for stroboscopy and sampling modes.
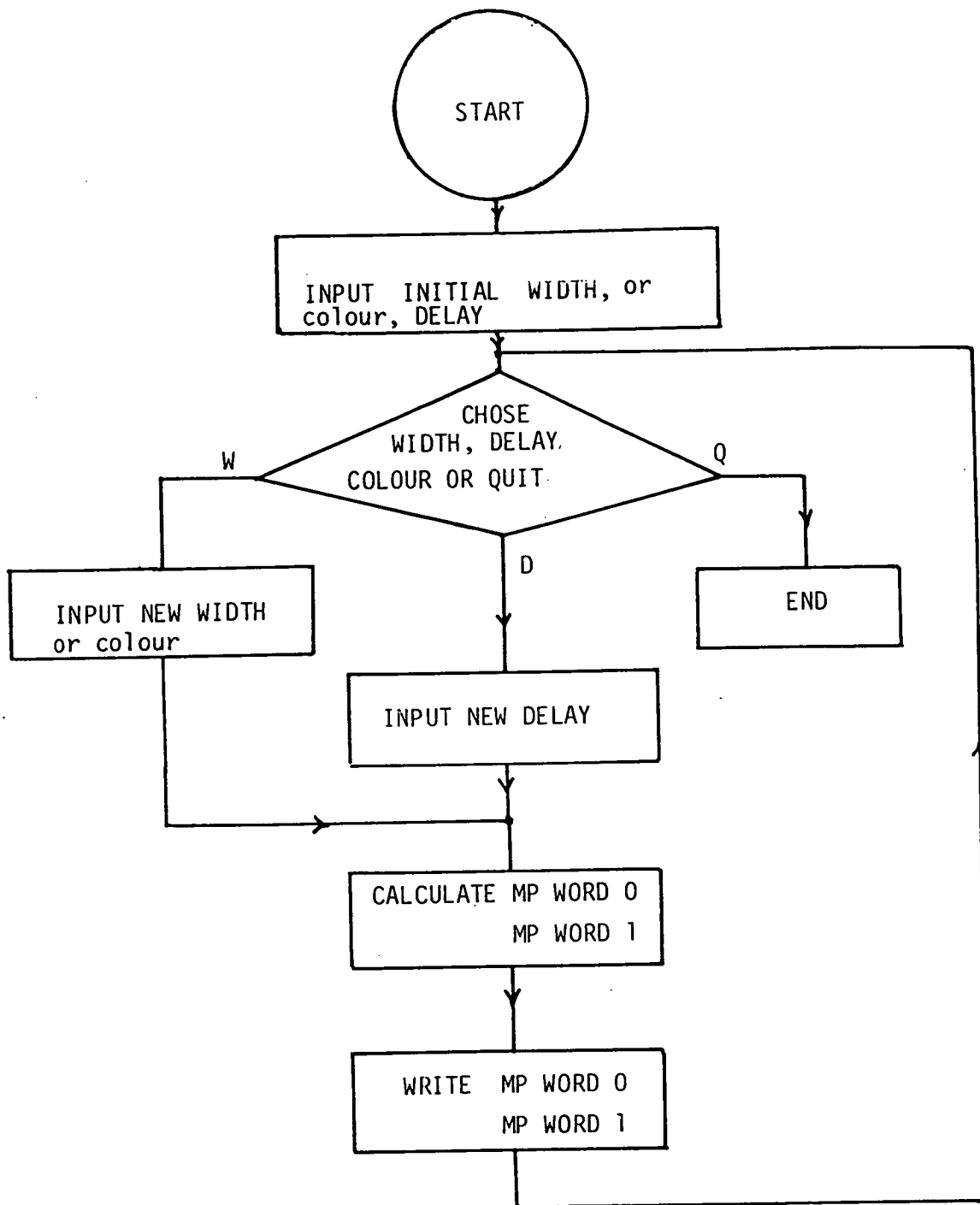
Figure 3: Shows Sampling Flowdiagram "CASE STATEMENT"
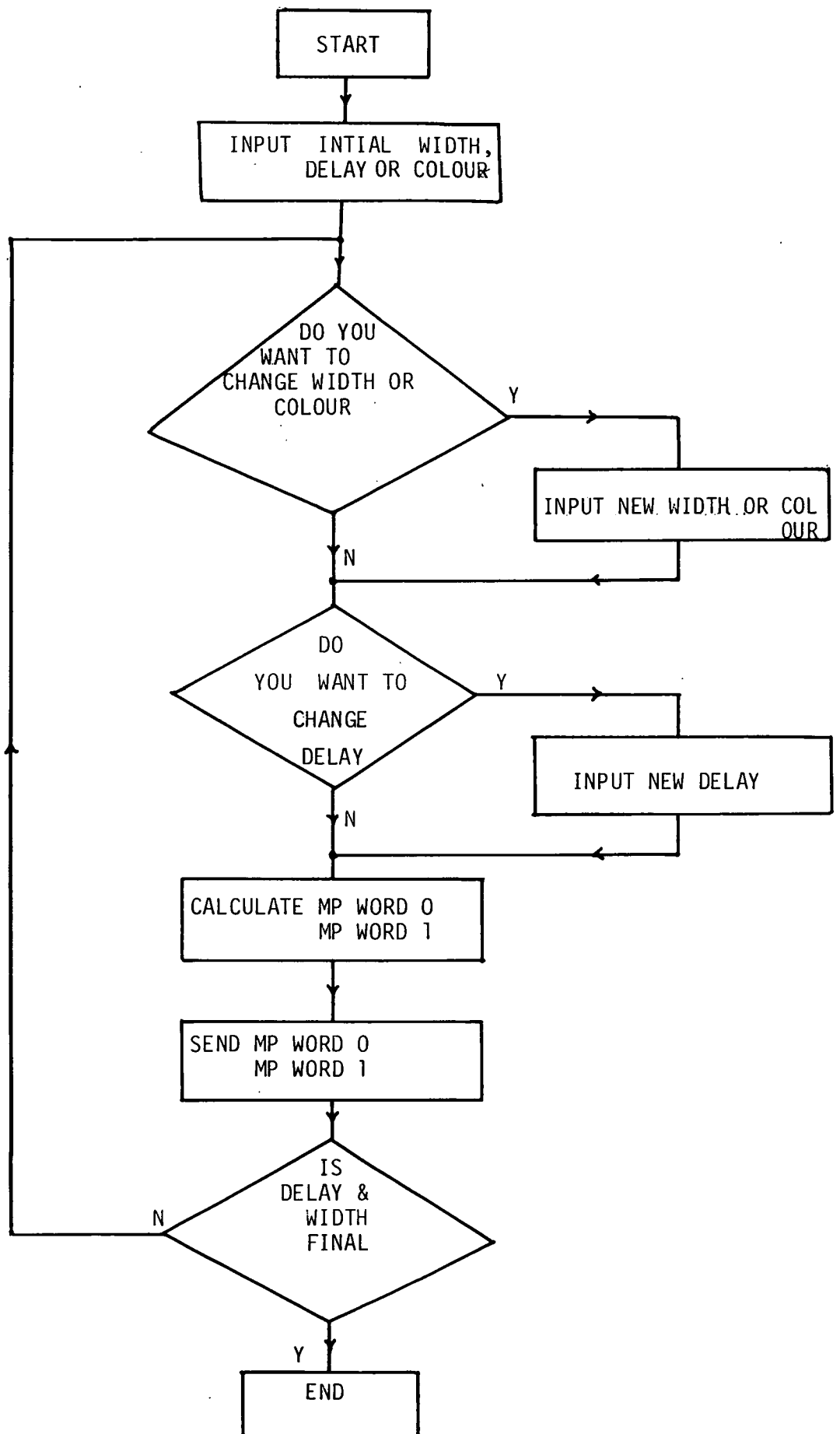
Figure 4: Shows Flow Diagram of Stroboscopy "IF STATEMENT"

Figure 5 : Shows Computer Program - flow diagram
"CASE STATEMENT" for stroboscopy,sampling modes
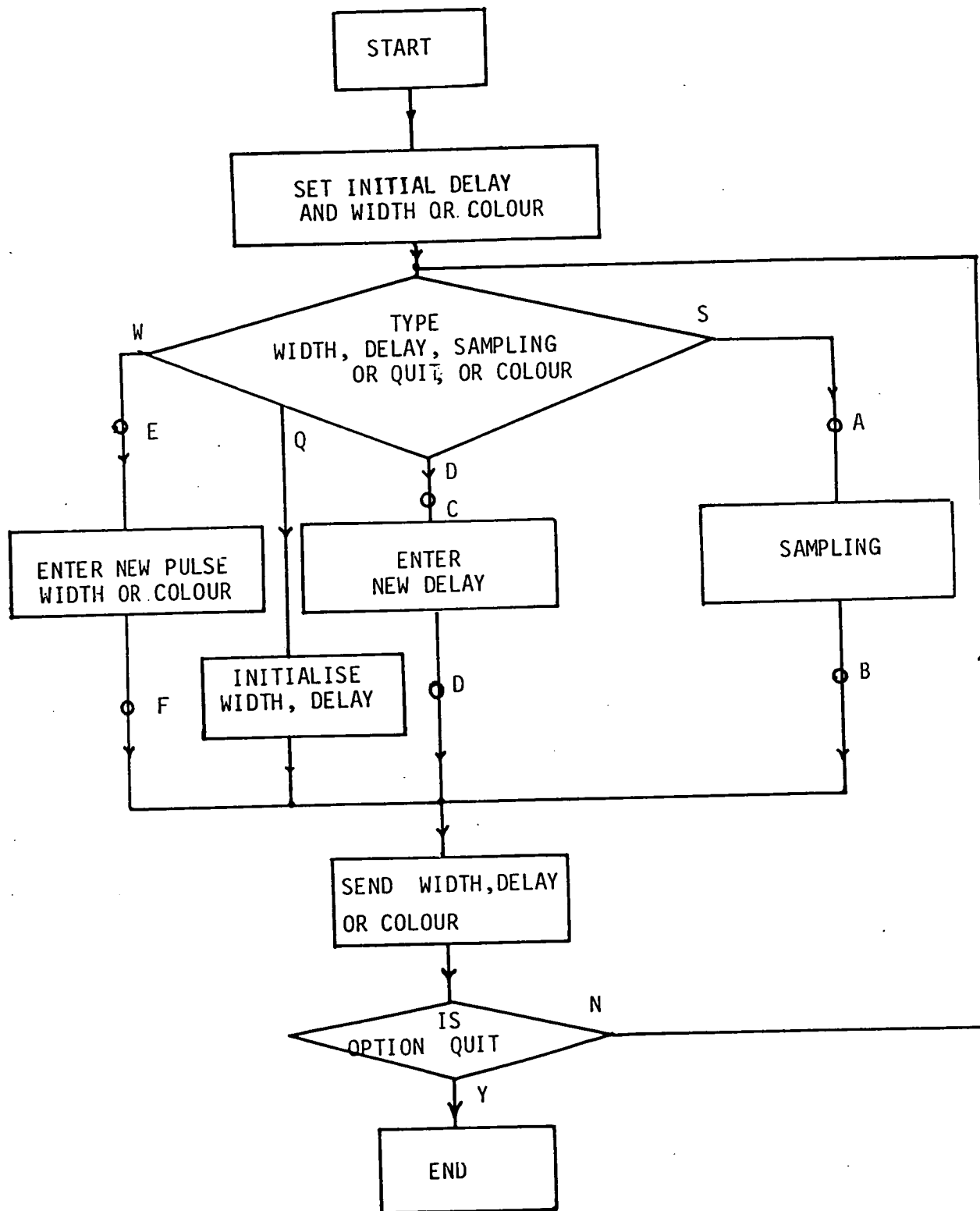
Figure 5: Shows Details of Case Statement Flow diagrams

C

INPUT NEW DELAY

is
delay D :
j <2.097 < E

N

Y

D

E

ENTER NEW PULSE-
WIDTH p.w or colour

is
p.w, or colour
in range 0...7?
...

N

Y

F

A

Enter D, delay
steps, delay
count, max cycle

REPEAT

SEND

WAIT SHORT
TIME

$\emptyset = \emptyset + t$

Have
you done
enough steps

N

Y

Have
you done en-
ough

N

Y cycle

START

CALCULATE MPWORD 0

CALCULATE MPWORD 1

CALCULATE OCTAL
CHARACTER

OUTPUT

END

SEND FLOW CHART
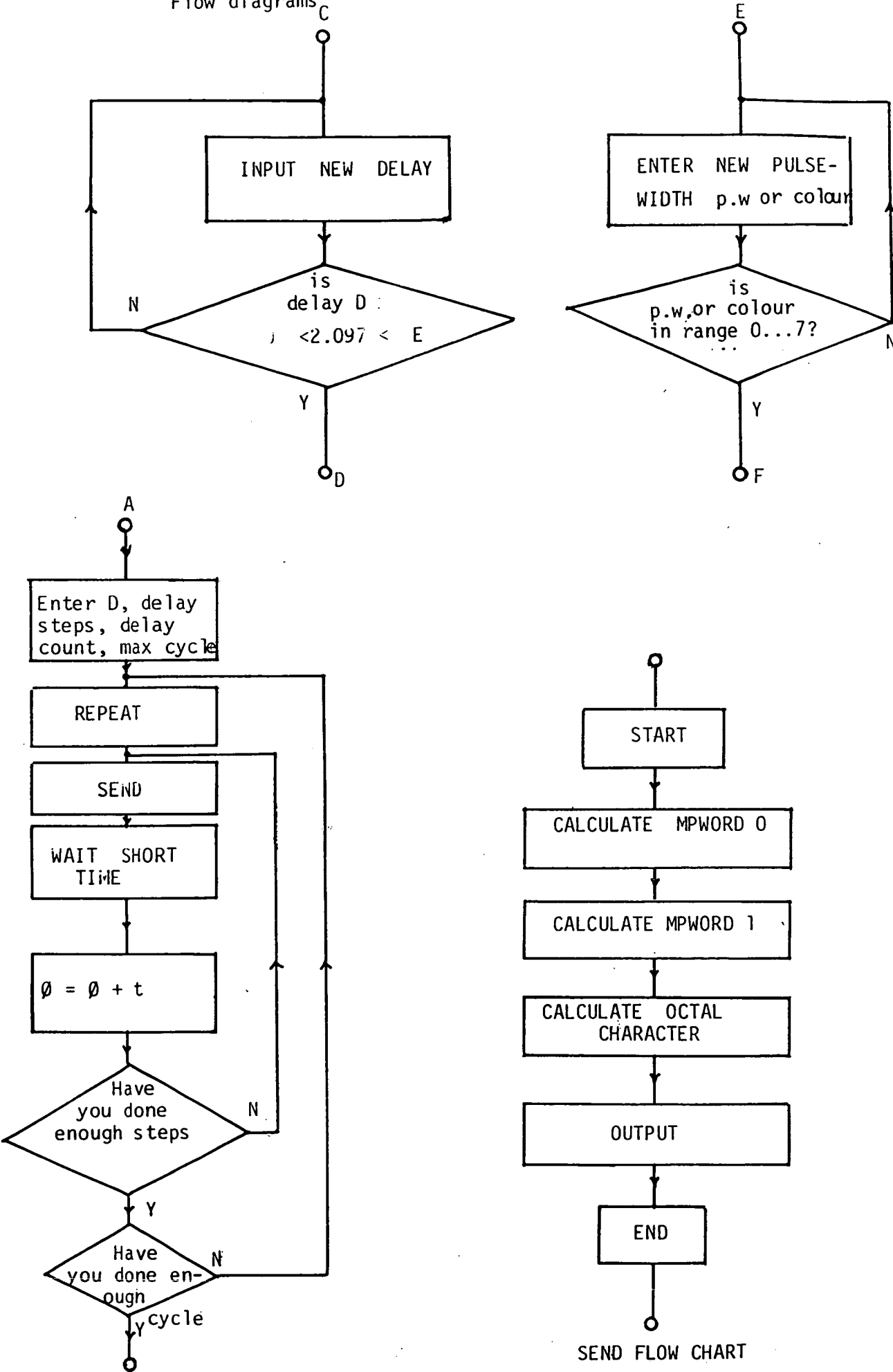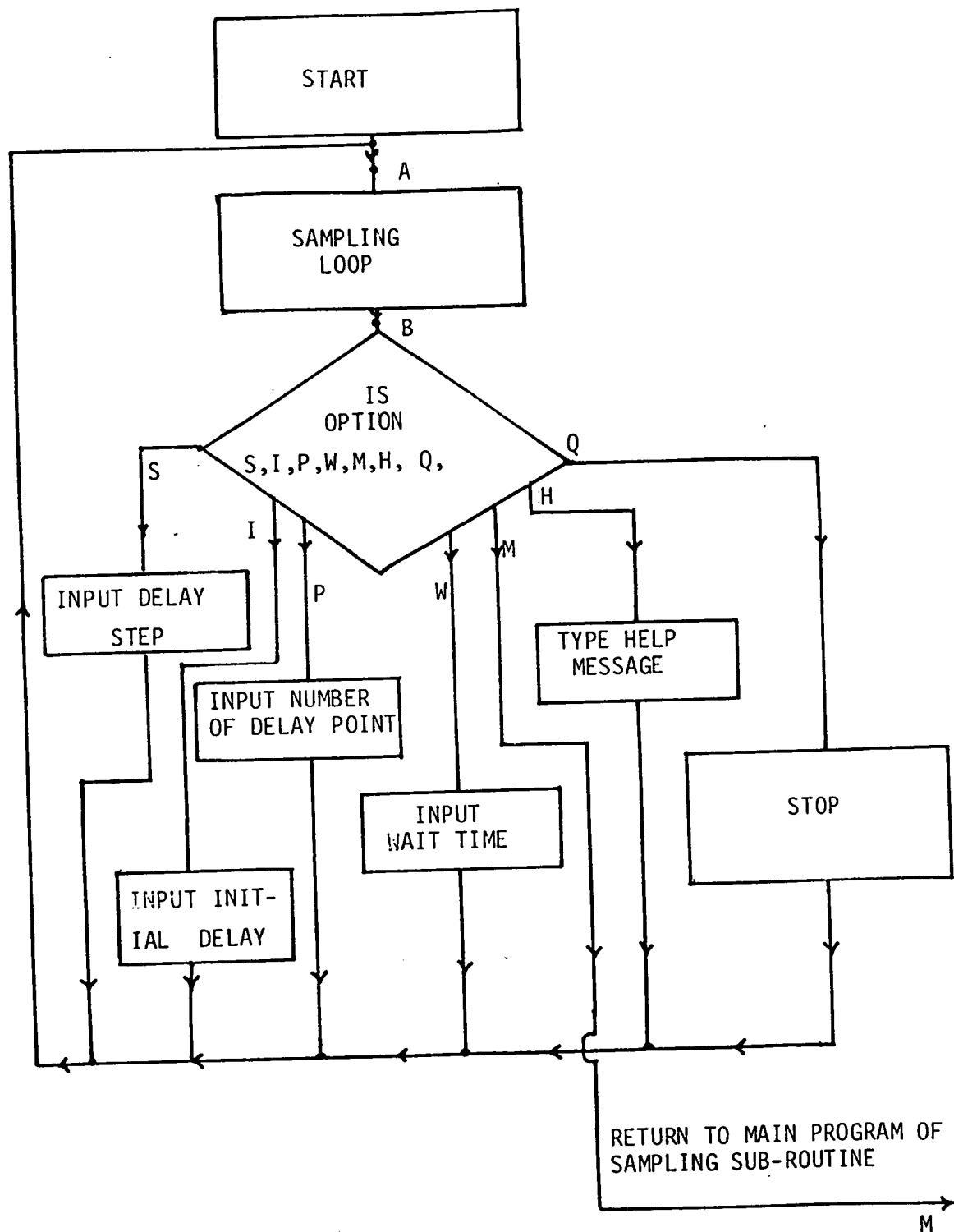
Figure   7   : Shows flow diagram for "delay control" program
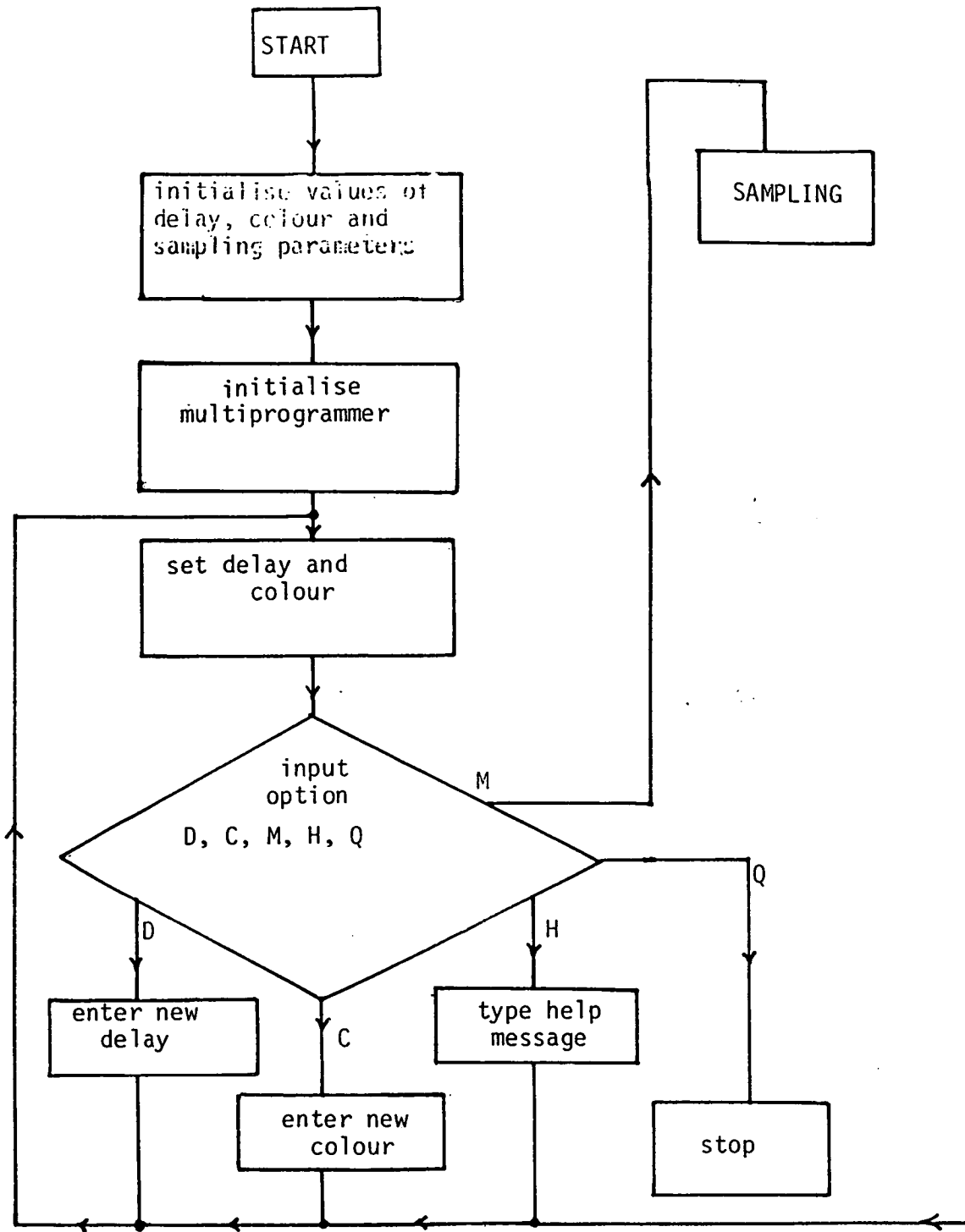
Figure 8 : Shows flow diagram for "delay control" program
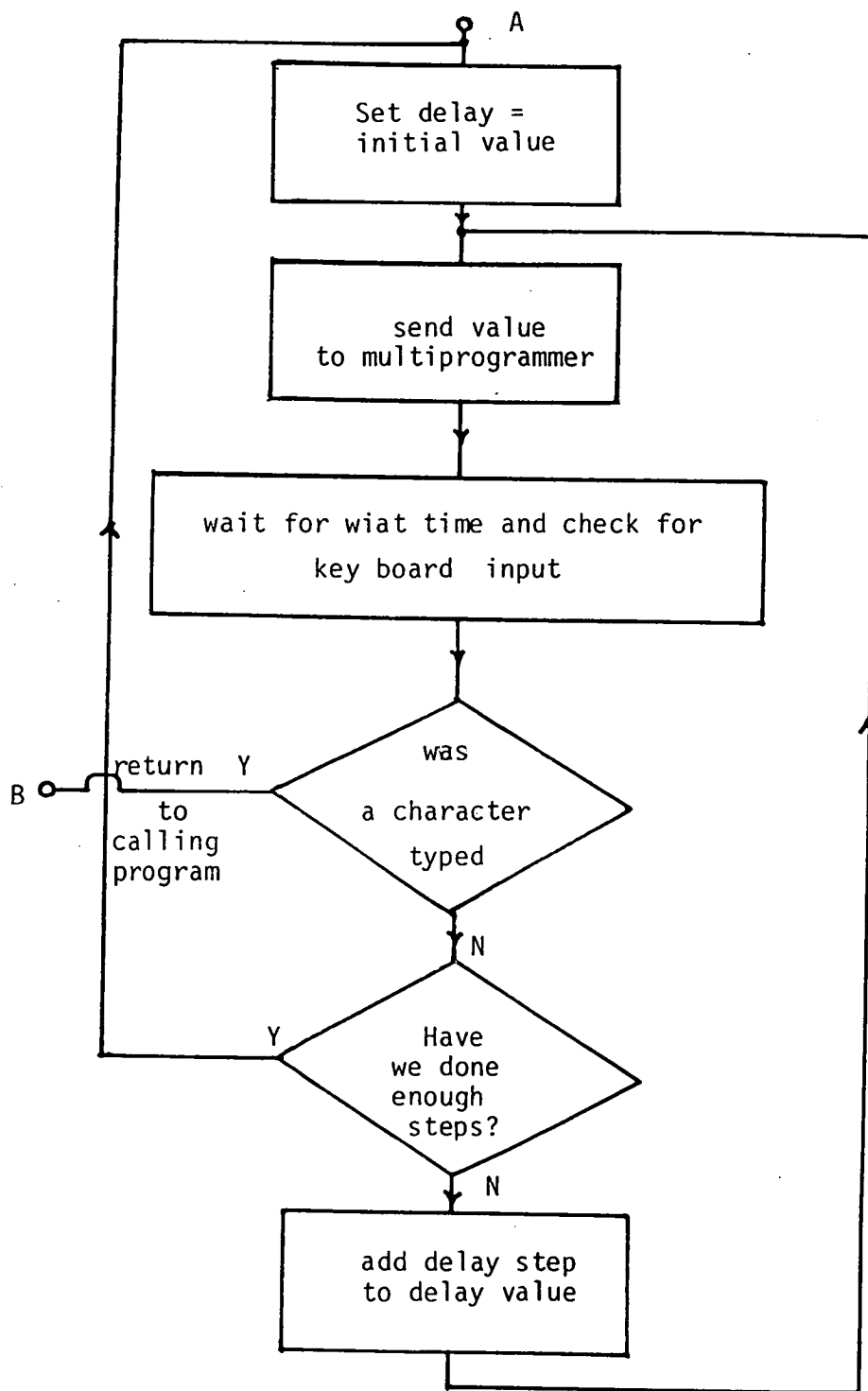
Figure .9 . Shows flow diagram of sampling loop
subroutine for "delay control" program.

```
Program choppingcontrol;

const k=0.76923;
   MP = 223;
   waitetime = 10;
var delay : real;
   option:char;
   rsb:1..8;
   x : packed array[1..12] of char;

procedure send(del: real; colour: integer );
var
   i,mpword1,mpword0 : integer;
begin
    x[8] := chr(colour + 48);
    del := del * k;
    mpword1 := trunc(del / 4096.0);
    mpword0 := round(del  - (mpword1 * 4096.0));
    for i := 5 downto 2 do begin
       x[i] := chr( mpword0 mod 8 + 48 );
       mpword0:=mpword0 div 8;
    end;
    for i:=11 downto 9 do begin
       x[i] := chr( mpword1 mod 8 + 48 );
       mpword1:=mpword1 div 8;
    end;
    unitwrite(MP, x, 12);
end;

procedure initialise;
begin
   delay:=0;rsb:=0
end;

Procedure sampling;
var
   step,stepcount,
   i, index : integer;
   statrec : array[1..30] of integer;
   intialphase, samdel : real;
begin
    write('Please enter intial delay ');
    readln(intialphase);
    write('Please enter delay step ');
    readln(step);
    write('Please enter number of steps ');
    readln(stepcount);
    write('Type any key to continue ');
    repeat
      samdel:=intialphase;
      for index:=1 to stepcount do begin
        send(samdel,rsb);
        for i:=1 to waitetime do begin end;
        samdel:=samdel+step
      end;
      unitstatus(1, statrec, 1)
    until statrec[1] <> 0;
    read(option); writeln
 end;
```

```
procedure delayenter;
begin
  repeat
    write('please enter the desired delay ');
    readln(delay);
  until((delay >= 0) and (delay * k < 2.097E+6))
end;

procedure rsbenter;
begin
  repeat
    write('please enter the desired rsb(0..7) ');
    readln(rsb);
  until(rsb >= 0) and (rsb <= 7)
end;

begin
  unitclear(231);
  x[1] := '0'; x[2] := '0'; x[3] := '1';
  x[4] := '4'; x[5] := '0'; x[6] := 'T';
  unitwrite(MP, x, 6);
  x[1] := '@'; x[7] := 'B'; x[12] := 'T';
  initialise;
  repeat
    write('please enter option, delay, colour, sampling, or quit ');
    read(option);
    writeln;
    case option of
      's': sampling;
      'd': delayenter;
      'c': rsbenter;
      'a': initialise;
    end;
    send(delay,rsb)
  until option='q'
end.
```

```pascal
program colourstroboscope;
   const HP = 223;
      knum = 10;
      kdenom = 13;
      max = 2097152;
   var
      mpword,i,index:integer;
      hibits, delay,delaystep,initialphase : integer[7];
      stat : array[1..30] of integer;
      x : packed array[1..12] of char;
      option : char;

begin
   x[1] := '0'; x[2] := '0'; x[3] := '1';
   x[4] := '4'; x[5] := '0'; x[6] := 'T';
   unitwrite(HP, x, 6);
   x[1] := '8'; x[7] := 'B'; x[12] := 'T';
   repeat
     repeat
        write('Please enter initial delay ');
        readln(initialphase);
        write('Please enter delay step ');
        readln(delaystep);
        initialphase:= (initialphase * knum) div kdenom;
        delaystep := (delaystep * knum) div kdenom;
     until initialphase + (7 * delaystep) < max;
     write('Type Q to quit, any other key to repeat ');
     repeat
        delay := initialphase;
        for index:=0 to 7 do begin
           hibits := delay div 4096;
           mpword := trunc(hibits);
           x[8] := chr(index + 48);
           for i:= 11 downto 9 do begin
               x[i]:= chr(mpword mod 8 + 48);
               mpword:=mpword div 8;
           end;
           hibits := delay - (hibits  * 4096);
           mpword := trunc(hibits);
           for i:=5 downto 2 do begin
               x[i]:= chr(mpword mod 8 + 48);
               mpword := mpword div 8;
           end;
           unitwrite(HP, x, 12);
           delay := delay + delaystep;
        end;
        unitstatus(1, stat, 1)
     until stat[1] <> 0;
     read(option);write(chr(12))
   until option = 'q'
end.
```

```
Prosram delay_control;

{    Prosram to control a delay unit, via a Hewlett-Packard Multiprosrammer
{    for samplins and stroboscopic use of the S.E.M.



uses screenops;
const
    MP = 223;
type
    delay_wrd = record hi, lo : inteser end;
var
    delay          : record case boolean of
                        false : (n  : delay_wrd);
                        true  : (oct : record
                                         hi, lo : packed array[0..3] of 0..7
                                       end)
                     end;
    RGB            : '0'..'7';
    MP_strins      : packed array[0..11] of char;

    bes_del,
    step           : delay_wrd;
    stepcount,
    waittime       : inteser;

procedure help;
begin
    SC_clr_screen;
    writeln; writeln(
'   This prosram operates in two modes, stroboscopic and samplins. The mode
    writeln(
'can be chansed by typins "M".');
    writeln(
'   In stroboscopic mode the static value of the delay and the colour can l
    writeln(
'chansed.');
    writeln(
'   In samplins mode the followins parameters may be varied:');
    writeln(
'       Initial delay   : The value of delay at the first phase point');
    writeln(
'       Step            : The interval between phase points.');
    writeln(
'       The number of phase points.');
    writeln(
'       Wait time       : The time for which the delay is held at each poi
    writeln; if space_wait(false) then besin end
end;
```

```
procedure MP_init;
const hi_slot = '@';
      lo_slot = 'B';

    procedure set_MP_string(str : string);
    var i : integer;
    begin
        for i := 1 to length(str) do MP_string[i - 1] := str[i]
    end;

begin
    unitclear(231);
    set_MP_string('00140T');
    unitwrite(MP, MP_string, 6);
    set_MP_string(concat(hi_slot, '0000T', lo_slot, '0000T'));
end;

procedure Set_init_values;

begin
    RGB := '0';
    delay.n.hi := 0;      delay.n.lo := 0;
    beg_del.hi := 0;      beg_del.lo := 0;
    step.hi    := 0;      step.lo    := 1;
    stepcount  := 256;    waittime   := 0;
end;

procedure write_long(del : delay_wrd);
var S  : string;
    L  : integer[7];
begin
    L := del.hi mod 512; L := L * 4096 + del.lo;
    str(L, S);
    write(S)
end;

procedure read_long(var del : delay_wrd);
var S : string;
    L : integer[7];
begin
    readln(L);
    del.hi := trunc(L div 4096);
    del.lo := trunc(L - (L div 4096) * 4096)
end;

procedure send_delay;
begin
    with delay.oct do begin
        MP_string[1]  := rgb;
        MP_string[2]  := chr(hi[2] + 48);
        MP_string[3]  := chr(hi[1] + 48);
        MP_string[4]  := chr(hi[0] + 48);
        MP_string[7]  := chr(lo[3] + 48);
        MP_string[8]  := chr(lo[2] + 48);
        MP_string[9]  := chr(lo[1] + 48);
        MP_string[10] := chr(lo[0] + 48)
    end;
    unitwrite(MP, MP_string, 12)
```

[F]

```
Procedure sampling;
var del_save      : delay_wrd;
    opt           : char;

   Procedure sample_loop;
   var  step_no,
        timer            : integer;
        statrec          : array[0..29] of integer;
   begin
      repeat
         delay.n := beg_del;
         with delay.n do begin
            for step_no := 1 to stepcount do begin
               send_delay;
               lo := lo + step.lo;
               if lo > 4095 then begin
                   lo := lo - 4096;
                   hi := succ(hi)
               end;
               hi := hi + step.hi;
               for timer := 0 to waittime do begin
                   unitstatus(1, statrec, 1);
                   if statrec[0] > 0 then exit(sample_loop)
               end
            end
         end
      until false
   end;
```

```pascal
begin
    del_save := delay.n;
    repeat
        sc_clr_screen;
        gotoxy(0,2); write('           Initial delay = '); write_long(beg_del);
        gotoxy(0,4); write('              Step size = '); write_long(step);
        gotoxy(0,6); write('   No of sample points = ', stepcount);
        gotoxy(0,8); write('              Wait time = ', waittime);
        SC_home;
        write(
'SAMPLING MODE...   I(nitial, S(tep, P(oints, W(ait, M(ode, H(elp, Q(uit ? ');
        sample_loop;
        read(keyboard, opt);
        case opt of
            'i', 'I' : begin
                        SC_erase_to_eol(24, 2);
                        read_long(beg_del)
                    end;
            's', 'S' : begin
                        SC_erase_to_eol(24, 4);
                        read_long(step)
                    end;
            'p', 'P' : begin
                        SC_erase_to_eol(24, 6);
                        readln(stepcount)
                    end;
            'w', 'W' : begin
                        SC_erase_to_eol(24, 8);
                        readln(waittime)
                    end;
            'm', 'M' : begin
                        delay.n := del_save;
                        exit(sampling)
                    end;
            'h', 'H' : help;
            'q', 'Q' : exit(program)
        end
    until false
end;
```

```
begin
    set_init_values;
    MP_init;
    repeat
        sc_clr_screen;
        gotoxy(4,2); write('Delay  = '); write_lons(delay.n);
        gotoxy(4,4); write('Colour = ', RGB);
        send_delay;
        case
            SC_prompt(
                'STROBOSCOPE MODE...   D(elay, C(olour, M(ode, H(elp, Q(uit ? ',
                -1, 0, 0, 0, ['D','C','M','H','Q'], false, '*' )
        of
            'D' : begin
                      SC_erase_to_eol(13, 2);
                      read_lons(delay.n)
                  end;
            'C' : RGB := SC_prompt('Enter new colour (0..7) ',
                                    13, 4, 0, 0, ['0'..'7'], false, '*' );
            'M' : sampling;
            'H' : help;
            'Q' : exit(program)
        end
    until false
end.
```

APPENDIX II

FIELD DISTRIBUTION AND ELECTRIC

FIELD OF CHOPPING PLATES

(A)   The electric field strength for bipolar   coordinates

Curved Plates

$$E_n = \frac{-(V_1 - V_2)}{a(n_1 - n_2)} \quad (\cosh n - \cos\theta) \tag{1}$$

where $n_1 - n_2 = \operatorname{Sinh}^{-1}(a/r_1) + \operatorname{Sinh}^{-1}(a/r_2)$ then

$$E_n = \frac{-(V_1 - V_2)(1 - \cos\theta)}{a(\operatorname{Sinh}^{-1}(a/r_1) + \operatorname{Sinh}^{-1}(a/r_2)} \tag{2}$$

(from Moon and Spencer 1961)

For present case $r_1 = r_2 =$ cylinder radius

   $a =$ distance from y axis to circle centre

(see Figure 3)

$$E_n = \frac{-(V_1 - V_2)(1 - \cos\theta)}{2a(\operatorname{Sinh}^{-1} a/r)} \tag{3}$$

$V_1 - V_2 =$ potential difference

for $n = 0, x = 0$
$\theta = \mp\pi$ $\} \quad 0 < \theta < 2\pi$

$y = \dfrac{a \sin\theta}{1 - \cos\theta}$

(See Figure 2B)

Thus the capacitance for $n_1 > n_2$ is

$$C = \frac{|Q|}{(V_1 - V_2)} = \frac{2\pi\varepsilon l}{n_1 - n_2}$$

Thus
$$C = \frac{2\pi\varepsilon l}{\text{Sinh}^{-1}(a/r_1) + \text{Sinh}^{-1}(a/r_2)}$$

$$\boxed{C = \frac{\pi\varepsilon l}{\text{Sinh}^{-1}(a/r)}} \qquad (4)$$

where l = length

(B)   The electric field strength for flat plates

The strength of the field depends on the difference of potential between the plates.

Considering now the t plane, if the potential of plate A is called zero and the potential of plate B is called V (see Figure 4A), the potential at any point is given by

$$\psi = \frac{V}{2\pi} q \tag{1}$$

Since 2π is the distance between the plates in the t plane

$$\frac{\partial \psi}{\partial q} = \frac{\partial \phi}{\partial p} \tag{2}$$

$$\phi + j\psi = \frac{V}{2\pi} (p + jq) \tag{3}$$

The density of charge:

$$\sigma = -\frac{\partial \psi}{\partial n} \varepsilon_o \tag{4}$$

(from Gibbs 1956).

σ = the normal component of the electric field and this proportional to the rate of change of ψ in direction perpendicular to the plate with negative sign.

To translate this into the Z plane it is necessary to multiply by

$$\frac{\partial t}{\partial z}$$

$$\sigma = -\frac{\partial \psi}{\partial n} \left| \frac{\partial t}{\partial z} \right| \varepsilon_0$$

but

$$\frac{\partial \psi}{\partial n} = \frac{\partial \Psi}{\partial q} = \frac{V}{2\pi} \tag{5}$$

Furthermore since

$$z = \frac{h}{2\pi} (e^t - t) \tag{6}$$

$$\frac{dz}{dt} = |e^p (\cos q + j \sin q) - 1| \tag{7}$$

$$\frac{dz}{dt} = \frac{h}{2\pi} |e^p - 1| \tag{8}$$

let $q = \pi$ in equation (7) because on the surface q is zero.

Hence $\qquad \sigma = \frac{V}{2\pi} \cdot \frac{2\pi}{h} \frac{1}{e^p - 1} \varepsilon_0$

$$\sigma = \frac{V \cdot \varepsilon_0}{2\pi} \left(\frac{dt}{dz}\right)$$

Hence the electric field

$$\boxed{E = \frac{V}{h(e^p + 1)}} \tag{9}$$

where p   = flux

    h = plates gap

    E   = electric field strength

    V   = potential difference

    Therefore the equation for negative values of p applies to
the inside of the plates. This type of plate shows fringes effect
at plates edges. (For more detail see Gibbs 1956).

CONCLUSION :

By estimating the electric field strength for both recently used plates
of flat and curved shape, using equations(2) page (A) and (9) page (D),
an approximate field strength is found in the center of the plates
gap(see figure 5) with the same conditions.To confirm this result and to
have further informations, to study
 the electron beam deflection with respect to the electric field
strength ,potential difference of the plates,deflection angles,plates
length, electron beam accelerating energy,transit time, shapes of the
plates,plates gap, and other factors, also to model a pattern for dif-
ferent shapes of the plates It is recommended to use the computer simu-
lation of Khursheed (1983) computer programme for this purposes.

N.B Most of mentioned equations are stated here for further work
     and as advantage for the reader as short cut .

APPENDIX II REFERENCES :

Gibbs, W.J. " Conformal Transformations in Electrical Engineering ",
Chapman and Hall Ltd. London, 1956.

Pipes, L.A. " Applied Mathematic For Engineers and Physicists ", 2nd ed-
ition, pp 561 - 582, NewYork, 1958.

Moon and Spencer . " Field Theory For Engineers ", Princeton, 1961.

(A)

$u = $ const.

$v = $ const.

$v = 0$

D

C

h

A

$v = \pi$

B

(B)

$u = $ const.

$u = $ const.

y

x

(C)

y

$-u$

$+u$

R

x

S

(D)

y

r_2

z

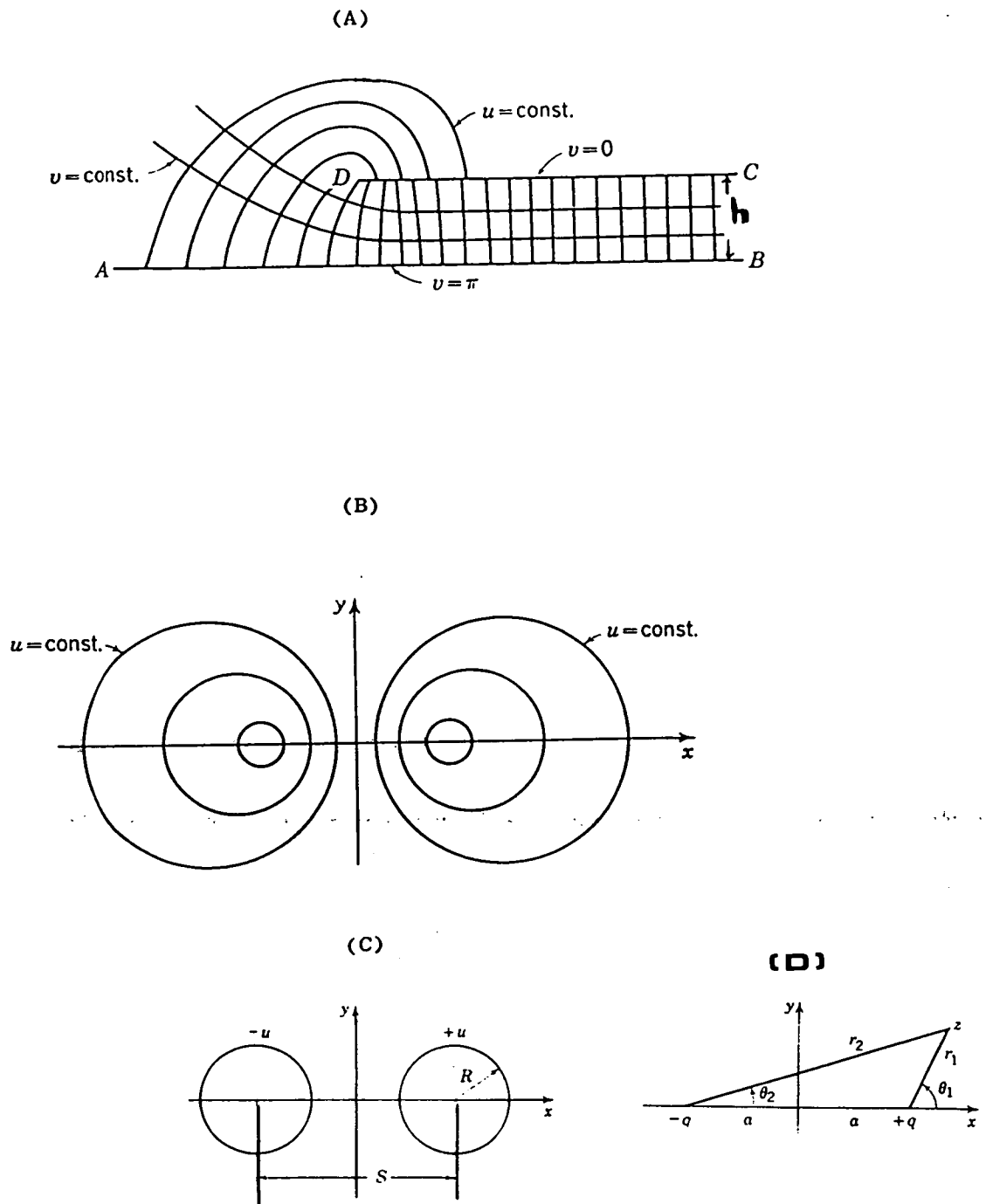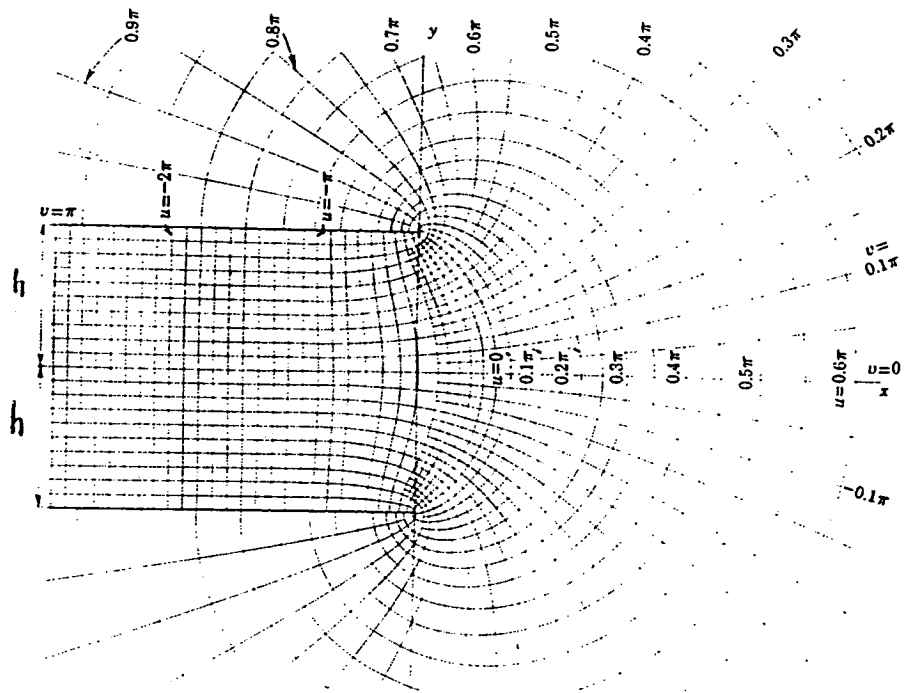r_1

θ_2
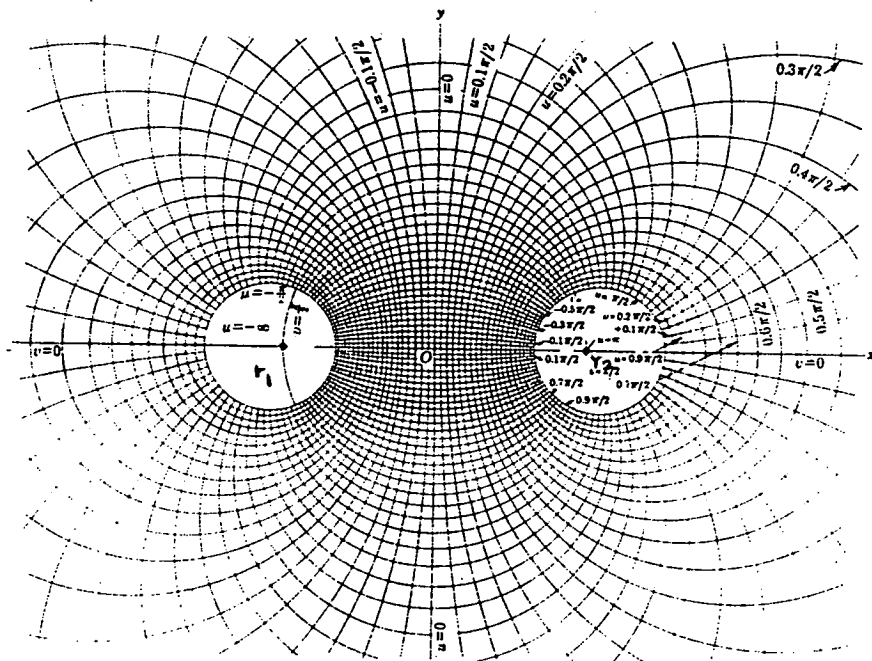
θ_1

$-q$

a

a

$+q$

x

Figure 1 : Shows two dimensional potential distribution of parallel flat plates capacitor of (A), (B), (C) are for curved plates (from Pipes 1958).

(A) Coordinate map obtained by transformation of a square grid in the W plane for flat plates.

(B) Bipolar coordinates obtained by transformation for cylindrical coordinate (curved plates).

Figure 2: Shows potential distribution of (A) flat plates and (B) cylindrical coordinated plates (from Moon and Spencer 1961).
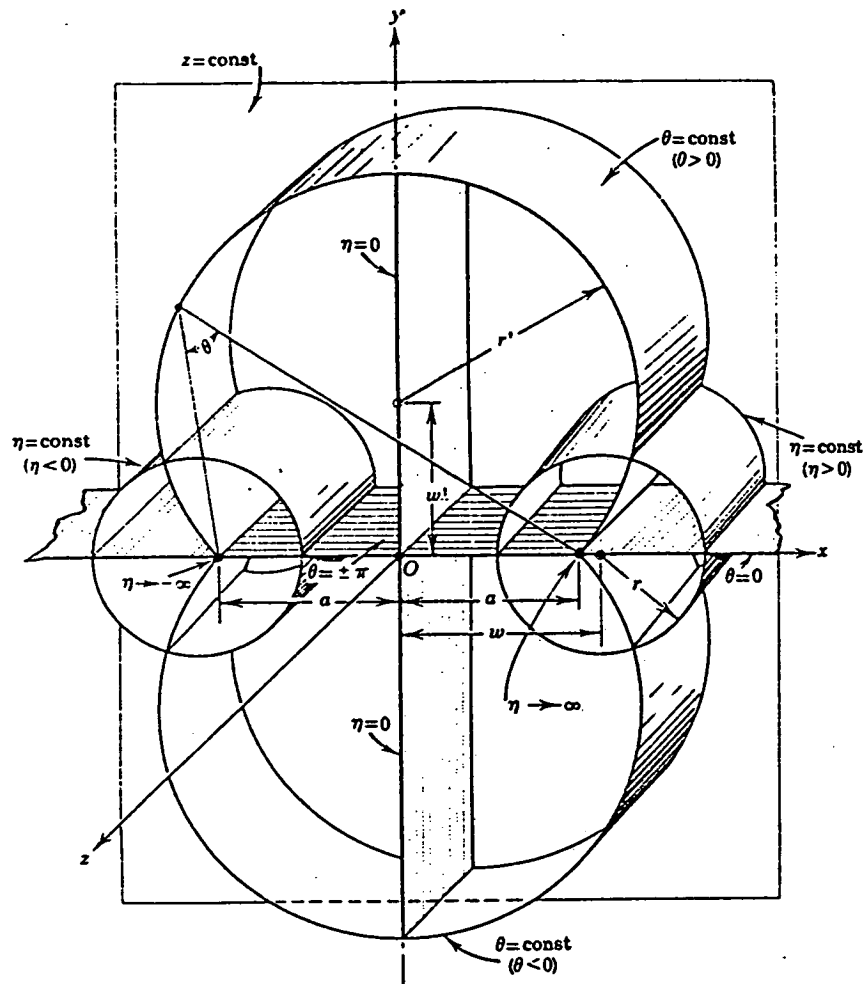
Figure 3: Shows bicylindrical coordinates. The surfaces n = constant
are circular cylinders with axes in the xz plane, surfaces θ
= constant are portions of circular cylinders with axes in
the yz plane, surfaces z = constant are parallel planes.
(from Moon and Spencer 1961).

(A)

q

t - plane

B
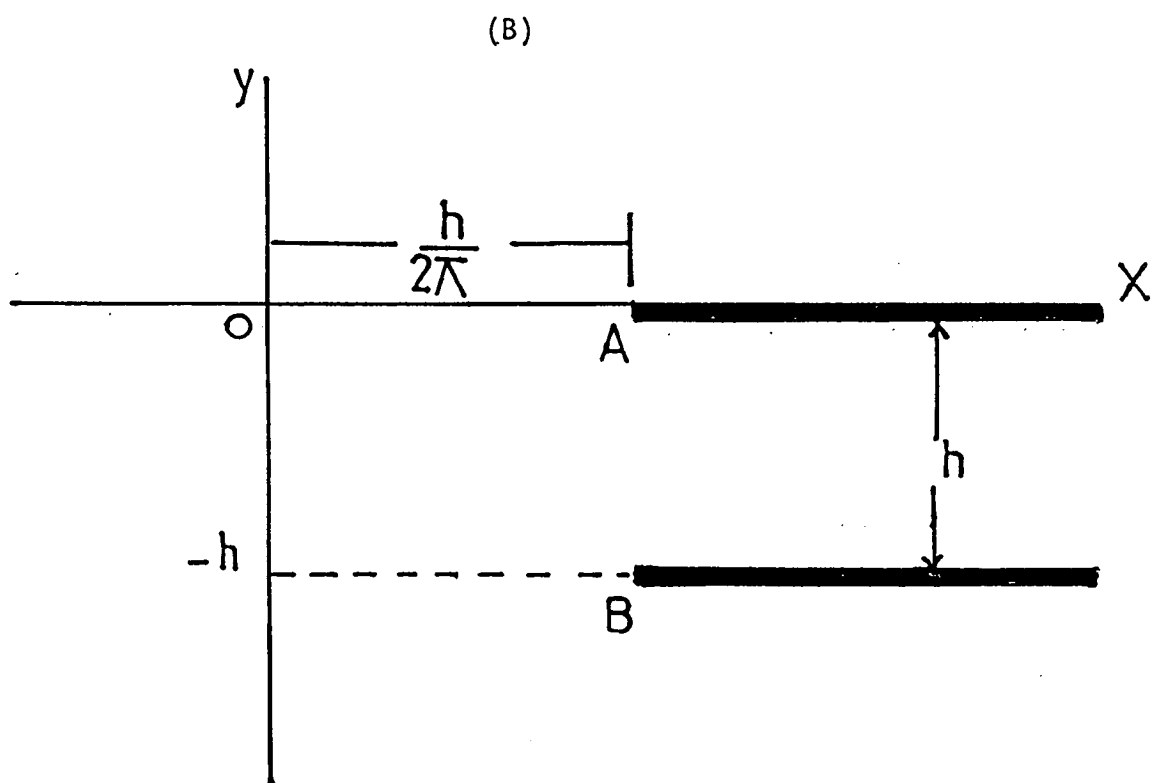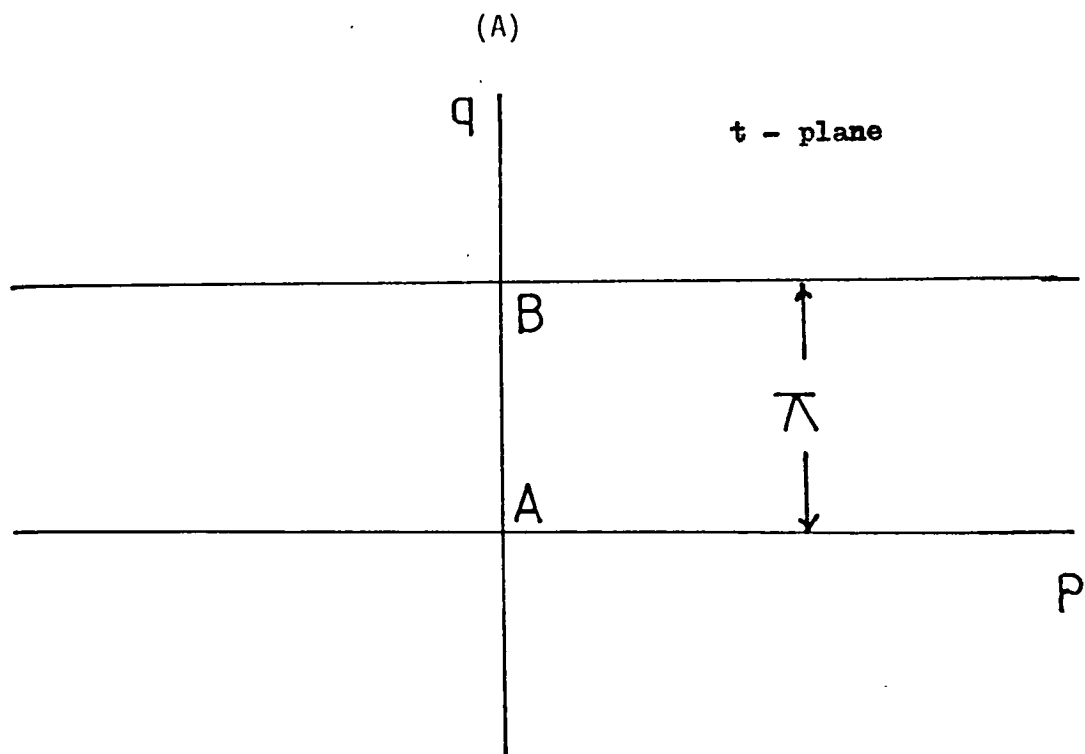
π

A

P

(B)

y

$\dfrac{h}{2\pi}$

X

O

A

h

-h

B

Figure 4 : Shows representation of two capacitor plates (A) Fixing
axes in the t plane (B) Axes in the Z plane. (From Gibbs,
W.J., 1956).

Electric field
V/m

For V = 1 Volt.

1. Electric field strength of flatplates:

$$E \longrightarrow \frac{V}{d}$$

2. Electric field strength of curved plates:

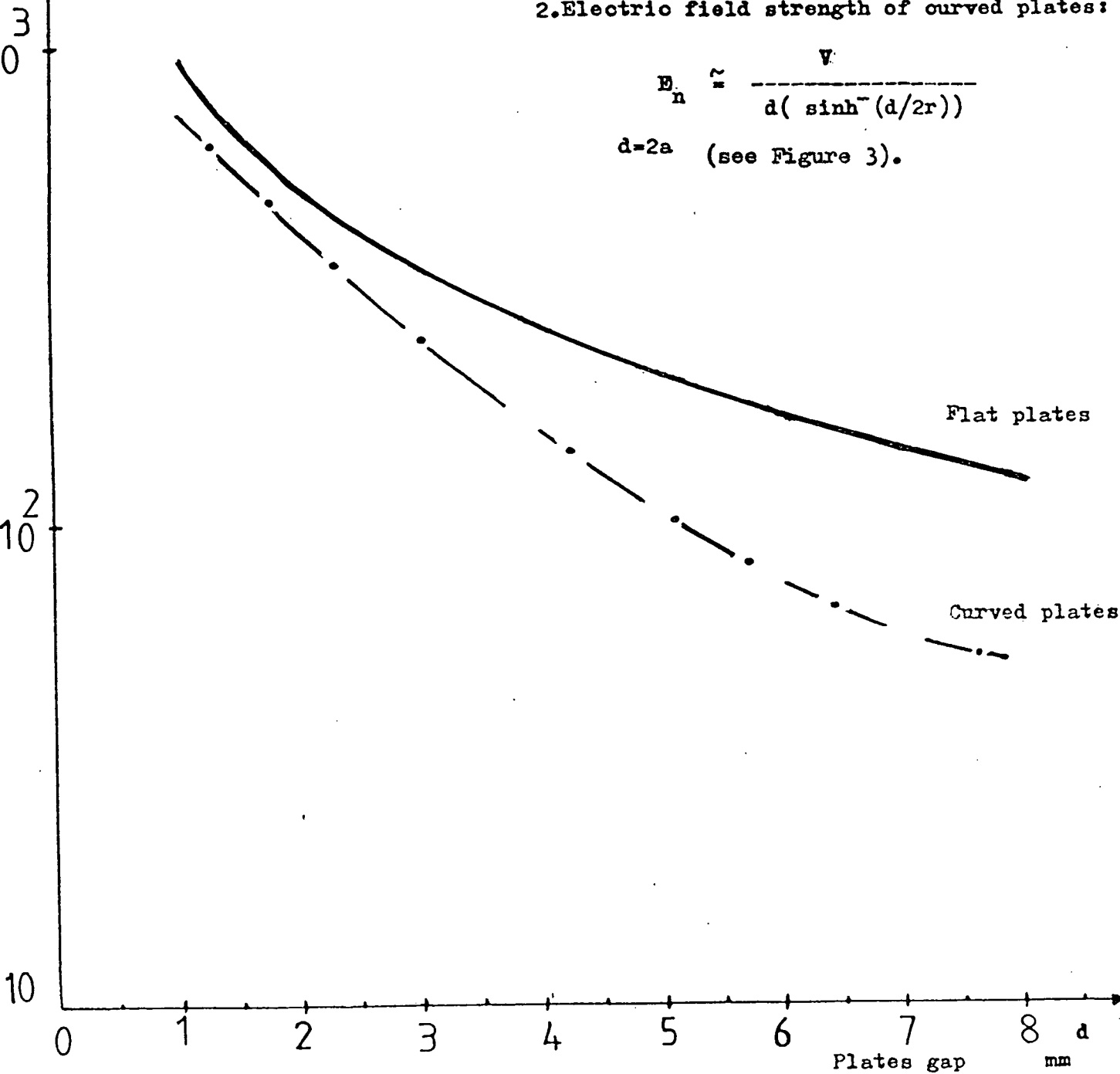$$E_n \cong \frac{V}{d(\ \sinh^-(d/2r))}$$

d=2a   (see Figure 3).

Flat plates

Curved plates

Plates gap

d

mm

Figure 5 : shows electric field strength of different plates shapes .

SEM COLOUR STROBOSCOPY FOR IMAGING OF TIMING
IN INTEGRATED CIRCUITS

S. Alshaban, A.R. Dinnis

*Electrical Engineering Department, University of Edinburgh,
King's Buildings, Edinburgh EH9 3JL, Scotland, UK.*

ABSTRACT

Colour stroboscopy aims to give timing information in the
form of colour on a 2-D image of the specimen. The present
work has no restriction on frequency of operation other than
that imposed by the beam-chopping system. The type of delay
unit employed, using digitally switched delays, is particu-
larly convenient in this application because the sampling
pulse delay can be almost instantly switched as the colour
display system demands.

1. INTRODUCTION

The basic principle, an extension of the method described
by Dinnis (1980), is that a different colour is allocated to
each phase of interest of a repetitive signal. The guns in
the colour TV display monitor are switched to display a fix-
ed sequence of colours; switching at line frequency can pro-
duce a picture which may be viewed in real time, although it
is noisy. As the display colours are switched, the phases
of the sampling pulses are switched correspondingly by means
of a system developed by Alshaban (1983) which works on a
digital principle.

Hence, if a point in the image is at low voltage when the
sampling pulse appears, then that colour will register on
the viewing screen. If a signal is low for only one sampling
phase during the cycle, then the conductor will appear in
that colour on the viewing screen. If the signal is low on
more than one sampling phase, then a mixture of colours will
appear; these can be arranged to simply superimpose to pro-
duce additive colour mixing or colour striations can be made
to appear.

This principle may be used in various modes, depending on
the application, and three cases are outlined below.

2. RESULTS

2.1 Pulse Position

If signal pulses are expected at certain points in the
cycle, then the sampling pulses are arranged to occur at
these points and all the conductors which are at zero or
negative voltage at the instants when the sampling pulses
are present will appear in the relevant colour, as shown in
Fig. 1, where the three primary colours are assigned to
three particular pulses. If the pulse on the circuit does
not occur at the expected time, then that colour does not
appear. The sampling point may then be shifted until the
colour appears, indicating that the pulse has been found.

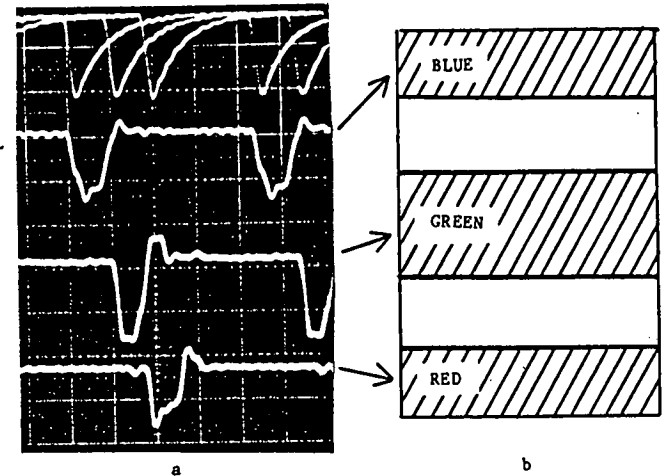a   b

*Fig. 1. Colour stroboscopy to indicate pulse position.
(a) The top trace is the voltage on the chopping plates;
the beam is on at the lowest point of the waveform. The
sequence of colours is B G R. The other three traces are
the voltages on adjacent conductors.
Horizontal scale: 50 ns/div. Vertical scale: 5 V/div.
(b) Indicates the colours appearing on the display.*

One application of this mode would be to detect any time delay error in a clock line on a large IC chip.

2.2 Pulse Length

Sampling points may be positioned at each end of a signal pulse, so that both colours superimpose so long as the pulse exceeds the preset length, as shown in Fig. 2.
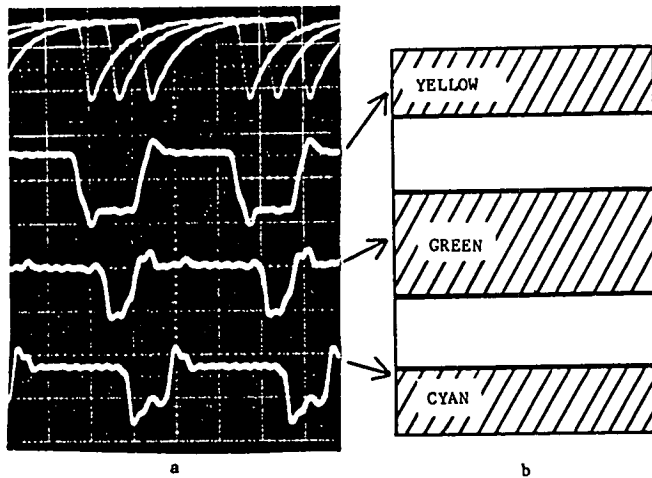

a   b

Fig. 2. Colour stroboscopy to indicate pulse length.
(a) The top trace is the voltage on the chopping plates.
The colour sequence is R G B. Horizontal scale: 50 ns/div.
Vertical scale: 5 V/div. (b) Indicates the colours
appearing on the display.

2.3 Transition Time

Here, sampling points are positioned at either side of a pulse transition (e.g. red and green). A primary colour (red) will result if the signal edge is correctly positioned and fast enough, as shown in Fig. 3. If the edge is slow, then the colours will mix (to give orange or yellow). A delay in the edge will give a similar effect, but this can be distinguished by shifting the sampling points, with the same interval between them, until they do cover the edge; if a primary colour can be achieved then the effect is pure delay. If a primary colour cannot be produced, then the transition time can be estimated by separating the sampling points until it is regained.
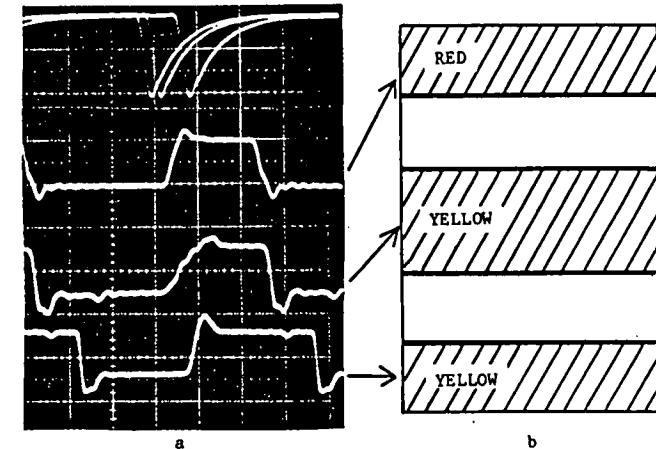

a   b

Fig. 3. Colour stroboscopy to indicate transition time.
(a) The top trace is the voltage on the chopping plates.
There is a 22 ns delay between the waveform reaching its
lowest point and the electron pulse reaching the
specimen. The colour sequence is R G B. The second trace
has a short risetime and so the conductor carrying it
appears red. The third trace has a long risetime and
appears yellow, as as does the fourth one, which has a
short risetime but is delayed. (b) Indicates the colours
appearing on the display.

3. SYSTEM DESIGN

The system shown in Fig. 4 was constructed to implement colour stroboscopy. The SEM was a Cambridge Instruments S-2 working with a beam accelerating voltage of 1.5 kV. It had beam chopping plates fitted between the gun and the first lens. These were driven by an amplifier fitted to the column which was driven by a 50 ohm matched coaxial line from the digitally controlled delay generator. The delay generator was triggered from the test signal generator which fed pulses to the specimen by 50 ohm coaxial lines with resistive terminations at the specimen IC. The latter was a specially designed device with various widths and spacings of conductors for testing the performance of voltage-contrast detectors.

The delay control circuit was used in the manually preset mode in this case, although it could also be set by computer. It was connected to the delay generator by 8 lines which controlled the first 8 bits of delay, which could therefore vary in 1.25 ns steps over a range of 320 ns. The delays for the three sampling points were set in the three 8-bit latches by setting the eight switches to the required delay for a particular colour and then loading the correct latch by pressing the appropriate button.

The digital scan-generator was used only in its TV scan mode in order that a real-time viewable colour display could be used. The display was a modified domestic receiver with additional inputs provided, one of which accepted a video signal with composite synchronising pulses which would normally produce a monochrome picture. The colour information was displayed by means of separate inputs to switch on the three guns in the display one at a time. The signals to control this were produced by a circuit which divided the line synchronising signal by three, so that the lines in the display were a continuous sequence; R-G-B-R-G-- . The same signals were fed to the delay control unit so that the delay was switched at the end of each line of the display. The line structure was clearly visible on the display but did not obscure the information in the picture and it became almost invisible on photographic recordings.

The signal frequency on the chip should be high enough that it does not produce noticeable patterning on the TV picture, i.e. it should be 5 MHz or greater. It should not be synchronised to the TV scan, again to reduce patterning effects.
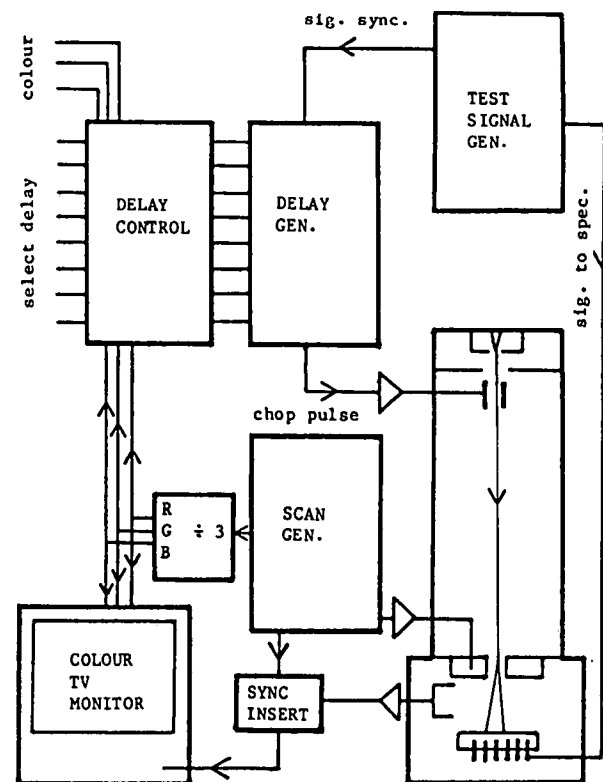

Fig. 4. Equipment for colour stroboscopy.

4. CONCLUSIONS

This work has shown that colour stroboscopy at high frequency to give a real-time TV display is both possible and useful. The maximum frequency which has been employed so far is about 10 MHz, with a time resolution in the region of 1ns. The frequency limitation is set by the chopping plates used to chop the beam and the associated delay generator rather than by the colour display system. While there is clearly a need for development and sophistication of the technique, it has already been shown that it can rapidly provide very precise timing information about pulses travelling through integrated circuit structures. Obtaining this information by other means would be laborious and time consuming. Once the method has been used to identify the places where trouble seems to be located, then the system can be switched to the conventional sampling mode and precise voltage waveforms can be traced out.

The type of delay unit employed using digitally switched delays, is particularly convenient in this application because the sampling pulse delay can be almost instantly switched as the colour display system demands. Most methods of delay generation should be able to change to the new value and settle to a stable state fairly rapidly. However, switching at line frequency requires that the time delay change within 12 microseconds, which is well within the capability of this system but could well cause problems in analogue-based systems. This delay unit also has low timing jitter compared with equivalent analogue systems.

In viewing the image produced by this system, the most noticeable defect is the poor signal-to-noise ratio. The spatial resolution is also somewhat degraded. The reason for these defects is the low duty cycle of the electron beam, which is necessary if good time resolution is to be achieved. In order to provide an image which is viewable at TV rate, it is necessary to use low demagnification of the gun crossover and a large final aperture, hence the poor spatial resolution. A brighter cathode is clearly one way to improve the situation.

Direct computer control of the delay unit has also been used but was found to be incapable of the speed which the hard-wired system provided and was therefore not capable of giving a directly viewable display. However, the advantages of computer control are so obvious that the next step in the development of this system must be to provide a computer-controlled system which would take over the present method of manually loading the delays corresponding to the three colours and provide other useful facilities.

6. REFERENCES

Alshaban,S. (1983). Ph.D. Thesis, University of Edinburgh.
Dinnis,A.R. (1980). Scanning, 3, 172-175.